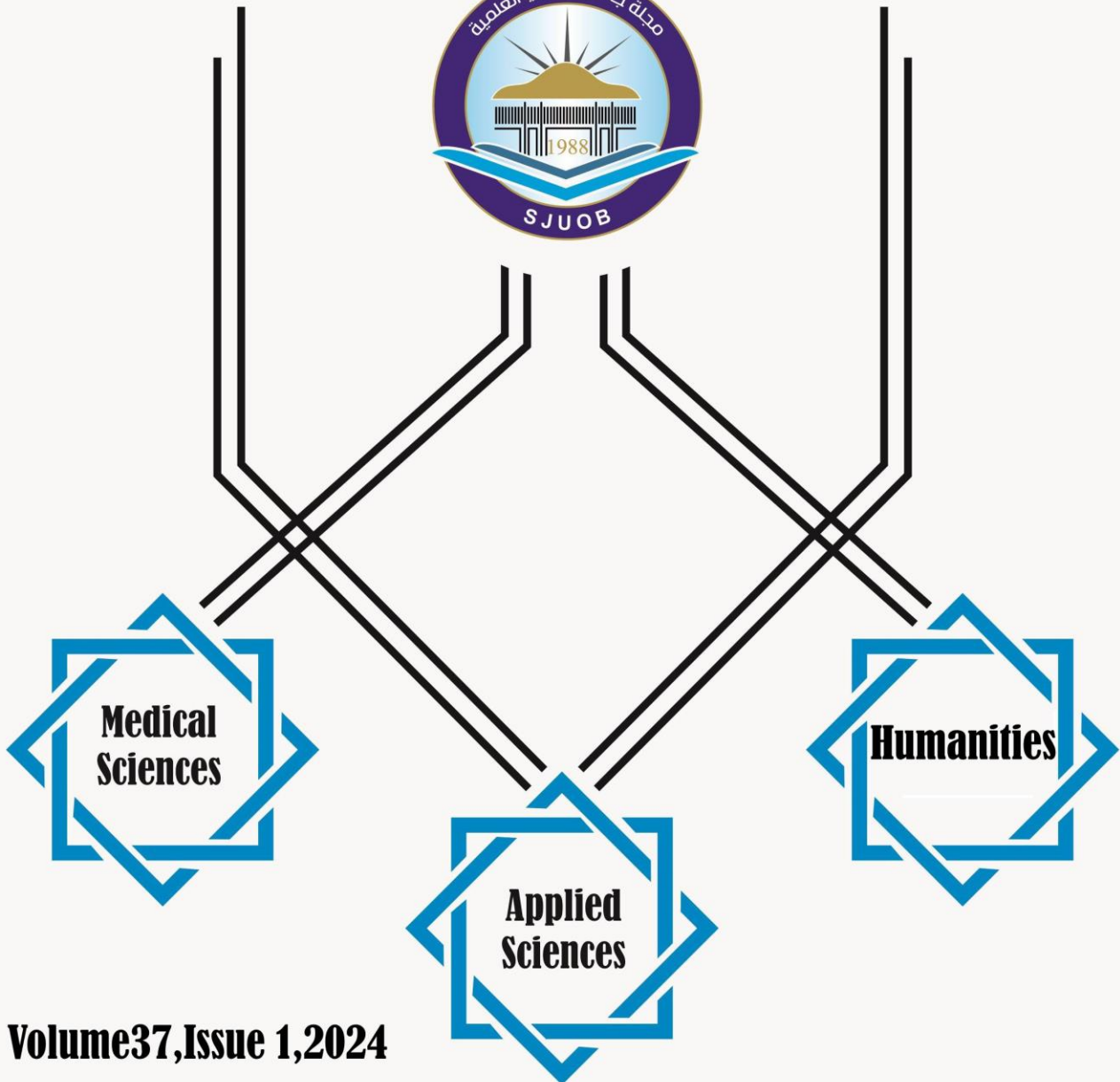


**University Of Benghazi**



**Scientific Journal of University of Benghazi**



**Volume37, Issue 1, 2024**

© 2024 University of Benghazi. All rights reserved. ISSN:Online 2790-1637, Print 2790-1629; National Library of Libya, Legal number : 154/2018

<http://journals.uob.edu.ly/sjuob>

**The preface of the first issue of the thirty-seventh  
volume for the year 2024**

**Greetings,**

We believe that focusing on scientific research leads to scientific progress and prosperity in all areas. The University of Benghazi plays a vital role in enriching knowledge and education with higher quality standards contributing to the development of our country. Our mission as an Editorial Board of the Scientific Journal of the University of Benghazi is to ensure the publication of high-quality scientific research papers undergoing blind peer-review by experts in various fields of humanity, applied, and medical sciences.

We are pleased to announce the publication of the first issue of the thirty-seventh volume for the year 2024 available electronically on the journal platform. In addition, we invite all researchers from all over the world to participate with their high-quality scientific research papers originally written in English for journal publication to enhance the rank of our university locally, regionally, and internationally.

Sincerely,

**Editor-in-chief**

**Prof. Dr. Marei El-ajaily**

# The Scientific Journal of University of Benghazi

Volume 37, Issue 1, (2024)

It deals with various branches of human, applied and medical knowledge  
Publishes research in English

## Editorial Board:



**Marei M. El-ajaily**  
Editor- in- Chief



**Daefalla M. Tawati**  
(Applied Sciences)



**Suliman S. Alfarawi**  
Executive Editor



**Abdelhamid Y. Alhassi**  
(Applied Sciences)



**Ahmad S. Emrage**  
(Humanities)



**Mayeen Uddin Khandaker**  
(Applied Sciences)



**Allaaeddin A. El Salabi**  
(Medical Sciences)



**Ahmed A. M. Ben Hosouna**  
(Medical Sciences)



**Abdelhakim M. Elbarsha**  
(Medical Sciences)

**Khalifa A. Al-Athram**  
(Technical coordinator)

University of Benghazi Scientific Journal - University of Benghazi, Office No.  
12, University of Benghazi - Al-Humaidah

Email: [sjuob@uob.edu.ly](mailto:sjuob@uob.edu.ly) - Website: <http://journals.uob.edu.ly/sjuob>

## **Guidelines for Submission**

- Only articles originally written in English (NOT translated to English) are accepted for submission.
- The submission has not been previously published or being under consideration elsewhere.
- The submission file is in Microsoft Word format (.doc,.docx)
- The submitted articles should adhere to originality and publishing ethics.
- The similarity of the article should not exceed 20%.
- The submission should include a separate title page, the main article and the journal submission form.
- Article should have no more than 6 authors.
- The main article should be divided into; Title, Abstract, Keywords, Introduction, Material and Methods, Results and Discussion, Conclusion and References.
- The text is single-spaced, Times New Roman with a 12-point font.
- The text must not be more than 3000 words excluding abstracts and references.
- All figures and tables should be well presented, organized and consistent with the text.
- All figures must be prepared as (.tiff) or (.jpeg) format for the width of A4 size (6.27 in) with a minimum resolution of 300 dpi.
- The role of authors should be provided.
- Ethical approval when applicable should be provided.
- Any conflict of interest should be declared.
- Vancouver referencing style should be used.
- URLs/DOIs in the references list should be included where available.

	Paper Title	Author	Page
<b>Humanities</b>			
1	Obstacles Face Sixth-Semester English Students in Translating Proverbs from Arabic into English	Fouzia Aleskandarani	6
2	Students' Preference of Theoretical and Practical Teaching in ELT Libyan Higher Education Setting: An Action Research Study on the Impact of Integrating Technology to Language Teaching	Najla Ali Hamad Suweekar	13
<b>Applied Sciences</b>			
1	Green Hydrogen Production from Seawater Using Metal Oxide Catalysts	Hamdy AB. Matter Tariq M. Ayad	21
2	The Sardar sub-equation technique for obtaining some optical solitons of cubic nonlinear Schrödinger equation involving beta derivatives with Kerr law nonlinearity	Abdulmalik A. Altwaty Jaffalah J. Amhalhil Ahmed El Sakori Nglia F. Meriki	28
3	Taguchi Grey Relational Analysis of Mechanical Properties of Structural Steel Welding Made by Gas Tungsten Arc Welding	Saleh Suliman Saleh Elfallah	37
4	Experimental Investigation of Steel Corrosion in Concrete Structures by Acoustic Emission Analysis	Hisham A. Elfergani	47
5	Using the Weather Index Classification System for Canadian Forest Fires over the Al-Jabal Al-Akhdar in Libya	Haifa M. Ben Miloud	55
6	Selecting the Optimal Airfoil for Automotive Rear Wings: Performance Assessment	Osama Maddani Saleh Etaig Al-Hadi Ebrahim Islam AlJhani	65
7	Effect of Intercritical Annealing Parameters on The Hardness Property: Statistical Study Using Taguchi	Asma F. Haiba Farag I. Haider Mohamed Gebril Dawod Elabar Ayad O. Abdalla	81
8	Detection of Autism Spectrum Disorder by A Case Study Model Using Machine Learning Techniques An Experimental Analysis on Child, Adolescent and Datasets	Najat S. Bousidrah Zahow M. Khamees Sana M. Ali	87
9	On Convergent Filters in Soft Topological Spaces	Rukaia Mahmoud Mohammed Rashed	101
<b>Medical Sciences</b>			
1	Knowledge, Attitude, and Practices Regarding Safe and Hygienic Food among Food Handlers in some Benghazi Hospitals	Sara Ahmed Elsherif Aya Abdallah Mohammed Budor Omar Mansor Manar Wanis Elbarghathi Najwa Faraj Elmodabel	110
2	Exploring Smell Loss Patterns and Recovery Factors Among Covid-19 Patients in Benghazi, Libya	Balgeis Elfallah	120
3	Prevalence of Obesity in Adult Hypertensive Patients and its Effect on Antihypertension Drugs Polypharmacy in Primary Health Care Clinics in Benghazi	Adel Saleh Adela Ebsat	130
4	The Analytical Descriptive Study of the Effect of Drinking Water Contamination on the Spread of Hepatitis A Virus in DARAA Governorate-Syria	Wisal Alhommada Tameem Alkrad khaldon Alkrad	141





## Obstacles Face Sixth-Semester English Students in Translating Proverbs from Arabic into English

Fouzia Aleskandarani <sup>1\*</sup>

*1 Department of Translation -Faculty of Languages -University of Benghazi.*

Received: 15 / 03 / 2024; accepted: 28 / 05 / 2024

### ABSTRACT

Translating proverbs is challenging, as they are culturally bound items. Thus, finding the most accurate equivalence causes problems for novice translators and learners. These problems are related to linguistic, cultural, and inaccurate use of translation techniques. Therefore, it is not reasonable to translate a proverb literally by just looking at the meaning of its individual words in a dictionary because they are culturally bound items. The current study attempts to investigate the problems that sixth-semester students encounter while translating Arabic proverbs into English and analyze the methods employed by them. The sample consists of 37 students in the English Department. The students were given a list of proverbs that contained 11 Arabic proverbs to be translated into English. The results revealed that students faced difficulties in translating proverbs due to cultural differences as well as overusing literal translation. The study recommended that students should use communicative translation, memorize some proverbs and their counterpart translations as well as practice.

**KEYWORDS:** culturally-bound, equivalence, proverbs, sixth-semester.

### 1. INTRODUCTION

Translation serves as a bridge that fills the gaps. Furthermore, it is a communicative process that transfers the message of a source language text to a target language. In this respect, translation should not be viewed from a single perspective since it requires more than just rendering words and sentence patterns from one language to another. It also involves a network of ideas, meanings, and most importantly, sociocultural norms. In translating proverbs, translators face some linguistic difficulties due to the lexical, stylistic, and cultural differences between the SL and the TL <sup>1</sup>. Achieving effective equivalence when rendering proverbs from one language to another can be problematic for translators, especially novice translators. In order to overcome such a problem, translators need to be aware of both cultures (SL and TL) and adopt the appropriate translation method to provide accurate translation <sup>2</sup>.

### 2. OBJECTIVE OF THE STUDY

The main objective of the study is to investigate the obstacles that the sixth-semester students at the University of Benghazi, Faculty of Languages encounter while translating Arabic proverbs to English. Moreover, to investigate the strategies the students employed to render the proverbs.

### *Equivalence*

Translation plays a crucial role in communication between nations and in bridging the cultural and linguistic gaps among them. The main challenge of translation is finding the most appropriate equivalence of meaning. In this respect, "Translation consists in reproducing in the receptor language the closest natural equivalent of the source-language message" <sup>3, p.12</sup>. Thus, translation is not a mere transfer of words and grammatical structure from one language to another, rather it is a transformation of messages using the most appropriate equivalence. That is to say, translation depends heavily on the transfer of culture. The problem becomes even more sophisticated when dealing with two different cultures: English and Arabic. In addition to the linguistic differences, Arabic and English do not belong to the same family of languages. Thus, the task of the translator is not easy since (s) he should create an effect on the target text reader that is similar to that of the original. Translators, however, frequently encounter several problems when translating texts from English into Arabic and vice versa. Equivalence is one of the problems that translators face. When translating texts with words that do not have a direct equivalent in the target language, the translator is compelled to translate them communicatively or merely translate the meaning. <sup>4</sup>

In the case of translating idioms, sayings, and proverbs which are culturally bound, the translator attempts to find the equivalence that would be known to the speech community of the target language and would imply adequate meaning. For instance, in *Carrying Coals to*

\*Correspondence: Fouzia Aleskandarani

[fouzia.aleskandarani@uob.edu.ly](mailto:fouzia.aleskandarani@uob.edu.ly)

*Newcastle*, the proverb sounds irrelevant if transformed literally into Arabic because the audience of the TL has no idea about Newcastle (A place famous for coal mining in Great Britain). Therefore, the appropriate equivalent in Arabic would be *بييع الماء في حارة الساقيين*. It has been argued that rendering proverbs by identifying word-for-word equivalence is not possible. This emphasizes the importance of considering proverbs beyond their denotative meaning. Thus, it is crucial to consider the cultural layers in the translation process<sup>5</sup>. All in all, equivalence is an important phenomenon in translation, and it involves an attempt to convert the content while retaining the context and meaning of the original.

### Translation and Culture

Communication between individuals from diverse cultural backgrounds is made feasible through translation. Indeed, translation plays a significant role in cultural exchange. Likewise, culture plays a crucial role in the translation process. Thus, translation and culture are interwoven. In this respect, translators have been entrusted with the highly demanding task of representing cultures for decades<sup>6</sup>. Newmark established the relationship between culture and translation. According to him, although this process has been supposed not to be difficult, in reality, translators have been facing the complex task of translating and conveying culture for a long time. Since the translator is considered a cultural mediator (s)he should be both bilingual and bicultural. To put it another way, (s)he has good knowledge of both SL and TL cultures. Therefore, he/she can render cultural messages to produce a text that has the same tone as the original one. The lack of such cultural knowledge of the SL and TL may cause cultural and semantic problems in conveying the intended meaning from one language to another.

Undoubtedly, culture has a significant impact on language; the two are closely linked "Language does not exist apart from culture"<sup>7</sup>, p.207. In other words, language is the mirror that reflects the culture of a particular community. Language obstacles are caused by culture; challenges that translators encounter due to cultural variations between the source and target languages might be more severe than those resulting from linguistic differences. Such challenges are obvious when it comes to the translation between two different languages Arabic and English. This problem becomes more complicated when dealing with culturally specific terms such as proverbs. Culture-specific items are words and expressions that are embedded within a particular language and culture, and they are not familiar to the TL and culture. These items represent a specific type of food, religious practice, specific habits, etc. For example, in Western culture owl is associated with wisdom, whereas in Arabic culture it is a symbol of pessimism. In the same vein, the Arabic proverb *أكلتم تمرى وعصيتم أمرى*, a literal translation of the previous will inevitably distort the meaning. The appropriate

equivalence would be *pig-headed*; the English people do not use the word "date" because this type of fruit does not grow in the country, so the translator needs to replace the word "date" with the word "pig" as it is a Western animal's pet and becomes a nutritious food for them.

### Proverbs

A proverb is a short well-known saying, that expresses wisdom and is derived from common real-world experience. Proverbs were defined as "special, fixed, unchanged phrases which have special, fixed, unchanged meanings"<sup>8</sup>, p.138. Proverbs can be very difficult to understand from single words since the literal meaning can mean something different from the figurative meaning. Hence, translating proverbs is challenging as they create problems in the process of understanding and translating them. Even if a proverb has a linguistic equivalent in the TL, there may be a cultural difference involved. For example, the English proverb *A bird in hand is worth two in the bush* has a similar linguistic equivalent in Arabic, however, the cultural equivalent is slightly different due to the cultural languages between the two languages. Although literal translation can be understood *عصفور في اليد خير من اثنين على الشجرة*, communicative translation matches the cultural equivalence *عصفور في اليد خير من عشرة على الشجرة*. In this case, proverbs cannot be translated literally since they may sometimes have no natural figurative equivalents in TL. Each proverb conveys a specific meaning in a specific context of a situation. Therefore, a proverb should be transformed accurately to carry the same cultural conventions of the original proverb<sup>5</sup>. It is not reasonable to translate a proverb literally by just looking at the meaning of its individual words in a dictionary because they are culturally bound items.

### Language of Proverbs

Proverbs are different from ordinary speech because they are made up of figurative language. A proverb may contain metaphor, personification, paradox, and other stylistic devices that identify the figurative nature of the language of proverbs<sup>4</sup>. This causes difficulty for translators since (s)he should render the figurative meaning of the proverb as well as their communicative, for example, simile is a metaphorical device used in the Arabic proverb *كالمستجير من الرمضاء بالنار*. Nonetheless, the literal device (simile) may not be the same in the translated form. For translators to accurately translate this proverb into Arabic, they must first identify the relevant counterpart in Arabic, which is "out of the fire into the frying pan." The proverb, which is used metaphorically in both Arabic and English, implies that one is going from a difficult circumstance to one that is even worse. Similarly, the English proverb "birds of a feather flock together" and its Arabic equivalent are metaphorically employed to illustrate how individuals who have similar traits gravitate towards each other's companionship. It can be said that

proverbs cannot be understood from the individual meanings of their elements and can yield different sentiments when treated as separate words. This is due to the fact that most proverbs are metaphoric expressions, such as *اليوم خمر وغدا أمر*. The previous proverb does not refer to *خمر* as wine, but it carries a connotative meaning. In this respect, proverbs resemble literary works in that they are like mirrors reflecting the picture of the customs and cultural values of various communities; they depict the experiences and customs of different nations. Most proverbs extend far beyond the literal meaning, which is the most preferred and practiced by people because of their great impact on capturing the audience's intention<sup>9</sup>.

### Obstacles of Translating Proverbs

Translators mainly novices encounter problems during the process of translation. These problems arise when the translator struggles to accurately comprehend the message or find its equivalent in the target language. One of these problems is the nature of the proverbs because proverbs are figurative and -culturally specific items, giving them a literal translation may distort their intended meaning. There are three main problems that translators face while translating proverbs<sup>10</sup>. These problems are linguistic, cultural, and the use of inaccurate translation methods.

### Linguistic Problems

Since English and Arabic originate from separate linguistic families, they are two distinct languages; English is a Germanic language, while Arabic is a Semitic one. Students face difficulties in translation due to the difference in semantics and grammar caused by the origins of these languages<sup>11</sup>. In the case of semantics, some proverbs have more than one equivalent in the TL. That causes confusion to the learners and novice translators. For instance, the Arabic proverb *لا تلد الذئبة إلا ذئبا* can be rendered in English either as *like father, like son* or *apple does not fall apart from tree*<sup>12</sup>. This is also attributed to the English proverbs when they are transformed into Arabic, for example, the English proverb *after black clouds, clear weather* is translated into Arabic as *ما بعد رجح بخفي حنين* or *إن مع العسر يسرا*. Moreover, some proverbs are difficult to understand in the SL like *رجح بخفي حنين*, novice translators who are not well grounded in the Arabic language will either interpret *حنين* as a female name or nostalgia. In addition, words like *خير* sometimes rendered as *better* as prevention is better than cure, whereas it is transferred worth as in *A bird in the hand is worth two in the bush*. Learners may have problems in rendering such words and they may rely on using the same word whenever they translate another proverb.

Structural mistakes occur when translating proverbs without paying much attention to the grammatical differences between SL and TL, for example, *الوقت من ذهب* is a nominal phrase in Arabic, however, it becomes a

verbal phrase when it is rendered to English (*Time is money*).

### Cultural Problems

the inability to translate culturally-bound words/expressions effectively providing an irrelevant translation of the proverb. "Translating involves not just two languages, but a transfer from one culture to another"<sup>12</sup>, p.28. These differences are more challenging than the linguistic ones because each culture has its specificities such as religion, literature, and way of living, these cultural problems make the task of translating proverbs difficult. Some proverbs have a direct equivalent in the TL, but many proverbs are specific to the TL. These proverbs may have a historical event like *أكرم من سمول*, or they are derived from SL literature<sup>13</sup> as *السيف أصدق أنباء من الكتب*. Therefore, translators need not only to have bilingual competence but also a good knowledge of the cultures of the languages concerned since literal translation and lack of linguistic and cultural knowledge in both languages cause problems in fully understanding the intended meaning.

### The Use of Inaccurate Translation Techniques

Most novice translators and learners are unable to adopt effective procedures that match the translation situation<sup>14</sup>. Some translators overuse literal translation, but this is not useful in translating proverbs that contain culturally bound words. For instance, *لا يلدغ المؤمن من جحر مرتين*. Undoubtedly, the use of literal translation will distort the intended meaning. Therefore, translators and translation learners should employ communicative translation to render the meaning properly.

## 3. METHODOLOGY

The data of the study is a collection of some proverbs, Arabic proverbs, and their translation counterparts that were selected from *Learn the Bases of Translation* (2010)<sup>15</sup>. 11 Arabic proverbs written in standard Arabic were chosen to be used as a test. The test was designed to assess the students' ability to translate Arabic proverbs into English. Some of the selected proverbs have absolute equivalence in the TL while others have different equivalence. The sample of the current study contained students who are studying English at the University of Benghazi, Faculty of Languages. They are in the 6<sup>th</sup> semester. This sample has been selected for the following reasons. Since they have been in the 6<sup>th</sup> semester, they have been practicing both A/ E and E/ A translation. In addition, they were introduced to different translation theories. The sample consisted of 37 students, and the selection of the sample was based on the Morgan Sampling Table to determine the sample size needed for the study. The students were given a test that consisted of the 11 selected Arabic proverbs to be translated into English. The test lasted about an hour and the students were allowed to

use dictionaries mainly online dictionaries such as Google Translate and Almaany.

The results were examined after the data had been gathered. 3 alternatives were used in scoring the test. First, the answer was correct if the proverb was translated by

using cultural equivalence. Second, the answer was wrong if the proverb is translated by using a literal translation. Finally, no answer if the students did not provide any translation. In order to assess the translation strategies employed by the students, Newmark translation strategies were utilized.

#### 4. RESULTS

Table 1

Arabic Proverb and its Translated Version			Correct Answer	Wrong Answer	No Answer	Total
أهل مكة أدري بشعابها	Transliteration	Students' numbers	3	19	15	37
Know something like the back of your hand.	'ahl makkeh 'adraa bishieabiha	Percentages	8.89%	48.89%	42.22%	100%

As seen in the table above, many students failed to render the proverb accurately. The best evidence is the percentage of incorrect answers 48.89%. They transformed the proverb literally as the people of Mecca know best

about its paths. The students neglected cultural differences between the two languages, Arabic and English. However, very few students 8.89% attempted to find the correct equivalent. Furthermore, 42.22% are left blank.

Table 2

Arabic Proverb and its Translated Version			Correct Answer	Wrong Answer	No Answer	Total
لا تلقوا بأيديكم إلى التهلكة	Transliteration	Students' numbers	10	25	2	37
Don't put your head in the lion's mouth.	la talqawa bi'aydikum 'iilaa altahluka	Percentages	27.03%	67.57%	5.41%	100%

The table above shows that the majority of the students translated the proverb inaccurately. Those students represent the highest sample by 67.57%. Most of them rendered this proverb literally as *do not throw yourself into*

*destruction*. This proverb is culturally bound, and literal translation does not fulfill the intended meaning. However, only ten students succeeded in providing an accurate interpretation. 5.41% are left blank.

Table 3

Arabic Proverb and its Translated Version			Correct Answer	Wrong Answer	No Answer	Total
الوقاية خير من العلاج	Transliteration	Students' numbers	35	2	0	37
Prevention is better than cure.	alwiyayat khayr min aleilaj	Percentages	94.59%	5.41%	0.00%	100%

Nearly all the students translated the proverb correctly 94.59% because it has a direct equivalence in the TL. Only four students rendered it literally as *protection is better*

*than treatment*. In addition, the percentage of no answer is 0.00%.

Table 4

Arabic Proverb and its Translated Version			Correct Answer	Wrong Answer	No Answer	Total
سبق السيف العذل.	Transliteration	Students' numbers	0	16	21	37
It's no use crying over spilled milk.	sabaq alsayf aleudhl	Percentages	0.00%	43.24%	56.76%	100%

56.76% of the respondents did not submit a translation for the proverb as seen from the table above. This can be due to the students' unfamiliarity with the proverb and the difficulty of finding the most appropriate equivalence. On the other hand, 43.24% incorrectly rendered the proverb as

*the sword preceded the humiliation*. Indeed, such a translation is inaccurate, and it distorts the meaning. In addition, none of the participants provided a correct translation.

Table 5

Arabic Proverb and its Translated Version			Correct Answer	Wrong Answer	No Answer	Total
الضرورات تبيح المحظورات. Necessity needs no rules.	Transliteration	Students' numbers	9	20	8	37
	aldarurat tubih almahzurati	Percentages	24.32%	54.05%	21.62%	100%

This table indicates that the highest percentage is the wrong answer where the students render the proverb improperly; they employed a literal translation. In addition,

21.62% are left unfilled spaces and only nine students succeeded in transforming the verb accurately.

Table 6

Arabic Proverb and its Translated Version			Correct Answer	Wrong Answer	No Answer	Total
الأقربون أولى بالمعروف. Charity begins at home.	Transliteration	Students' numbers	15	19	3	37
	al'aqrabun 'awlaa bialmaeruf	Percentages	40.54%	51.35%	8.11%	100%

This proverb is culturally religious bound. In addition, it is widely used by Arabic speakers. 40.54% succeeded in providing an accurate translation. Nevertheless, 51.35% gave other irrelevant answers such as *the closet, the*

*relatives*. Those participants failed to render the meaning because they used literal translation. In addition, 8.11% did not translate the proverb at all.

Table 7

Arabic Proverb and its Translated Version			Correct Answer	Wrong Answer	No Answer	Total
لا دخان بدون نار. No smoke without fire.	Transliteration	Students' numbers	33	4	0	37
	la dukhan bidun nari	Percentages	89.19%	10.81%	0.00%	100%

The table above shows that the proverb لا دخان بدون نار seems easy to be understood and the majority of the students are at ease with this proverb. The best evidence is the percentage of correct answers 89.19%. In addition, this

proper interpretation is mainly due to the wide use of the proverb in English. In contrast, only four failed to transform this proverb accurately.

Table 8

Arabic Proverb and its Translated Version			Correct Answer	Wrong Answer	No Answer	Total
يزيد الطين بلة. Add fuel to fire.	Transliteration	Students' numbers	11	22	4	37
	yazid altiyn bila	Percentages	29.73%	59.46%	10.81%	100%

59.46% of the students responded with *increasing the wet of the clay*, this means that they transferred the proverb literally. Although the proverb is commonly used in Arabic contexts, students failed to find the appropriate

equivalence. Furthermore, 10.81% did not answer; they did not translate this proverb. 11 students provided the correct translation.

Table 9

Arabic Proverb and its Translated Version			Correct Answer	Wrong Answer	No Answer	Total
اللبيب من الإشارة يفهم. A word is enough to a wise man.	Transliteration	Students' numbers	5	21	11	37
	allabib min al'iisharat yafhamu	Percentages	13.51%	56.76%	29.73%	100%

The percentage of students who did not translate the phrasal verb accurately implies a greater percentage, as seen in the table above, which is 56.76%. The students translated the proverb literally. The literal translation was seen as both unacceptable and inaccurate, they translated

the proverb as follows *smart understands from the sign*. Such translation does not fulfill the intended meaning. Moreover, the number of the blanks is 29.73%. Just five students had translated the proverb correctly.

Table 10

Arabic Proverb and its Translated Version			Correct Answer	Wrong Answer	No Answer	Total
احذر عدوك مرة واحذر صديقك ألف مرة. A good enemy is better than a false friend.	Transliteration	Students' numbers	11	21	5	37
	ahdhar eaduuq mara w ahdhar sadiqak 'alf mara	Percentages	29.73%	56.76%	13.51%	100%

The table indicates that more than half of the students failed to transform the proverb properly. They relied on the literal translation *be aware of your enemy once and be aware of your friend a thousand times* neglecting the use

of communicative translation. Therefore, the literal translation does not match the meaning. Moreover, the number of blanks is 13.51%. In contrast, very few participants rendered the proverb accurately.

Table 11

Arabic Proverb and its Translated Version			Correct Answer	Wrong Answer	No Answer	Total
عصفور في اليد خير من عشرة على الشجرة. A bird in hand is worth two in the bush.	Transliteration	Students' numbers	25	12	0	37
	eusfur fi alyad khayr min easharat ealaa alshajarati	Percentages	67.57%	32.43%	0.00%	100%

As seen in the table, the number of students who translated the aforementioned proverb is very high because of the students' familiarity with the verb as well as its usage. On the contrary, very few students provided the wrong translation, and they represent 32.43%. They rendered the proverb literally as *a bird in the hand is better than ten on the tree*. None of the students left them without providing any answer.

## 5. DISCUSSION

The results of the study revealed that most students faced some difficulties when translating Arabic proverbs into English. Many students failed to find the appropriate equivalence, and they depended solely on the literal translation. They ignored that literal translation distorts the meaning of these culturally bound items. This can be attributed to many reasons. First, the students were unable to infer the meaning of some proverbs in their mother

tongue like *سبق السيف العذل*, therefore, they either gave a poor translation or gave no response at all. Second, some of the proverbs are related to culture, and any misinterpretation will lead to inaccurate translation. Such proverbs as *أهل مكة أدرى بشعابها*. Many participants did not transform the proverb correctly. In addition to being culturally bound, Arabic proverbs are closely interwoven with religion. For example, *لا تلقوا بأيديكم إلى التهلكة*, most students were not able to provide the target language equivalence. Thirdly, for some proverbs like *الوقاية خير من العلاج*, the participants attempted to render this proverb accurately; however, they used the word *protection* instead of prevention to transform *الوقاية* and the word *treatment* rather than using cure to render *العلاج*. Another example is *اللبيب* many students translated as *the smart person*. This is due to the fact that when rendering individual words from Arabic to English, the word may have more than one translation. In this case, students are facing difficulty in

choosing the closest equivalent. On the other hand, proverbs that have absolute equivalence do not pose any difficulties for students, such as لا دخان بدون نار since the literal translation matches the meaning of the original. It can be said that students overused literal translation to render the proverbs, however, they did not successfully provide the proper translation. Furthermore, the lack of knowledge of the TL culture compelled the learners to utilize the literal translation.

Despite using an electronic dictionary to assist them in translating proverbs from Arabic to English, the students translated many proverbs inaccurately because online dictionaries, like Google, only offer literal translations rather than the intended meaning in the target language. As a result, students need to first understand the proverb in their native language. Then search for the appropriate equivalent in the target language. Students are recommended to utilize dictionaries like المنجد في اللغة *almunjid fi allugha* because it contains various Arabic proverbs with elaboration. Moreover, they are recommended to use *The Oxford Dictionary of Proverbs* to understand the meaning of English proverbs.

To overcome the difficulties of translating proverbs, students should not rely on literal translation because it distorts the meaning of those proverbs that do not have absolute equivalence in the TL. Moreover, they need to memorize a wide range of proverbs in both languages as well as understand the cultural meaning and do more practice. Since these culturally bound expressions cannot be translated literally, students should be familiar with different translation techniques as it is one of the obstacles that students encounter. Therefore, students need to be trained to use translation techniques properly to provide accurate translation.

## 6. CONCLUSION

Translation of proverbs poses a challenge for novice translators since these items are closely related to culture. In addition, literal translation is problematic because it distorts the meaning. Therefore, translators need not only to be bilingual, but they have to be bicultural to render the cultural words and expressions accurately. The current study recommended that students should be taught translation courses as practical training not only as theoretical to assist them overcome the challenges when translating from Arabic into English and vice versa. These courses should include independent courses that focus on the best strategies that can help the students to translate accurately. Students should be involved in translation tasks to be able to select the appropriate techniques. In addition, proverbs should be introduced as part of the material to make students aware of the cultural and syntactic differences between the SL and TL.

## 7. REFERENCES

1. Dweik BS, Thalji MB. Obstacles Faced by the Jordanian Novice Translators in Translating Arabic Proverbs. *International Journal of English Language & Translation Studies* (online). 2015, 3 (4), 50-59. Available from: <http://www.eltsjournal.org>
2. Almjlal S. How the Saudi EFL Students at Undergraduate Level Translate English Proverbs into Arabic: Problems, Strategies and Solutions. *AWEJ* (online). 2023, 7 (4), 61-76, [Accessed 25 December 2023]. Available from: <https://papers.ssrn.com/sol3/papers>
3. Nida EA, Taber CR. *The Theory and Practice of Translation*. E. J. Brill, Leiden, 1969.
4. Sally A. Difficulties of Translating Proverbs from Arabic to English and Vice Versa Semester Four English Students as a Case Study, 2019. Cadi Ayyad University: Faculty of Letters.
5. Mollanazar H. *Principles and Methodology of Translation*. Tehran: Samt, 2001.
6. Newmark P A. *Textbook of Translation*. New York: Prentice Hall, 1988.
7. Sapir, E. *Language*. London: Rupert Hart-Davi, 1921.
8. Ghazala H. *Translation Problems and Solution. A coursebook for University Students and Trainee Translators*. Beirut: Dar WaMaktabet Al-Hilal, 1995.
9. Fahmi M. A Cross-Cultural Study of Some Selected Arabic Proverbs and their English Translation Equivalents: A Contrastive Approach. *International Journal of Comparative Literature & Translation Studies*. 2016, 4 (2): 51- 57, [Accessed 23 March 2021]. Available from: <http://journals.aiac.org.au/index.php/IJCLTS>
10. Mollanazar H. *Principles and Methodology of Translation*. Tehran: SAMT, 2001.
11. Meider W. *Proverbs: A handbook*. Connecticut: Greenwood Publishing Group. 2004.
12. Dickins J, Hervey S, Higgins I. *Thinking Arabic Translation: A Course in Translation Method: Arabic to English*. London: Routledge, 2002.
13. Dawood I, Khalil A, Yassin A. Investigating Linguistic Difficulties Arising from Translating Proverbs from English into Arabic. *IJ SS H Research* (online). 2019; 7 (1), 679-689, [Accessed 6 December 2022]. Available from: <https://www.researchpublish.com/>
14. Dickens J. *Thinking Arabic Translation. A course in Translation Method Arabic to English*. Sander Hervey: Ian Higgin's, 2002.
15. Hasan H. *Learn the basis of translation*. Dar alkootbalmesria, 2010.



## Students' Preference of Theoretical and Practical Teaching in ELT Libyan Higher Education Setting: An Action Research Study on the Impact of Integrating Technology to Language Teaching

Najla Ali Hamad Suweekar <sup>1\*</sup>

*1 Department of English Language and Linguistics -Al.Marj- Faculty of Arts and Sciences -University of Benghazi.*

Received: 25 / 02 / 2024; accepted: 07 / 06 / 2024

### ABSTRACT

Shifting the focus from merely theoretical teaching to balancing between theory and practicum in English Language Teaching (ELT) in Libyan Higher Education setting is a challenge, and it is the concern of this article. ELT Libyan students need to be capable enough to implement what they learn in universities and to integrate technology in language classrooms. At the Department of English Language in the University of Benghazi Al. Marj Campus, the author –a teacher and educator- investigated 47 eighth semester students to know their feedback about the style of instruction they are experiencing and what they prefer instead, their opinions about the practical and technological classes of the subject Technology and Language Learning E506 (taught by the author), and to assess their immediate performance after attending a workshop. Unlike their educational experience which relies on providing only theoretical knowledge, students expressed a desire to equate theoretical and practical education. They enjoyed participating in workshops as well as using technology in teaching and learning. Students performances were evident to be better, therefore, the current study recommends that attending workshops helps students teachers to revise and apply what they are learning to improve their teaching and technical skills.

**KEYWORDS:** ELT Libyan Higher Education Setting, Practical Teaching, Theoretical Content, Educational Technology, Educational Applications, Students' Preference, Students' Performance, Teaching and Learning Skills.

### 1. INTRODUCTION

Theoretical concepts are important in any educational process as well as the practical implementations related to such concepts. It is said that these two types of knowledge are two sides of the same coin Such conceptual understanding can be achieved not through blind learning but through experience and exploration which lead to genuine understanding, pieces of information we discover are absorbed more effectively than information we are taught <sup>1</sup>. Learning by doing is considered to be one of the best methods of acquiring new knowledge and skills. Supporting teaching with job-related learning makes the transition from being students to employment easier, this can be reached through stimulating classroom interest by the application of academic content to job situations. In Higher Education context it is the Ministry of Higher Education role to make cooperation with organizations, institutions and business community in providing practicum programs to university students <sup>2</sup>.

In Libya, Colleges of Arts do not offer practicum sessions, as the outputs will go to sectors other than education. On the other hand, it is the Education Faculties' function to prepare students practically in order to become teachers. It seems to be a perfect situation, but in the Libyan Higher Education context it is important to repeatedly remind that the outcomes of universities and colleges (Arts, Education and Sciences) are all directed toward schools, so the skills of new teachers must match the students' needs. The problem according to Halliday <sup>3, p. 38</sup> is that "the sort of instruction which young people get in their colleges does not easily match industrial reality". The field of work often requires theoretical knowledge that supported by practical skills, these two educational phases are referred to by Warnock <sup>4, p. 170</sup> as "the two great arms of the educational system".

Lovell and Lawson <sup>5</sup> state that the first method of acquiring knowledge is by personal experience (observation and records). To grasp a piece of information is to experience its practice. In terms of language education, language acquisition comes across two stages, knowing about the language (structure) and knowing the language (communication) <sup>6</sup>. Therefore, consideration must be given to practices, especially in Libyan Higher Education settings (Arts Colleges) where theoretical teaching is the dominant. According to <sup>7, p. 14</sup> "because of this dominance Libyan universities are far away from

\*Correspondence: Najla Ali Hamad Suweekar

[najla.suweekar@uob.edu.ly](mailto:najla.suweekar@uob.edu.ly)

applying strategies that promote effective learning". Shafter and Ruth <sup>8, p. 20</sup> stated "theoretical teaching led to deficiencies in the activation of educational activities and student services and an inability to meet students' needs".

Students' needs are changing due to the new generations dependence on using technology and the internet. All international educational systems utilize technological practices inside and outside classrooms. In ELT classrooms students' skills can be better improved by integrating technology to teaching and learning considering that technical experience has a vital role in shifting from merely theoretical education to practicum. Isman <sup>9</sup> defined technology as the practical application of knowledge, involving machines, tools and interactions with humans and the environment.

### **Research Questions**

1. To determine the dominant education style at the Department of English Language in Al.Marj Faculty of Arts and Sciences at Benghazi University.
2. To determine the type of teaching environment that students prefer.
3. To find out what students think of practical classes in general and of the subject Technology and Language Learning E506 in particular.
4. To assess the students' performance after attending a workshop class of the course Technology and Language Learning E506.

## **2. PREVIOUS STUDIES**

### **2.1. Why not to reach practical competences in Libyan Higher Education contexts:**

According to Shafter and Ruth <sup>8, p. 22</sup> "competency is the knowledge, skills, and attitudes that human force should have and establish to facilitate the ability to function appropriately at the job market". The authors pointed out that Higher Education in Libya has encountered several and severe challenges to the government, faculties, departments, teachers, students, and society at large. The reason why the expansion of universities and the growth in the enrolment are considered shortcomings not features <sup>8</sup>.

Alsanousi <sup>10, p. 139</sup> states that "Higher Education contributes to the national development by producing higher-level skills and competencies needed for a shift towards knowledge-based economy". Brydan and Abdalnabi <sup>11</sup> studied the students' benefits of Higher Education internationalization in Libya and concluded that it is important for universities and technical institutions to achieve the targeted employability skills in order to produce graduates who are ready to join the labor market.

Regarding English language teaching, the surrounded circumstances often lead to bad results, as for instance, laboratories in some English departments at Libyan

universities suffer from the lack of equipment and overcrowding due to the large numbers of students, these conditions prevent the implementation of theoretical content the students extensively learn in their syllabus. In addition, the Libya Organization of Policies and Strategies (LOOPS) <sup>12</sup> listed some obstacles that face the sector of Higher Education including the poor curricula and teaching methods, the universities unclear policy of implementation, the cheating in secondary school exams that produces students who are unable to pass the introductory courses at the university level, and theoretical exams that result in students poor ability to deal with the practical reality in their majors after graduation. Also the deficiency of the teaching staff members and other workers in terms of qualification, performance and number.

### **2.2. Changing the orientation: Transition to practicum and technology:**

As shown in the previous section, the desired change seems to be long-lasting. The thrill of analyzing a problem, detecting errors, experimenting solutions and finally watching that it has been solved successfully, brings to the researcher a joy of research, a desire to gain knowledge and apply activities to solve some of the most demanding problems faced by the English Language Teaching ELT in Libyan Higher Education environment. In this respect, the researcher as a teacher had the chance to build a new vision for a specific syllabus design to put its objectives in use through the application of a new technique (teaching instruction integrates theory, practice and technology using educational applications). According to Isman <sup>9, p. 209</sup> a technique is a body of technical methods or a method of accomplishing a desired aim. Chukwuere and Kuttikattu <sup>13</sup> adopted a narrative literature review (NLR) research approach to look at some academic materials determining their usage of mobile educational applications for their academic purposes. They concluded that university students invest a good amount of time using mobile educational applications to improve their academic performance. However, limited studies exist on the usage of mobile educational applications at the university level <sup>13</sup>.

### **2.3. Technology and language learning E506: General aims and intended outcomes:**

The course Technology and Language Learning E506 is offered to students in the last semester at the Department of English Language in Al.Marj Faculty of Sciences and Arts at Benghazi University. It was prepared and developed by the teacher (the researcher) in order to obtain the following general aims mentioned in the course description form:

- Teaching about educational technology.
- Teaching with educational technology.

- Integrating educational technology into the design and delivery of curricula.
- Engaging in research regarding the use and effects of educational technology in the teaching/learning process.

To achieve the ultimate goal of making balance between theoretical knowledge and practical implementations, the intended outcomes of this course are divided into four types (according to the course description template):

- Knowledge and Understanding. (theoretical)
- Intellectual Skills. (theoretical)
- Professional and Practical Skills. (practical)
- General and Transferable Skills. (practical)

The variety of modules ranging between lectures, small group discussions, applications and practical sessions, provides a good balance between theoretical and practical knowledge. The various projects of lesson planning, presentations on Google Slides, PowerPoint and Canva, browsing educational websites and experimenting online platforms provide students an opportunity to apply their theoretical knowledge in practical situations. The uniqueness of this subject lies in the fact that its modules focused on improving employability skills like lesson planning, lesson designing, lesson presenting and team working.

### 3. METHODOLOGY

The present study took place at the Department of English Language in Al.Marj Faculty of Arts and Sciences at Benghazi University. The department was established in 1990. It is Applied Linguistics general section that offers a variety of educational materials, including literature, language skills, linguistics, applied linguistics, translation and educational technology. All staff members in the department are Libyan. Some of them graduated from Benghazi University, others from the Libyan Academy, whereas the rest of the teaching staff members received their degrees from native-English speaking countries. The educational system of the department was based on academic year system for several years and then changed to semesters system, three months for each semester. Throughout this period students are required to complete specialized academic subjects, and then present graduation papers in order to be certified by Bachelor of Arts in English language.

#### 3.1 The study design

The study was carried out during regular lectures according to the department timetable, so that the students do not feel discomfort, and that they are under study. Within six months (two academic semesters) two groups of

students participated, each group was taught for three months using the same teaching strategies and educational technologies. Throughout this period the teacher (the researcher) used different types of tools to collect data and evaluate students. A descriptive research model was utilized. According to Lovell and Lawson<sup>5, p. 23</sup> it is "A type of educational research that concerned with both syllabus and curriculum reform and with an examination of the aims and methods" A variety of data collection instruments were adopted to insure the validity of this study, questionnaire, lesson plan templates to be filled by students and students' narratives feedback. The instruction used was based on making balance between theoretical and practical teaching methods using technology.

#### 3.2. Participants

The participants of this study were 47 eighth semester students studying in the Department of English Language in Al.Marj Faculty of Arts and Sciences at Benghazi University. They were about to graduate, and their ages range from 22 to 25 years old.

#### 3.3. Data collection and analysis

As mentioned above, three data collection instruments were used, questionnaire, lesson plan forms and narrative feedback. The questionnaire was distributed to students online through the private Telegram channel of the course. So that, students' responses were smoothly and confidently collected, 47 forms were submitted. The main purpose of using questionnaire in this study was to collect students' opinions about two subjects, firstly, their preference of theoretical or practical teaching. Secondly, their opinions about the practical sessions of the subject Technology and Language Learning E506. The questionnaire consisted of fifteen closed multiple choice questions, seven questions for the first subject and eight for the second. This questionnaire was created by the researcher and revised by a faculty member from Benghazi University and then modified in light of the feedback provided. Lesson plan templates also used as a tool for data collection to assess the students' performance after attending a workshop entitled (the lesson planner). A sample of 19 lesson plan templates were collected from students. The third instrument that used for data collection is narrative of student's feedback which is considered as a tool of reflection that teachers can use to observe and evaluate the way they behave in their classroom<sup>14</sup>, the researcher asked students to give feedback about the method used to deliver the subject Technology and Language Learning E506 as well as their opinions about the instruction they are experiencing. A Google Slides presentation was shared with 25 students to collect their feedback narratives, a total of 14 students commented on the slide.

The researcher depended on inductive content analysis to categorize the raw data into concepts. The technique involves reducing the raw data, grouping similar relevant

material under certain categories and then calculating the frequency of the students' responses <sup>15</sup>. The findings of this study were divided into two main themes, the discrepancy between the prevailing teaching style and the type of education desired by students, and students' opinions and performance in practical classes.

#### 4. FINDINGS AND DISCUSSION

##### 4.1. The discrepancy between the prevailing teaching style and the type of education desired by students:

From the students' narratives, it is concluded that their educational experience was based on enhancing theoretical knowledge. Whereas practical implementation is considered to be new for them. This determines the type of teaching method dominated at the Department of English Language in A.Marj Faculty of Arts and Sciences which is traditional lecturing. Some of students' narratives about the instructional change that they have experienced with practicum and technology reflected their desire to develop some practical skills, they stated:

Student (13)

*We as graduate students and students of the English language need to have a skill in studying and teaching. Mastering the language is practical and not theoretical....*

Student (12)

*It was a new and special method...This experience taught me a lot through the new teaching, unlike ever before...*

Student (11)

*I had the opportunity to know a new teaching method...one of the useful methods...it is not just depend on the method itself, but on the teacher...*

Student (7)

*...the old methods are no longer contemporary with educational technology*

Data in table (1) below answered the research question about teaching style preference, a good number of students prefer to be taught using a mixed teaching method that contains both theoretical knowledge and practical experience. From their humble experience attending some practical classes, students tend to choose equality and balance between practical and theoretical classes. Only five participants from the forty-seven prefer to be taught theoretically.

**Table (1): Teaching Style Preference**

Teaching Style Preference	Students' Number	Percentage
Theoretical	5	10.64 %
Practical	12	25.53 %
Mixed	30	63.83 %

In addition to the above data, the majority of the participants (97.87%) stated that some theoretical subjects they are learning need to be supported by working on projects, and that (72.34 %) of them like to work in groups not individually, as well as (68.09%) strongly agreed that doing projects facilitates learning. The data in table (2) shows students' preference of working on presentations.

**Table (2): Project Type Preference**

Project Types	Students' Number	Percentage
Presentation	26	55.32 %
Assignment	5	10.64 %
Portfolio	7	14.89 %
Research Paper	9	19.15 %

According to the students' responses, subjects that need to be supported by practical classes are as follows:

**Table (3): Subjects need practical support**

Subject	Number of Students	Percentage
Listening	25	13.23 %
Translation	20	10.58 %
CALL	20	10.58 %
Speaking	20	10.58 %
Teaching Methodology	17	8.99 %
Phonetics and Phonology	15	7.94 %
Language Acquisition	13	6.88 %
Language Testing	11	5.82 %
Grammar	11	5.82 %
Writing	10	5.29 %
Semantics	8	4.23 %
Reading	8	4.23 %
Morphology and Syntax	6	3.17 %
Pragmatics	5	2.65 %

The table above illustrates two types of subjects that have been focused on by students to be supported by practical classes, subjects that teach language skills (e.g. listening, speaking and translation), and subjects that teach teaching skills (e.g. teaching methodology and computer assisted language learning (CALL)). This indicates the students understanding of their needs as future teachers. In addition, there is a considerable low percentage that goes to some linguistic subjects (e.g. morphology, syntax, semantics and pragmatics) apart from their importance in acquiring the language skills, students put these subjects at the end of the chart clarifying that some linguistic details might not carry the characteristic of being practical.

**4.2. Students' opinions and performance in practical classes:**

All the participants (100%) agreed that using technology in the language classroom is a top priority, they enjoyed working on educational applications (Google Slides, PowerPoint and Canva) and using AI tools (chatGPT) during Technology and Language Learning E506 classes. Mobile educational applications greatly impact the learning process and progress and make open access for all <sup>13</sup>.

The majority (91.49%) stated that workshops of the subject Technology and Language Learning E506 are valuable, they narrated that this method is a useful idea to know the appropriate techniques for each level, a pleasant way that facilitates lessons, a great environment to learn, and a distinctive method that will make a big difference in the future. (93.61%) of them will use technological devices that their teachers use. Table (4) below shows the types of devices used by teachers in this department:

**Table (4): Devices used by teachers**

Device	Number of students	Percentage
Projectors and laptops	34	72.34 %
Smart phones	13	27.66 %
Smart boards / screens	0	0 %

In addition, (89.36%) of the students think that using the internet might improve teaching and learning processes, some of them indicate that it is the best way to inform and receive information, they wrote:

Student (3):

*....communication and reminders of the details of lectures on social networking sites motivating the students to think outside the box and develop their creative thought...*

Student (10):

*Sending e-mails, add comments on it, doing a midterm exam Online, sharing exam scores by e-mail, and repeat what was said in the lectures on Telegram Channel....All of these methods helped and gave everyone of us the opportunity to receive information by interesting ways...*

Student (4):

*We did not worry about the midterm exam, as it was very interesting and we wished that the all exam materials were like this or in a similar way...*

Students' performance was also questioned after working on lesson plan templates, they showed a higher level of thinking, responsibility, and creativity while filling on the templates, they were excited to reach the intended goal of each activity, and their results were ranging from good to excellent.

**5. CONCLUSION**

It is obvious from the above data that practical activities and sessions e.g. workshops, small group discussions and working on projects are somewhat ignored in the study context, and the entire program relates itself to theory more than practice. This finding reflects the extent to which Higher Education in Libya is ineffective in terms of providing students with practical skills that they need for their future career. Despite their advanced level in this department some of the participants lack communication skills as well as teaching skills. This is due to several reasons including the department's policy in dealing with practical subjects, the absence of workshops and discussion seminars, and the lack of students' self-development. Students teachers need to revise and apply what they are learning, to seek new lines in teaching methods and techniques to cope with what is happening around the world, and to improve some skills that enrich their work (e.g. learning how to teach and doing action research). The role of technology in facilitating teaching and learning was focused on from the participants, as they presented preference to variation in using teaching and learning methods. In addition, the types of activities and tasks in practicum motivated students to communicate, work together and with teacher, improve language skills, integrate technology in teaching and learning, and perform better.

**5.1. Recommendations**

This study recommends that the current type of instruction may be changed by adding accredited practical classes for each course, and providing the required places, equipment and tools. The study also highlights that all the previous projections lead to the possibility of classifying courses of Applied Linguistics offered by Libyan Arts Faculties as continuing professional development programs for those in English language departments. On one hand,

this type of programs could be available in the evenings and weekends, and planned to be as practical as possible to provide students with opportunities to activate their knowledge by playing teacher roles in classroom-like environments, or through collaborations between Arts Faculties and schools in the frame of observational visits. In addition, these programs should supply effective use of communication technologies in teaching, especially now that the world is turning to digital education. As in-service training is not available for teachers in Libya, it would be better to provide students teachers with opportunities for pre-service professional development sessions during their active learning.

### 5.2. Acknowledgement

The researcher would like to express profound gratitude to eighth semester students (fall\spring semesters -2023) in the Department of English Language and Linguistics in Al.Marj Faculty of Arts and Sciences, whose dynamism, vision, sincerity and motivation have positively affected all aspects of the field study. As well as their contributions (opinions, responses and narratives) that have strongly supported the research by reliability and validity. Special thanks are also acknowledged to the Department of English Language and Linguistics in Al.Marj Faculty of Arts and Sciences for its help, support and flexibility in conducting scientific research.

## 6. REFERENCES

1. Harmer J. The Practice of English Language Teaching. 3rd edition. Longman; 2005.  
[https://openlibrary.org/works/OL4480543W/The\\_Practice\\_of\\_English\\_Language\\_Teaching?edition=key%3Abooks/OL7880916M](https://openlibrary.org/works/OL4480543W/The_Practice_of_English_Language_Teaching?edition=key%3Abooks/OL7880916M)
2. Wimberly High School. Benefits of practicum. Wimberly ISD. Accessed May 30, 2024.  
<https://www.wimberleyisd.net/Domain/8>
3. Halliday J. Markets, Managers and Theory in Education. The Falmer Press; 1990.  
[https://openlibrary.org/works/OL2830674W/Markets\\_managers\\_and\\_theory\\_in\\_education](https://openlibrary.org/works/OL2830674W/Markets_managers_and_theory_in_education)
4. Warnock HM. A Common Policy For Education. Oxford. Oxford University Press; 1988.  
[https://openlibrary.org/works/OL10619848W/A\\_common\\_policy\\_for\\_education](https://openlibrary.org/works/OL10619848W/A_common_policy_for_education)
5. Lovell K, Lawson KS. Understanding research in education. Hodder and Stoughton LTD; 1970.  
[https://openlibrary.org/works/OL6605585W/Understanding\\_research\\_in\\_education](https://openlibrary.org/works/OL6605585W/Understanding_research_in_education)
6. Balboni PE. A theoretical framework for language education and teaching. Cambridge Scholars Publishing; 2018.  
<https://e-journal.org/index.php/ejall/article/view/vol7-issue2-2020-2376905x-12-222>
7. Suweekar NA. Exploring the natural match between communicative and cooperative learning strategies. Global Libyan Journal. 2018; 40 (6):1-24.
8. Shafter ME, Ruth C. State of higher education in Libya: A game change administrative approach. Shanlax International Journal of Education.2020; 8(3):19-23.  
<https://www.files.eric.ed.gov/fulltext/EJ1256069.pdf>
9. Isman A. Technology and technique: An educational perspective. The Turkish Online Journal of Educational Technology. 2012; 11(2):207-213.  
<http://tojet.net/articles/v11i2/11222.pdf>
10. Alsanousi AM. The effect of higher education quality on economic growth in Libya. International Journal of Academic Research in Business and Social Sciences. 2017; 7(3):139-149.  
[https://www.knowledgewords.com/images/The\\_Effect\\_of\\_Higher\\_Education\\_quality\\_on\\_Economic\\_Growth\\_in\\_Libya.pdf](https://www.knowledgewords.com/images/The_Effect_of_Higher_Education_quality_on_Economic_Growth_in_Libya.pdf)
11. Brydan R, Abdulnabi M. Benefits of higher education internationalization in Libya: case study of Omar Al-Mukhtar University. Journal of Contemporary Business and Economic Studies. 2022; 5(2):11-25.  
[https://www.researchgate.net/publication/360291878\\_Students\\_Benefits\\_of\\_Higher\\_Education\\_Internationalization\\_In\\_Libya\\_Case\\_Study\\_of\\_Omar\\_Al-Mukhtar\\_University](https://www.researchgate.net/publication/360291878_Students_Benefits_of_Higher_Education_Internationalization_In_Libya_Case_Study_of_Omar_Al-Mukhtar_University)
12. The Libya Organization of Policies and Strategies (LOOPS). The reality of Higher Education in Libya; 2016.  
<https://www.mena-forum.com/need-rebuild-libya-higher-education-system/>
13. Chukwuere JE, Kuttikattu VJ. A narrative study on the usage of mobile educational applications by the university students. International Conference on Emerging Technology and Interdisciplinary Sciences (ICETIS). Jozak Publishers. 2021.  
<https://doi.org/10.57040/icetis.vi.3>
14. Widya T, Asri F, Santiana S. Students feedback as a tool for reflection: A narrative of an Indonesian pre-service teacher. Journal of Teaching and Learning English in Multicultural Contexts. 2020; 4(1): 1-11.  
<https://jurnal.unsil.ac.id/index.php/tlemc/article/view/1775/1170>
15. Flick U. An introduction to qualitative research. SAGE Publications Ltd. 2009.  
[https://elearning.shisu.edu.cn/pluginfile.php/35310/mod\\_resource/content/2/Research-Intro-Flick.pdf](https://elearning.shisu.edu.cn/pluginfile.php/35310/mod_resource/content/2/Research-Intro-Flick.pdf)

**Appendix****Questionnaire items****1. What type of teaching do you prefer?**

Theoretical \ Practical \ Mixture

**2. Do you occasionally have practical sessions or workshops in your department?**

Sometimes \ Rarely / Never

**3. Do you think that some theoretical subjects need to be supported by working on projects?**

Yes \ No / Sometimes

**4. What is your opinion about using technology inside the language classroom?**

The most important priority / A top priority / Not very important priority

**5. Do your instructors use technological devices in teaching?**

Yes / No / Some of them

**6. what type of technology do they use?**

Projectors / Laptops / Smart phones

**7. Do you exchange assignments online with teachers?**

Usually / Rarely / Never

**8. What do think about the practical sessions of the course Technology and Language learning E506?**

Extremely valuable / Somewhat valuable / Not so valuable

**9. Will you make efforts to use technology in your classes?**

Yes / No / Maybe

**10. Do you think that using the internet may improve teaching and learning processes?**

Yes / No / Sometimes

**11. Do you think that using technology might turn some boring theoretical material into interesting ones?**

Yes / No / Sometimes

**12. What are the courses that you think they must have practical sessions?**

Teaching methodology/Language Acquisition /Language Testing/CALL/Translation/

Semantics/Morphology and Syntax/Phonetics and Phonology/Pragmatics/Listening

Writing/Reading/Speaking/Grammar

**13. Do you like working on projects? In groups\ individually?**

In groups / Individually / I don't like working on projects

**14. What type of projects do you enjoy working on?**

Presentation / Assignment / Portfolio / Research paper

**15. Do you agree that making projects facilitates learning?**

Strongly agree / Neutral / Disagree

مجلة جامعة بنغازي العلمية

# Applied Sciences

1988

SJUOB



# Green Hydrogen Production from Seawater Using Metal Oxide Catalysts

Hamdy AB. Matter <sup>1\*</sup>- Tariq M. Ayad <sup>1</sup>

*1 Department Chemistry- Faculty Arts and science/El-Wahat – University of Benghazi.*

Received: 01 / 03 / 2024; Accepted: 02 / 04 / 2024

## ABSTRACT

In this work, five electrodes were studied to produce green hydrogen (GH) versus the graphite electrode (as a positive electrode). The electrodes are Fe, Cu, Al, Zn, and Pb. It was found that Zn electrode produces the most hydrogen from seawater, then Pb, the least ones are Fe, Cu, and Al. Oxides (Cu<sub>2</sub>O, Cr<sub>2</sub>O<sub>3</sub>, V<sub>2</sub>O<sub>5</sub>, ZnO, SnO<sub>2</sub>, Pb<sub>3</sub>O<sub>4</sub>, NiO, MnO<sub>2</sub>, Fe<sub>3</sub>O<sub>4</sub>, and SiO<sub>2</sub>) were used and added at a fixed concentration to the five electrodes, and the extent of the effect of these oxides on the production of GH were studied. Some of them were inhibitory, some were a helpful factor and worked to stimulate the production of GH, and some had no effect. However, most oxides inhibit hydrogen production at the Al electrode, most of them did not affect H<sub>2</sub> production at the Fe and Cu electrodes, while oxides such as ZnO, SnO<sub>2</sub>, Pb<sub>3</sub>O<sub>4</sub>, NiO, MnO<sub>2</sub>, and Fe<sub>3</sub>O<sub>4</sub> showed an increase in H<sub>2</sub> production at the zinc electrode. On the contrary, V<sub>2</sub>O<sub>5</sub>, SnO<sub>2</sub>, and SiO<sub>2</sub>, were found to increase H<sub>2</sub> production at the zinc and Pb electrodes.

**KEYWORDS:** metal oxides - Huffman voltammeter - sea water - catalysts - green hydrogen.

## 1. INTRODUCTION

Electrolysis is used to produce green hydrogen (GH) and is considered an environmentally friendly solution to reduce carbon emissions and preserve the environment. GH is produced through the electrolysis of freshwater supported by renewable energy systems to reduce the emission of CO<sub>2</sub> gases. Therefore, a large amount of freshwater is used to produce H<sub>2</sub> at the cathode and O<sub>2</sub> at the anode. It is preferable to use seawater because it is the most abundant water source. However, the obstacles are the reaction of unwanted chlorine gas at the anode and the resulting corrosion. The development of effective chemical catalysts of oxides for non-precious metals with industrial current density is important for the production of H<sub>2</sub> from acidic or alkaline water/seawater in order to alleviate the energy crisis and environmental pollution. Hydrogen is considered a promising source of renewable and green energy to meet energy needs and achieve the prevention of carbon dioxide emissions. It is, therefore, preferable to use abundant and relatively cheap seawater as opposed to fresh water. However, the production of highly effective and efficient chemical and electrocatalysts with long-term viability under harsh corrosive conditions remains a challenging topic for large-scale seawater electrolysis technology.

Transition metal electrocatalysts for hydrogen production fall into four different classes, namely alloys, layered double hydroxides (LDHs), transition metal dichalcogenides (TMDs), and single-atom catalysts (SACs) <sup>[1]</sup>. Pt-MoP-MoO<sub>3</sub>/C an efficient electro-photo catalyst was constructed to enhance Pt catalytic capacity via the uniform integration of Pt nanoparticles and MoP on carbon black (Vulcan-C), in which Vulcan-C was used as a support material <sup>[2]</sup>. Ga doped Co<sub>0.6</sub>Cu<sub>0.4</sub>Fe<sub>2</sub>O<sub>4</sub> nano catalysts was fabricated via sol-gel auto-combustion (SGA) for the production of GH generation <sup>[3]</sup>. Ni species were deposited as a single atom onto TiO<sub>2</sub>/g-C<sub>3</sub>N<sub>4</sub> (TCN) composite photocatalyst with an S-scheme heterojunction to produce H<sub>2</sub> <sup>[4]</sup>. Alloy, noble metals, transition metals, carbides, oxides, nitrides, phosphides, synthesis of novel catalysts, and especially the design for seawater electrolysis are prospected <sup>[5]</sup>. Rare earth compounds, N-doped carbon and bimetallic carbide were demonstrated to accelerate the H<sub>2</sub> evolution process in acid-base electrolytes and seawater <sup>[6]</sup>. A carbon-based composite photocatalyst (CQM) was fabricated for photocatalytic production of H<sub>2</sub>O<sub>2</sub>. The metal ions strongly affect the photocatalytic activity of the CQM catalyst with the order of Mg<sup>2+</sup>> Al<sup>3+</sup>> Ca<sup>2+</sup>> K<sup>+</sup> <sup>[7]</sup>. Cr-Cu<sub>2</sub>S Nanoflakes supported on Cu-foam (Cr-Cu<sub>2</sub>S-CF) for alkaline water electrolyze for H<sub>2</sub> production at an industrial scale <sup>[8]</sup>. In addition, Ni-doped WO<sub>2</sub> was proposed to realize H<sub>2</sub> production from seawater, Ni doping can enhance the H<sub>2</sub> evolution reaction activity of WO<sub>2</sub> with excellent inhibitor corrosion <sup>[9]</sup>. A ternary Pt, Ru, and Ti (PRT) catalyst with a minimized Pt level

\*Correspondence: Hamdy AB. Matter

[hamdy.matter@uob.edu.ly](mailto:hamdy.matter@uob.edu.ly)

(Pt<sub>0.06</sub>Ru<sub>0.24</sub>Ti<sub>0.70</sub>O<sub>x</sub>) drives chloride oxidation reaction (CIOR) at a Faradaic efficiency (FE) of ~100% in saline water at current density <sup>[10]</sup>. Co/W5N4 catalyst with porous structure is innovatively constructed <sup>[11]</sup>. The self-supporting electrode is prepared by in-situ growth of nickel and boron on porous hydrophilic filter paper (HP) via mild electroless plating at 298 K <sup>[12]</sup>. Indeed, the existence of various ions in seawater is a barrier to efficient H<sub>2</sub> production via photocatalytic splitting <sup>[13]</sup>. Co/Co<sub>9</sub>S<sub>8</sub> electrocatalyst with hollow spherical structure. As-prepared material exhibited excellent electrocatalytic activity in H<sub>2</sub> evolution reaction (HER) in alkaline seawater <sup>[14]</sup>. A bifunctional Ni foam supported NiFe<sub>2</sub>O<sub>4</sub> was as spinel catalyst (i.e., NiFe<sub>2</sub>O<sub>4</sub>/NF) that is capable of facilitating the coupling of (HER) with selective methanol oxidation reaction (SMOR) in seawater to produce format via a CO-free pathway <sup>[15]</sup>. N and P doped carbon nanoparticles decorated with tiny amounts of Pt nanoparticles (~6.0 wt%) were synthesized and investigated for the catalytic performances to H<sub>2</sub> and Cl<sub>2</sub> generation from fresh and seawater <sup>[16]</sup>. Moreover, strong metal-support interaction (SMSI) and Pt-p-block alloys (PtM-CNT, M = Ga, In, Pb, and Bi) to construct a stable electronic perturbation and achieve acidic seawater H<sub>2</sub> evolution <sup>[17]</sup>. CoSe<sub>2</sub>-CoO/CF catalysts are prepared by a simple electrodeposition method <sup>[18]</sup>. Carbon-encapsulated Pt was fabricated core-shell supported CoMo<sub>2</sub>S<sub>4</sub>-NGNF as an efficient electrocatalyst for the H<sub>2</sub> evolution reaction (HER) <sup>[19]</sup>. The unique 3D nanorose structure and the optimized electronic structure of the heterostructure enable Ni<sub>2</sub>P/Co(PO<sub>3</sub>)<sub>2</sub>/NF super-hydrophilic and super-aerophobic characteristics, and highly facilitate (HER) kinetics in alkaline seawater <sup>[20]</sup>. P-Ni<sub>4</sub>Mogrow on the surface of the copper foam (CF) substrate to synthesize an efficient seawater electrolysis catalyst (P-Ni<sub>4</sub>Mo/CF) <sup>[21]</sup>. Se/NiSe<sub>2</sub> was developed to exhibit energy saving for alkaline seawater splitting in urea <sup>[22]</sup>. A highly conjugative  $\pi$ -acceptor type ligand with metal ions (M = Co<sup>2+</sup>, Zn<sup>2+</sup>, Cu<sup>2+</sup> and Ni<sup>2+</sup>) was used as a catalyst for the evolution of H<sub>2</sub> as alternate fuel <sup>[23]</sup>. Ru, P dual-doped NiMoO<sub>4</sub> multichannel nanorods in situ grown on nickel foam (Ru/P-NiMoO<sub>4</sub>-NF), which can achieve chlorine-free H<sub>2</sub> production <sup>[24]</sup>. High-performance catalysts were designed for seawater electrolysis <sup>[25]</sup>. Wind energy is used for the electrolysis method used in H<sub>2</sub> production <sup>[26]</sup>. An Egyptian Atlas for GH production utilizing water electrolysis powered by the available wind (wind turbines, WTs) and solar (PV panels) energies <sup>[27]</sup>. Offshore Wind Technology (OWF) was used for H<sub>2</sub> production through water electrolysis, as well as the storage and transportation of the produced H<sub>2</sub> for use in H<sub>2</sub> fuel stations <sup>[28]</sup>. The reaction between metal scrap and steam is studied for H<sub>2</sub> production, the scrap materials are used as nanomaterials in the generation of GH, and the production pathways for nanomaterials have also been addressed <sup>[29]</sup>. The most

significant challenge in the thermally driven reaction is finding a metal oxide that can be reduced at practical temperatures with acceptable reaction kinetics, whereas, the most important challenge for photocatalytic reactions is to find a stable semiconductor-based material capable of splitting water using a large fraction of sunlight <sup>[30]</sup>. Metal-oxide electrocatalysts, including noble metal oxides, non-noble metal oxides and their compounds, and spinel- and perovskite-type oxides, for seawater splitting. We elucidate their chemical properties, excellent the oxygen evolution reaction OER selectivity, <sup>[31]</sup> the nonmetallic electrode is made of surface rock portions that have high porosity and pore volume and high permeability and pore connectivity and is saturated with saline water. Surface rocks with the above properties exhibit very low resistivity and hence conduct electricity like metallic electrodes <sup>[32]</sup>, the Novel Solution. A low-cost but powerful solution to the corrosion problem is introduced, tested, and experimentally proved. The novelty of the solution relies on replacing the classic special high-cost metallic positive electrode with a nonmetallic, no-cost, one. The nonmetallic electrode is made of surface rock portions that have high porosity and pore volume and high permeability and pore connectivity and is saturated with saline water. Surface rocks with the above properties exhibit very low resistivity and hence conduct electricity like metallic electrodes. The voltage and the current conducted by such electrodes are controlled by the electrode geometry.

In this work, five electrodes were studied to produce GH versus the graphite electrode (as a positive electrode). The electrodes are Fe, Cu, Al, Zn, and Pb. It was found that the Zn electrode produces the most H<sub>2</sub> from seawater.

## 2. THE EXPERIMENT

### 2.1. Materials and Chemicals:

Five different electrodes 3cm in length and 2ml diameter (0.1cm<sup>2</sup>) for product H<sub>2</sub> (Fe, Cu, Al, Zn and Pb) against graphite electrode at Hoffman Voltammeter (Picture 1) with modified the cathode electrode to put 1g of 10 metal oxides as the catalyst: Cuprous oxide (Cu<sub>2</sub>O), Chromium (III) oxide (Cr<sub>2</sub>O<sub>3</sub>), Vanadium pentoxide (V<sub>2</sub>O<sub>5</sub>), Zinc oxide (ZnO), Stannic oxide (SnO<sub>2</sub>), Red lead oxide (Pb<sub>3</sub>O<sub>4</sub>), Nickel oxide (NiO), Manganese dioxide (MnO<sub>2</sub>) black iron oxide (Fe<sub>3</sub>O<sub>4</sub>), and Silicon Oxide (SiO<sub>2</sub>) are used, 3.5% NaCl as seawater electrolyte solution, DC electric source.



Picture 1: Hoffman Voltammeter

2.2. Method

The Huffman voltmeter is connected to a 5–12-Volt direct current source with different electrodes without adding a catalyst and measuring the amount of H<sub>2</sub> produced. Then, after an hour, add a specific concentration of the catalyst and measure the percentage of H<sub>2</sub> produced at the same time, with the same electrodes, and change the catalysts. The volumes of H<sub>2</sub> gas produced were as in the following table:

Table 1. The volume by ml of H<sub>2</sub> product /h.cm<sup>2</sup> at different electrodes with ten metal oxides.

C/H <sub>2</sub>	nil	Cu <sub>2</sub> O	Cr <sub>2</sub> O <sub>3</sub>	V <sub>2</sub> O <sub>5</sub>	ZnO	SnO <sub>2</sub>	Pb <sub>3</sub> O <sub>4</sub>	NiO	MnO <sub>2</sub>	Fe <sub>3</sub> O <sub>4</sub>	SiO <sub>2</sub>
Fe	8 ml	5	6.5	3.1	8	8	3	1	2.5	7	7
Cu	11.2	10	14.5	12	13.7	8	13.2	14	13.4	12.5	13.2
Al	20	11	6	2.5	13	10	7	4.3	8.5	5.5	17.5
Zn	42	7	30	5	60	60	58	57	60	57	28.2
Pb	36	28	31	59	26	56.3	8	40	42.3	14.3	60

3. RESULTS AND DISCUSSION

Fig. 1 depicts the sequence of electrodes that yield the highest hydrogen (H<sub>2</sub>) production without the utilization of oxides as catalysts or inhibitors. These electrodes are ranked as follows: Zn, Pb, Al, Cu, and Fe. Additionally, it is observed that Cu<sub>2</sub>O functions as an inhibitor of H<sub>2</sub> production at the Zn electrode, with its inhibitory effect diminishing progressively at the Pb and Al electrodes, and being least pronounced at the Cu and Fe electrodes.

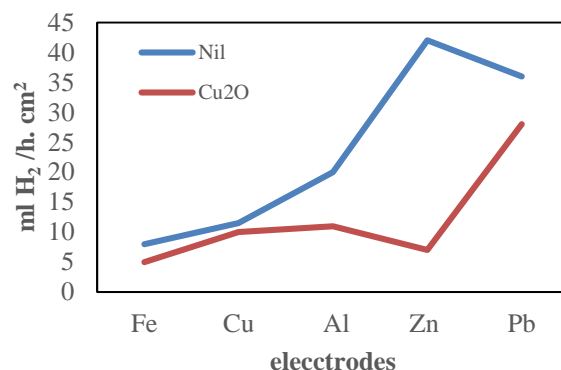


Fig.1. The effect of Cu<sub>2</sub>O for production of H<sub>2</sub> at electrodes.

Figure 2 illustrates that Cr<sub>2</sub>O<sub>3</sub> serves as an inhibitor of hydrogen (H<sub>2</sub>) production at the aluminum (Al) electrode. Conversely, its impact is less pronounced at zinc (Zn) and lead (Pb) electrodes, and it has no effect on copper (Cu) and iron (Fe) electrodes.

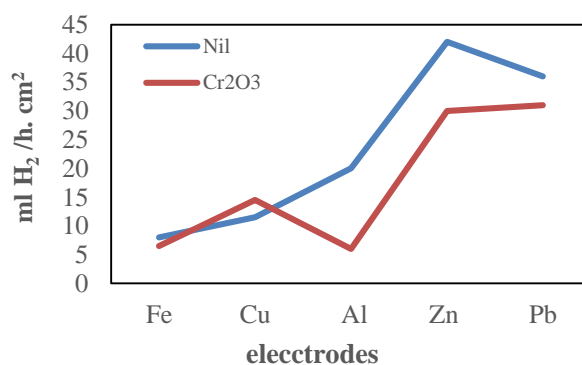
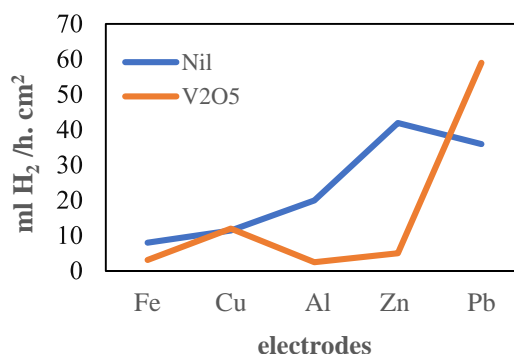


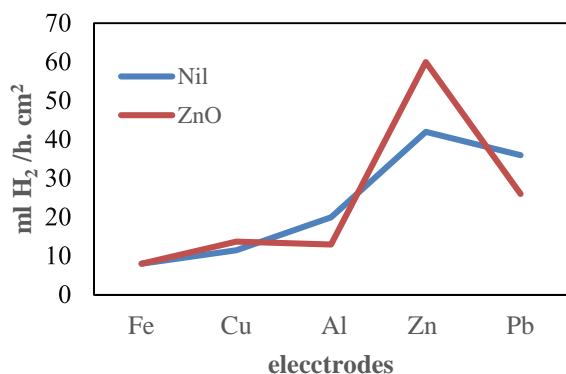
Fig.2. The effect of Cr<sub>2</sub>O<sub>3</sub> on the production of H<sub>2</sub> at electrodes.

Fig. 3 demonstrates that V<sub>2</sub>O<sub>5</sub> functions as a catalyst for hydrogen (H<sub>2</sub>) production at the lead (Pb) electrode. Conversely, it acts as an inhibitor for H<sub>2</sub> production at the zinc (Zn) and aluminum (Al) electrodes, while it has no effect on H<sub>2</sub> production at the copper (Cu) and iron (Fe) electrodes.



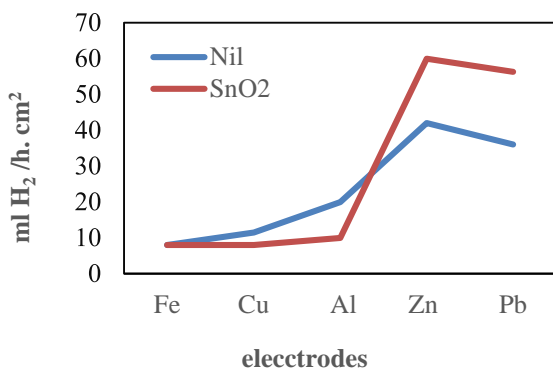
**Fig.3. The effect of V2O5 on the production of H2 at electrodes.**

Fig. 4 illustrates that ZnO serves as a catalyst for hydrogen (H2) production specifically at the zinc (Zn) electrode. However, it does not exert any influence on H2 production at the lead (Pb), aluminum (Al), copper (Cu), and iron (Fe) electrodes.



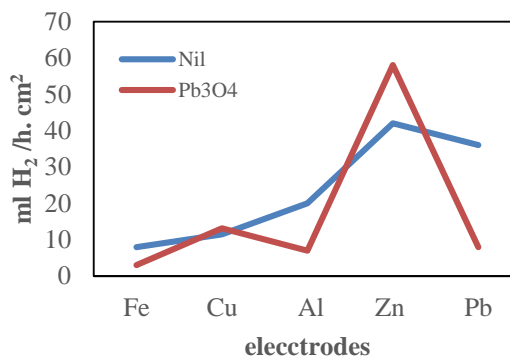
**Fig.4. The effect of ZnO on the production of H2 at electrodes.**

Fig. 5 displays that SnO2 functions as a catalyst for hydrogen (H2) production at both the lead (Pb) and zinc (Zn) electrodes. Conversely, it acts as an inhibitor at the aluminum (Al) electrode and has no effect on H2 production at the copper (Cu) and iron (Fe) electrodes.



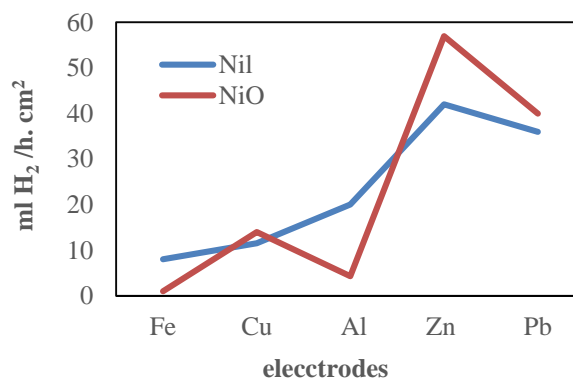
**Fig.5. The effect of SnO2 on the production of H2 at electrodes.**

Fig. 6 demonstrates that Pb3O4 serves as an inhibitor of hydrogen (H2) production at both the lead (Pb) and aluminum (Al) electrodes. Conversely, it acts as a catalyst at the zinc (Zn) electrode and has no effect on H2 production at the copper (Cu) and iron (Fe) electrodes.



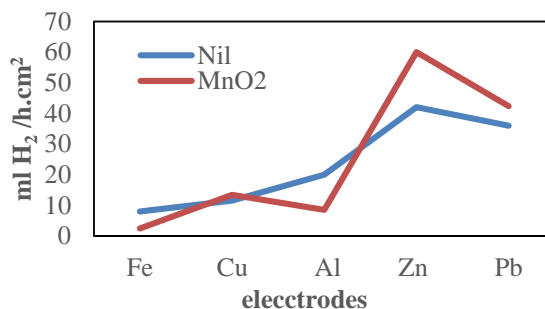
**Fig.6. The effect of Pb3O4 on the production of H2 at electrodes.**

Fig. 7 illustrates that NiO functions as an inhibitor of hydrogen (H2) production specifically at the aluminum (Al) electrode. Conversely, it acts as a catalyst at the zinc (Zn) electrode and does not affect H2 production at the copper (Cu) and iron (Fe) electrodes.



**Fig.7. The effect of NiO on the production of H2 at electrodes.**

Fig. 8 demonstrates that MnO2 serves as an inhibitor of hydrogen (H2) production specifically at the aluminum (Al) electrode. Conversely, it acts as a catalyst for H2 production at the zinc (Zn) electrode and has no effect on H2 production at the lead (Pb), copper (Cu), and iron (Fe) electrodes.



**Fig.8. The effect of MnO2 on the production of H2 at electrodes.**

Fig. 9 demonstrates that Fe3O4 serves as an inhibitor of hydrogen (H2) production specifically at the aluminum (Al) electrode. Conversely, it acts as a catalyst for H2 production at the zinc (Zn) electrode and has no effect on H2 production at the lead (Pb), copper (Cu), and iron (Fe) electrodes.

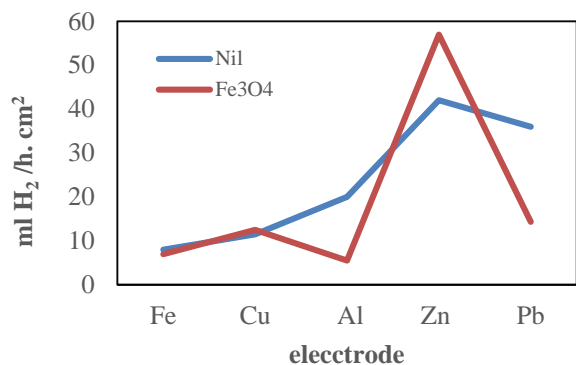


Fig.9. The effect of Fe3O4 on the production of H2 at electrodes.

Fig. 10 illustrates that SiO2 acts as a catalyst for hydrogen (H2) production specifically at the lead (Pb) electrode. Conversely, it functions as an inhibitor at the zinc (Zn) electrode and has no effect on H2 production at the aluminum (Al), copper (Cu), and iron (Fe) electrodes.

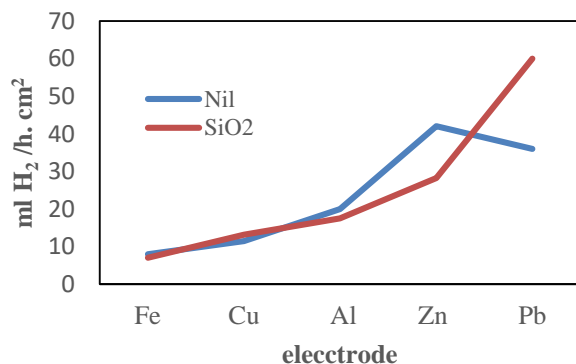


Fig.10. The effect of SiO2 on the production of H2 at electrodes.

Fig. 11 illustrates that the metal oxides NiO, MnO2, Pb3O4, V2O5, Cu2O, and Cr2O3 function as inhibitors at the iron (Fe) electrode. On the other hand, ZnO, SnO2, Fe3O4, and SiO2 have no effect on the Fe electrode.

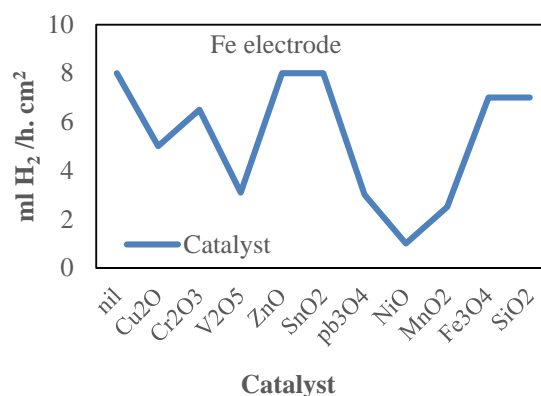


Fig.11. The effect of metal oxides at Fe electrode.

Figure 12 demonstrates that the metal oxides SnO2 and Cu2O act as inhibitors at the copper (Cu) electrode, whereas ZnO, Fe3O4, Cr2O3, NiO, MnO2, Pb3O4, V2O5, and SiO2 exhibit relatively weak effects at the Cu electrode.

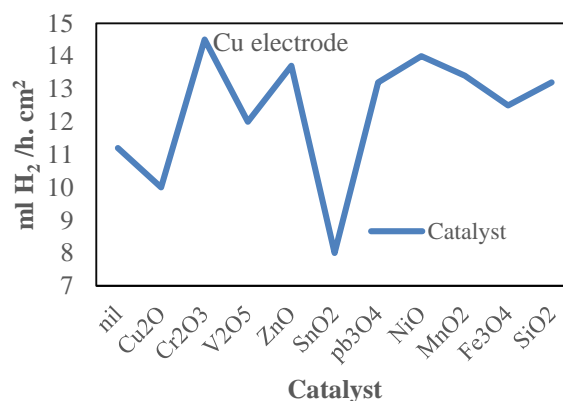


Fig.12. The effect of metal oxides at Cu electrode.

Fig. 13 illustrates that the metal oxides V2O5, NiO, Cr2O3, Fe3O4, Cu2O, MnO2, Pb3O4, SnO2, ZnO, and SiO2 act as inhibitors at the aluminum (Al) electrode.

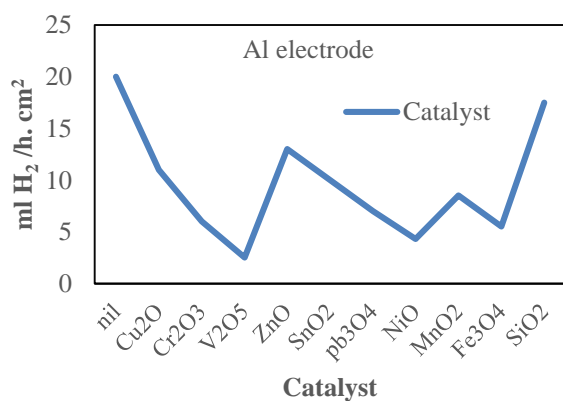


Fig.13. The effect of metal oxides at Al electrode.

Fig. 14 demonstrates that the metal oxides V2O5, Cu2O, Cr2O3, and SiO2 act as inhibitors at the zinc (Zn) electrode. Conversely, ZnO, SnO2, Fe3O4, Pb3O4, NiO, and MnO2 serve as good catalysts for the production of GH.

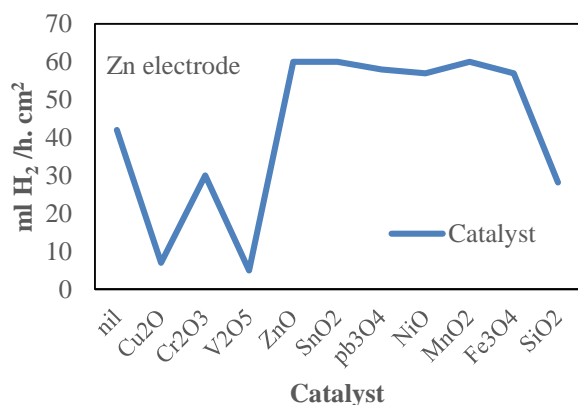


Fig.14. The effect of metal oxides at Zn electrode.

Fig. 15 illustrates that the metal oxides Pb3O4, Fe3O4, ZnO, Cu2O, Cr2O3, and SiO2 act as inhibitors at the lead (Pb) electrode. Conversely, SiO2, SnO2, V2O5, NiO, and MnO2 serve as good catalysts for the production of GH.

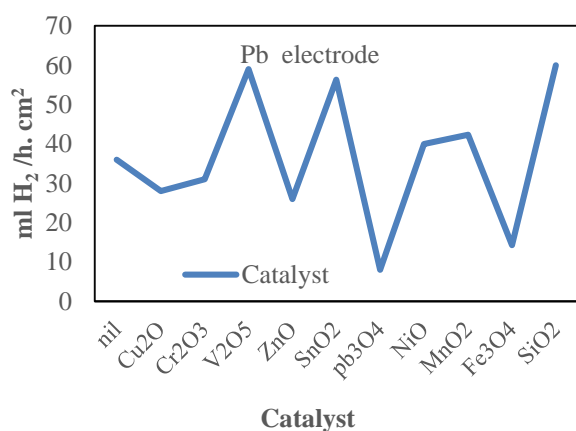


Fig.15. The effect of metal oxides at Pb electrode.

#### 4. CONCLUSION

It was possible to produce GH in quantities exceeding normal production from seawater using zinc and lead electrodes in the presence of catalysts, such as oxides of ZnO, SnO2, pb3O4, NiO, MnO2 and Fe3O4at the zinc electrode, as well as oxides of V2O5, SnO2 and SiO2 at Pb electrode. They showed an increase in H2 production.

#### 5. REFERENCES

1. Kwon HR, Park H, Jun SE, Choi S, Jang HW. High performance transition metal-based electrocatalysts for GH production. *Chem Commun.* 2022. <https://doi.org/10.1039/D2CC02423C>.
2. Peng J, Shi Y, Xiao Z, Ye Y, Li Z, Lin S. Promotional effects of MoP on its efficient electro-photo catalysis of Pt-MoP-MoO<sub>3</sub>/C catalyst for hydrogen evolution. *Mater Res Bull.* 2023;166:112341. <https://doi.org/10.1016/j.materresbull.2023.112341>
3. Kotwal P, Jasrotia R, Nidhi AV, Ahmed J, Thakur S, Kandwal A, et al. Photo/electro catalytic GH production promoted by Ga modified Co<sub>0</sub>. 6Cu<sub>0</sub>. 4Fe<sub>2</sub>O<sub>4</sub> nano catalysts. *Environ Res.* 2023;117669. <https://doi.org/10.1016/j.envres.2023.117669>
4. Yang S, Wang K, Chen Q, Wu Y. Enhanced photocatalytic hydrogen production of S-scheme TiO<sub>2</sub>/g-C<sub>3</sub>N<sub>4</sub> heterojunction loaded with single-atom Ni. *J Mater Sci Technol.* 2024;175:104-114. <https://doi.org/10.1016/j.jmst.2023.07.044>
5. Feng C, Chen M, Yang Z, Xie Z, Li X, Li S, et al. Electrocatalytic seawater splitting for hydrogen production: recent progress and future prospects. *J Mater Sci Technol.* 2023. <https://doi.org/10.1016/j.jmst.2023.03.058>
6. Liu J, Song X, Gao S, Chen F, Lang X, Zhang T, et al. Collaborative coupling catalytic interface enabling efficient hydrogen evolution in universal-pH electrolytes and seawater. *Int J Hydrogen Energy.* 2023. <https://doi.org/10.1016/j.ijhydene.2023.11.128>
7. Li J, Shi H, Li Z, Wang J, Si H, Liao F, et al. Interaction of metal ions in high efficiency seawater hydrogen peroxide production by a carbon-based photocatalyst. *Appl Catal B Environ.* 2023;123541. <https://doi.org/10.1016/j.apcatb.2023.123541>
8. Trivedi N, Joshi KK, Siraj S, Sahatiya P, Patel V, Sumesh CK, et al. Self-supported Cr-Cu<sub>2</sub>S nanoflakes for hydrogen production from seawater. *Int J Hydrogen Energy.* 2023. <https://doi.org/10.1016/j.ijhydene.2023.11.036>
9. Liang W, Zhou M, Lin X, Xu J, Dong P, Le Z, et al. Nickel-doped tungsten oxide promotes stable and efficient hydrogen evolution in seawater. *Appl Catal B Environ.* 2023;325:122397. <https://doi.org/10.1016/j.apcatb.2023.122397>
10. Liang NN, Han DS, Park H. Membraneless unbuffered seawater electrolysis for pure hydrogen production using PtRuTiO<sub>x</sub> anode and MnO<sub>x</sub> cathode pairs. *Appl Catal B Environ.* 2023;324:122275. <https://doi.org/10.1016/j.apcatb.2022.122275>
11. Geng S, Chen L, Kang L, Li R, Chen H, Cheng L, et al. Synergistic dp Hybridized Co/W<sub>5</sub>N<sub>4</sub> Heterostructure Catalyst for Industrial Alkaline Water/Seawater Hydrogen Evolution. *Appl Catal B Environ.* 2023;123486. <https://doi.org/10.1016/j.apcatb.2023.123486>

12. Zhou Z, Liang R, Weng S, Lei F, Qian Y, Yang Z, et al. Construction of filterable and intelligent flexible NiB-Based catalytic electrode toward efficient overall seawater splitting. *Appl Surf Sci.* 2023;640:158415. <https://doi.org/10.1016/j.apsusc.2023.158415>
13. Hassan IU, Naikoo GA, Salim H, Awan T, Tabook MA, Pedram MZ, et al. Advances in photochemical splitting of seawater over semiconductor nano-catalysts for hydrogen production: A critical review. *J Ind Eng Chem.* 2023. <https://doi.org/10.1016/j.jiec.2023.01.006>
14. Li J, Sun J, Meng X. Spherical Co/Co<sub>9</sub>S<sub>8</sub> as electrocatalyst for hydrogen production from alkaline solution and alkaline seawater. *Int J Hydrogen Energy.* 2023. <https://doi.org/10.1016/j.ijhydene.2023.04.175>
15. Du X, Tan M, Wei T, Kobayashi H, Song J, Peng Z, et al. Highly efficient and robust nickel-iron bifunctional catalyst coupling selective methanol oxidation and freshwater/seawater hydrogen evolution via CO-free pathway. *Chem Eng J.* 2023;452:139404. <https://doi.org/10.1016/j.cej.2022.139404>
16. Huang Y, Seo KD, Jannath KA, Park DS, Shim YB. Heteroatoms doped carbon decorated with tiny amount Pt nanoparticles as a bifunctional catalyst for hydrogen and chlorine generation from seawater. *Carbon.* 2022;196:621-632. <https://doi.org/10.1016/j.carbon.2022.05.017>
17. Nie N, Zhang D, Wang Z, Ge S, Gu Y, Yang B, et al. Stable p-block metals electronic perturbation in PtM- CNT (M= Ga, In, Pb and Bi) for acidic seawater hydrogen production at commercial current densities. *Appl Catal B Environ.* 2022;322:122100. <https://doi.org/10.1016/j.apcatb.2022.122100>
18. Feng S, Rao P, Yu Y, Li J, Deng P, Kang Z, et al. Self-assembled Heterojunction CoSe<sub>2</sub>- CoO Catalysts for Efficient Seawater Electrolysis. *Electrochim Acta.* 2023;142870. <https://doi.org/10.1016/j.electacta.2023.142870>
19. Vijayapradeep S, Logeshwaran N, Ramakrishnan S, Kim AR, Sampath P, Kim DH, et al. Novel Pt-carbon core-shell decorated hierarchical CoMo<sub>2</sub>S<sub>4</sub> as efficient electrocatalysts for alkaline/seawater hydrogen evolution reaction. *Chem Eng J.* 2023;145348. <https://doi.org/10.1016/j.cej.2023.145348>
20. Zhang M, Chen WZ, Liu Z, He J, Wang YQ. Super-hydrophilic/super-aerophobic Ni<sub>2</sub>P/Co (PO<sub>3</sub>)<sub>2</sub> heterostructure for high-efficiency and durable hydrogen evolution electrocatalysis at large current density in alkaline fresh water, alkaline seawater and industrial wastewater. *Int J Hydrogen Energy.* 2023;48(47):17783-17800. <https://doi.org/10.1016/j.ijhydene.2023.01.238>
21. Li G, Feng S, Li J, Deng P, Tian X, Wang C, et al. P-Ni<sub>4</sub>Mo Catalyst for Seawater Electrolysis with High Current Density and Durability. *Chin J Struct Chem.* 2022;41(7):2207068-2207073. <https://doi.org/10.14102/j.cnki.0254-5861.2022-0110>
22. Khatun S, Roy P. Mott-Schottky heterojunction of Se/NiSe<sub>2</sub> as bifunctional electrocatalyst for energy efficient hydrogen production via urea assisted seawater electrolysis. *J Colloid Interface Sci.* 2023;630:844-854. <https://doi.org/10.1016/j.jcis.2022.10.149>
23. Gladis EE, Nagashri K, Joseph J. Transition metal chelates with multifunctional 1, 10-phenanthroline derivative towards production of hydrogen as alternative fuel from sea water: Design, synthesis, characterization and catalytic studies. *Int J Hydrogen Energy.* 2021;46(9):6573-6587. <https://doi.org/10.1016/j.ijhydene.2020.11.206>
24. Guo L, Chi J, Zhu J, Cui T, Lai J, Wang L. Dual-doping NiMoO<sub>4</sub> with multi-channel structure enable urea-assisted energy-saving H<sub>2</sub> production at large current density in alkaline seawater. *Appl Catal B Environ.* 2022;320:121977. <https://doi.org/10.1016/j.apcatb.2022.121977>
25. Zhang F, Yu L, Wu L, Luo D, Ren Z. Rational design of oxygen evolution reaction catalysts for seawater electrolysis. *Trends Chem.* 2021;3(6):485-498. <https://doi.org/10.1016/j.trechm.2021.03.003>
26. Emeksiz C, Tan M. An innovative adaptive hybrid prediction model based on deep learning methods (CEEMDAN-GRU) for GH production, In case study: Turkey. *Int J Hydrogen Energy.* 2023. <https://doi.org/10.1016/j.ijhydene.2023.11.026>
27. Nasser M, Hassan H. Egyptian GH Atlas based on available wind/solar energies: Power, hydrogen production, cost, and CO<sub>2</sub> mitigation maps. *Int J Hydrogen Energy.* 2023. <https://doi.org/10.1016/j.ijhydene.2023.09.127>
28. Akdağ O. The operation and applicability to hydrogen fuel technology of GH production by water electrolysis using offshore wind power. *J Clean Prod.* 2023;425:138863. <https://doi.org/10.1016/j.jclepro.2023.138863>
29. Müller LA, Leonard A, Trotter PA, Hirmer S. GH production and use in low-and middle-income countries: A least-cost geospatial modelling approach applied to Kenya. *Appl Energy.* 2023;343:121219. <https://doi.org/10.1016/j.apenergy.2023.121219>



# The Sardar sub-equation technique for obtaining some optical solitons of cubic nonlinear Schrödinger equation involving beta derivatives with Kerr law nonlinearity

Abdulmalik A. Altwaty <sup>1\*</sup> - Jaffalah J. Amhalhil <sup>2</sup> - Ahmed El Sakori <sup>1</sup> - Ngla F. Meriki <sup>1</sup>

<sup>1</sup> Department of Mathematics, Faculty of Arts & Science, University of Benghazi, Al Marj, Libya.

<sup>2</sup> Department of Mathematics, Faculty of Education, Sirte University, Libya.

Received: 14 / 03 / 2024; Accepted: 10 / 05 / 2024

## ABSTRACT

This study investigates new optical and chirped optical solitons for the space-time fractional cubic nonlinear Schrödinger equation using the Sardar sub-equation technique in the presence of Kerr law nonlinearity. The solutions are expressed in terms of hyperbolic and trigonometric functions, revealing a diverse range of behaviors within the system. The identified optical and chirped optical soliton types include dark, bright, kink, and periodic, showcasing a rich spectrum of phenomena. Representing soliton solutions using 2D and 3D graphs with varying parameters leads to a better understanding of their formation and characteristics. The findings contribute to the comprehension of nonlinear dynamics, offering insights into phenomena relevant to nonlinear optics, quantum mechanics, and condensed matter physics.

**KEYWORDS:** Cubic nonlinear Schrödinger equation, Kerr law nonlinearity, beta derivative, optical solitons, Sardar sub-equation technique.

## 1. INTRODUCTION

Nonlinear models have been used to explain a variety of real-world occurrences, revealing significant information in the process. Advanced classes of differential equations that produce better outcomes are represented by fractional nonlinear evolution equations. Due to their important uses, these equations aid in the illustration of complex physical events and draw a large number of researchers to work in this subject. The nonlinear Schrödinger equation is an essential component of fractional nonlinear evolution equations and is applied in quantum mechanics, biology, optical fiber, plasma physics, fluid mechanics, electricity, shallow water wave phenomena, heat flow, finance, and fractal dynamics.

The intricate interplay between the nonlinear and dispersive components of solitons within a medium has revealed that their wave-like structure remains preserved during propagation. The soliton solutions originating from Fractional Nonlinear Evolution Equations (FNLEEs) offer a wide array of practical and commercial advantages across numerous industries. In the realm of fiber optic technology <sup>[1-3]</sup>, these soliton solutions contribute to enhancing data transmission speeds and reliability, crucial for meeting the growing demands of high-speed communication networks.

Within the telecommunications sector <sup>[4]</sup>, FNLEE solitons play a pivotal role in ensuring seamless connectivity and efficient signal transmission. In signal processing applications <sup>[5]</sup>, these solutions aid in the precise analysis and manipulation of data signals, facilitating advancements in fields such as digital communications and information processing. Moreover, in image processing <sup>[6]</sup>, FNLEE solitons are utilized for advanced image enhancement techniques, enabling clearer and more detailed visual representation. System identification benefits from the application of soliton solutions by providing accurate modeling tools for complex systems, aiding in predictive analysis and control. Water treatment processes leverage FNLEE solitons for optimized purification methods, enhancing the efficiency of wastewater treatment and desalination processes. In the realm of plasma physics, these solutions assist in understanding and controlling plasma behavior, essential for various applications ranging from fusion research to materials processing. Medical device sterilization procedures benefit from the use of soliton solutions, ensuring effective and reliable sterilization processes in healthcare settings. Furthermore, in the field of chemistry, FNLEE solitons offer valuable insights into intricate chemical reactions and phenomena, aiding in the development of novel materials and pharmaceuticals. These diverse applications underscore the versatility and impact of soliton solutions derived from FNLEEs in

\*Correspondence: Abdulmalik A. Altwaty

[abdulmalik.altwaty@uob.edu.ly](mailto:abdulmalik.altwaty@uob.edu.ly)

addressing challenges and driving innovation across a broad spectrum of industries and disciplines.

Various dynamic approaches have been introduced and implemented in the literature to solve nonlinear fractional differential equations (NFDES) and obtain analytical traveling wave solutions, for example, the fractional differential transform method [7], the fractional modified Kudryashov method [8], the generalized differential transform method [9], the fractional finite difference method [10-12], the fractional finite element method [13-15], the fractional boundary element method [16-18], the fractional radial basis function method [19-21], the fractional homotopy analysis method [22,23], the fractional homotopy perturbation transform method [24,25].

In this paper, we will utilize for the first time the fractional cubic NLFSE with Kerr law nonlinearity by using Sardar sub-equation technique. The fractional cubic NLFSE with the Kerr law nonlinearity is stated as [26, 27].

$$iD_t^\alpha u + a_1 D_t^\alpha D_x^\alpha u + a_2 D_x^{2\alpha} u + a_3 |u|^2 u = 0. \quad (1)$$

The wave profile with complex values is represented by  $u(x,t)$ . Here  $a_1, a_2, a_3$  are real coefficients, and  $(0 \leq \alpha \leq 1)$ . The cubic fractional nonlinear Schrödinger equation, which includes beta derivatives in both space and time, is utilized to represent various nonlinear optical phenomena. For instance, it can be applied to model the behavior of solitons in optical fibers, showcasing their unique propagation characteristics and stability in the presence of nonlinear effects.

The structure of this article is outlined as follows: Section 2 discusses the characteristics of the beta derivative. The methodology of the proposed approach is detailed in Section 3. A mathematical analysis is presented in Section 4. The article is concluded in Section 5.

## 2. DEFINITION OF BETA DERIVATIVE AND ITS PROPERTIES

In recent years, researchers have introduced various definitions of fractional derivatives, including the Riemann-Liouville, modified Riemann-Liouville, Caputo, Caputo-Fabrizio, conformable fractional derivative, and Atangana-Baleanu derivatives. These fractional derivatives often deviate from the familiar properties of classical calculus, such as the chain rule, the Leibniz rule, and the derivative of a constant being zero. To address this, Atangana and colleagues proposed a novel and significant definition known as the beta derivative. This beta derivative adheres to the fundamental properties of classical calculus, marking a crucial advancement in the field of fractional calculus.

Definition 1: Given  $\alpha \in \mathbb{R}$  and a function  $h=h(x)$  defined on the interval  $[\alpha, \infty) \rightarrow \mathbb{R}$ , the beta derivative of

order  $\alpha$  with respect to  $x$  is formally defined as follows [28]:

$$D_x^\alpha (h(x)) = \lim_{\epsilon \rightarrow 0} \frac{h\left(x + \epsilon \left(x + \frac{1}{\Gamma(\alpha)}\right)^{1-\alpha}\right) - h(x)}{\epsilon}, \quad (2)$$

where  $\Gamma$  is the gamma function and  $D_x^\alpha h(x) = d/dx h(x)$  for  $\alpha=1$ . Given that  $h(x)$  and  $g(x)$  are  $\alpha$ -order differentiable for  $x > 0$ , and  $a$  and  $b$  are real constants, the beta derivative exhibits the following properties:

1.  $D_x^\alpha (a h(x) + b g(x)) = a D_x^\alpha h(x) + b D_x^\alpha g(x)$ .
2.  $D_x^\alpha (k) = 0$ , where  $k$  is a constant.
3.  $D_x^\alpha (h(x) g(x)) = h(x) D_x^\alpha g(x) + g(x) D_x^\alpha h(x)$ .
4.  $D_x^\alpha \left(\frac{h(x)}{g(x)}\right) = \frac{g(x) D_x^\alpha (h(x)) - h(x) D_x^\alpha (g(x))}{g^2(x)}$ .
5.  $D_x^\alpha (h^{-1}(x)) = -\frac{D_x^\alpha (h(x))}{h^2(x)}$ .
6.  $D_x^\alpha h(x) = \left(x + \frac{1}{\Gamma(\alpha)}\right)^{1-\alpha} \frac{dh(x)}{dx}$ .

Utilizing these properties of the beta derivative, fractional differential equations can be effectively reduced to ordinary differential equations. Notably, the beta derivative has demonstrated a comprehensive fulfillment of properties equivalent to those observed with integer-order derivatives without encountering any discernible limitations thus far.

## 3. ALGORITHM OF THE SARDAR SUB-EQUATION TECHNIQUE

In this section, we introduced the Sardar sub-equation technique as a powerful tool. This method empowers us to derive new and extensive analytical solutions for the model (1). By leveraging this technique, we can convert fractional partial differential equations into ordinary differential equations, streamlining the computational procedure. The algorithm outlining this process is detailed below:

**Step 1:** Let

$$H(u, u_x, u_t, D_t^\alpha u, D_x^\alpha u, D_{tt}^{2\alpha} u, D_{xt}^{2\alpha} u, D_{xx}^{2\alpha} u, \dots) = 0, \quad (3)$$

Where  $\mathcal{F}$  is a polynomial of  $u(x,t)$ , and  $D_t^\alpha$  is a fractional derivative of  $\alpha$ -order. Consider the wave transformation  $u = \varphi(\xi) e^{i(\vartheta(\xi) - \omega t)}$ , where  $\xi = \frac{1}{\alpha} \left(x + \frac{1}{\Gamma(\alpha)}\right)^\alpha - \frac{v}{\alpha} \left(t + \frac{1}{\Gamma(\alpha)}\right)^\alpha$  and  $v, \omega$  are respectively velocity and wave number. According to the definition provided in reference [29], we have:

$$\delta w = -\frac{\partial(\vartheta(\xi) - \omega t)}{\partial t} = \vartheta(\xi)'$$

Using the considerable transformation, Eq. (3) reduced to the following ordinary differential equation:

$$\mathcal{H}(u, u', u'', u''', \dots) = 0 \tag{4}$$

**Step 2:** the exact solution of Eq. (4) given as

$$u(\xi) = \sum_{l=0}^N b_l M^l(\xi); \quad b_l \neq 0, \tag{5}$$

Where  $b_l (0 \leq l \leq N)$  are constant coefficients to be evaluated later and  $M(\xi)$  satisfies the following ordinary differential equation,

$$M'(\xi) = \sqrt{\mu + \gamma M(\xi)^2 + M(\xi)^4}, \tag{6}$$

Where  $\mu$  and  $\gamma$  are real constants. The general solutions of Equation (6) are given as.

(1) If  $\gamma > 0$  and  $\mu = 0$  then

$$\begin{aligned} M_1^\pm(\xi) &= \pm \sqrt{-pq\gamma} \operatorname{sech}_{pq}(\sqrt{\gamma} \xi) \\ M_2^\pm(\xi) &= \pm \sqrt{pq\gamma} \operatorname{csch}_{pq}(\sqrt{\gamma} \xi) \end{aligned}$$

(2) If  $\gamma < 0$  and  $\mu = 0$  then

$$\begin{aligned} M_3^\pm(\xi) &= \pm \sqrt{-pq\gamma} \operatorname{sec}_{pq}(\sqrt{-\gamma} \xi) \\ M_4^\pm(\xi) &= \pm \sqrt{-pq\gamma} \operatorname{csc}_{pq}(\sqrt{-\gamma} \xi) \end{aligned}$$

(3) If  $\gamma < 0$  and  $\mu = \frac{\gamma^2}{4}$  then

$$\begin{aligned} M_5^\pm(\xi) &= \pm \sqrt{\frac{-\gamma}{2}} \operatorname{tanh}_{pq} \left( \sqrt{\frac{-\gamma}{2}} \xi \right), \\ M_6^\pm(\xi) &= \pm \sqrt{\frac{-\gamma}{2}} \operatorname{coth}_{pq} \left( \sqrt{\frac{-\gamma}{2}} \xi \right), \\ M_7^\pm(\xi) &= \pm \sqrt{\frac{-\gamma}{2}} \left( \operatorname{tanh}_{pq}(\sqrt{-2\gamma} \xi) \pm i \sqrt{pq} \operatorname{sech}_{pq}(\sqrt{-2\gamma} \xi) \right) \\ M_8^\pm(\xi) &= \pm \sqrt{\frac{-\gamma}{2}} \left( \operatorname{coth}_{pq}(\sqrt{-2\gamma} \xi) \pm \sqrt{pq} \operatorname{csch}_{pq}(\sqrt{-2\gamma} \xi) \right) \\ M_9^\pm(\xi) &= \pm \sqrt{\frac{-\gamma}{8}} \left( \operatorname{tanh}_{pq} \left( \sqrt{\frac{-\gamma}{8}} \xi \right) + \operatorname{oth}_{pq} \left( \sqrt{\frac{-\gamma}{8}} \xi \right) \right) \end{aligned}$$

(4) If  $\gamma > 0$  and  $\mu = \frac{\gamma^2}{4}$  then

$$\begin{aligned} M_{10}^\pm(\xi) &= \pm \sqrt{\frac{\gamma}{2}} \operatorname{tan}_{pq} \left( \sqrt{\frac{\gamma}{2}} \xi \right) \\ M_{11}^\pm(\xi) &= \pm \sqrt{\frac{\gamma}{2}} \operatorname{cot}_{pq} \left( \sqrt{\frac{\gamma}{2}} \xi \right) \\ M_{12}^\pm(\xi) &= \pm \sqrt{\frac{\gamma}{2}} \left( \operatorname{tan}_{pq}(\sqrt{2\gamma} \xi) \pm \sqrt{pq} \operatorname{sec}_{pq}(\sqrt{2\gamma} \xi) \right) \\ M_{13}^\pm(\xi) &= \pm \sqrt{\frac{\gamma}{2}} \left( \operatorname{cot}_{pq}(\sqrt{2\gamma} \xi) \pm \sqrt{pq} \operatorname{csc}_{pq}(\sqrt{2\gamma} \xi) \right) \\ M_{14}^\pm(\xi) &= \pm \sqrt{\frac{\gamma}{8}} \left( \operatorname{tan}_{pq} \left( \sqrt{\frac{\gamma}{8}} \xi \right) + \operatorname{cot}_{pq} \left( \sqrt{\frac{\gamma}{8}} \xi \right) \right) \end{aligned}$$

Where

$$\begin{aligned} \operatorname{tan}_{pq}(\xi) &= -i \frac{pe^{i\xi} - qe^{-i\xi}}{pe^{i\xi} + qe^{-i\xi}}, \quad \operatorname{cot}_{pq}(\xi) = i \frac{pe^{i\xi} + qe^{-i\xi}}{pe^{i\xi} - qe^{-i\xi}} \\ \operatorname{tanh}_{pq}(\xi) &= \frac{pe^\xi - qe^{-\xi}}{pe^\xi + qe^{-\xi}}, \quad \operatorname{coth}_{pq}(\xi) = \frac{pe^\xi + qe^{-\xi}}{pe^\xi - qe^{-\xi}} \\ \operatorname{sec}_{pq}(\xi) &= \frac{2}{pe^{i\xi} + qe^{-i\xi}}, \quad \operatorname{csc}_{pq}(\xi) = \frac{2i}{pe^{i\xi} - qe^{-i\xi}} \\ \operatorname{sech}_{pq}(\xi) &= \frac{2}{pe^\xi + qe^{-\xi}}, \quad \operatorname{csch}_{pq}(\xi) = \frac{2}{pe^\xi - qe^{-\xi}} \end{aligned}$$

**Step 3:** The integer  $N$  calculated by balancing the capitals. Substituting Eq. (5) into Eq. (4) we obtain a system of algebraic equations in terms of  $M^l(\xi)$  where  $(l = 0, 1, 2, \dots, N)$ .

**Step 4:** Solving these algebraic equations, we determine the values of the unknown parameters.

#### 4. Mathematical Analysis

In this section, we delved into the study of the space-time fractional cubic Nonlinear Fractional Schrödinger Equations (NLFSEs) with the aim of obtaining broader and more conventional exact wave solutions. To achieve this, we applied the Sardar sub-equation technique, a method that simplifies the solution process for fractional partial differential equations by transforming them into ordinary differential equations.

Furthermore, we conducted a comprehensive mathematical analysis of these wave solutions to gain a deeper understanding of their behavior and properties. By utilizing a fractional transformation, we converted the original Equation (1) into an ordinary differential equation that accounts for both the real and imaginary components of the solution. This transformation facilitated the derivation of analytical solutions that provide insights into the dynamics and characteristics of the system under study.

$$\begin{aligned} (v + a_1 \theta) \phi \phi' + \theta \phi + (a_1 v - a_2) \phi (\phi')^2 + (a_2 - a_1 v) \phi'' + a_3 \phi^3 &= 0, \\ (v - a_1 \theta) \phi' + 2(a_2 - a_1 v) \phi' \phi' + (a_2 - a_1 v) \phi \phi'' &= 0. \end{aligned} \tag{8}$$

Integrating Eq.(8) yields

$$\phi' = \frac{a_1 \theta - v}{a_2 - a_1 v} + C \phi^{-2}. \tag{9}$$

Concurrently, the chirp is shown by

$$\delta \omega = - \left[ \frac{a_1 \theta - v}{a_2 - a_1 v} + C \phi^{-2} \right]. \tag{10}$$

Substituting into the real part we get

$$A_0\varphi^4 + A_1\varphi^2 + A_2 + A_3\varphi^3\varphi'' + a_3\varphi^6 = 0. \tag{11}$$

Where  $A_0 = \frac{(v+a_1\theta)^2-2v}{4(a_2-a_1v)} + \theta, A_1 = 2Cv, A_2 = C^2(a_1v - a_2), A_3 = (a_2 - a_1v),$  and  $C$  is the integration constant.

Now balancing between  $\varphi^3\varphi''$  and  $\varphi^6$  the highest order derivatives and highest power of the nonlinear term in Eq. (11), we obtain  $N = 1$ . Therefore, the solution of Eq. (11) is of the form

$$\varphi(\xi) = b_0 + b_1 M(\xi). \tag{12}$$

Upon substituting Eq. (11) together with Eq. (6), we derive a polynomial expression in  $M^l(\xi)$ . Setting this polynomial to zero, representing the coefficient power of  $M^l(\xi)$ , we formulate a system of algebraic equations that incorporate the variables  $b_0, b_1, \mu,$  and  $\gamma$ . Solving this system of algebraic equations using Matlab provides the parameter values as follows:

$$b_0 = b_0, \quad b_1 = b_1, \quad \mu = \mu, \quad \gamma = \gamma, \quad v = \frac{a_2C - a_3b_0^6}{2b_0^2 + a_1C},$$

$$\theta = -\frac{a_2}{a_1^2} + \frac{a_2C - a_3b_0^6}{4a_1b_0^2 + 2a_1^2C} \pm 2\sqrt{\frac{a_2}{a_1}\left(\frac{a_2}{a_1^3} - \frac{a_2C - a_3b_0^6}{2b_0^2 + a_1C}\right)},$$

Where  $\omega$  is real if and only if  $C \geq -\frac{a_1^3a_3b_0^6 + 2a_2b_0^2}{a_1a_2 - a_1^3a_2}$ .

Substituting into (12) and the hypothesis of the auxiliary equation for different conditions, we establish the travelling wave solutions of (1) which are given as:

**Case 1:** When  $\gamma > 0$  and  $\mu = 0$ , then the solutions are as follows:

$$u_1 = \{b_0 \pm b_1\sqrt{-pq\gamma} \operatorname{sech}_{pq}(\sqrt{\gamma}\xi)\} e^{i\left(\vartheta(\xi) - \left(-\frac{a_2}{a_1^2} + \frac{a_2C - a_3b_0^6}{4a_1b_0^2 + 2a_1^2C} \pm 2\sqrt{\frac{a_2}{a_1}\left(\frac{a_2}{a_1^3} - \frac{a_2C - a_3b_0^6}{2b_0^2 + a_1C}\right)}\right)t\right)} \tag{13}$$

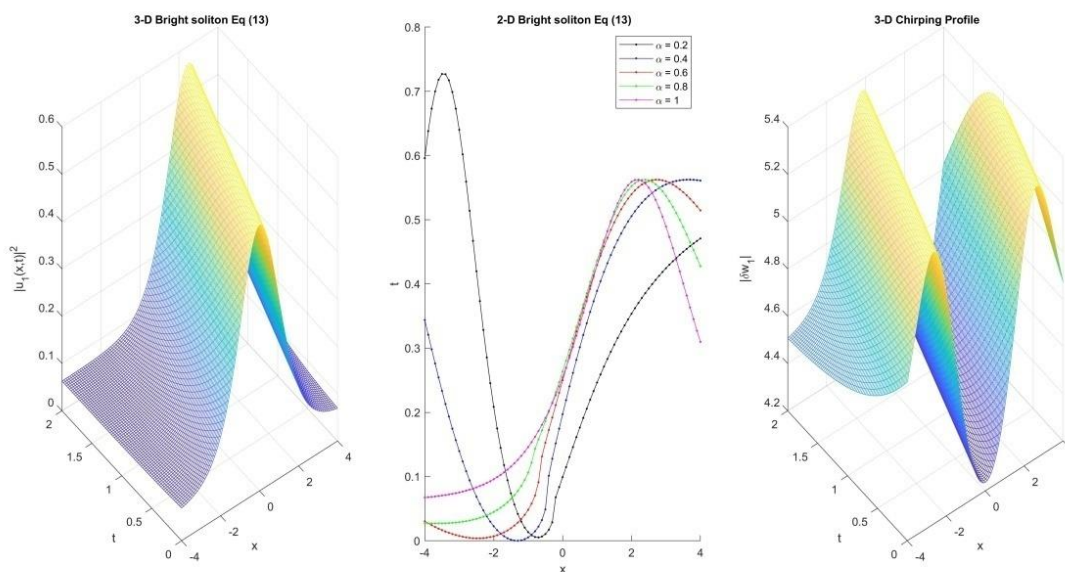


**Figure 1:** 3D, 2D and 3D chirped Bright soliton solutions of Equation (13) for  $a_1 = 0.15, a_2 = 0.5, a_3 = 2, b_0 = 0.25, \gamma = 0.5, b_1 = 1, C = 0.5,$  and  $\alpha = 1,$  with  $x \in [-4, 4]$  and  $x \in [0, 2].$

$$\delta\omega_1 = -\left[\frac{a_1\omega - v}{a_2 - a_1v} + C(b_0 \pm b_1\sqrt{-pq\gamma} \operatorname{sech}_{pq}(\sqrt{\gamma}\xi))^{-2}\right], \tag{14}$$

$$u_2 = \{b_0 \pm b_1\sqrt{-pq\gamma} \operatorname{csch}_{pq}(\sqrt{\gamma}\xi)\} e^{i\left(\vartheta(\xi) - \left(-\frac{a_2}{a_1^2} + \frac{a_2C - a_3b_0^6}{4a_1b_0^2 + 2a_1^2C} \pm 2\sqrt{\frac{a_2}{a_1}\left(\frac{a_2}{a_1^3} - \frac{a_2C - a_3b_0^6}{2b_0^2 + a_1C}\right)}\right)t\right)}, \tag{15}$$

$$\delta\omega_2 = -\left[\frac{a_1\omega - v}{a_2 - a_1v} + C(b_0 \pm b_1\sqrt{-pq\gamma} \operatorname{csch}_{pq}(\sqrt{\gamma}\xi))^{-2}\right]. \tag{16}$$

**Case 2:** When  $\gamma < 0$  and  $\mu = 0$ , we obtain

$$u_3 = \{b_0 \pm b_1 \sqrt{-pq\gamma} \sec_{pq}(\sqrt{-\gamma}\xi)\} e^{i\left(\theta(\xi) - \left(\frac{a_2}{a_1^2} + \frac{a_2 C - a_3 b_0^6}{4a_1 b_0^2 + 2a_1^2 C} \pm 2 \sqrt{\frac{a_2}{a_1} \left(\frac{a_2}{a_1^3} - \frac{a_2 C - a_3 b_0^6}{2b_0^2 + a_1 C}\right)}\right) t\right)} \tag{17}$$

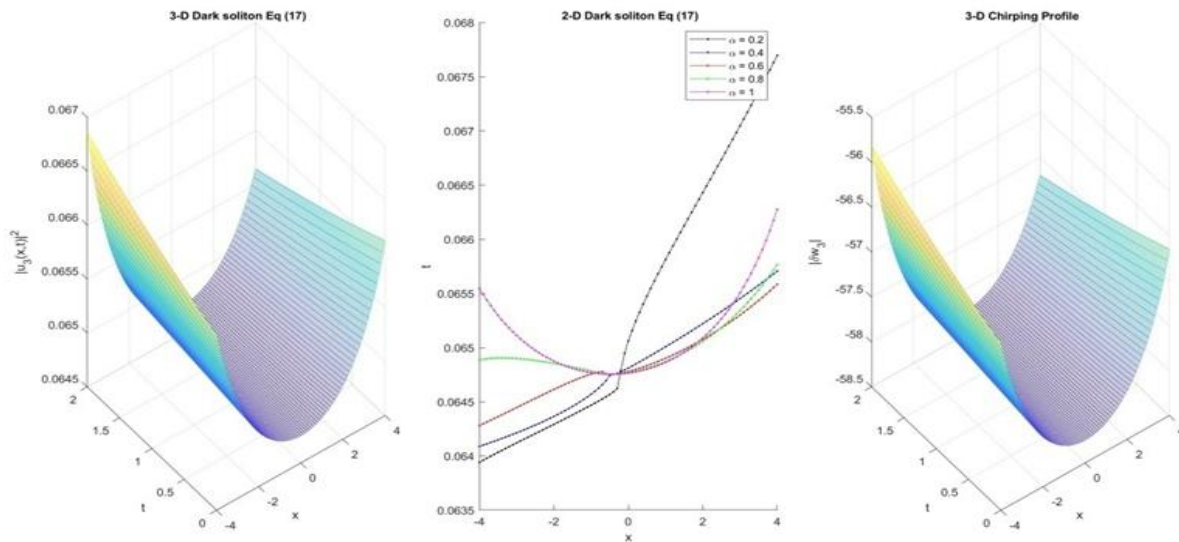


**Figure 2:** 3D, 2D and 3D chirped Dark soliton solutions of Equation (17) for  $a_1 = 0.15, a_2 = 0.05, a_3 = 0.2, b_0 = 0.25, \gamma = -0.05, b_1 = 0.02, C = 5,$  and  $\alpha = 1,$  with  $x \in [-4, 4]$  and  $x \in [0, 2].$

$= 1,$  with  $x \in [-4, 4]$  and  $x \in [0, 2].$

$$\delta\omega_3 = -\left[\frac{a_1\omega - v}{a_2 - a_1 v} + C (b_0 \pm b_1 \sqrt{-pq\gamma} \sec_{pq}(\sqrt{-\gamma}\xi))^{-2}\right], \tag{18}$$

$$u_4 = \{b_0 \pm b_1 \sqrt{-pq\gamma} \csc_{pq}(\sqrt{-\gamma}\xi)\} e^{i\left(\theta(\xi) - \left(\frac{a_2}{a_1^2} + \frac{a_2 C - a_3 b_0^6}{4a_1 b_0^2 + 2a_1^2 C} \pm 2 \sqrt{\frac{a_2}{a_1} \left(\frac{a_2}{a_1^3} - \frac{a_2 C - a_3 b_0^6}{2b_0^2 + a_1 C}\right)}\right) t\right)}, \tag{19}$$

$$\delta\omega_4 = -\left[\frac{a_1\omega - v}{a_2 - a_1 v} + C (b_0 \pm b_1 \sqrt{-pq\gamma} \csc_{pq}(\sqrt{-\gamma}\xi))^{-2}\right]. \tag{20}$$

**Case 3:** When  $\gamma < 0$  and  $\mu = \frac{\gamma^2}{4},$  we obtain

$$u_5 = \{b_0 \pm b_1 \sqrt{\frac{-\gamma}{2}} \tanh_{pq}\left(\sqrt{\frac{-\gamma}{2}}\xi\right)\} e^{i\left(\theta(\xi) - \left(\frac{a_2}{a_1^2} + \frac{a_2 C - a_3 b_0^6}{4a_1 b_0^2 + 2a_1^2 C} \pm 2 \sqrt{\frac{a_2}{a_1} \left(\frac{a_2}{a_1^3} - \frac{a_2 C - a_3 b_0^6}{2b_0^2 + a_1 C}\right)}\right) t\right)}, \tag{21}$$

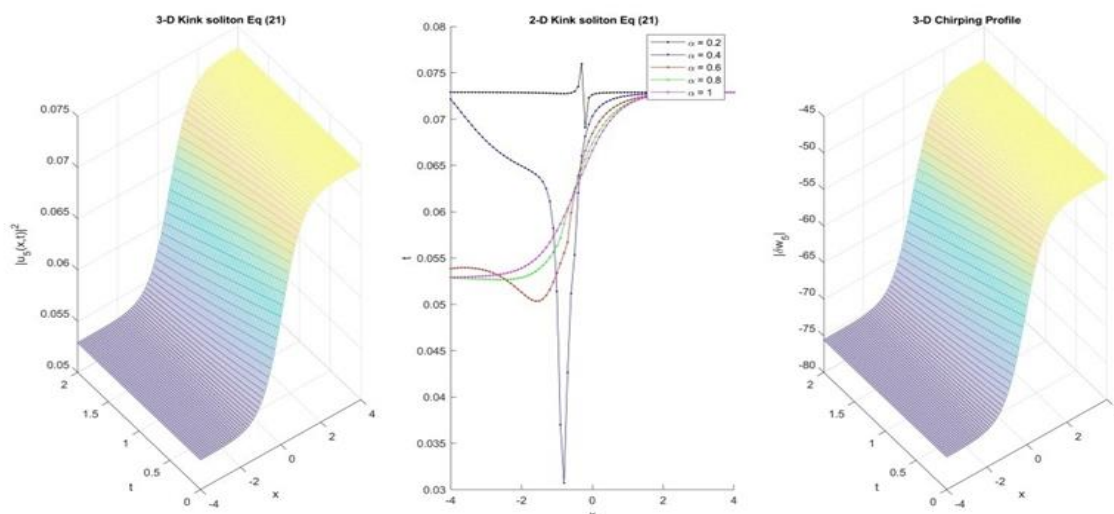


**Figure 3:** 3D, 2D and 3D chirped Kink soliton solutions of Equation (21) for  $\mathbf{a}_1 = \mathbf{0.15}, \mathbf{a}_2 = \mathbf{0.05}, \mathbf{a}_3 = \mathbf{0.2}, \mathbf{b}_0 = \mathbf{0.25}, \mathbf{\gamma} = \mathbf{-2}, \mathbf{b}_1 = \mathbf{0.02}, \mathbf{C} = \mathbf{5},$  and  $\alpha = \mathbf{1}$ , with  $\mathbf{x} \in [-4, 4]$  and  $\mathbf{x} \in [0, 2]$ .

$$\delta\omega_5 = - \left[ \frac{a_1\omega - v}{a_2 - a_1v} + C \left( b_0 \pm b_1 \sqrt{\frac{-\gamma}{2}} \tanh_{pq} \left( \sqrt{\frac{-\gamma}{2}} \xi \right) \right)^{-2} \right], \tag{22}$$

$$u_6 = \left\{ b_0 \pm b_1 \sqrt{\frac{-\gamma}{2}} \coth_{pq} \left( \sqrt{\frac{-\gamma}{2}} \xi \right) \right\} e^{i \left( \phi(\xi) - \left( \frac{a_2}{a_1^2} + \frac{a_2C - a_3b_0^6}{4a_1b_0^2 + 2a_1^2C} \pm 2 \sqrt{\frac{a_2 \left( \frac{a_2}{a_1^3} - \frac{a_2C - a_3b_0^6}{2b_0^2 + a_1C} \right)}{a_1}} \right) t \right)}, \tag{23}$$

$$\delta\omega_6 = - \left[ \frac{a_1\omega - v}{a_2 - a_1v} + C \left( b_0 \pm b_1 \sqrt{\frac{-\gamma}{2}} \coth_{pq} \left( \sqrt{\frac{-\gamma}{2}} \xi \right) \right)^{-2} \right], \tag{24}$$

$$u_7 = \left\{ b_0 \pm b_1 \sqrt{\frac{-\gamma}{2}} (\tanh_{pq}(\sqrt{-2\gamma}\xi) \pm i\sqrt{pq} \operatorname{sech}_{pq}(\sqrt{-2\gamma}\xi)) \right\} e^{i \left( \phi(\xi) - \left( \frac{a_2}{a_1^2} + \frac{a_2C - a_3b_0^6}{4a_1b_0^2 + 2a_1^2C} \pm 2 \sqrt{\frac{a_2 \left( \frac{a_2}{a_1^3} - \frac{a_2C - a_3b_0^6}{2b_0^2 + a_1C} \right)}{a_1}} \right) t \right)}, \tag{25}$$

$$\delta\omega_7 = - \left[ \frac{a_1\omega - v}{a_2 - a_1v} + C \left( b_0 \pm b_1 \sqrt{\frac{-\gamma}{2}} (\tanh_{pq}(\sqrt{-2\gamma}\xi) \pm i\sqrt{pq} \operatorname{sech}_{pq}(\sqrt{-2\gamma}\xi)) \right)^{-2} \right], \tag{26}$$

$$u_8 = \left\{ b_0 \pm b_1 \sqrt{\frac{-\gamma}{2}} (\coth_{pq}(\sqrt{-2\gamma}\xi) \pm \sqrt{pq} \operatorname{csch}_{pq}(\sqrt{-2\gamma}\xi)) \right\} e^{i \left( \phi(\xi) - \left( \frac{a_2}{a_1^2} + \frac{a_2C - a_3b_0^6}{4a_1b_0^2 + 2a_1^2C} \pm 2 \sqrt{\frac{a_2 \left( \frac{a_2}{a_1^3} - \frac{a_2C - a_3b_0^6}{2b_0^2 + a_1C} \right)}{a_1}} \right) t \right)}, \tag{27}$$

$$\delta\omega_8 = - \left[ \frac{a_1\omega - v}{a_2 - a_1v} + C \left( b_0 \pm b_1 \sqrt{\frac{-\gamma}{2}} (\coth_{pq}(\sqrt{-2\gamma}\xi) \pm \sqrt{pq} \operatorname{csch}_{pq}(\sqrt{-2\gamma}\xi)) \right)^{-2} \right], \tag{28}$$

$$u_9 = \left\{ b_0 \pm b_1 \sqrt{\frac{-\gamma}{8}} \left( \tanh_{pq} \left( \sqrt{\frac{-\gamma}{8}} \xi \right) + \coth_{pq} \left( \sqrt{\frac{-\gamma}{8}} \xi \right) \right) \right\} e^{i \left( \phi(\xi) - \left( \frac{a_2}{a_1^2} + \frac{a_2C - a_3b_0^6}{4a_1b_0^2 + 2a_1^2C} \pm 2 \sqrt{\frac{a_2 \left( \frac{a_2}{a_1^3} - \frac{a_2C - a_3b_0^6}{2b_0^2 + a_1C} \right)}{a_1}} \right) t \right)}, \tag{29}$$

$$\delta\omega_9 = - \left[ \frac{a_1\omega - v}{a_2 - a_1v} + C \left( b_0 \pm b_1 \sqrt{\frac{-\gamma}{8}} \left( \tanh_{pq} \left( \sqrt{\frac{-\gamma}{8}} \xi \right) + \coth_{pq} \left( \sqrt{\frac{-\gamma}{8}} \xi \right) \right) \right)^{-2} \right]. \tag{30}$$

**Case 4:** When  $\gamma > 0$  and  $\mu = \frac{\gamma^2}{4}$ , we obtain

$$u_{10} = \left\{ b_0 \pm b_1 \sqrt{\frac{\gamma}{2}} \tan_{pq} \left( \sqrt{\frac{\gamma}{2}} \xi \right) \right\} e^{i \left( \phi(\xi) - \left( \frac{a_2}{a_1^2} + \frac{a_2C - a_3b_0^6}{4a_1b_0^2 + 2a_1^2C} \pm 2 \sqrt{\frac{a_2 \left( \frac{a_2}{a_1^3} - \frac{a_2C - a_3b_0^6}{2b_0^2 + a_1C} \right)}{a_1}} \right) t \right)}, \tag{31}$$

$$\delta\omega_{10} = - \left[ \frac{a_1\omega - v}{a_2 - a_1v} + C \left( b_0 \pm b_1 \sqrt{\frac{\gamma}{2}} \tan_{pq} \left( \sqrt{\frac{\gamma}{2}} \xi \right) \right)^{-2} \right], \tag{32}$$

$$u_{11} = \left\{ b_0 \pm b_1 \sqrt{\frac{\gamma}{2}} \cot_{pq} \left( \sqrt{\frac{\gamma}{2}} \xi \right) \right\} e^{i \left( \theta(\xi) - \left( \frac{a_2}{a_1^2} + \frac{a_2C - a_3b_0^6}{4a_1b_0^2 + 2a_1^2C} + 2 \sqrt{\frac{a_2}{a_1} \left( \frac{a_2}{a_1^3} - \frac{a_2C - a_3b_0^6}{2b_0^2 + a_1C} \right)} \right) t \right)}, \tag{33}$$

$$\delta\omega_{11} = - \left[ \frac{a_1\omega - v}{a_2 - a_1v} + C \left( b_0 \pm b_1 \sqrt{\frac{\gamma}{2}} \cot_{pq} \left( \sqrt{\frac{\gamma}{2}} \xi \right) \right)^{-2} \right], \tag{34}$$

$$u_{12} = \left\{ b_0 \pm b_1 \sqrt{\frac{\gamma}{2}} (\tan_{pq}(\sqrt{2\gamma}\xi) \pm \sqrt{pq} \sec_{pq}(\sqrt{2\gamma}\xi)) \right\} e^{i \left( \theta(\xi) - \left( \frac{a_2}{a_1^2} + \frac{a_2C - a_3b_0^6}{4a_1b_0^2 + 2a_1^2C} + 2 \sqrt{\frac{a_2}{a_1} \left( \frac{a_2}{a_1^3} - \frac{a_2C - a_3b_0^6}{2b_0^2 + a_1C} \right)} \right) t \right)}, \tag{35}$$

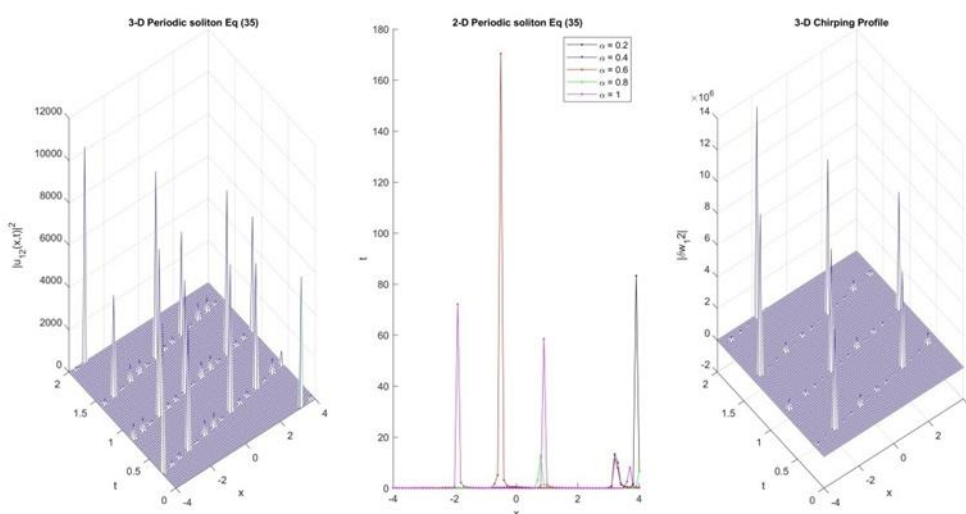


**Figure 4:** 3D, 2D and 3D chirped Periodic soliton solutions of Equation (35) for  $a_1 = 0.15$ ,  $a_2 = 1.5$ ,  $a_3 = 0.12$ ,  $b_0 = 0.25$ ,  $\gamma = 0.12$ ,  $b_1 = 0.5$ ,  $C = -1.5$ , and  $\alpha = 1$ , with  $x \in [-4, 4]$  and  $t \in [0, 2]$ .

$$\delta\omega_{12} = - \left[ \frac{a_1\omega - v}{a_2 - a_1v} + C \left( b_0 \pm b_1 \sqrt{\frac{\gamma}{2}} (\tan_{pq}(\sqrt{2\gamma}\xi) \pm \sqrt{pq} \sec_{pq}(\sqrt{2\gamma}\xi)) \right)^{-2} \right], \tag{36}$$

$$u_{13} = \left\{ b_0 \pm b_1 \sqrt{\frac{\gamma}{2}} (\cot_{pq}(\sqrt{2\gamma}\xi) \pm \sqrt{pq} \csc_{pq}(\sqrt{2\gamma}\xi)) \right\} e^{i \left( \theta(\xi) - \left( \frac{a_2}{a_1^2} + \frac{a_2C - a_3b_0^6}{4a_1b_0^2 + 2a_1^2C} + 2 \sqrt{\frac{a_2}{a_1} \left( \frac{a_2}{a_1^3} - \frac{a_2C - a_3b_0^6}{2b_0^2 + a_1C} \right)} \right) t \right)}, \tag{37}$$

$$\delta\omega_{13} = - \left[ \frac{a_1\omega - v}{a_2 - a_1v} + C \left( b_0 \pm b_1 \sqrt{\frac{\gamma}{2}} (\cot_{pq}(\sqrt{2\gamma}\xi) \pm \sqrt{pq} \csc_{pq}(\sqrt{2\gamma}\xi)) \right)^{-2} \right], \tag{38}$$

$$u_{14} = \left\{ b_0 \pm b_1 \sqrt{\frac{\gamma}{8}} \left( \tan_{pq} \left( \sqrt{\frac{\gamma}{8}} \xi \right) + \cot_{pq} \left( \sqrt{\frac{\gamma}{8}} \xi \right) \right) \right\} e^{i \left( \theta(\xi) - \left( \frac{a_2}{a_1^2} + \frac{a_2C - a_3b_0^6}{4a_1b_0^2 + 2a_1^2C} + 2 \sqrt{\frac{a_2}{a_1} \left( \frac{a_2}{a_1^3} - \frac{a_2C - a_3b_0^6}{2b_0^2 + a_1C} \right)} \right) t \right)}, \tag{39}$$

$$\delta\omega_{14} = - \left[ \frac{a_1\omega - v}{a_2 - a_1v} + C \left( b_0 \pm b_1 \sqrt{\frac{\gamma}{8}} \left( \tan_{pq} \left( \sqrt{\frac{\gamma}{8}} \xi \right) + \cot_{pq} \left( \sqrt{\frac{\gamma}{8}} \xi \right) \right) \right)^{-2} \right]. \quad (40)$$

The soliton solutions obtained in this study are diverse and novel, originating from the general solutions.

#### 4. CONCLUSION

This article discusses the use of the Sardar sub-equation approach to produce novel optical and chirped optical solitons from the space-time fractional cubic nonlinear Schrödinger equation with Kerr law nonlinearity. The solutions show a wide range of behaviors within the system and are stated in terms of trigonometric and hyperbolic functions. A wide range of phenomena are displayed by the several varieties of optical and chirped optical solitons that have been found, including dark, bright, kink, and periodic. These solutions are shown in two and three-dimensional graphics. The results provide a thorough understanding of nonlinear dynamics and shed some light on phenomena related to condensed matter physics, quantum mechanics, and nonlinear optics.

#### 5. REFERENCES

- Agarwal A. Fiber-Optic Communication Systems. Wiley. 2010.  
<https://onlinelibrary.wiley.com/doi/book/10.1002/9780470918524>
- Altwaty AA, Hassan SM, Baleanu D. Soliton and wave solutions to the extended Gerdjikov-Ivanov equation in DWDM system with auxiliary equation method. Math SciLett. 2020;9(3):57-63.  
<https://doi.org/10.18576/msl/090302>
- Altwaty AA. Optical solitons in Fiber Bragg Gratings for the coupled form of the nonlinear (2+1)-dimensional Kundu-Mukherjee-Naskar equation via four powerful techniques. Results Phys. 2023;44:106205.  
<https://doi.org/10.1016/j.rinp.2022.106205>
- Rappaport TS. Wireless communications: principles and practice. Pearson Education; 2019.
- Oppenheim AV, Schaffer RW, Buck JR. Discrete-time signal processing. Pearson; 2020.
- Gonzalez RC, Woods RE. Digital image processing. Pearson; 2017.
- Saha Ray S, New Techniques on Fractional Reduced Differential Transform Method. In: Nonlinear Differential Equations in Physics. Springer, Singapore 2020.  
[https://doi.org/10.1007/978-981-15-1656-6\\_7](https://doi.org/10.1007/978-981-15-1656-6_7)
- Fushun L, Yuqiang F. The modified generalized Kudryashov method for nonlinear space-time fractional partial differential equations of Schrödinger type. Results in Physics Volume 53, October 2023, 106914.  
<https://doi.org/10.1016/j.rinp.2023.106914>
- Mustafa Ekici. Exact Solutions to Some Nonlinear Time-Fractional Evolution Equations Using the Generalized Kudryashov Method in Mathematical Physics. Symmetry 2023, 15(10), 1961.  
<https://doi.org/10.3390/sym15101961>
- Rana TS. A Novel Approach for Solving Nonlinear Time Fractional Fisher Partial Differential Equations. Journal of Advances in Mathematics Vol 22 (2023).  
<https://doi.org/10.24297/jam.v22i.9558>
- Jocemar QC, Giuliano G, La G, Ervin KL. A finite difference method for a class of nonlinear fractional advection-diffusion equations. Partial Differential Equations in Applied Mathematics. Volume 4, December 2021, 100090.  
<https://doi.org/10.1016/j.padiff.2021.100090>
- Azin A, Habibirad A, Baghani O. Legendre-finite difference method for solving fractional nonlinear Sobolev equation with Caputo derivative. Journal of Computational Science. Volume 74, December 2023, 102177.  
<https://doi.org/10.1016/j.jocs.2023.102177>
- Muhammad BH, Marek K. Fractional Spectral and Fractional Finite Element Methods: A Comprehensive Review and Future Prospects. Archives of Computational Methods in Engineering. 2024.  
<https://doi.org/10.1007/s11831-024-10083-w>
- Malatip A, Wansophark N, Dechaumphair P. Fractional four-step finite element method for analysis of thermally coupled fluid-solid interaction problems. Applied Mathematics and Mechanics. Volume 33, pages 99–116, 2012.  
<https://doi.org/10.1007/s10483-012-1536-9>
- Lakhlifa S, Tania AL, Ishak H. Conformable finite element method for conformable fractional partial differential equations. AIMS Mathematics. 2023, Volume 8, Issue 12: 28858-28877.  
<https://doi.org/10.3934/math.2023147>
- Changtao S, Jie S. A Hybrid Spectral Element Method for Fractional Two-Point Boundary Value Problems. Numerical Mathematics: Theory, Methods and Applications, Volume 10, Issue 2, May 2017, pp. 437 – 464.  
<https://doi.org/10.4208/nmtma.2017.s11>
- Baoli Y, Yang L, Hong L, Zhimin Z. Finite Element Methods Based on Two Families of Second-Order Numerical Formulas for the Fractional Cable Model with Smooth Solutions. J Sci Comput 84, 2 (2020).  
<https://doi.org/10.1007/s10915-020-01258-1>

18. Bruch, E.K. Introduction to the Boundary Element Method. In: The Boundary Element Method for Groundwater Flow. Lecture Notes in Engineering, vol 70. Springer, Berlin, Heidelberg, 1991.  
[https://doi.org/10.1007/978-3-642-84577-2\\_3](https://doi.org/10.1007/978-3-642-84577-2_3)
19. Liu Q, Zhuang P, Liu F. et al. An investigation of radial basis functions for fractional derivatives and their applications. *ComputMech* 65, 475–486 (2020).  
<https://doi.org/10.1007/s00466-019-01779-z>
20. Tseng CC, Lee SL, "Design of fractional delay FIR filter using radial basis function, IEEE International Symposium on Circuits and Systems, Taipei, Taiwan, 2009, pp. 485-488,  
<https://doi.org/10.1109/ISCAS.2009.5117791>.
21. Hussain M, Haq S. Radial Basis Functions Collocation Method for Numerical Solution of Coupled Burgers' and Korteweg-de Vries Equations of Fractional Order. *Iran J SciTechnol Trans Sci* 45, 707–725 (2021).  
<https://doi.org/10.1007/s40995-021-01065-9>
22. Shaiq MS, Iqbal Z, Mohyud-Din ST. Homotopy Analysis Method for Time-Fractional Wave-Like Equations. *Comput Math Model* 24, 592–603 (2013).  
<https://doi.org/10.1007/s10598-013-9201-2>
23. Saratha SR, Bagyalakshmi M, SaiSundara Krishnan G. Fractional generalisedhomotopy analysis method for solving nonlinear fractional differential equations. *Comp. Appl. Math.* 39, 112 (2020).  
<https://doi.org/10.1007/s40314-020-1133-9>
24. Shah,NA, El-Zahar ER, Aljoufi MD. et al. An efficient approach for solution of fractional-order Helmholtz equations.*Adv Differ Equ* 2021, 14 (2021).  
<https://doi.org/10.1186/s13662-020-03167-x>
25. Nadeem M, He JH, The homotopy perturbation method for fractional differential equations: part 2, two-scale transform, *International Journal of Numerical Methods for Heat & Fluid Flow*,2022, Vol. 32 No. 2, pp. 559-567.  
<https://doi.org/10.1108/HFF-01-2021-0030>
26. Tasnim F, Akbar MA, Osman MS. The Extended Direct Algebraic Method for Extracting Analytical Solitons Solutions to the Cubic Nonlinear Schrödinger Equation Involving Beta Derivatives in Space and Time. *JAMA*. 2023.  
<https://doi.org/10.3390/fractalfract7060426>
27. Gang-Zhou W, Li-Jun Y, Yue-Yue W, Fractional optical solitons of the space-time fractional nonlinear Schrödinger equation, *Optik* Volume 207, April 2020, 164405.  
<https://doi.org/10.1016/j.ijleo.2020.164405>
28. Atangana A, Alqahtani RT. Modelling the Spread of River Blindness Disease via the Caputo Fractional Derivative and the Beta-Derivative. *Entropy*. 2016;18:40.  
<https://doi.org/10.3390/e18020040>
29. Sharma VK. Chirped soliton-like solutions of generalized nonlinear Schrödinger equation for pulse propagation in negative index material embedded into a Kerr medium. *Indian J Phys*. 2016;90:1271-1276.  
<https://doi.org/10.1007/s12648-016-0840-y>

## Taguchi Grey Relational Analysis of Mechanical Properties of Structural Steel Welding Made by Gas Tungsten Arc Welding

Saleh Suliman Saleh Elfallah <sup>1\*</sup>

*1 College of Mechanical Engineering Technology - Benghazi.*

Received: 22 / 03 / 2024; Accepted: 12 / 05 / 2024

### ABSTRACT

Welding is a widely used method in industry for joining metals. Its applications include structures, fabrications, automobiles, oil and gas production, and others. Gas Tungsten Arc Welding (GTAW) is a common welding technique that produces higher-quality welds. Its application is mostly for stainless steel and aluminum welding due to its stable arc and focused heat source that produces a narrower heat-affected zone (HAZ). However, optimizing the welding process is a challenge for better-quality welds. This study utilizes the Grey-Taguchi method to optimize welding parameters for maximum tensile strength and hardness of structural steel welds. Structural steel, one of the most common materials involved in local industry, is normally welded by shielded metal arc welding (SMAW), while this work inspects the mechanical and microstructure properties of welds made by GTAW. The results presented higher tensile strength of weldments with decreased welding current. The V-groove-shaped weldments' tensile strength was higher than that of the samples with X-groove-shaped weldments. The Taguchi method has obtained that welding tensile strength is mostly influenced by the welding current, followed by groove shape, while welding speed has the least impact on the tensile strength. The grey relational analysis (GRA) concluded that groove shape had a higher impact on multi-response analysis. The welding factor's optimum settings are 170 A, groove shape V, and a welding speed of 150 mm/min.

**KEYWORDS:** Structural steel, GTAW, Tensile strength, Hardness, Grey-Taguchi method.

### 1. INTRODUCTION

Welding is considered one of the most common manufacturing techniques in the industry for joining metallic alloys. It's simple, flexible, and produces high-strength joints. Gas tungsten arc welding (GTAW) is a known welding process used mostly to weld aluminum, stainless steel, and dissimilar alloys. Furthermore, it uses non-consumable tungsten as an electrode. Moreover, GTAW is advantageous for producing high-quality welds with focused heat generated between the electrode and the welding joint, which produces minimum distortion welds with maximum penetration. In addition, GTAW is fumeless, spatter-free, and normally requires no finishing process. Besides, it's affordable. <sup>[1,2,3]</sup>

Carbon steel is extensively utilized in various engineering applications, such as structures, gears, vices, cutting tools, shafts, railways in fabrication, and others. Each application selects the suitable carbon steel based on properties that are determined principally by the alloy's carbon content. Structural steel, or low-alloy steel, is widely involved in fabrication in local industry.

It is shaped by various fusion welding techniques such as shielded metal arc welding (SMAW), gas metal arc welding (GMAW), and gas tungsten arc welding (GTAW). Also, non-fusion techniques such as friction stir welding (FSW). <sup>[4,5]</sup>

The issue with weldments in general is that the differences in mechanical characteristics between the base metal, the fusion zone (FZ), and the heat-affected zone (HAZ) can lead to failure. This is a result of the variations in grain size and structure among them. <sup>[4,6]</sup> Weldment needs to have higher mechanical qualities, such as tensile strength and hardness, in order to prevent microscopic flaws and eventual failure. <sup>[7]</sup> Therefore, for high-quality weldments with improved mechanical properties, it's critical to optimize the welding parameters that govern the characteristics of the final weldment. <sup>[8]</sup> The tensile test is a well-known mechanical test that examines how much a material can extend before breaking, and in the case of testing welds, it is considered a common test. The hardness of materials or welds normally correlates linearly with their tensile strength. <sup>[9,10]</sup>

Various researchers studied the effect of GTAW welding parameters such as welding current, welding speed, filler material and diameter, root gap, gas flow rate, and others on the final weldment characteristics of

\*Correspondence: Saleh Suliman Saleh Elfallah

[sselfallah87@gmail.com](mailto:sselfallah87@gmail.com)

steel and other metal alloys. [2,11] For instance, Korkmaz et al. studied the effect of welding current and welding speed tensile strength on the welding of XPF800 steel by GTAW and 99.9% argon (Ar) as shield gas. The results found that higher tensile strength (777 MPa) was shown at 140 A and 100 mm/min [12]. The Taguchi method is a technique that is common in process optimization in industry [13]. It promotes the orthogonal array (OA) as a process design that requires fewer experiments than other design of experiment (DoE) methods [14]. Researchers have repeatedly utilized the Taguchi method to optimize GTAW weldment responses [15]. Numerous studies have experienced Taguchi's design to optimize the steel welding parameters made by GTAW on mechanical properties such as tensile strength and hardness. A study by Yadav et al. focused on dissimilar welding of AA5083 and AA6082 aluminum alloys and ER4043 as welding fillers. The work experimentation followed L9 OA and concluded that welding speed had a higher effect on the tensile strength and Brinell hardness, followed by welding current, while filler diameter had the least significant influence on the responses [11]. Mohanty et al. reported on low-carbon steel welding using welding filler grade ER309L and pure Ar as a shielding gas. The experiments designed according to L9 Taguchi's orthogonal array showed that welding current had a higher effect on welding tensile strength and hardness. The results revealed that the hardness was more affected by the welding speed, whereas the tensile strength was more affected by the welding voltage and current. Furthermore, a drop in welding voltage and current and an increase in welding speed were associated with an increase in tensile strength. Moreover, the FZ hardness varied as the welding tensile strength increased; at a maximum tensile strength of 473 MPa, the hardness was 147.2 HB, but at a maximum welding hardness of 151.2 HB, the tensile strength was 462.8 MPa [1]. Abima et al. reported on the welding of AISI 1008 low-carbon steel by welding filler ER70S-6 and found that lower welding current (140 A) and gas flow rate (15 L/mm) showed higher hardness (189.22 HV for FZ and 152.5 HV for HAZ). Furthermore, an increased tensile strength (432.89 MPa) was obtained at a higher welding current of 180 A and a gas flow rate of 19 L/mm [16]. Additionally, Jawad et al. reported on welding AISI 1045 medium steel that a maximum tensile strength of 625 MPa and Rockwell hardness of 80.19 HRB achieved at optimum welding speed, welding current, and gas flow rate. The study further concluded that increased tensile strength was detected at decreased welding speeds [17]. These studies and others infer that common welding parameters influence the tensile strength and hardness of weldments; however, the results show a change in the influence of parameters from one study to another. Nevertheless, according to the literature, the welding current had mostly higher control over the final weldment properties.

This work aims to optimize the GTAW welding process to produce reliable and quality S235JR structural steel weldments. GTAW is not familiar with welding structural steel; however, more research is needed to investigate the potential for GTAW to enhance structural steel weldments and increasingly emerge in the industry along with common techniques such as SMAW and GMAW in steel welding. The parameters that could have higher order effects have been included in addition to the groove shape, as it has not been commonly reported, as well as the welding current and welding speed as welding parameters. The objective of this study is to improve the tensile strength and hardness for quality and reliable weldment. The influence of each response was determined by the Taguchi method, while the effect of tensile strength and hardness was computed by the Grey Relational Analysis (GRA) method in multi-response optimization. In addition, the impact weights of the parameters on the objective functions were computed with the aid of the analysis of variance (ANOVA) approach.

## 2. MATERIALS AND METHODS

The structural steel also called low-alloy steel grade S235JR follows European Steel and Alloy (1.0038) is common in the local market in plate form. The plate that is 10 mm in thickness was cut by a computer numerical control (CNC) laser cutter in the Tasamim workshop at Benghazi to 50 mm by 450 mm. These rectangular shapes will bear the tensile strength and hardness samples after the welding process. The tensile strength samples followed the American Society of Testing Materials (ASTM) E8 / E8M [18] as shown in Figure 1. The grooves took V and X-like shapes with 60° for each angle (Figure 1). After the welding process, the rectangular parts were shaped into tensile samples by cutting through the reduced section (Figure 1), and those excess parts were taken to test the hardness of weldments. The welding of the samples has taken place at Altaibat Food Inc. The welded samples (weldments) are seen in Figure 2. The welding was processed using a power supply GTAW with tungsten as an electrode, a Daewoo Inverter Welder, tungsten inert gas / manual metal arc welding TIG/MMA, and a welding speed device that controls the electrode, the YSG-12 Beetle Portable Gas Cutter. The shielding gas for welding used is composed of 90% Ar and 10% carbon dioxide (CO<sub>2</sub>) with a flow rate of 10 L/min. Normally, a binary gas mixture of 80% Ar and 20% CO<sub>2</sub> is common in the welding of structural steel in the local industry, and 95% Ar and 5% CO<sub>2</sub> in other countries as shielding gas. The Ar protects the weld pool from atmospheric oxidation while the CO<sub>2</sub> promotes penetration depth in steel welding although in cases sputtering [19] (Mariappan et al., 2021). However, a study by Murali et al. showed slightly decreased tensile strength for alloy steel welded using 80% Ar and 20% CO<sub>2</sub>

mixture gas compared to pure Ar [20]. The welding filler utilized for welding is mild steel E6013 with a size of 2.5 mm. Table 1 lists the composition of the base metal and filler wire. Table 2 obtain the tensile strength and hardness properties of the structural steel or base metal and welding filler.

The parameters that vary in GTAW are welding current (A), welding speed (B), and groove shape (C) as mentioned earlier each has two levels, as listed in Table 3. The voltage is estimated to be between 20 V and 30 V. The welding experiments follow the 2-level's three parameters, resulting in a total of 8 runs as seen in codes in Table 4. This method is known as Taguchi's L8 array. Table 5 lists the experiments with the results, the tensile strength, and hardness values. The analysis was computed by Minitab 18®.

The tensile test was performed on the universal testing machine Shimadzu (UEH-20) at the Libyan Iron and Steel Company. The samples following the test are shown in Figure 3 presenting fractures in the welding area. The samples that failed quickly were repeated to guarantee the consistency of the results. The hardness test was carried out by Ernst Rockwell with a pressure force of 100 kg (HRB) and ball indenter sized 1/16 at the College of Mechanical and Engineering Technology. The tensile strength and Rockwell hardness HRB are presented in Table 5.

The heat input generated by welding as presented in Table 5 was calculated from Equation 1:

$$H = \frac{f_1 \times E \times I}{v} \quad (1)$$

Where  $f_1$  is the heat transfer factor or efficiency (0.6),  $E$  is the voltage (V),  $I$  is the current (A), and  $v$  is the travel speed (mm/s). The voltage was considered 30 V knowing that voltage of the welder machine reduces with working time due to the decreased efficiency.

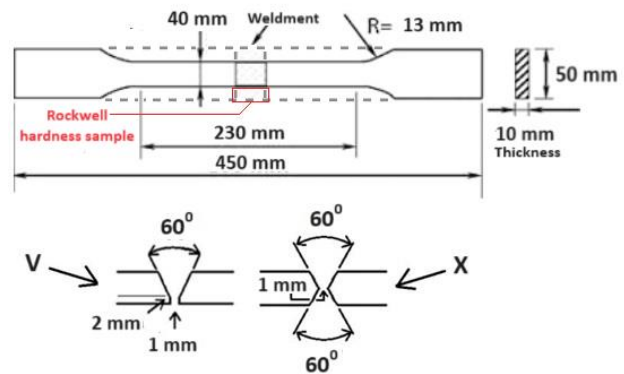


Fig.1. Samples dimensions for tensile test made according to ASTM E8/E8M [18]

Table 1. The chemical compositions of the base metal and welding filler used in the experiment [21]

Component	Composition									
	C	Mn	S	Ni	Cr	P	Si	Cu	Mo	V
Base metal (S235JR)	0.17%	1.4%	0.025%	0.012%	-	0.025%	-	0.55%	-	-
Welding filler (E6013)	0.10%	0.6%	0.03%	0.3%	0.2%	0.035%	0.5%	0.35%	0.2%	0.05%



Fig.2. Weldments

**Table 2. The tensile strength and hardness of base metal and welding filler** <sup>[22,23,24]</sup>

Component	Tensile properties		Hardness properties	
	Yield strength	Tensile strength	Elongation	Rockwell hardness B
Base metal (EN 10025-2)	235	360-510	26%	66.7 HRB
Filler wire (E6013)	458MPa (66.5ksi)	527MPa (76.5ksi)	25%	83 HRB

**Table 3. Parameters of the welding process each has two levels**

Code	Parameters	Unit	Level 1	Level 2
A	Welding current	A	170	200
B	Welding speed	mm/min	100	150
C	Groove shape	-	V	X

**Table 4. The orthogonal array layout L8 (2<sup>3</sup>) in a coded layout**

Trial	A	B	C
1	1	1	1
2	1	1	2
3	1	2	1
4	1	2	2
5	2	1	1
6	2	1	2
7	2	2	1
8	2	2	2

**Table 5. The experiments L8 and their corresponding responses (Tensile strength and hardness)**

Trial	Welding current (A)	Welding speed (mm/min)	Groove shape	Tensile strength (N/mm <sup>2</sup> )	Heat input (J/mm)	Hardness (HRB)	EL %
1	170	100	V	232	1836	82.5	4
2	170	100	X	202	1836	80.7	3
3	170	150	V	219	1224	84.8	4
4	170	150	X	191	1224	83.5	3
5	200	100	V	184	2160	83.8	3
6	200	100	X	158	2160	81.6	3
7	200	150	V	205	1440	80.4	4
8	200	150	X	169	1440	78.1	3



Fig.3. Weldments after tensile test showing fracture in the welds (FZ and HAZ)

### 3. RESULTS AND DISCUSSION

#### a. Effect of Welding Parameters on the Mechanical Properties

Table 5 illustrates how tensile strength has frequently increased with decreasing hardness and vice versa. For instance, the welding hardness increased from 82.5 HRB to 84.8 HRB at 170 A due to the lowered tensile strength from 232 to 219 N/mm<sup>2</sup> at V-groove-shaped weldments-shaped welding samples or trials. The enhanced tensile strength from 158 to 169 N/mm<sup>2</sup> at X-groove-shaped weldments-shaped welding samples, however, revealed a drop in welding hardness from 81.6 HRB to 78.1 HRB at 200 A. With an increase in welding speed, there has also been variation in the tensile strength. Overall, the increase in welding current from 170 A to 200 A and the rise in average heat input, which is influenced by welding speed and welding current, have resulted in a loss in tensile strength and hardness. In addition, it was greater at welding samples with V-groove-shaped weldment shapes. The sample elongated to 4% increase in length at a tensile strength of 232 N/mm<sup>2</sup>, compared to 3% at 158 N/mm<sup>2</sup>, indicating that the elongation was higher at the increased tensile strength.

Table 5 illustrates how increased welding current with decreased welding speed led to increased welding heat input. Equation 1 is used to compute the welding heat input. For instance, in trials 1 and 5 in Table 5, the welding current rose from 170 to 200 A, resulting in an increase in the heat input from 1836 to 2160 J/mm. Additionally, the heat input has dropped from 1836 to 1224 J/mm due to the higher welding speed of 100 to 150 mm/min.

Increased internal tensions resulting from the fusion zone's greater dilution caused by the welding's prolonged heat [25]. Lower weldment tensile strength and hardness in

the welding looked to be a result of the greater internal stresses. Table 5 makes it evident that increased heat input was observed at increased welding amperage, which is correlated with decreased hardness and tensile strength. The Taguchi method study will include a presentation of the increased influence of welding current later on. The samples with lower weldment tensile strength are the ones that were manufactured at an X-groove shaped weldments shape and the samples made at a V-groove shaped weldments shape at a higher welding current (200 A), as shown in Figure 3 for samples (trials) 2, 4, 5, 6, 7, and 8. A longer cooling rate is a result of the increased heat input from a microstructural standpoint. As a result, the welding area has coarser grains due to a longer microstructural recrystallization time [26]. In a previous similar study made on structural steel welded by GTAW, it was found that faster welding speeds led to reduced heat input, coarser  $\alpha$ -ferrite grain formation, and less carbide and Widmanstatten ferrite in the welding area. Higher weldment tensile strengths in welding have resulted from it [27]. While lower heat input due to lower welding current has caused the formation of finer  $\alpha$ -ferrite and increased precipitation of Widman Tatten ferrite, a study by Abima et al. on low-carbon steel welding metallurgy agrees that lower heat input has increased welding weldment tensile strength and HAZ hardness [16]. The data do not clearly show that increased weldment tensile strength is a function of increased welding hardness. As was previously mentioned, the welding tensile strength has been demonstrated to be influenced by the groove shape, and the dilution is the outcome of the welding heat input caused by the welding current. As Table 2 illustrates, the tensile strength of welding has generally been demonstrated to be lower than the tensile strength of base metal and welding filler. As Table 2 illustrates, the hardness of the welding was comparable to that of the welding filler. Stated

differently, the weldment tensile strength of the welding was unaffected by the hardness differential between the welding area and the nearby base metal. The failure at the edge of the welding region due to the softening of HAZ is believed to be caused by increased heat input, which led to increased strains in the welding area, even if the dilution wasn't higher for the experiments that were exposed to lower heat input. It was stated that HAZ has larger residual stresses than the welding area [28], and its softening is the cause of the hardness loss [29].

**b. Taguchi Method**

The primary impacts of signal-to-noise (S/N) ratios for tensile strength and hardness are presented in Table 6, while the plot for mean S/N ratio for tensile strength and hardness are shown in Figures 4 and 5, respectively. S/N ratio demonstrates the impact of the welding settings measuring the noise level under various noise situations for the response.

**Table 6. S/N ratios correspond to the tensile strength and hardness values**

Trial	Welding current (A)	Welding speed (mm/min)	Groove shape	Tensile strength S/N ratio	Hardness S/N ratio
1	170	100	V	47.3098	38.3291
2	170	100	X	46.1070	38.1375
3	170	150	V	46.8089	38.5679
4	170	150	X	45.6207	38.4337
5	200	100	V	45.2964	38.4649
6	200	100	X	43.9731	38.2338
7	200	150	V	46.2351	38.1051
8	200	150	X	44.5577	37.8530

The experiment goal, which is to maximize the responses as indicated by equation 2, is correlated with the greater S/N ratio, which is designated as "Larger is Better".

$$\frac{S}{N} = -10 \log\left[\frac{1}{n} \sum_{i=1}^n \frac{1}{y_i^2}\right] \quad (2)$$

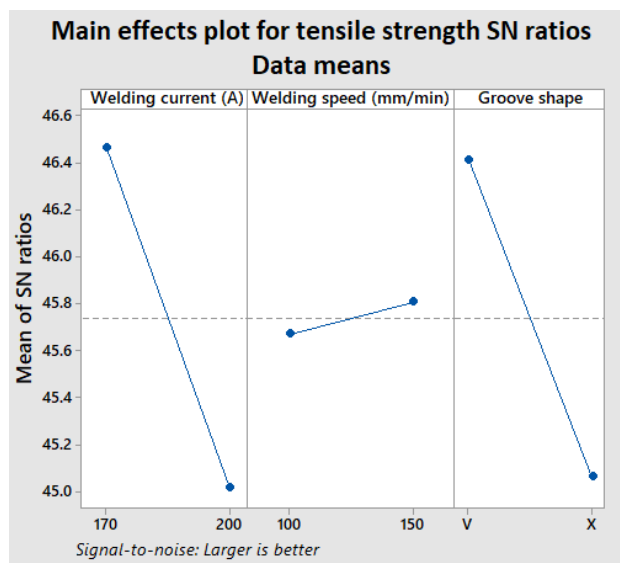


**Fig.4. Main effect plot of S/N ratios for weldments tensile strength**

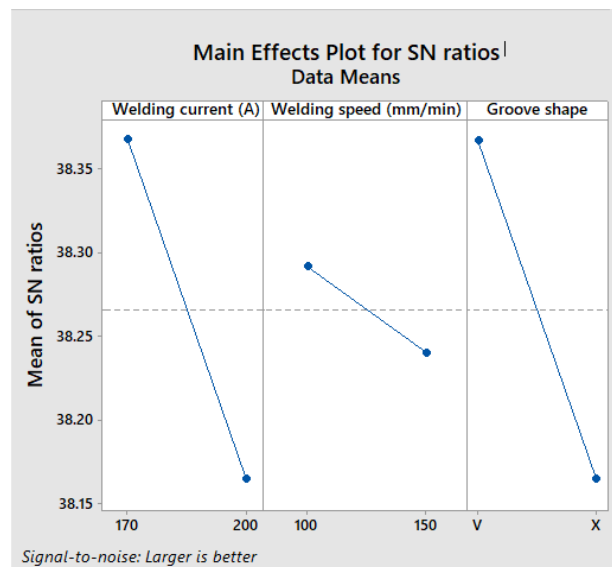


**Fig.5. Main effect plot of S/N ratios for weldments hardness**

The means of S/N ratios that are presented in Figure 4 and Figure 5 are listed in Table 7 and Table 8 respectively. The ranking in Table 7 and Table 8 are based on the higher delta value, which is the result of the S/N ratio of level 1 minus the value of level 2. The ranking presents the relative strength of each factor. As shown in Table 7, a welding current of 170 A has a greater S/N ratio (46.46) than a welding current of 200 A

(45.02). Comes second to the V-groove shaped weldments-shaped welding demonstrated a higher S/N ratio (46.41), compared to the X-groove shaped weldments-shaped welding, which demonstrated a 45.06 noise ratio. These values correspond to level 1 and level 2, respectively. As indicated by 150 mm/min, the welding speed had the least impact on the increased tensile strength, with a noise ratio of 45.67. The welding current 170 A and groove shape V both had the same ranking, thus similar impact on the weldment hardness. The welding current was ranked first in Table 7 and Table 8, which indicates it has higher influence or impact on the tensile strength and hardness of weldments.

The ANOVA in Table 9 and Table 10 confirm Taguchi's showing the higher contribution of welding current by 19.32 % and 1.59 % on the effect of the tensile strength and hardness respectively. The contribution values are listed as F in the tables. However, the P-value (population value) for the welding parameter has shown non-significant on the weldment hardness (Table 10) since the level of significance taken is 0.05. While the welding current and groove shape have shown a significance impact on the tensile strength (0.012 and 0.015 respectively) as presented in Table 9.

**Table 7. Ranking for means of S/N ratios for weldments tensile strength**

Level	Welding current (A)	Welding speed (mm/min)	Groove shape
1	46.46	45.67	46.41
2	45.02	45.81	45.06
Delta	1.45	0.13	1.35
Rank	1	3	2

\*Larger is better

**Table 8. Ranking for means of S/N ratios for weldments hardness**

Level	Welding current (A)	Welding speed (mm/min)	Groove shape
1	38.37	38.29	38.37
2	38.16	38.24	38.16
Delta	0.20	0.05	0.20
Rank	1	3	2

\*Larger is better

**Table 9. ANOVA for tensile strength S/N ratios**

Source	DF	Seq SS	Adj SS	Adj MS	F	P
Welding current (A)	1	4.18187	4.18187	4.18187	19.32	0.012
Welding speed (mm/min)	1	0.03592	0.03592	0.03592	0.17	0.705
Groove shape	1	3.63354	3.63354	3.63354	16.79	0.015
Residual Error	4	0.86572	0.86572	0.21643		
Total	7	8.71705				

**Table 10. ANOVA for hardness S/N ratios**

Source	DF	Seq SS	Adj SS	Adj MS	F	P
Welding current (A)	1	0.082290	0.082290	0.082290	1.59	0.276
Welding speed (mm/min)	1	0.005276	0.005276	0.005276	0.10	0.766
Groove shape	1	0.081805	0.081805	0.081805	1.58	0.277
Residual Error	4	0.207438	0.207438	0.051859		
Total	7	0.376809				

**c. Grey relational analysis (GRA)**

GRA is a technique developed to solve multi-objective or multi-response optimization. In order to obtain optimum tensile strength and hardness of weldments<sup>30</sup>. First, normalization was made on the response results by Equation 3 and shown in Table 11.

$$Y_i^*(k) = \frac{y_i(k) - \min(y_i(k))}{\max(y_i(k)) - \min(y_i(k))} \quad (3)$$

Where  $i = 1, \dots, m$ ;  $k = 1, 2, \dots, n$ ;  $m$  is the number of experimental data,  $n$  is the number of factors,  $y_i(k)$  = original sequence,  $Y_i^*(k)$  = value after grey relational generation (GRG),  $\min y_i(k)$  is the minimum value of  $y_i(k)$  and  $\max y_i(k)$  is its maximum value. The grey relational coefficient (GRC) is computed by Equation 4 and the coefficients are shown in Table 12.

$$\varepsilon_j(k) = \frac{\Delta_{\min} + \omega \Delta_{\max}}{\Delta_{oi}(k) + \omega \Delta_{\max}} \quad (4)$$

Where,  $\Delta_{oi}$  is the deviation among  $Y_0^*(k)$  and  $Y_i^*(k)$ ,  $Y_0^*(k)$  is the ideal reference sequence,  $\Delta_{\min}$  is the least value of  $\Delta_{oi}(k)$  and  $\Delta_{\max}$  is the highest value of  $\Delta_{oi}(k)$ . Table 4 gives the calculated Grey relation coefficients. The grey rational grade (GRG) is calculated by Equation 5 and shown in Table 12.

$$\Gamma_i = \frac{1}{n} \sum_1^Q i(k) \quad (5)$$

Where,  $Q$  = total quantity of responses  $n$  is the number of output responses, while  $i$  is the level of the relationship between the reference and the comparative sequence. The means plot S/N ratio for GRG is shown in Figure 6, while Table 13 shows the ranking based on the S/N means and Table 14 presents the ANOVA.

**Table 11. Normalization of tensile strength and hardness results**

Trial	Welding current (A)	Welding speed (mm/min)	Groove shape	Tensile strength (Normalized)	Hardness (Normalized)
1	170	100	V	1.000	0.666
2	170	100	X	0.640	0.398
3	170	150	V	0.060	0.019
4	170	150	X	0.494	0.812
5	200	100	V	0.397	0.856
6	200	100	X	0.000	0.010
7	200	150	V	0.678	0.353
8	200	150	X	0.175	0.000

**Table 12. GRC and GRG for the tensile strength and Hardness**

Trial	Welding current (A)	Welding speed (mm/min)	Groove shape	Tensile strength GRC	Hardness GRC	GRG	S/N
1	170	100	V	1.429471	1.4742	1.451836	3.23835
2	170	100	X	0.495935	0.494022	0.494978	-6.10828
3	170	150	V	1.401621	1.449979	1.4258	3.08117
4	170	150	X	1.414338	1.479786	1.447062	3.20974
5	200	100	V	1.411469	1.481461	1.446465	3.20616
6	200	100	X	1.399882	1.44966	1.424771	3.07490
7	200	150	V	1.419805	1.462378	1.441092	3.17383
8	200	150	X	1.404977	1.449297	1.427137	3.08931

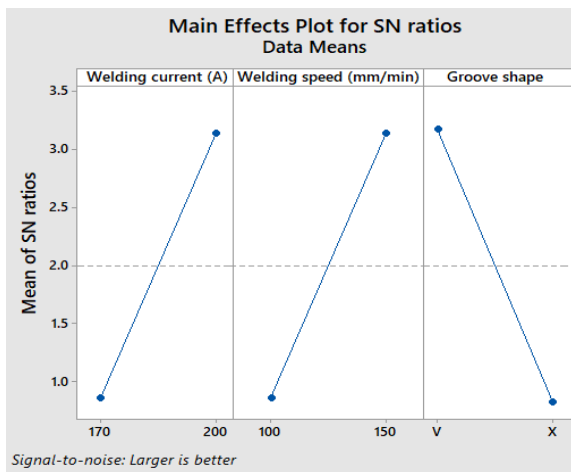


Fig.6. Main effect plot of S/N ratios for GRG

Table 13. Ranking for means of S/N ratios for GRG

Level	Welding current (A)	Welding speed (mm/min)	Groove shape
1	0.8552	0.8528	3.1749
2	3.1361	3.1385	0.8164
Delta	2.2808	2.2857	2.3585
Rank	3	2	1

Table 14. ANOVA for GRG S/N ratios

Source	DF	Seq SS	Adj SS	Adj MS	F	P
Welding current (A)	1	10.40	10.40	10.40	0.97	0.381
Welding speed (mm/min)	1	10.45	10.45	10.45	0.97	0.381
Groove shape	1	11.12	11.12	11.12	1.03	0.367
Residual Error	4	43.11	43.11	10.78		
Total	7	75.08				

The S/N ratio with optimal conditions is predictable by Equation 6:

$$\eta_{opt} = \eta_m + \sum_{i=1}^f (\bar{\eta}_i - \eta_m) \quad (6)$$

Where  $\eta_m$  = the mean of S/N ratio means,  $f$  = the number of parameters,  $\eta_i$  = the mean of the signal-to-noise ratios at the optimal level of each factor  $i$ .

Table 13 shows that groove shape has shown a higher rank which indicates it has a higher impact on the tensile strength and hardness and it showed a higher contribution on the response influence according to the F value in Table 14. However, none of the welding parameters has presented significance on both the tensile strength and hardness based on ANOVA.

It is evident from Taguchi method that the welding speed has the least impact on the weldment’s tensile strength and weldment hardness, while the welding current, has demonstrated a stronger influence. The GRA showed based on multi-response analysis that groove shape showed a higher impact on the responses. The optimal welding conditions according to GRA are 170 A, V-shaped welding, and 150 mm/min.

#### 4. CONCLUSIONS

Structural steel was welded using GTAW with various welding settings. The effects of a combination of welding current, welding speed, and groove form on the hardness and weldment welding tensile strength were investigated. The Taguchi method is applied to the analysis. The outcomes showed that reduced welding current led to higher welded tensile strength. The tensile strength of the welding samples with a V-groove-shaped weldments was higher than that of the samples with an X-groove-shaped weldments. According to Taguchi, the welding tensile strength is mostly influenced by the welding current, with the groove shape having a somewhat similar effect. The welding speed has the least impact on the tensile strength. Furthermore, the GRA showed that groove shape had a higher effect on multi-response analysis. The welding factor's optimum combination is 170 A, groove shape V, and a welding speed of 150 mm/min.

#### 5. ACKNOWLEDGMENT

The author would like to thank his family for their support and encouragement throughout this study. A sincere appreciation goes to the Libyan Iron and Steel

Company for their help, to the staff of the welding laboratory at Altaibat Food Inc. An appreciation goes to the College of Mechanical Engineering Technology, Benghazi.

## 6. REFERENCES

- Mohanty S, Mohanta GK, Senapati AK, Rath KC. Taguchi grey relational analysis for optimal process parameter of low carbon steel welded by GTAW by using ER309L filler material. *Mater Today: Proc*, 2021;44:2556-2561.  
<https://doi.org/10.1016/j.matpr.2020.12.631>
- Assefa AT, Ahmed GMS, Alamri S, Edacherian A, Jiru MG, Pandey V, et al. Experimental investigation and parametric optimization of the tungsten inert gas welding process parameters of dissimilar metals. *Mater*, 2022;15(13): 4426.  
<https://doi.org/10.3390/ma15134426>.
- Shrivastava M, Kumar R. Optimization of GTA welding parameters for AISI 304 stainless steel using Taguchi method. *Int. Conf. Adv. Res. Innov.* 2020. Available from:  
[https://papers.ssrn.com/sol3/papers.cfm?abstract\\_id=3566687](https://papers.ssrn.com/sol3/papers.cfm?abstract_id=3566687)
- İrsel G. Study of the microstructure and mechanical property relationships of shielded metal arc and TIG welded S235JR steel joints. *Mater Sci Eng A*. 2022; 830:142320.  
<https://doi.org/10.1016/j.msea.2021.142320>
- Dubey Y, Sharma P, Singh MP. Experimental investigation for GTAW optimization using genetic algorithm on S-1 tool steel. *Mater Today: Proc*. 2023.  
<https://doi.org/10.1016/j.matpr.2023.02.174>
- Hariprasath P, Sivaraj P, Balasubramanian V, Pilli S, Sridhar K. Effect of the welding technique on mechanical properties and metallurgical characteristics of the naval grade high strength low alloy steel joints produced by SMAW and GMAW. *CIRP J Manuf Sci Tech*, 2022;37:584-595.  
<https://doi.org/10.1016/j.cirpj.2022.03.007>
- Liu X, Guo Z, Bai D, Yuan C. Study on the mechanical properties and defect detection of low alloy steel weldments for large cruise ships. *Ocean Eng*. 2022; 258:111815.  
<https://doi.org/10.1016/j.oceaneng.2022.111815>
- Zhao D, Bezgans Y, Vdonin N, Radionova L, Glebov L, Bykov V (2023). Metallurgical and mechanical attributes of gas metal arc welded high-strength low-alloy steel. *Int J Adv Manuf Tech*. 2023; 225(3):1305-1323.
- Sakthivel P, Manobbala V, Manikandan T, Salik ZMA, Rajkamal G. Investigation on mechanical properties of dissimilar metals using MIG welding. *Mater Today: Proc*. 2021; 37:531-536.  
<https://doi.org/10.1016/j.matpr.2020.05.488>
- Jiang J, Peng ZY, Ye M, Wang YB, Wang X, Bao W. Thermal effect of welding on mechanical behavior of high-strength steel. *J Mater Civ Eng*. 2021;33(8):04021186.  
[https://doi.org/10.1061/\(ASCE\)MT.1943-5533.000383](https://doi.org/10.1061/(ASCE)MT.1943-5533.000383)
- Yadav AK, Agrawal MK, Saxena KK, Yelamasetti B. Effect of GTAW process parameters on weld characteristics and microstructural studies of dissimilar welded joints of AA5083 and AA6082: optimization technique. *Int J Interact Des Manuf*. 2023;1-10.  
<https://doi.org/10.1007/s12008-023-01230-x>
- Korkmaz E, Meran C. Mechanical properties and microstructure characterization of GTAW of micro-alloyed hot rolled ferritic XPF800 steel. *Eng Sci Tech Int J*. 2021;24(2):503-513.  
<https://doi.org/10.1016/j.jestch.2020.04.006>
- Hamzaçebi C. Taguchi method as a robust design tool. In: Li P, Pereira PAR, Navas H, editors. *Quality control - intelligent manufacturing, robust design and charts*. IntechOpen: London, UK; 2020.  
<https://doi.org/10.5772/intechopen.94908>
- Chauhan V, Kärki T, Varis J. Optimization of compression molding process parameters for NFPC manufacturing using Taguchi design of experiment and mold flow analysis. *Proc*. 2021;9(10):1853.  
<https://doi.org/10.3390/pr9101853>
- Karpagaraj A, Parthiban K, Ponmani S. Optimization techniques used in gas tungsten arc welding process-A review. *Mater Today: Proc*. 2020; 27:2187-2190.  
<https://doi.org/10.1016/j.matpr.2019.09.093>
- Abima CS, Akinlabi SA, Madushele N, Fatoba OS, Akinlabi ET. Experimental investigation of TIG-welded AISI 1008 carbon steel. *IOP Conf Ser: Mater Sci Eng*. 2021;1107(1):012036.  
<https://doi.org/10.1088/1757-899x/1107/1/012036>
- Jawad M, Jahanzaib M, Ali MA, Farooq MU, Mufti NA, Pruncu CI, et al. Revealing the microstructure and mechanical attributes of pre-heated conditions for gas tungsten arc welded AISI 1045 steel joints. *Int J Press Vessels Pip*. 2021; 192:104440.  
<https://doi.org/10.1016/j.ijpvp.2021.104440>
- American Society for Testing and Materials. Standard test methods for tension testing of metallic materials (ASTM E8/E8M-21). *ASTM Int* [Internet];2022. Available from:  
[https://doi.org/10.1520/E0008\\_E0008M-21](https://doi.org/10.1520/E0008_E0008M-21)
- Mariappan M, Parthasarathi NL, Ravindran R, Lenin K, Raja A. Effect of alternating shielding gases in gas metal arc welding of SA515 Gr 70 carbon steel. *Mater Res Express*. 2021;8(9):095601.  
<https://doi.org/10.1088/2053-1591/ac21e9>

20. Murali P, Gopi R. Experimental investigation of tungsten inert gas welding (TIG) using Ar/Ar-CO<sub>2</sub> shielding gas on alloy steels. *Mater Today: Proc.* 2021; 39:812-817.  
<https://doi.org/10.1016/j.matpr.2020.09.776>
21. World Material. EN 1.0038 steel S235JR material equivalent, properties, composition [Internet]. 2024 [Cited 21 Mar 2024]. Available from:  
<https://www.theworldmaterial.com/1-0038-steel-s235jr-material/>
22. Weld Wire. E6010 welding electrode properties [Internet]. 2024 [Cited 21 Mar 2024]. Available online:  
[https://www.weldwire.net/weld\\_products/ww6013/](https://www.weldwire.net/weld_products/ww6013/)
23. Ratiwi YR, Wibowo SS, The effect of electrode and number of passes on hardness and micro structure of shielded metal arc welding. *IOP Conf Ser: Mater Sci Eng.* IOP Publ. 2019; 515(1): 012072.  
<https://doi.org/10.1088/1757-899x/515/1/012072>
24. ISO, Metallic Materials - Conversion of Hardness Table, ISO 18265 [Internet]. 2024 [Cited 21 Mar 2024]. Available online:  
<https://www.iso.org/obp/ui/#iso:std:iso:18265:ed-2:v1:en>
25. Sonar T, Balasubramanian V, Malarvizhi S, Venkateswaran T, Sivakumar D. An overview on welding of Inconel 718 alloy-Effect of welding processes on microstructural evolution and mechanical properties of joints. *Mater Charact.* 2021; 174:110997.  
<https://doi.org/10.1016/j.matchar.2021.110997>
26. Araújo HR, Torres EA, Apolinário LHR, Vicente ADA, da Silva Júnior DC Santos TFDA. Evaluation of mechanical performance and microstructural aspects of AISI 304 stainless steel welded joints produced by controlled short circuit GMAW and GTAW. *Weld World.* 2022;66(12):2443-2459.  
<https://10.1007/s40194-022-01383-5>
27. Elfallah S. Effect of GTAW on the tensile strength and hardness of mild steel. *Annals of "Dunarea de Jos" University of Galati. Fascicle XII, Weld Equip Technol.* 2022;33:95-100.  
<https://doi.org/10.35219/awet.2022.08>
28. Britto JG, John RA, Murugesan G, Prabhakaran R, Jeevahan J Mageshwaran G. Enhancement of mechanical properties of alloy steel by GTAW with different purge/shielding gases. *FME Trans.* 2020;48(1):149-154.  
<https://doi.org/10.5937/fmet2001149B>
29. Kumar A, Pandey S M, Sirohi S, Fydrych D, Pandey C. P92 steel and inconel 617 alloy welds joint produced using ERNiCr-3 filler with GTAW process: Solidification mechanism, microstructure, mechanical properties and residual stresses. *Heliyon.*2023; e18959.  
<https://doi.org/10.1016/j.heliyon.2023.e18959>
30. Kumar A, Mukherjee S, Agrawal S. Optimization of parameters of dissimilar gas tungsten arc welding using grey relational analysis. *Int. J. Veh. Struct. Syst.* 2020;12(2):157-161.  
<https://doi.org/10.4273/ijvss.12.2.09>



# Experimental Investigation of Steel Corrosion in Concrete Structures by Acoustic Emission Analysis

Hisham A. Elfergani <sup>1\*</sup>

*1 Mechanical Engineering Department- Faculty of Engineering- University of Benghazi.*

Received: 29 / 03 / 2024; Accepted: 16 / 05 / 2024

## ABSTRACT

Corrosion represents a significant issue in various structures, with reinforced and prestressed concrete particularly susceptible. In certain applications, it demands specific attention and mitigation strategies, special attention must be paid to ensure that failure does not occur, as it could lead to loss of life and incur significant financial expenses.

This paper examines the role of Acoustic Emission (AE) as a non-destructive testing (NDT) technique for reinforced concrete structures. The work focuses on the development of experimental techniques and data analysis methods for the detection, location, and assessment of AE from reinforced concrete specimens due to steel wire corrosion.

The results reveal that AE can be used to detect the onset of corrosion activity in wire in the interface between prestressed concrete and mortar as found in prestressed concrete pipes.

It has been shown that by using AE and the relationship between RA and AF value, the crack area can be located and identified. Hence, it could be possible to provide a corrosion alarm and location prior to any wire breaks. Furthermore, the results offer encouragement for the use of the AE technique to detect early corrosion and macro cracks in large concrete pipe structures.

**KEYWORDS:** Acoustic Emission, Steel Corrosion, reinforced concrete, prestressed concrete.

## 1. INTRODUCTION

Corrosion of steel is a significant problem in numerous reinforced and prestressed concrete structures. It is reported that the costs of repair and maintenance of corroded structures exceed billions of dollars per year <sup>[1, 2]</sup>. For example, the projected yearly direct expense of corrosion for U.S. highway bridges totals \$13.6 billion, with approximately 40% stemming from corrosion in traditional reinforced concrete (RC).<sup>[3]</sup> Infrastructure maintenance and the resulting downtime caused by steel corrosion and its associated issues consume a significant portion of the annual budget allocated for civil structures in numerous countries. The costs vary depending on the condition of the concrete structures, including the cause of damage, degree of damage, and effect of damage on structural behaviour. The risk of corrosion in this particular type of structure requires careful attention as failure could lead to either loss of life in extreme cases or, at the very least, financial losses.

For example, in the collapse of the Polcevera viaduct in Genoa (2018, Italy), which killed 43 people and injured 16, corrosion played a significant role in the collapse, exerting a devastating impact on the inadequately robust design featuring RC stay cables. Additionally, the abrupt collapse of a residential building in Miami (2021, USA), resulting in the loss of 97 lives, was linked to the deterioration of the RC substructure in a marine setting <sup>[3]</sup>.

The majority of studies suggest that the primary cause of failure in buildings, bridges, and concrete pipes is corrosion occurring shortly after their construction.

The primary factors leading to the initiation of corrosion in reinforcing and prestressing steel are the infiltration of chloride ions and carbon dioxide onto the steel surface. Once corrosion begins, the resultant corrosion products, typically iron oxides and hydroxides, are commonly deposited within the confined space in the concrete surrounding the steel. Their formation within this confined area generates expansive stresses, leading to cracking and spalling of the concrete cover. Consequently, this process leads to the gradual deterioration of the concrete. <sup>[4]</sup>

Reinforced concrete is recognized as one of the most extensively used building materials. It is relatively cheap, due to the availability of raw materials, versatile,

\*Correspondence: Hisham A. Elfergani

[Hisham.elfergani@uob.edu.ly](mailto:Hisham.elfergani@uob.edu.ly)

allowing a wide range of forms and applications, and durable if designed and executed in a proper way. The primary factor leading to the degradation of reinforced concrete structures is the corrosion of the steel reinforcement within them.

As a consequence, the expenses associated with repairs constitute a significant portion of current infrastructure spending. Ensuring quality control, maintenance, and planning for the restoration of these structures necessitates non-destructive inspection and monitoring techniques capable of detecting corrosion at an early stage.

The infrastructure of water-carrying concrete pipes has experienced corrosion issues. For instance, the pipes employed in The Man-Made River Project of Libya have experienced this issue. Five instances of pipe failures resulting from corrosion have been documented since their installation. The primary cause of the damage is the corrosion of prestressed wires within the pipes, which occurs due to the penetration of chloride ions from the adjacent soil. Detection of the corrosion in its early stages is very important to avoid water interruption to homes and industries.

The Acoustic Emission (AE) technique has found extensive application in civil engineering for structural health monitoring. Its advantages over other non-destructive techniques include the ability to pinpoint the location of developing cracks and the capability to test the entire structure without disrupting its operation.

Acoustic emission refers to the generation of transient elastic waves resulting from the rapid release of energy from localized sources within a material. AE is generated and propagates during the formation and spreading of cracks in all materials. It can also be defined as the sudden release of elastic waves caused by the rapid energy discharge from localized sources within a material [5]. This abrupt release of elastic energy, known as the AE event, travels through the structure until it reaches the location where a piezoelectric transducer is installed. These transducers identify surface displacement at various points and transform it into a functional electrical signal. Analysing the resulting waveform based on characteristics such as amplitude, energy, and time of arrival enables the evaluation of the severity and origin of the AE source as illustrated in Figure 1.

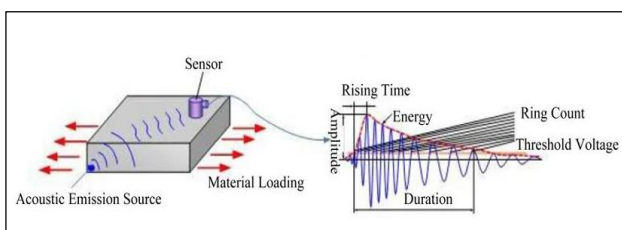


Fig. 1: Acoustic Emission Testing [5].

AE parameters such as amplitude, rise time, average frequency, signal strength, and energy can be further analysed to assess the extent of damage and characterize it. Numerous researchers have devised methodologies for assessing the severity of damage and categorizing cracks using acoustic emission (AE) signal parameters. These methods have used information on the hits, amplitude, frequency, and wave energy [6].

As per multiple studies (references [7, 8, 9, 10, 23, 24, 25]), the connection between RA values (rise time/amplitude) and average frequencies (counts/duration) can serve to categorize different stages of damage in structures. Their findings indicate that a low average frequency and a high RA value in an AE signal denote a shear-type crack, while a high average frequency coupled with a low RA value signifies a tensile-type crack as shown in Figure 2.

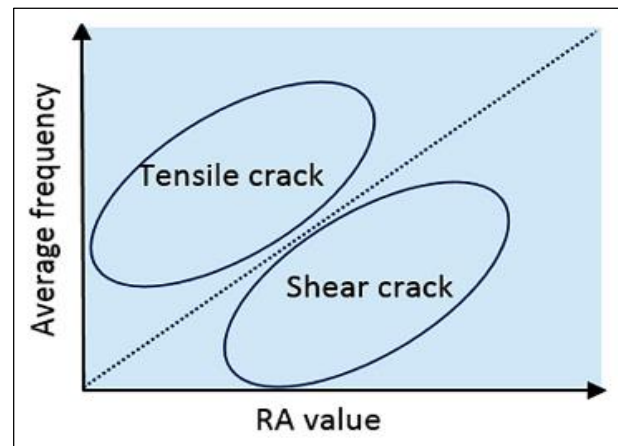


Fig. 2: Crack classification [4]

Concrete pipes used for water transportation are a prime example of structures that have been affected by corrosion. For example, the pipes of The Man-Made River project of Libya have suffered from the effect of corrosion. Five pipe failures have occurred due to corrosion since their installation. This project conveys water through an extensive network of nearly 4000 kilometers of Prestressed Concrete Cylinder Pipe (PCCP) infrastructure [3, 11, 12].

The construction of the concrete pipe involves a 4.0meter diameter, 7.5 meters length and 225 mm thick concrete core encased within a steel cylinder and externally reinforced by prestressed wires. High-tensile steel wires are applied through over-wrapping at a close interval under uniform tension. These prestressed wires are shielded by a 19 mm thick layer of cement mortar. After ten years of operation, there were five severe breakdowns in four-meter-diameter white pipes following a decade of use. The primary cause was the corrosion of the prestressed wires within the pipes, resulting from the assault of chloride ions present in the soil. Early detection of this corrosion is crucial to prevent further pipe failures that could disrupt water flow.

Apart from the ongoing challenge of preventing future corrosion, engineers are actively working to identify the most effective methods for detecting corrosion and halting the deterioration of these pipes [17]. The objective of the Man-Made River project is to employ the Acoustic Emission (AE) method for identifying the initial phases of corrosion before the degradation and ultimate breakdown of concrete structures occur.

While most non-destructive (NDT) methods employed in the project can identify wire breaks, they lack the capability to detect corrosion. Consequently, areas with substantial damage may remain unnoticed in sections where excavation hasn't taken place. In this context, Acoustic Emission (AE) holds a notable advantage over other non-destructive testing methods. It demonstrated the capability of the AE method for detecting the initial stages of the corrosion process, even before significant damage to the concrete occurs. Moreover, it can gauge the extent of damage being inflicted on the concrete [13, 14, 15, 16, 22].

## 2. EXPERIMENTAL SETUP

### • Wire preparation

As the aim of this study was to replicate the authentic physical environment surrounding the high-strength steel wires in concrete pipes, it was crucial to position and sustain all pertinent wire samples under tension equivalent to 60% of their ultimate tensile strength in PCCP. To achieve this objective a tension frame was designed and constructed. The framework comprises two blocks measuring 190mm x 45mm x 45mm each, along with two threaded steel bars (studding) with a diameter of

20 mm and a length of 500 mm. Two holes (20 mm diameter) and two (6mm) are drilled in each block. The two blocks are connected using two threaded bars secured by eight nuts. The two working high-strength steel wire samples were used. The metallurgical composition and mechanical properties of wire are summarized as follows: Carbon steel (carbon 0.8-0.84%, 0.85-1.00%Mn, 0.030 %Max S, 0.035% Max P, 0.20-0.35% Si) [26]. The wires exhibit a tensile strength of approximately 1738 MPa. The two wire samples were passed through 6 mm diameter holes in the steel blocks and then two modified bolts and nuts. Finally, a steel cylinder was threaded over the wire and then was compressed in a load machine. By adjusting the bolts and nuts, each wire was subjected to a tensile force of 20 kN, which was monitored using strain gauges attached to the wires. [16, 17, 20].

### • Concrete and mortar preparation

The concrete specimen (200\*200\*50mm), representative of the inner pipe was prepared according to the technical specification for PCCP manufacturing used in the Man-Made River Project, which is in accordance with AWWA C301-92 (Standard for Pre-stressed Concrete Pressure Pipe, Steel Cylinder Type, for Water and Other Liquids) [3]. Three days following the casting of the concrete specimen, the wires, along with their holding frame, were positioned on the upper surface of this specimen. Finally, the mortar 200\*200mm and 20 mm thickness was coated on the upper surface of the concrete. The mortar consists of one part cement to not more than three parts fine aggregate by weight [6, 18, 21]. The final construction is shown in Figure 3.



Fig. 3: Concrete and mortar sample

### • Accelerated corrosion technique

In order to examine the impacts of corrosion within a practical timeframe, it may be essential to speed up the beginning phase and at times regulate the corrosion rate as it progresses. To simulate the corrosion of steel wires,

the corrosion cell was induced by an impressed current ( $100\mu\text{A}/\text{cm}^2$ ). This is documented as representing the maximum corrosion rate for concrete under laboratory conditions and has been utilized by numerous researchers in their laboratory experiments, as discussed by Li and Zhang [18]. In this experimental setup, wire corrosion was

induced by applying an impressed current of  $100\mu\text{A}/\text{cm}^2$ . The prestressed wires were integrated into an electrical circuit with the positive pole of the power supplier, while the negative pole was connected to a stainless-steel plate (30\*150 mm) positioned on the upper mortar. A 4% NaCl solution was poured on the surface of the mortar. Silicon sealant was employed to create a pool of the solution on the upper surface.

• *Acoustic emission set-up*

Typically, AE instrumentation comprises transducers, filters, amplifiers, and analysis software. Four AE sensors (R3I – resonant frequency is 30 kHz) were mounted to the surface of the mortar as shown in Figure 4. The four AE sensors were affixed using silicon sealant and secured onto the upper surface of the mortar with a U-shaped plate. This plate was screwed in place to firmly hold down the sensors and ensure effective coupling. Then the sensitivity of the sensors was checked by using the Hsu-Neilson source [19]. The Schematic diagram and a photo of experimental test set up are shown in Figures 4 and 5.

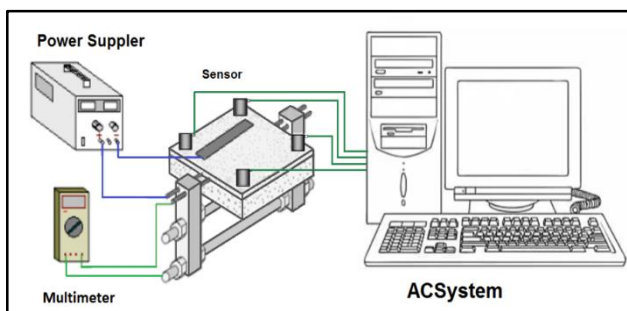


Fig. 4: Detailed schematic view of experimental set-up

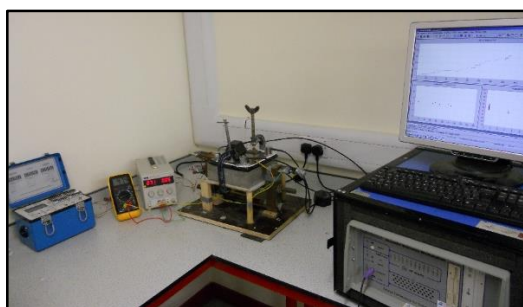


Fig. 5: A Photo of Experimental Set-up

3. RESULTS AND DISCUSSION

Figure 6 depicts a schematic representation of the specimen post-testing, illustrating the placement of sensors on the mortar surface, wire positioning, the stainless-steel plate, and the shape of the crack. Figures 7 display photographic images of the top surface of the mortar after the finish of the test.

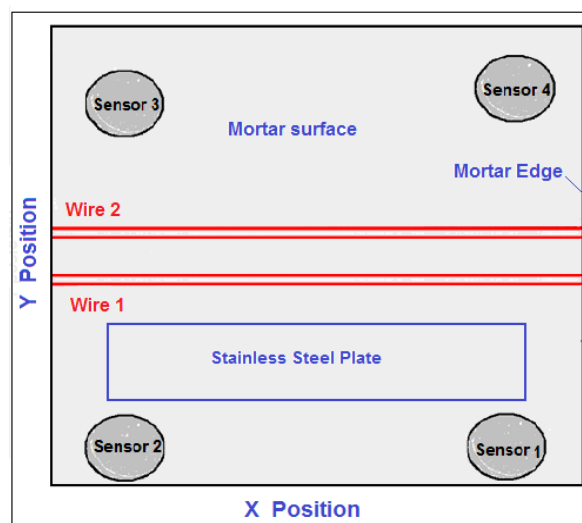


Fig. 6: Schematic Diagram of top mortar surface

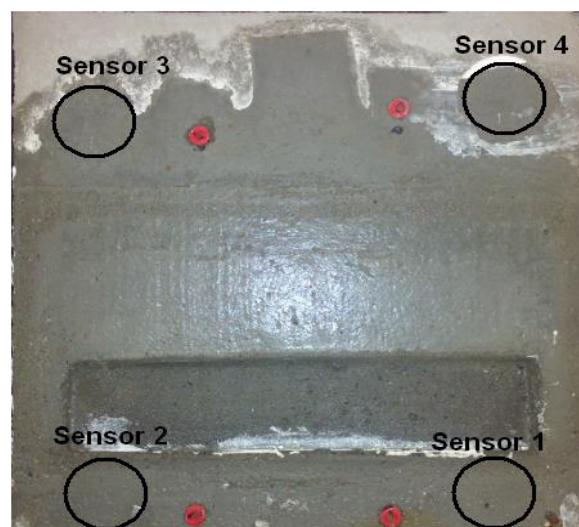


Fig. 7: photo of top mortar surface

Figure 8 shows the cumulative acoustic energy as detected by all sensors with a minimum amplitude 42 dB for almost 100 hr of continuous monitoring. The graph demonstrates the behaviour of the energy emission in two regions of time.

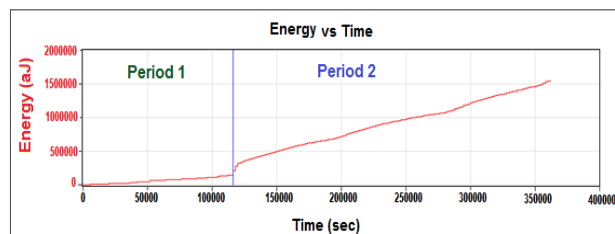
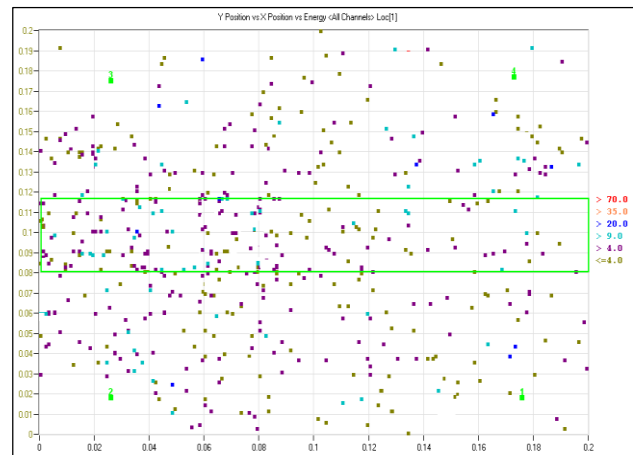


Fig. 8: Energy of detected signals for the duration of the investigation

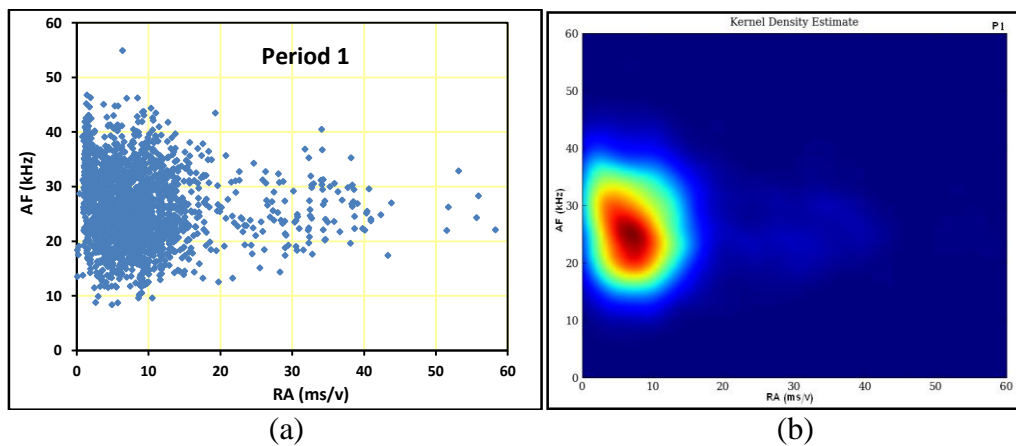
It can be noted that the whole time of the test can be divided into two significant stages as shown in Figure 8, the first stage which is the first 30 hr (0-120,000 sec) is named period 1. There are a small number of hits and with low energy. The second stage which is 70 hr (120000-370000) is named period 2. It can be noted that there is a sudden increase in the number of hits and higher energy emitted is attributed to the onset of corrosion and the build-up of corrosion products on the corroding wire surface.

Figure 9 shows the source location of the sample of period 1 before supplying current (no corrosion) for about 30 hours. It can be seen that there is a low level of events prior to the onset of corrosion. Additionally, a color-coded legend is provided to indicate the number of signals detected at each position.



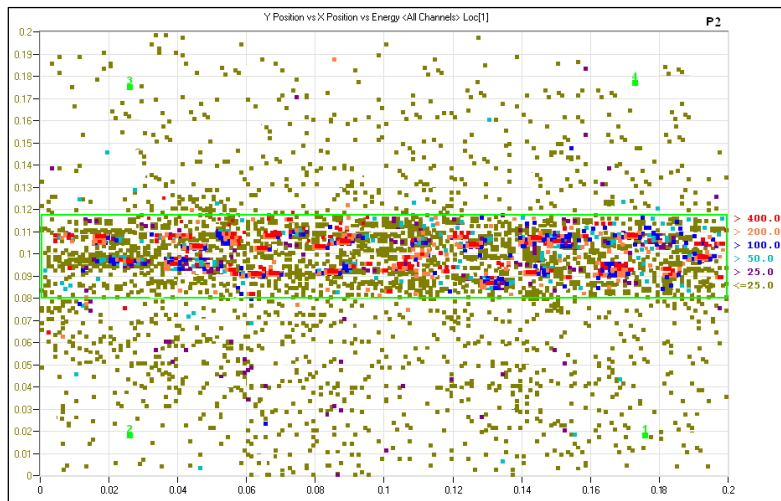
**Fig. 9: Source locations before supplying current (no corrosion)**

Figure 10 (a) illustrates the trends of the relation between the RA-value and AF-value of all hits for period 1 of concentration of events on the surface of the mortar. Furthermore, these areas can be visualised by using Kernel Density Estimation Function (KDEF) as shown in Figure 10 (b). Areas with high concentrations are more readily identifiable. The concentration value of the data is represented by different colours, brown for the highest number of data points and blue for the lowest. It can be noted that the RA vs AF relationship has a broad horizontal distribution (0-20 ms/v) which is representative of non-corrosion signals.



**Fig. 10: Relation between the RA value and AF, (a) graph and (b) Kernel Density Estimation Function**

Figure 11 illustrates the source locations of signals during this period 2. It can be noted that the highest hits concentration and highest energy in the region coincides with the maximum wire corrosion products area which was visibly observed post-test as shown in Figure 12.



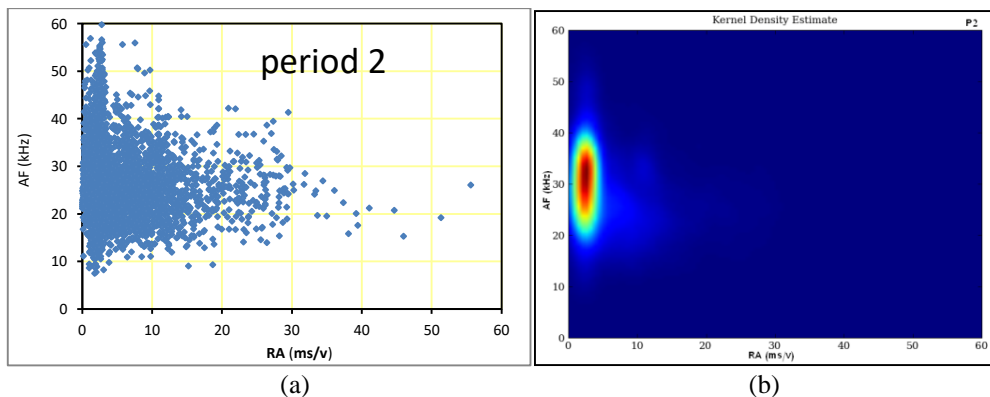
**Fig. 11: Source locations for period 2**

Figure 12 displays the corroded wires and corrosion products after the mortar has been removed. It is evident that significant corrosion occurred in the upper where a vast majority of AE signals were detected and pinpointed.



**Fig. 12: Photo of the upper concrete surface and corroded wires**

Figure 13 illustrates the trends of relation between the RA-value and AF-value of all hits of the period, which are represented via graph and KDEF. It can be seen that the most of data points have various AF values and low RA values (less than 10 ms/v) which are termed a “vertical trend”, this indicates the wire corrosion activity.



**Fig. 13: Relation between the RA value and AF, (a) graph and (b) Kernel Density Estimation Function of period 2**

It has been shown that by using AE and the relationship between RA and AF value, the corrosion area can be located and identified (Figures 11 and 12). Hence, it could be possible to provide a corrosion alarm and location to pipe engineers prior to any wire breaks. Furthermore, it is possible to identify the corrosion activity area before the mortar fails to appear.

#### 4. CONCLUSION

The results demonstrated that the acoustic emission method is an excellent non-destructive method to monitor the different stages of deterioration of concrete structure. It was shown that the AE method is sensitive to detect the stages of steel corrosion prior to the deterioration of reinforced concrete structures. In addition, it can identify the onset of corrosion activity by analysing AE signal parameters and the relationship between RA value and AF value. It was shown that using AE it is possible to give indications of damage at earlier stages than traditional techniques. Furthermore, the results offer encouragement for the use of the AE technique to detect early corrosion and macro cracks in large concrete pipe structures.

#### 5. REFERENCES

- Ann K.Y., Ahn J. H., Ryou J. S. (2009). The importance of chloride content at the concrete surface in assessing the time to corrosion of steel in concrete structures, *Construction and Building Materials*, 23, pp239–245.  
<https://doi.org/10.1016/j.conbuildmat.2007.12.014>
- Zhe L., Zuquan J., Penggang W., Tiejun Z. (2021) Corrosion mechanism of reinforced bars inside concrete and relevant monitoring or detection apparatus: A review, *Construction and Building Materials Journal* Vol. 279, 12 April, pp 122432.  
<https://doi.org/10.1016/j.conbuildmat.2021.122432>
- Verstryngne E., Steen C., Vandecruys E., Wevers M. (2022). Steel corrosion damage monitoring in reinforced concrete structures with the acoustic emission technique: A review, *Construction and Building Materials*, Volume 349, 26 September, 128732.  
<https://doi.org/10.1016/j.conbuildmat.2022.128732>
- Fujian T., Guoshuai Z., Hong-Nan L., Els V. (2021). A review on fiber optic sensors for rebar corrosion monitoring in RC structures, *Construction and Building Materials Journal*, Vol. 313, 27 December, pp 125578.  
<https://doi.org/10.1016/j.conbuildmat.2021.125578>
- Miller R. K., Hill E. V. K., Moore P. O. (2005). *Non-destructive Testing Handbook, Acoustic Emission Testing*, Volume 6, USA.
- Elfergani H. (2024). Acoustic Emission Analysis for Crack Classification and Localization in Prestressed Concrete Structures, *International Science and Technology Journal*, vol. 33, Issue 2, January, pp 1-15.
- JCMS-III B5706. (2003). *Monitoring method for active cracks in concrete by AE*, Tokyo: Japan Construction Material Standards.
- Ohtsu M. and Tomoda Y. (2007). Corrosion process in reinforced concrete identified by acoustic emission, *Materials Transactions*, Vol. 48, No. 6, pp1184-1189.  
<https://doi.org/10.2320/matertrans.I-MRA2007844>
- Ohno K. And Ohtsu M. (2010). Crack classification in concrete based on acoustic emission, *Construction and Building Materials* 24, pp 2339-2346.  
<https://doi.org/10.1016/j.conbuildmat.2010.05.004>
- Aggelis D. (2011). Classification of cracking mode in concrete by acoustic emission parameters, *Mechanics Research Communications* 38, pp153-157.  
<https://doi.org/10.1016/j.mechrescom.2011.03.007>
- Kuwairi A. (2006). Water mining: the Great Man-made River, Libya, *Proceedings of ICE Civil Engineering* 159 May, pp 39-43 paper 14382.  
<https://doi.org/10.1680/cien.2006.159.5.39>
- Essamin O. and Holley M. (2004). Great Man Made River Authority (GMRA): The Role of Acoustic Monitoring in the Management of the World Largest Prestressed Concrete Cylinder Pipe Project, *Proceedings of the ASCE Annual International Conference on Pipeline Engineering and Construction*, August 1-4, San Diego, California.  
[DOI: 10.1061/40745\(146\)28](https://doi.org/10.1061/40745(146)28)
- Ing M., Austin S., Lyons R. (2005). Cover zone properties influencing acoustic emission due to corrosion, *Cement and Concrete Research* 35 pp 284– 295.  
<https://doi.org/10.1016/j.cemconres.2004.05.006>
- Hellier C. J. (2001). *Handbook of Non-destructive Evaluation*, McGraw-Hill, USA.
- Carpinteri A., Lacidogna G., Pugno N. (2007). Structural damage diagnosis and life-time assessment by acoustic emission monitoring. *Engineering Fracture Mechanics* 74, pp273–289.  
<https://doi.org/10.1016/j.engfracmech.2006.01.036>
- Elfergani H., Pullin R., Holford K. (2011). Acoustic Emission Analysis of Prestressed Concrete Structures. *Journal of Physics: Conference Series* 305, 012076.  
<https://doi.org/10.1088/1742-6596/305/1/012076>
- Elfergani H., Pullin R., Holford K. (2013). Damage assessment of corrosion in prestressed concrete by acoustic emission, *Construction & Building Materials Journal*, Vol. 40, pp 925-933.  
<https://doi.org/10.1016/j.conbuildmat.2012.11.071>
- Li X. and Zhang Y. (2008). Analytical Study of piezoelectric Paint for Acoustic Emission-Based Fracture Monitoring, *Fatigue and Fracture of Engineering Materials and Structures* 31, pp. 684-694.  
<https://doi.org/10.1111/j.1460-2695.2008.01249.x>

19. Hsu N N, and Breckenridge, F. R. (1981). Characterization and Calibration of Acoustic Emission Sensor. *Materials Evaluation* 39 (1) pp. 60-68.
20. Shahidan S., Pulin R., Bunnori N. M., Holford K. M. (2013). Damage classification in reinforced concrete beam by acoustic emission signal analysis, *Construction and Building Materials*, Vol. 45, August , pp 78-86.  
<https://doi.org/10.1016/j.conbuildmat.2013.03.095>
21. Elfergani H. (2024). Monitoring Stages of Damage in Concrete Structures by Using the Acoustic Emission Technique, *African Journal of Advanced Pure and Applied* vol. 3, Issue 1, January – Marc, pp 127-133.
22. Liu F., Guo R., Lin X., Zhang X., Huang S., Yang F., Cheng X. (2022). Monitoring the damage evolution of reinforced concrete during tunnel boring machine hoisting by acoustic emission, *Construction and Building Materials Journal*, Vol. 327, 11 April, pp 127000.  
<https://doi.org/10.1016/j.conbuildmat.2022.127000>
23. Lian S., Zheng K., Zhao Y., Bi J., Wang C., Huang Y. (2023). Investigation the effect of freeze–thaw cycle on fracture mode classification in concrete based on acoustic emission parameter analysis, *Construction and Building Materials Journal* Vol. 362, 2 January, pp 129789.  
<https://doi.org/10.1016/j.conbuildmat.2022.129789>
24. Yong N., Xiao-Ping Z., Filippo B. (2020). Evaluation of fracture mode classification in flawed red sandstone under uniaxial compression, *Theoretical and Applied Fracture Mechanics Journal*, Vol. 107, June, 102528.  
<https://doi.org/10.1016/j.tafmec.2020.102528>
25. Abarkane C., Florez-Tapia A., Odriozola J., Artetxe A., Lekka M., García-Lecina E., Grande H., Vega J. (2023). Acoustic emission as a reliable technique for filiform corrosion monitoring on coated AA7075-T6: Tailored data processing, *Corrosion Science* Vol.214, 15 April,110964.  
<https://doi.org/10.1016/j.corsci.2023.110964>
26. ASTM A663/A663M-89. 2000. Specification for Steel Bars, Carbon, Merchant Quality, Mechanical Properties, American Society for Testing and Materials.



# Using the Weather Index Classification System for Canadian Forest Fires over the Al-Jabal Al-Akhdar in Libya

Haifa M. Ben Miloud <sup>1\*</sup>

*1 Atmospheric science - College of Science - Tripoli University.*

Received: 21 / 02 / 2024; Accepted: 26 / 04 / 2024

## ABSTRACT

Due to the noticeable change in temperatures in the world as a whole, fires in forests have become more prevalent in the summer. The current study sheds light on using the Canadian classification of forest burning on Al-Jabal Al-Akhdar in Libya, it aims to study the climatic variation of the fire weather index in Libya for the 24-27<sup>th</sup> day of July at noon for a long period 1940-2022. For Fire Weather Index (FWI) to occur, it is necessary to go through levels and analyze their data. The first level, which is the Fine Fuel Moisture Code (FFMC) code, is high in the middle and extends to the south of the region, while the Duff Moisture Code (DMC) code decreases in the north of the region and increases in the south. However, the Drought Code (DC) code shows the increase and decrease in the south as we head north, while in the second level, the Initial Spread Index (ISI) shows that it is high in the middle of the region. The Build-Up Index (BUI) increases to the south and decreases to the north, and for the occurrence of the Fire Weather Index (FWI) in the third level, it reaches above 60, and thus it is considered very high, and this was clear on the 24th and decreased on the 27th during the period 1940-2022 for July at 12 noon. When dividing the periods from 1940-1981 and 1982-2022, it becomes clear that the first period is more widespread than the second period, and the intensity of the second period is higher than the first period. This indicates climate change in temperatures and the occurrence of drought. Over the coming years, the fire weather index will increase in the future.

**KEYWORDS:** Climate change, Drought Code (DC), Duff Moisture Code (DMC), Fire Weather Index (FWI), Libya.

## 1. INTRODUCTION

Globally speaking, fire is the main cause of disturbance to terrestrial ecosystems. Climate, ecosystems, the cycles of carbon and water, and human activity are all closely related to it <sup>[1]</sup>, so temperature, moisture, and wind the Weather elements that contribute to "hot, dry, and windy" weather conditions direct physical on wild land fires <sup>[2]</sup>, which are a serious natural hazard on ecosystems and populations <sup>[3]</sup>.

Wildland fires pose a serious threat to natural ecosystems in areas with a Mediterranean climate, causing enormous losses in terms of both economic and ecological resources <sup>[4]</sup>. The Mediterranean basin is particularly vulnerable to forest fires, with an estimated yearly average of over 50,000 fires burning an area roughly equivalent to 1.3–1.7% of all Mediterranean forests, but starting in the early 1970s, there has been a noticeable rise in the number of forest fires in Mediterranean basin regions where data dating back to the 1950s are available <sup>[5]</sup>.

According to the IPCC AR6 report, fire weather has changed in some regions (like the Mediterranean) compared to preindustrial times in terms of distribution, duration, and intensity. These changes are predicted to worsen as global warming levels rise <sup>[6]</sup>.

In Libya, a rise in temperatures over the past years has caused several fires to break out in different areas and occasions, including the fire that broke out in an agricultural project near the city of Ghat, in the southwest of the country, which caused major material losses after a large number of palm trees burned in the year 2021 <sup>[7]</sup>. All global models indicated that the summer season is very hot, especially in North Africa during the year 2023, which makes the possibility of the outbreak of more fires possible, especially in forests and agricultural projects, this was evident in the eastern region, where a massive fire broke out in the Ain Mara Forest, due to high temperatures, as well as a huge fire that broke out in the Zala area in the south and caused widespread destruction, burning more than 800 palm trees.

Last summer, the city of Bani Walid, southwest of Tripoli, witnessed a major fire in the city's government hospital as a result of the explosion of the electrical control box due to high temperatures, which resulted in the fire igniting parts of the hospital, which contained

\*Correspondence: Haifa M. Ben Miloud

[Regcm00@yahoo.com](mailto:Regcm00@yahoo.com)

many inmates, before it was brought under control. Without any human casualties [8].

## 2. OBJECTIVES OF THE STUDY

1. In recent years, it has been shown that temperatures have increased significantly in Libya during the summer months and its impact on the environment through the outbreak of fires.
2. To understand fire weather, knowing the weather factors that affect the size, intensity, and speed of forest fires, in addition to their predictability and their ability to expose society to danger.

## 3. SOURCE OF DATA

The ECMWF ERA5 reanalysis's weather forecasts from past simulations are used to calculate the fire weather index. The fire weather index is part of a dataset produced by the Copernicus Emergency Management Service (CEMS). The data was from day 24-27 of July at noon for the period 1940-2022[8].

### *Climatological Analysis of Fire Weather Index over Libya*

In Libya, the climate is considered desert in most of the country, except for the areas overlooking the Mediterranean Sea, which take on the climatic characteristics of the sea [9]. When analyzing the data for most of the country, it became clear that the fire weather index in the south is very high, due to the high temperature and lack of rain, which consequently increases the expansion of drought areas in the country. We note that in the north of the country, it decreases more than in the south, but it is considered somewhat high, according to the classification of the fire weather index greater than (Extreme) 50 is considered high, as shown in Table 1 [10].

Upon analysis from the 24<sup>th</sup> to the 27<sup>th</sup> of July at 12 p.m. in the afternoon for the period 1940-2022, it became clear that the fire weather index increases in the south and decreases in the north, and the 24<sup>th</sup> is considered higher than the 25<sup>th</sup>, and this was clear in the eastern region, where there are trees represented in the Green Mountain area. It increases on the 26<sup>th</sup> and decreases further on the 27<sup>th</sup>. Therefore, the study was focused on using the Canadian Forest Fire Weather Index classification system over the Green Mountain area, which overlooks the sea and is characterized by vegetation.

**Table 1. FWI value classification**

FWI Danger	Level
very low	0-5.2
Low	5.2-11.2
middle	11.2-21.3
High	21.3-38
very high	38-50
Extreme	>50

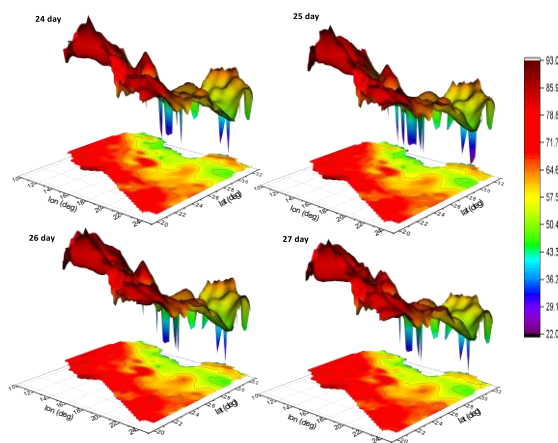


**Fig. 1: Average Fire weather index (FWI) over Libya from 24-27 days at noon for July for the period 1940-2022, [8].**

### *Area of Study*

The spread of forests in the world and their burning every year in the summer months due to the noticeable climate change in rising temperatures has been an area of interest for many studies, the classification system has used the fire weather index for Canadian forests in the world as a whole. The Green Mountain region was among the regions of the world, (this is a region our study), at longitudes 21.2-22 and latitudes 31.19-33N<sup>0</sup>. Although the fire weather includes all areas since these areas do not have vegetation cover, the burning speed is more evident in the forests, so it was concentrated more on the forests.

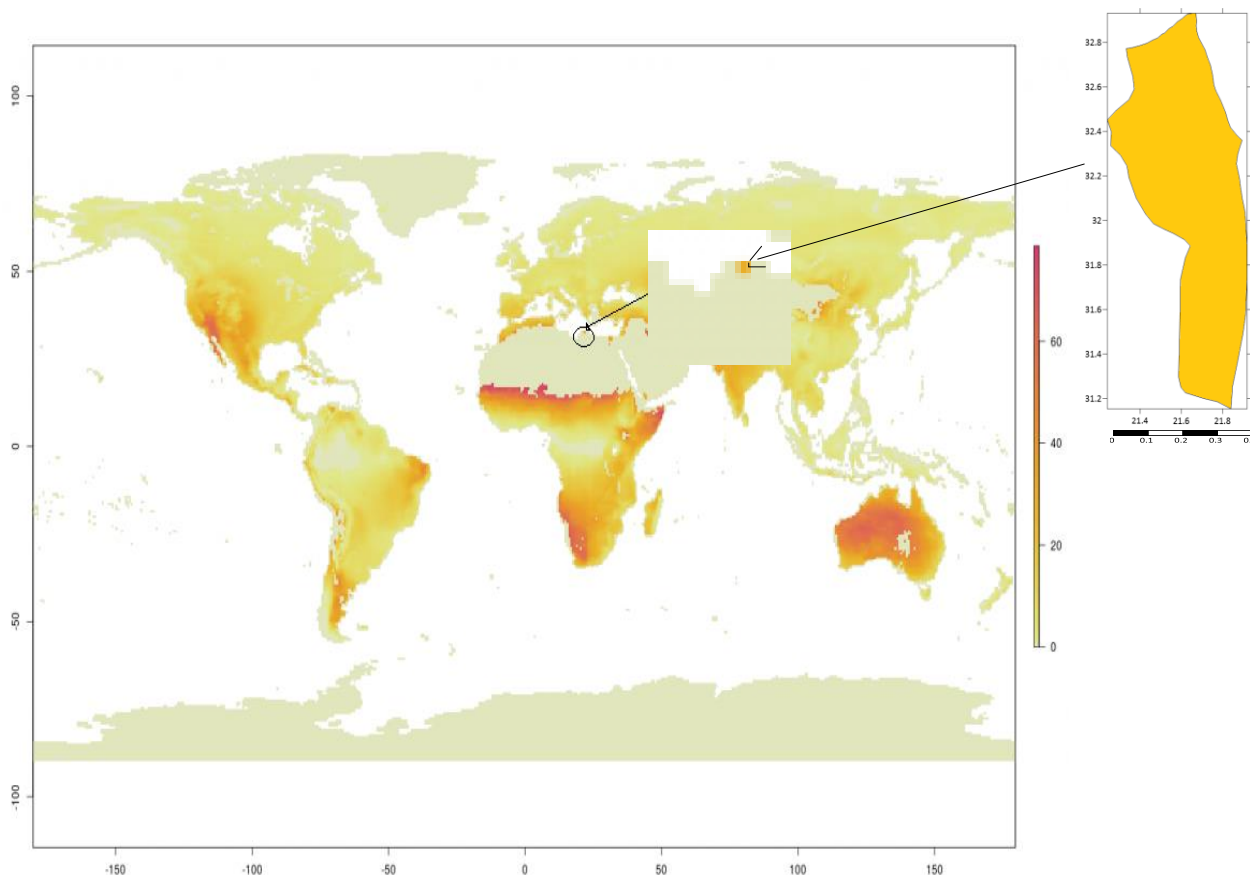


Fig .2: Area study Al-Jabal Al-Akhdar. mean FWI in the period 1980-2017<sup>[11]</sup>.

#### 4. METHODS

##### Fire Weather Index System

**Definition** The fire weather index indicates fire intensity by combining the rate of fire spread with the amount of fuel being consumed. The fire weather index is calculated using the Canadian Forest Service Fire Weather Index rating system (FWI) <sup>[12]</sup>. The fire danger model takes into account temperature, relative humidity, wind speed, precipitation, drought conditions, fuel availability, vegetation characteristics, and topography <sup>[13]</sup>.

The FWI is calculated in three main tiers. In the first tier, three moisture codes are calculated. The Fine Fuel Moisture Code (FFMC) is calculated using temperature, precipitation, wind speed, and relative humidity. The FFMC represents moisture levels on daily time scales and in litter that is 2cm or less deep. The Duff Moisture Code (DMC) is calculated using temperature, precipitation, and

relative humidity. The DMC represents moisture levels on ~2-week time scales and in litter and soil 5-10 cm deep. The Drought Code (DC) is calculated using temperature and precipitation. The DC represents moisture levels on ~2-month scales and in litter and soil 10-20 cm deep. All three moisture codes are unitless.

The second tier, the Build-Up Index (BUI) is defined as “a number that reflects the combined cumulative effects of daily drying and precipitation in fuels with a 10-day time lag constant” <sup>[13]</sup>, and the Initial Spread Index (ISI) is calculated using the derived codes in the first tier. The BUI is calculated using the DMC and DC and represents the total fuel available for combustion through long-term drying. The ISI is calculated using the FFMC and wind speed to represent the rate of fire spread. In the third tier, the FWI is calculated using the BUI and ISI, and represents fire danger given the meteorological conditions, and the fire intensity, if a fire were to be ignited <sup>[15]</sup>.

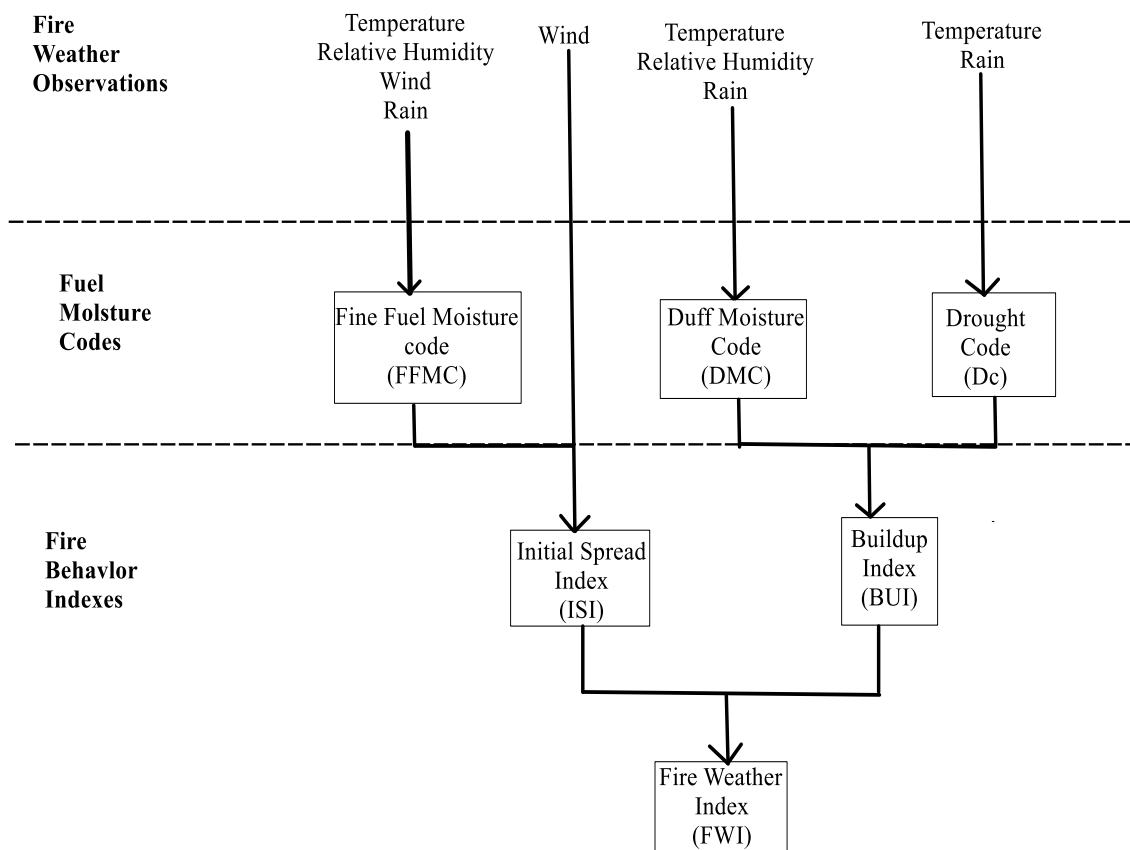


Fig. 3: fire weather index system [12].

### 5. RESULTS AND DISCUSSION

Applying the Canadian classification for forest burning on the Green Mountain in Libya, which has a picturesque natural beauty and the density of its trees, which are concentrated in the center and south of the region more than in the north overlooking the sea. By analyzing the average Fine Fuel Moisture Code (FFMC) for each day from the 24<sup>th</sup> to the 27<sup>th</sup> at 12 in the afternoon for July during the period 1940-2022, it is clear that it increases in the south of the mountain and decreases in the north, and that its spread and density increases on the 26<sup>th</sup> and then on the 27<sup>th</sup> and decreases on the 24<sup>th</sup> and 25<sup>th</sup>, as shown in Figure (4, a), which shows the density function, the Fine Fuel Moisture Code for days, When calculating the total average from the 24<sup>th</sup> to the 27<sup>th</sup> at noon in July for the periods 1940-1981 and 1982-2022 to determine the increase, it became clear that the period 1982-2022 is more widespread and dense than the period 1940-1981, as shown in the Figure (4, b).

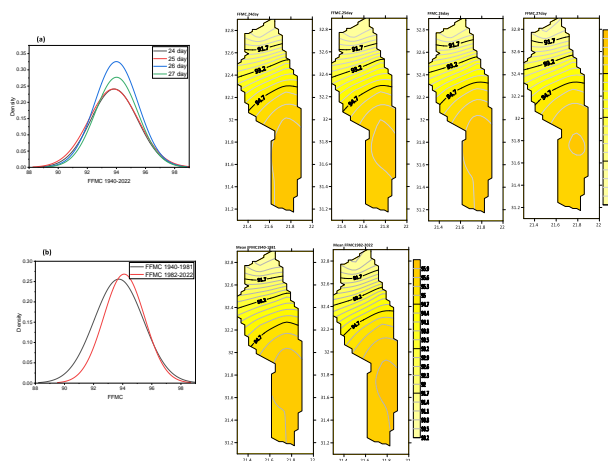
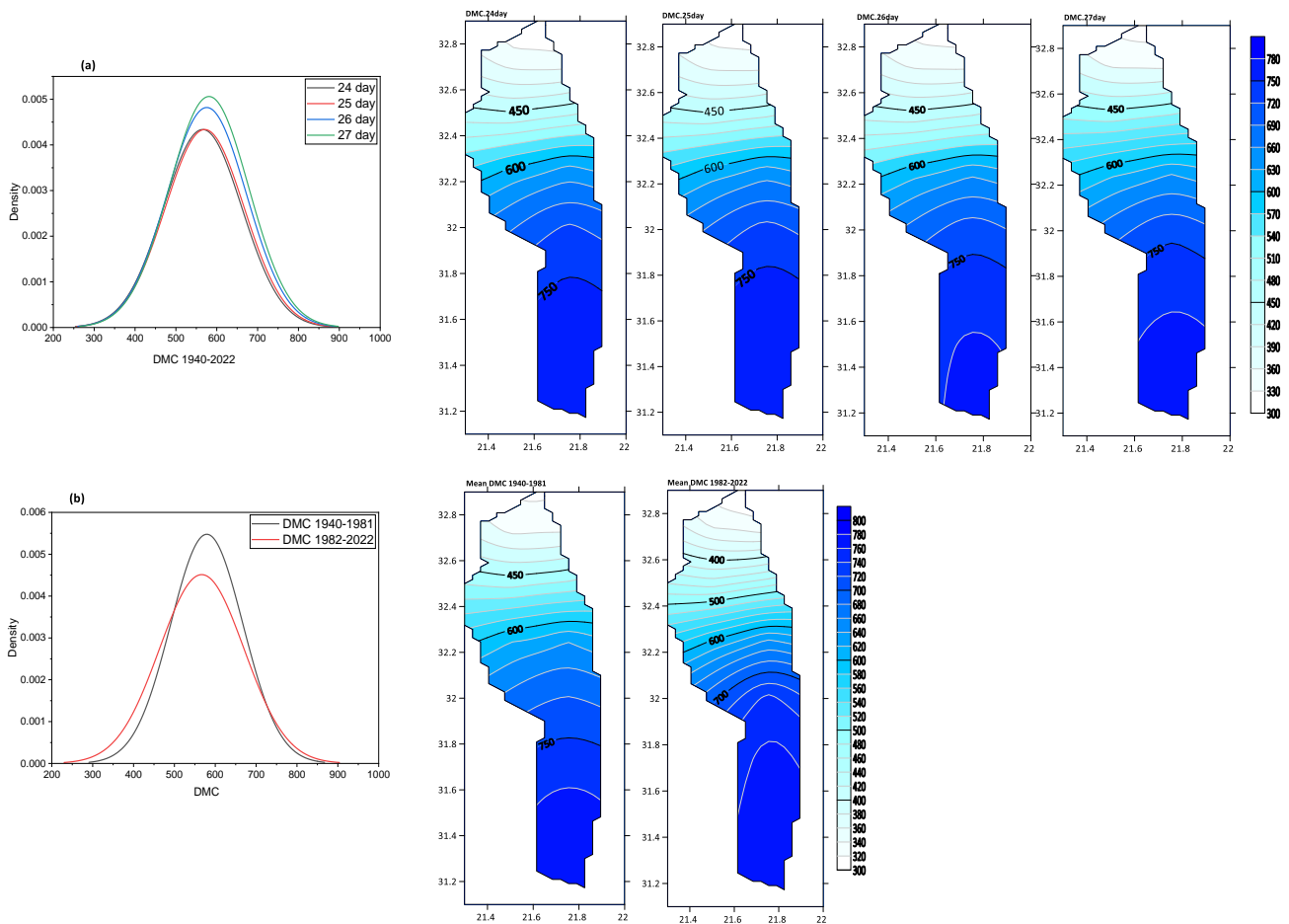


Fig. 4: Distribution and density of the average Fine Fuel Moisture Code (FFMC) over the Al-Jabal Al-Akhdar(a) 24-27 days at noon in July for the period 1940-2022, (b) 24-27 days at 12 noon in July for the period 1940-1981 and 1982-2022.

Figure (5.a) shows Duff Moisture Code (DMC) that increases in the south of the region and decreases as we rise higher. On the 27<sup>th</sup> and 26<sup>th</sup>, it is higher than on the 24<sup>th</sup> and 25<sup>th</sup>. Likewise, in the period 1940-1981, its density was higher, but less widespread than the period 1982-2022. As shown in Figure (5, b).



**Fig. 5: Distribution and density of the average Duff Moisture Code (DMC) over the Al-Jabal Al-Akhdar (a) 24-27 days at 12 noon in July for the period 1940-2022, (b) 24-27 days at 12 noon in July for the period 1940-1981 and 1982- 2022.**

In Figure (6, A) the average Drought Code (DC) is shown, showing its equal distribution for all days except Day 27. There is a very slight change, while for the period 1940-1981 it is more widespread and intense than the period 1982-2022 shown in Figure (6, B). This is due to climate changes and Rainfall amounts have increased in recent years, as forests are considered humid areas compared to other regions in the country, but the curve for the second period shows that it will increase during the coming years, and this is what climate models such as CMIP6 [16]. For the second level of the occurrence of the

Fire Weather Index, the Initial Spread Index (ISI) is calculated. Shows that on the 24<sup>th</sup> at 12 noon in the month of July, the Initial Spread Index (ISI) , density was greater than the rest of the days, followed by the 25<sup>th</sup> and then the 27<sup>th</sup> in terms of density, but on the 26<sup>th</sup> it was greater in spread than on the 25<sup>th</sup> and 27<sup>th</sup> and less dense than them, as shown in Figure (7.a), while in Figure (7.b) it shows that the period 1940-1981 is more widespread and less intense than the second period 1982-2022, and this is what is shown by the drought code in Figure (6.b).

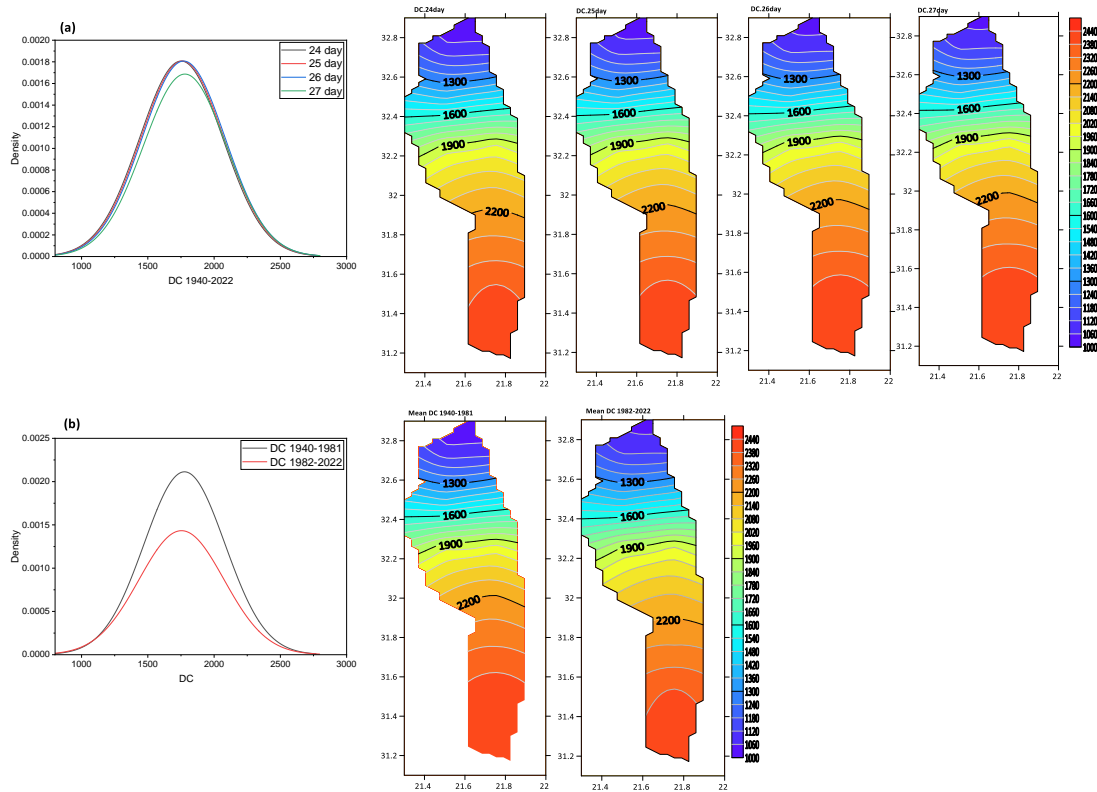


Fig. 6: Distribution and density of the average Drought Code (DC) over the Al-Jabal Al-Akhdar (a) 24-27 days at 12 noon in July for the period 1940-2022, (b) 24-27 days at 12 noon in July for the period 1940-1981 and 1982- 2022.

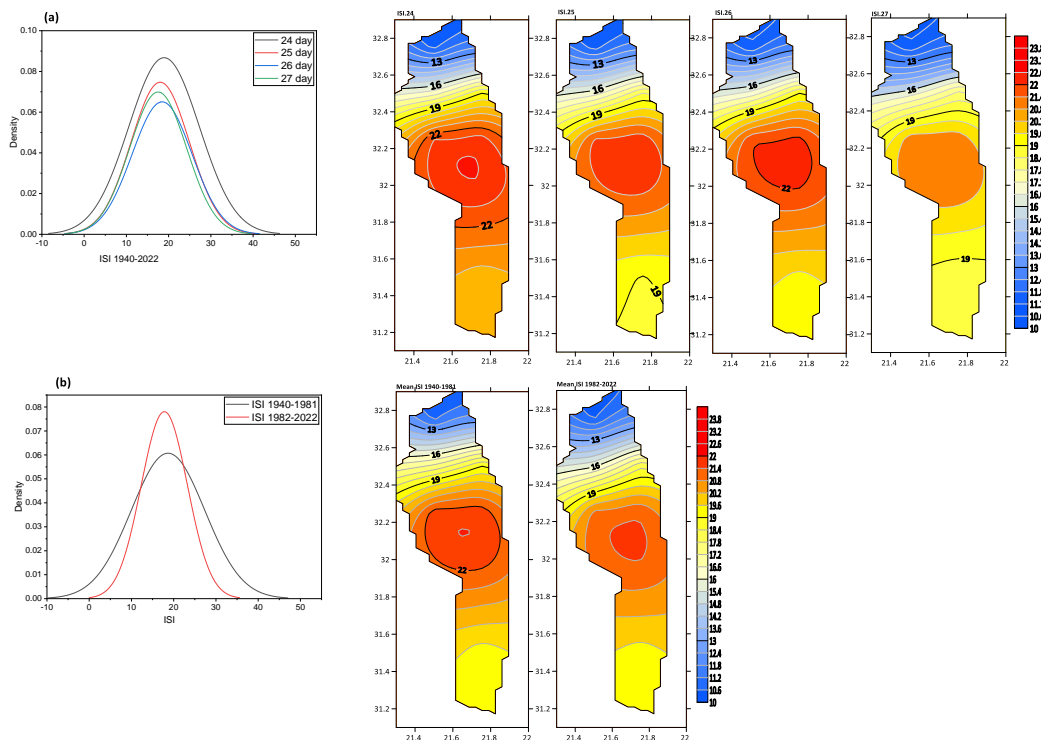
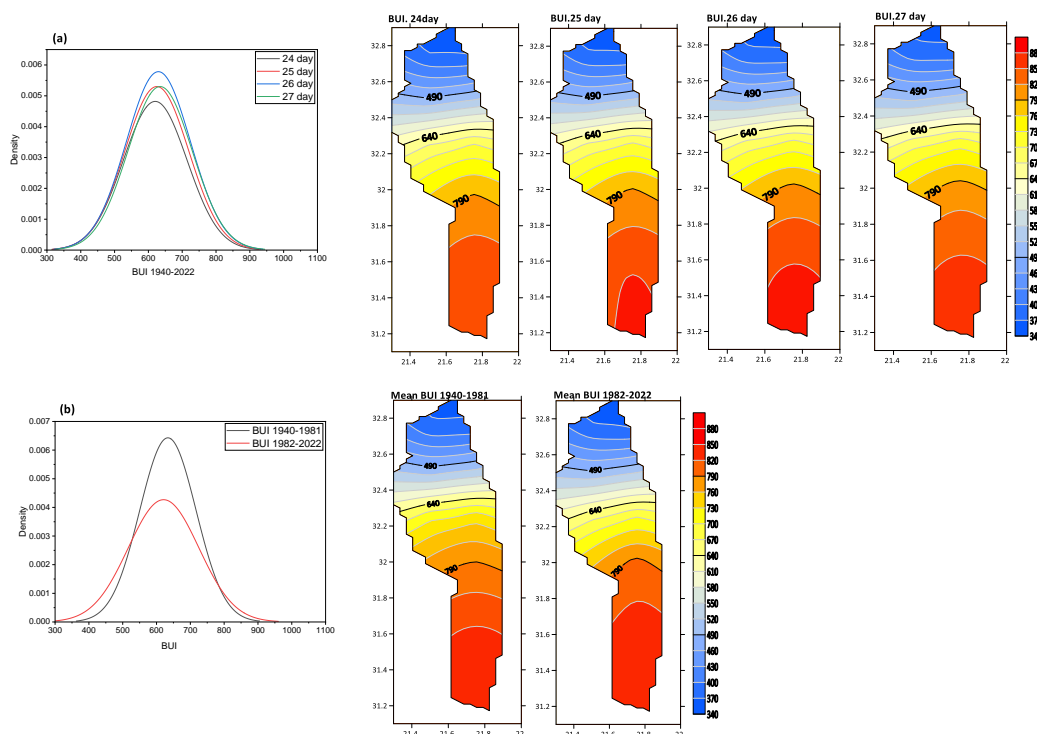


Fig. 7: Distribution and density of the average Initial Spread Index (ISI) over the Al-Jabal Al-Akhdar (a) 24-27 days at 12 noon in July for the period 1940-2022, (b) 24-27 days at 12 noon in July for the period 1940-1981 and 1982- 2022.

In Figure (8, a) the Build-Up Index (BUI) is shown. It is noted that day 26 is more widespread than days 25 and 27, and day 24 is less dense. While analyzing the periods in Figure (8, b), we see that the period 1982-2022 is more widespread and less dense than the period 1940-1981.



**Fig. 8: Distribution and density of the average Build-Up Index (BUI) over the Al-Jabal Al-Akhdar (a) 24-27 days at 12 noon in July for the period 1940-2022, (b) 24-27 days at 12 noon in July for the period 1940-1981 and 1982- 2022.**

At the last level, the Fire Weather Index (FWI) was the highest possible and most widespread on days 24 and 26, reaching a value of more than 60 from the south of the region to its center, and decreasing as we headed towards the north, followed by the 25<sup>th</sup>, while the 27<sup>th</sup> was less widespread, as shown in Figure (9, a). While it is noted in Figure (9, b) that the period 1940-1981 is more widespread than the period 1982-2022, with the passage of the coming years, the intensity of fire weather increases, and this is shown in the intensity curve for this period.

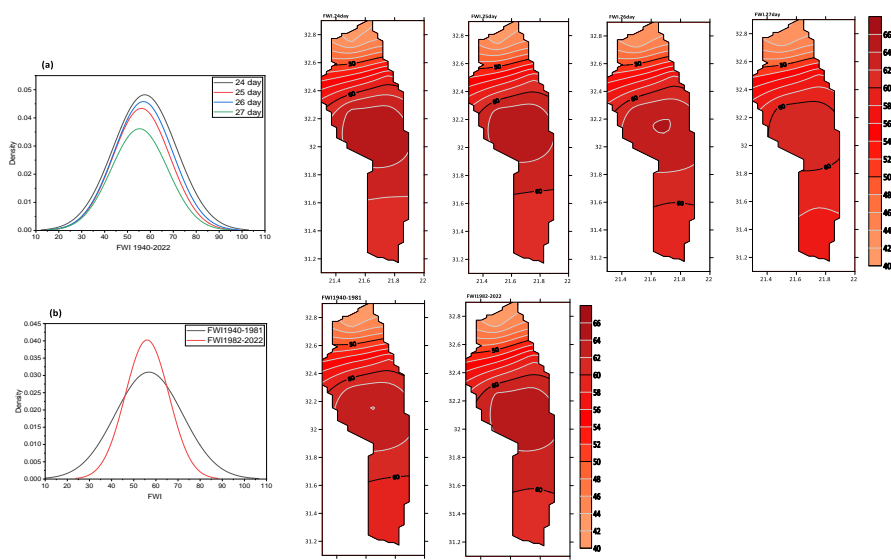


**Fig. 9: Distribution and density of the average Fire Weather Index (FWI) over the Al-Jabal Al-Akhdar (a) 24-27 days at 12 noon in July for the period 1940-2022, (b) 24-27 days at 12 noon in July for the period 1940-1981 and 1982- 2022.**

To know the increase and decrease in the Fire Weather Index (FWI), for Canadian classification, the difference between the periods 1940-1981 and 1982-2022 was taken. It is noted that the FFMC code increases in the south of the region and decreases in the north, while the DMC code increases in the north and gradually decreases in the south. On the other hand, the DC code increases in the south and decreases in the north. Whereas the ISI code increases in the middle of the region, it decreases in the north and south. The BUI code, however; it decreases in the central part and extends to increase in the north and increases somewhat in the south, and the FWI is highest in the center of the region and decreases towards the north, where there is less vegetation cover and marine climate. See Figure 10.

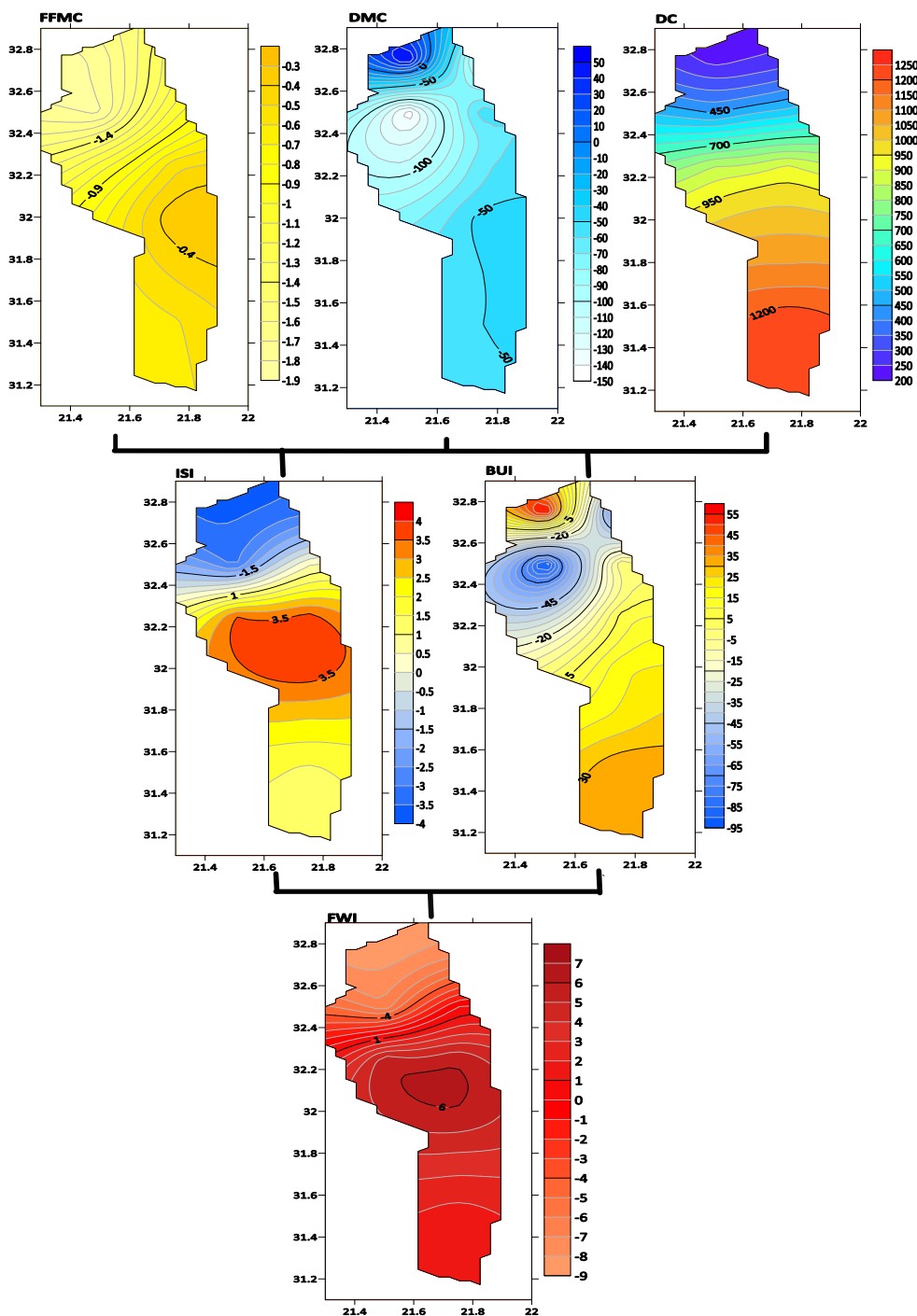


Fig. 10: The difference between the period 1982-2022 and the period 1940-1981 for the Canadian classification of the Fire Weather Index over the Al-Jabal Al-Akhdar for the 24-27 days of July at 12 noon.

## 6. CONCLUSION

Climate change has become clear in terms of an increase in temperatures across both continents and oceans, resulting in floods in some countries and, on the other hand, the spread of fires in other parts of some countries. Here in this study, the Canadian classification for burning forests in the Green Mountain region was used, has it dense with trees, although Libya considers the fire weather index to be very high in all of Libya, but when this classification is used on forests to reach the fire weather index (FWI), it requires measuring all of the following: The first level, which is the Fine Fuel Moisture Code (FFMC), is high in the center and extends to the south of the region, and it was more evident in On the 26<sup>th</sup>, compared to the rest of the days, its spread and density are high, while the Duff Moisture Code (DMC) decreases in the north of the region and increases in the south, and it was clear on the 27<sup>th</sup> day, then on the 26<sup>th</sup>, and its spread in the period 1982-2022 is more than the period 1940-1981, while the Drought Code (DC) shows the increase and decrease in the south as we headed north and its spread in the period 1940-1981 was higher than the period 1982-2022 due to the increasing amounts of rain in recent years, but its spread will increase and this is shown in the curve for the second period due to the increase in temperature and lack of rain in the coming years, while in the second level The Initial Spread Index (ISI) shows that it is high in the middle of the region, and the Build-up Index (BUI) increases to the south and decreases to the north, and due to the occurrence of fire weather (FWI) at the third level, it reaches above 60, and thus it is considered very high, shown on the 24<sup>th</sup> and 26<sup>th</sup> days more than on the 25<sup>th</sup> and 27<sup>th</sup> days.

Because of the Intergovernmental Panel on Climate Change) IPCC) warnings of climate changes on the Earth's surface, the fire weather index will increase in the coming years, and the Libyan state must take caution and be careful of these changes in the future.

**Author Contribution:** The design of the study, the analysis of the data and the final results and conclusion have been carried out by the author.

**Funding:** This work was not supported financially in any way. No funding was received to help in the preparation of this manuscript.

**Data Availability Statement:** The climatic data used in this research paper was obtained from

<https://cds.climate.copernicus.eu/>

**Acknowledgments:** Thanks and appreciation to the Copernicus services for the good data to cover the event with distinction

**Conflicts of Interest:** The author affirms that they have no known financial or interpersonal conflicts that

would have appeared to have an impact on the research presented in this study.

## References

1. John TA, Williams .PA, Renaud. B. Global Emergence of Anthropogenic Climate Change in Fire Weather Indices. AGU. 2019 Jan; 46 (1), 326–336 :  
<https://doi.org/10.1029/2018GL080959>.
2. Alan FS, Joseph JC, Brian EP, Scott LG. The Hot-Dry-Windy Index: A New Fire Weather Index. MDPI .2018 Jul; 9(7), 1-11:  
<https://doi.org/10.3390/atmos9070279>.
3. Miguel .MP, Carlos .CD, Alexandra. H, Ricardo .MT, Isabel FT. Enhancing the fire weather index with atmospheric instability information. IOP. 2020Sep; 15(9), 1-12:  
<https://doi.org/10.1088/1748-9326/ab9e22>
4. Dimitrakopoulos AP, Bemmerzouk AM, Mitsopoulos ID. Evaluation of the Canadian fire weather index system in an eastern Mediterranean environment. RMetS. 2011 Feb; 18(1),83- 93:  
<https://doi.org/10.1002/met.214>.
5. Hasan T, Murat T. Climatological evaluation of Haines forest fire weather index over the Mediterranean Basin. RMetS. 2013 Feb; 21(3), 545 -552 :  
<https://doi.org/10.1002/met.1367>.
6. Seneviratne SI, Zhang. X, Adnan. M, Badi. W, Dereczynski C, Di LA, et al. Weather and Climate Extreme Events in a Changing Climate. In Climate Change .IPCC\_AR6\_WGI\_Chapter 11.2021;1513-1766:  
<https://doi:10.1017/9781009157896.013>.
7. NSA warns eastern Libya's public of bad weather:  
<https://ar.libyaobserver.ly>.
8. Copernicus Climate Data Store:  
<https://cds.climate.copernicus.eu>.
9. El-Tantawi MM . Climate Change in Libya and Desertification of Jifara Plain Using Geographical Information System and Remote Sensing Techniques. Ph.D thesis. University in Mainz. 2005;1-261.
10. Nikolaos. N, Marios .S, Lampros .V ,Nikitas.M. Contribution to the Study of Forest Fires in Semi-Arid Regions with the Use of Canadian Fire Weather Index Application in Greece. MDPI. 2022Sep;10(10) 143, 2-29:  
<https://doi.org/10.3390/cli10100143>.
11. Catalogue of ANYWHERE Products for Hazard Forecasting and Impact Localization due to Weather and Climate Events:  
<http://aqua.upc.es/anywhere-catalogue>

12. Tables for the Canadian forest fire weather index system, Canadian forestry service Environment Canada. 1984;1-73.
13. Climate ADAPT :  
<https://climateadapt.eea.europa.eu/en/metadata/indicators/fire-weather-index-monthly-mean-1979-2019>.
14. A Working Group for NCDFR MTM. 2009 May,1 -5.
15. Touma, Danielle , NCAR . The Climate Data Guide: Canadian Forest Fire Weather Index (FWI). 2023Aug .  
<https://climatedataguide.ucar.edu/climate-data/canadian-forest-fire-weather-index-fwi>
16. Yann. Q, Fulden. B, Andreia. FS, Ryan .SP, Sonia. I . Fire weather index data under historical and shared socioeconomic pathway projections in the 6th phase of the Coupled Model Intercomparison Project from 1850 to 2100. ESSD. 2023 May; 1-25:  
<https://doi.org/10.5194/essd-15-2153-2023>.



# Selecting the Optimal Airfoil for Automotive Rear Wings: Performance Assessment

Osama Maddani<sup>1</sup> - Saleh Etaig<sup>1\*</sup> - Al-Hadi Ebrahim -<sup>1</sup> Islam AlJhani<sup>1</sup>

*1 Mechanical Engineering department - Faculty of Engineering - University of Benghazi.*

Received: 22 / 03 / 2024; Accepted: 15 / 05 / 2024

## ABSTRACT

This study investigates the potential performance and safety improvements achievable through the application of inverted airfoils on a BMW 3-series (E36) car. Computational fluid dynamics (CFD) simulations were employed to assess the aerodynamic characteristics of three distinct airfoil designs: NACA 0012, NACA 4412, and Eppler E423. Evaluations were conducted at 0° in freestream and at 14° angles of attack (AOA) when used in the automotive application to analyze the impact on lift and drag forces. The findings revealed unique aerodynamic profiles for each airfoil. The angle of attack for the airfoils in freestream was chosen to be 0 degrees to isolate the effect of the different airfoil shapes on their performance. This allows us to better understand how their performance translates to the automotive application. Considering automotive applications, the Eppler E423 demonstrated superior potential for enhanced acceleration and cornering speeds compared to the other airfoils. The NACA 4412 also displayed comparable performance to the Eppler E423 in these aspects. Overall, the inclusion of an Eppler E423 airfoil positioned as an inverted wing at a 14° AOA emerged as the configuration offering the optimal balance between performance and safety benefits for the BMW 3-series (E36). This research underscores the significant potential of strategically incorporating aerodynamic devices, such as inverted wings, to achieve improvements in both vehicle safety and performance characteristics.

**KEYWORDS:** Automotive aerodynamics, Numerical simulation, Airfoil, Turbulence models.

## 1. INTRODUCTION

In recent years, automotive aerodynamics has garnered significant attention within the industry, largely driven by increased awareness of fuel consumption. The streamlined shapes of vehicles play a crucial role, as less aerodynamic resistance force, commonly known as drag, is generated. Consequently, overcoming this drag necessitates more engine power, ultimately leading to higher fuel consumption. Moreover, the escalating speeds attained by both sports road vehicles and motorsport racing cars accentuate the need for enhanced stability. Achieving this stability typically involves balancing the lift forces acting on the vehicle's body, among other factors.

Several studies have investigated the use of CFD for airfoil analysis and selection, demonstrating the effectiveness of different turbulence models and highlighting key considerations for unmanned aerial vehicles (UAVs)

Douvi et al<sup>1</sup> achieved the most accurate results for the NACA 0012 airfoil when using the Spalart-Allmaras turbulence model, compared to k-ε and SST k-ω models. Their study emphasizes the importance of rigorous model validation for reliable outcomes.

Kevadiya and Vaidya<sup>2</sup> obtained good results for the NACA 4412 airfoil using Spalart-Allmaras. Their work focused on a lower angle of attack range (0°-12°) compared to Douvi et al<sup>1</sup>.

Reza et al<sup>3</sup> conducted a comprehensive analysis of various airfoils for high-lift, low-Re UAVs. They initially evaluated EPPLER, SELIG, WORTMANN, AG35, and NLF 0115 airfoils. Further analysis based on drag polar at a standard Re for low-speed UAVs led them to select E420, E423, FX74-CL5-140, and S1223 for further scrutiny. Ultimately, S1223 emerged as the most suitable option due to its superior C<sub>l</sub> and C<sub>m</sub> characteristics and slightly higher stall angle compared to E420.

Parhcal<sup>4</sup> computationally modeled a NACA 4412 airfoil as both front and rear wings for a racing vehicle, aiming to increase downforce and enhance stability. His study analyzed the ground effect, varying angles of attack, and optimized configurations for maximum downforce and minimum drag, finding potential design parameters

\*Correspondence: Saleh Etaig

[Saleh.Etaig@uob.edu.ly](mailto:Saleh.Etaig@uob.edu.ly)

Ahmad et al.<sup>5</sup> validated 2D flow simulations of a NACA 0012 airfoil using the  $k-\omega$  SST turbulence model, comparing against experimental data from Theory of Wing Sections<sup>6</sup>. Employing this validated technique, they analyzed a plain flapped NACA 0012 airfoil at varying flap angles revealing that drag coefficients (CD) remain relatively constant.

Abobaker et al.<sup>6</sup> numerically investigated the impact of wind tunnel walls on airfoil measurements, specifically focusing on the lift curve slope correction factor ( $K_a$ ). They analyzed subsonic flow over a NACA 0012 airfoil at varying angles of attack and domain heights using CFD with SST- $k-\omega$  turbulence modeling. Their numerical results, validated against experimental data, demonstrate the importance of CFD in understanding and correcting for wind tunnel wall effects.

In their study, Dinesh Bhatia et al.<sup>7</sup> conducted simulations of a 2D NACA 0012 airfoil. They highlighted that positioning the sharkskin denticles at 0.16 of the airfoil's chord length in the normal direction resulted in a maximum drag reduction of 3% and an enhancement in lift-to-drag ratio (L/D) of 1.5%. These optimal improvements were observed at angles of attack (AOA) of 0° and 4°. Several efforts focused on studying turbulence models such as<sup>8</sup>

In a separate investigation focusing on modifications of the NACA 0012 airfoil, Sogukpinar<sup>9</sup> explored the impact of varying thicknesses on the lower surface of the airfoil. The resultant data were then compared with observational data from NASA<sup>11,12</sup> to validate the accuracy of the computational approach.

Karim et al.<sup>10</sup> investigated the behavior of a hydrofoil submerged in water, focusing on the influence of the water surface boundary position. Their study involved 2D simulations of a NACA 0015 hydrofoil, with an angle of attack (AOA) of 5°. The realizable  $k-\epsilon$  turbulence model was employed for turbulence modeling.

Azim et al.<sup>11</sup> determined that implementing a suction slot modification effectively delayed separation in a NACA 4412 airfoil operating at Mach number 0.6 and an angle of attack (AOA) of 12°. They utilized the Spalart-Allmaras turbulence model. Consequently, the lift-to-drag ratio ( $C_l/C_d$ ) increased approximately 2.24 times compared to the airfoil without suction.

Hossain et al.<sup>12</sup> concluded that for practical applications, the NACA 4412 airfoil outperforms the NACA 6409. Their comparison was based on the results of coefficient of drag ( $C_d$ ) and coefficient of lift ( $C_l$ ) obtained under identical boundary conditions, specifically at angles of attack (AOA) of 0° and 5°.

Singh et al.<sup>13</sup> conducted a comparison study indicating that the NACA 4412 airfoil is well-suited for sports planes, whereas the S1223 airfoil is more appropriate for

heavy lift cargo planes. Their simulations were carried out within an angle of attack (AOA) range of 0° to 10°.

Amit Saraf et al. conducted investigations on the NACA 4412 airfoil in 2D, as detailed in their studies<sup>14</sup> and<sup>15</sup>. Their findings suggest that turbulence models namely the standard  $k-\epsilon$ ,  $k-\omega$ , and Spalart-Allmaras models, do not yield accurate results at high angles of attack (AOA). The simulations were conducted at a flow velocity of 50 m/s, spanning an AOA range of 0° to 15°.

Petinrin and Onoja<sup>16</sup> investigated the accuracy of turbulence models, particularly focusing on the NACA 4412 airfoil. Their study revealed that the SST  $k-\omega$  transport turbulence model demonstrates superior accuracy compared to the Spalart-Allmaras model. Additionally, the authors observed that the increase in aerodynamic performance of the airfoil diminishes exponentially with increasing Reynolds numbers.

Wina and Thian wiboon<sup>17</sup> conducted a comprehensive investigation using 2D simulations of the NACA 4412 airfoil, exploring variations in angles of attack (AOA). Their study covered an AOA range of 4° to 8° in ground effect in three height to chord length (H/C) ratios 0.1, 0.15 and 0.2. They concluded that as the H/C decreases, the coefficient of lift ( $C_l$ ) increases and the coefficient of drag ( $C_d$ ) decreases, leading to a higher lift-to-drag ratio in ground effect.

Ockfen and Matveev<sup>18</sup> presented a study on the NACA 4412 airfoil, focusing on small angles of attack (AOA). They observed that the coefficient of lift ( $C_l$ ) increases across all ground heights. However, they noticed a significant increase in the coefficient of drag ( $C_d$ ) as the flap is deflected.

Qiulin Qu et al.<sup>19</sup> investigated the influence of Dynamic Ground Effect (DGE) on the NACA 4412 airfoil through 2D simulations. They conducted simulations at an angle of attack of  $\alpha=3.6^\circ$ . To validate their simulations, they computed the flow past the Tyrrell-026 airfoil and compared the results with experimental data.

Huminic and Huminic<sup>20</sup> investigated the E423 airfoil and discovered that the Coandă effect, achieved through a curved slot in the underside of the airfoil located at 0.6 of the Chord and has a width of 0.7 mm and a curve radius of 5mm. This improvement enhanced the aerodynamic characteristics of the ailerons, ultimately leading to an enhancement in the aerodynamic behavior of the vehicle in terms of aerodynamic loads. Their study conducted at an angle of attack (AOA) range of 0° to 10°.

Omkar Bhatkar et al.<sup>21</sup> conducted a study on a modified version of the E423 airfoil and its impact on vehicle aerodynamics. They found that the generation of downforce substantially affect race car performance. The study focused on the NACA's E423 multi-elemental

airfoil's front wing and rear wing. Their results indicated a coefficient of lift ( $C_l$ ) of -1.37 for the front wing and -1.48 for the rear wing.

Sreejith and Sathyabhama <sup>22</sup>, conducted a study on the E216 airfoil, where they found that the implementation of a boundary layer trip could partially or completely eliminate the laminar separation bubble (LSB), thereby enhancing the aerodynamic performance of the airfoil. They observed that the maximum improvement in drag reached 15.48%, while the lift-to-drag ratio improved by 21.62% at an angle of attack (AOA) of 6° across all cases.

Guda et al <sup>23</sup> found that employing a double spoiler design, featuring both upper and lower spoilers, effectively reduced the coefficient of drag ( $C_d$ ) from 0.34 to 0.3 in a Maruti 800 car model. To ensure the accuracy of their findings, the authors validated their simulations against the actual model provided by the manufacturer.

Kumar et al <sup>24</sup> determined that among three spoilers added to a sedan car, the second spoiler yielded the most favorable results. They achieved a coefficient of drag ( $C_d$ ) of approximately 0.329 and a coefficient of lift ( $C_l$ ) of 0.106. The authors concluded that the addition of the spoiler resulted in a reduction in the coefficient of drag compared to the baseline configuration.

From the above explored survey of the literature, it can be concluded that there is a gap in studying various airfoils configurations in terms of performance as well as its impact in a rear wing car especially when it comes to an actual vehicle, hence the main contribution of the present study is focused on developing a numerical model and validating it to accurately predict the aerodynamic behavior of various bodies in freestream conditions, enhancing understanding of their performance characteristics.

The performance is thoroughly investigated by exploration of selected airfoils using diverse turbulence models, leading to a comprehensive analysis of their aerodynamic features and behaviors in freestream environments. The study comprises comparison of simulated results with experimental data, facilitating the validation process and strengthening the credibility of the numerical simulations. In addition, a detailed examination of the BMW 3-series (E36) both in its original, wingless state and with the addition of various inverted wings (Airfoils) is presented, shedding light on their respective aerodynamic properties and effectiveness.

## 2. NUMERICAL METHOD

The present work was conducted using CFD which is a robust tool to investigate and analyze sophisticated fluid flow cases. The governing equations, turbulence model and mesh test will be discussed in detail.

### Governing equations

The governing equations are: continuity equations which can be written as:

$$\frac{\partial \rho}{\partial t} + \left( \frac{\partial \rho u}{\partial x} + \frac{\partial \rho v}{\partial y} + \frac{\partial \rho w}{\partial z} \right) = 0 \quad (1)$$

The momentum equation which can be written as:

$$\rho \frac{dv}{dt} = \rho g - \nabla P + \nabla \tau_{ij} \quad (2)$$

The Navier stokes equations can be expressed in x, y and z directions as:

#### X- Momentum

$$\frac{\partial(\rho u)}{\partial t} + \frac{\partial(\rho u^2)}{\partial x} + \frac{\partial(\rho uv)}{\partial y} + \frac{\partial(\rho uw)}{\partial z} = -\frac{\partial p}{\partial x} + \frac{\partial}{\partial x} \left[ \lambda \nabla \cdot \mathbf{V} + 2\mu \frac{\partial u}{\partial x} \right] + \frac{\partial}{\partial y} \left[ \mu \left( \frac{\partial v}{\partial x} + \frac{\partial u}{\partial y} \right) \right] + \frac{\partial}{\partial z} \left[ \mu \left( \frac{\partial u}{\partial z} + \frac{\partial w}{\partial x} \right) \right] + \rho f_x \quad (3)$$

#### Y-Momentum

$$\frac{\partial(\rho v)}{\partial t} + \frac{\partial(\rho uv)}{\partial x} + \frac{\partial(\rho v^2)}{\partial y} + \frac{\partial(\rho vw)}{\partial z} = -\frac{\partial p}{\partial y} + \frac{\partial}{\partial x} \left[ \mu \left( \frac{\partial v}{\partial x} + \frac{\partial u}{\partial y} \right) \right] + \frac{\partial}{\partial y} \left( \lambda \nabla \cdot \mathbf{V} + 2\mu \frac{\partial v}{\partial y} \right) + \frac{\partial}{\partial z} \left[ \mu \left( \frac{\partial w}{\partial y} + \frac{\partial v}{\partial z} \right) \right] + \rho f_y \quad (4)$$

#### Z-Momentum

$$\frac{\partial(\rho w)}{\partial t} + \frac{\partial(\rho uw)}{\partial x} + \frac{\partial(\rho vw)}{\partial y} + \frac{\partial(\rho w^2)}{\partial z} = -\frac{\partial p}{\partial z} + \frac{\partial}{\partial x} \left[ \mu \left( \frac{\partial u}{\partial z} + \frac{\partial w}{\partial x} \right) \right] + \frac{\partial}{\partial y} \left[ \mu \left( \frac{\partial w}{\partial y} + \frac{\partial v}{\partial z} \right) \right] + \frac{\partial}{\partial z} \left( \lambda \nabla \cdot \mathbf{V} + 2\mu \frac{\partial w}{\partial z} \right) + \rho f_z \quad (5)$$

Reynolds average Navier stokes equations:

$$\begin{aligned} & \frac{\partial(\bar{\rho}\bar{U})}{\partial t} + \nabla \cdot (\bar{\rho}\bar{U}\bar{U}) \\ & = -\frac{\partial\bar{P}}{\partial x} + \nabla \cdot (\mu\nabla\bar{U}) \\ & + \left[ -\frac{\partial(\overline{\rho u'^2})}{\partial x} - \frac{\partial(\overline{\rho u'v'})}{\partial y} \right. \\ & \left. - \frac{\partial(\overline{\rho u'w'})}{\partial z} \right] + S_{Mx} \end{aligned} \quad (6)$$

$$\begin{aligned} & \frac{\partial(\bar{\rho}\bar{V})}{\partial t} + \nabla \cdot (\bar{\rho}\bar{V}\bar{U}) \\ & = -\frac{\partial\bar{P}}{\partial y} + \nabla \cdot (\mu\nabla\bar{V}) \\ & + \left[ -\frac{\partial(\overline{\rho u'v'})}{\partial x} - \frac{\partial(\overline{\rho v'^2})}{\partial y} \right. \\ & \left. - \frac{\partial(\overline{\rho v'w'})}{\partial z} \right] + S_{My} \end{aligned} \quad (7)$$

$$\begin{aligned} & \frac{\partial(\bar{\rho}\bar{U})}{\partial t} + \nabla \cdot (\bar{\rho}\bar{W}\bar{U}) \\ &= -\frac{\partial\bar{P}}{\partial z} + \nabla \cdot (\mu\nabla\bar{W}) \\ &+ \left[ -\frac{\partial(\overline{\rho u'v'})}{\partial x} - \frac{\partial(\overline{\rho v'w'})}{\partial y} \right. \\ &\left. - \frac{\partial(\overline{\rho w'^2})}{\partial z} \right] + S_{Mw} \end{aligned} \quad (8)$$

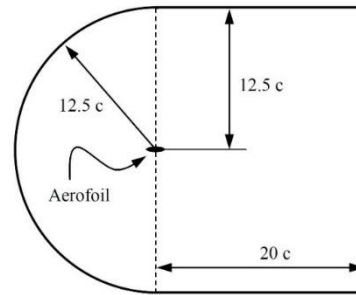


Fig. 1. Airfoil domain dimensions

Scalar transport equation:

$$\begin{aligned} & \frac{\partial(\bar{\rho}\bar{\phi})}{\partial t} + \nabla \cdot (\bar{\rho}\bar{\phi}\bar{U}) \\ &= \nabla \cdot \left( \Gamma_{\phi}\nabla\bar{\phi} + \left[ -\frac{\partial(\overline{\rho u'\phi'})}{\partial x} - \frac{\partial(\overline{\rho v'\phi'})}{\partial y} \right. \right. \\ &\left. \left. - \frac{\partial(\overline{\rho w'\phi'})}{\partial z} \right] + S_{\phi} \right) \end{aligned} \quad (9)$$

The models that were used in the current study are: Spalart-Allmaras (one equation), k-ε (Two equation), k – ω (Two equation), k-ω SST (two equation), k-kl-ω Transition Model, and Transition SST Model

coefficient of drag ( $C_d$ ), and the coefficient of lift ( $C_l$ ) are given by

$$C_d = \frac{D}{\frac{1}{2}\rho V^2 A} \quad (10)$$

$$C_l = \frac{L}{\frac{1}{2}\rho V^2 A} \quad (11)$$

Where D and L are the drag and the lift forces respectively, ρ is the air density, V is the air freestream velocity, and A is the projected area.

**Case Geometry:**

The airfoil's geometry and mesh were created using ANSYS ICEM CFD software, with a chord length of 1 meter and an angle of attack of 0 degrees. The choice of this angle of attack was chosen to highlight the effect the difference in camber and shape of the airfoil had on its performance, and how this could translate to its performance in the automotive application. A NACA0012 profile was utilized for the mesh test, which was then applied to other airfoils. The fluid domain dimensions are depicted in Figure 1 below:

The mesh was structured in a C-type configuration using blocks, as illustrated in Figure 2, to ensure organized meshing and smooth transition with minimal skewness and element distortion, facilitating a fine mesh. Achieving an accurate solution necessitated very fine mesh elements near the wall, thus a first layer spacing of  $8 \times 10^{-6}$  meters was employed, with a growth rate of 1.1

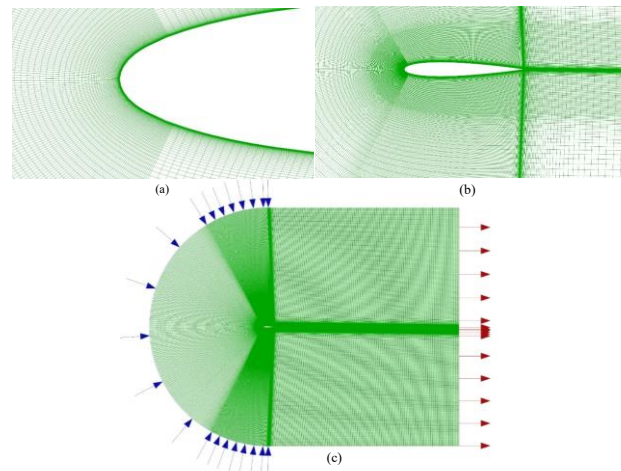


Fig. 2. (a) Airfoil leading edge mesh closeup, (b) Airfoil mesh closeup, (c) Airfoil domain mesh

**Car mesh:**

The car mesh was generated in 2-D modeled after a BMW 3 series (E36), the dimensions were taken from BMW's service manual, the mesh and geometry were created in ANSYS ICEM CFD as illustrated in Figure 3.

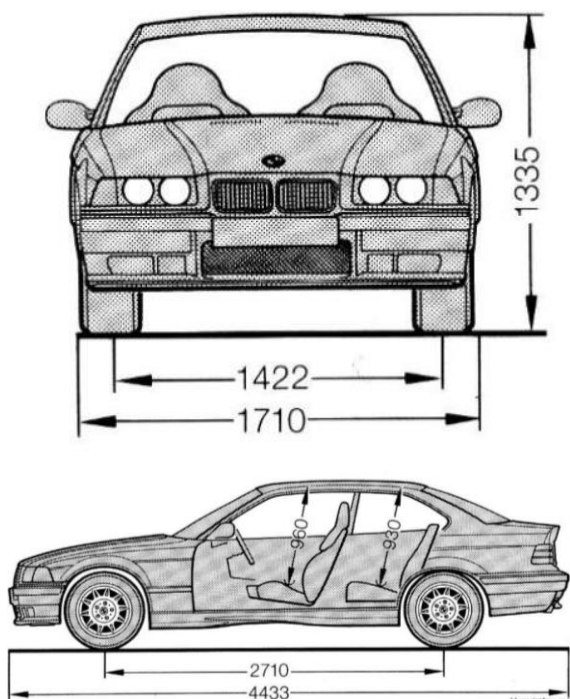


Fig. 3. BMW 3 series (E36) blueprint

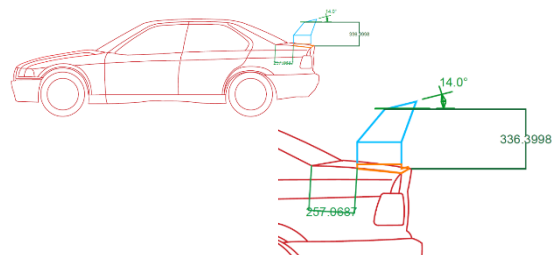


Fig. 4. (a) BMW 3 series (E36) CAD design of the rear wing, (b) BMW 3 series (E36) 2D drawing of the car body's outline used in the simulation

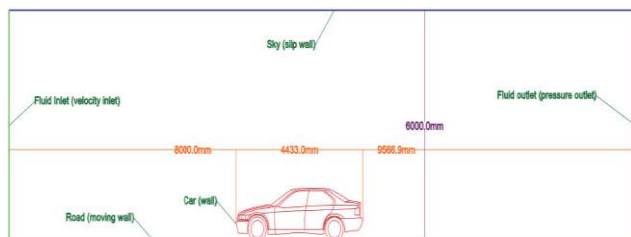


Fig. 5. BMW 3 series (E36) Fluid domain dimensions and boundaries

The mesh was refined by dividing the mesh blocks to avoid skewed elements and to improve quality. The fluid domain which represents the air flowing around the car was drawn as shown in Figure 5.

The boundaries are identified as shown in the Figure 5, sky is assumed a slip wall, the road as a moving wall, the car as wall, fluid inlet as a velocity inlet, and the fluid outlet as a pressure outlet, the airfoil was placed according to the CAD design in the Figure 4, the dimensions were referenced from a real wing used in BMW race cars, measurements were taken to replicate the real wing, although different airfoil sections were used, but all are at 14° AOA relative to the horizontal not the airstream coming down from the car's roof, although the angle could be optimised to avoid separation that may lead to (stall), but this wasn't within the objective of the current study, Stall is where the streamlines do not follow the airfoil shapes and the flow will be separated. This will result in dramatic loss of lift (stall) and sudden increase in drag, as shown in Figure 6 Below <sup>28</sup>.

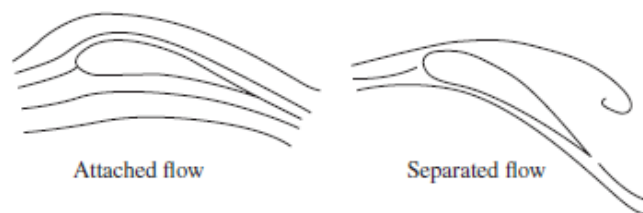


Fig. 6. Schematic description of the streamlines in airfoil attached and separated flow <sup>28</sup>

The airfoil was placed according to the CAD design in the Figure 5(a), the dimensions were referenced from a real wing used in BMW race cars, measurements were taken to replicate the real wing, although different airfoil sections were used, but all are at 14° AOA.

The airfoil (inverted wing) was drawn in its specified place) above the rear boot lid, and meshing was made. Figure 7 depicts the complete mesh of the fluid domain, blue arrows represent the air entering and red arrows represent the air leaving the domain.

The mesh minimum determinant quality was 0.7, and the minimum angle in the mesh was 18 degrees, the values of these mesh metrics are acceptable according to ICFM CFD's tutorial manual (29) which predicts a reasonable solution.

**Mesh test and model validation:**

In order to ensure that the solution is independent of the mesh, a mesh test is carried out. Two meshes were generated, one for the simulation of the airfoils, and one for the simulation of the car, which is the application of the present work for the airfoil.

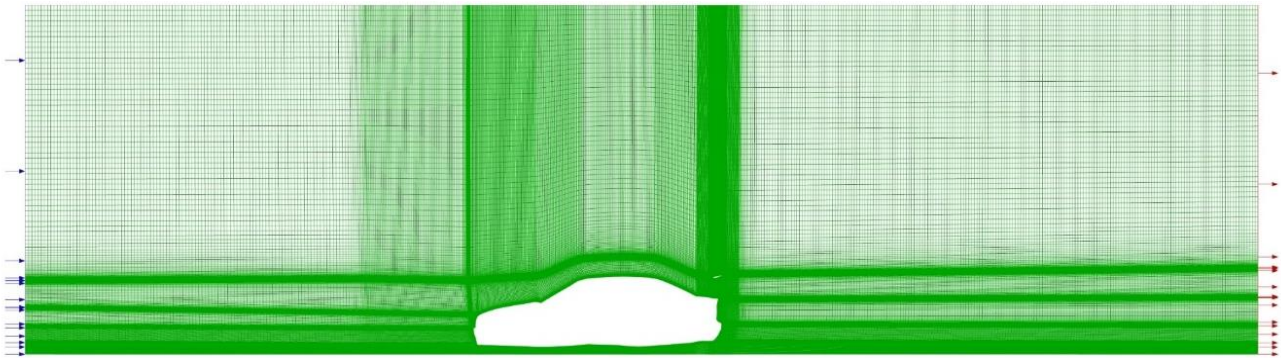


**Fig. 7. BMW 3 series (E36) Fluid domain dimensions and boundaries**

Several turbulence models were tested in order to ascertain the suitability of each model for given conditions

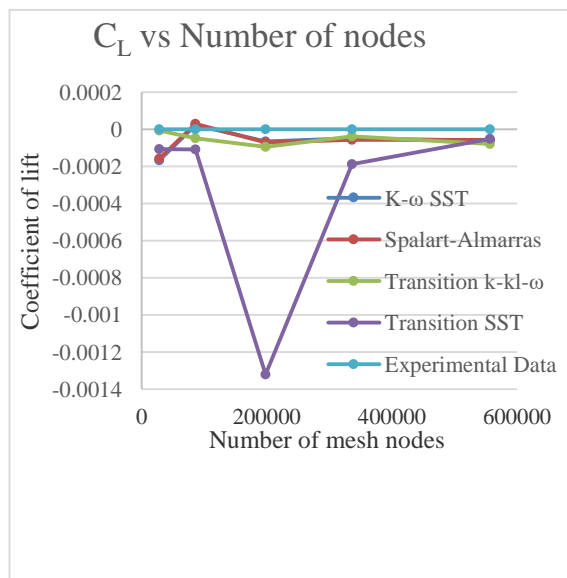


**Fig. 8.  $C_L$  vs number of nodes**

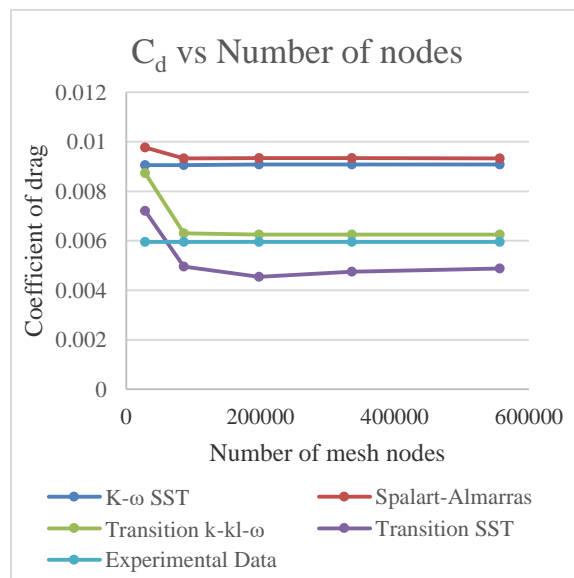


**Fig. 9.  $C_d$  vs number of nodes**

***Airfoil mesh test:***

The mesh is tested on a NACA0012 airfoil,

**Table 1 NACA0012 mesh sensitivity test**

Cd					
[Nodes\model]	K- $\omega$ SST	Spalart-Allmaras	Transition k-kl- $\omega$	Transition SST	Experiment Data
28380	0.009064248	0.009765499	0.008739613	0.00721464	0.00596
85792	0.009061483	0.009330248	0.006297206	0.004964117	
197932	0.009084467	0.009342926	0.006256086	0.004541023	
336124	0.009084229	0.009337151	0.00625686	0.004757129	
556604	0.009079381	0.009330945	0.006254567	0.004882753	
CL					
28380	-0.00016592	-0.00015697	-0.00000627	-0.00010534	0
85792	0.0000235	0.0000299	-0.000047	-0.00010735	
197932	-0.0000648	-0.0000701	-0.0000941	-0.00132037	
336124	-0.0000483	-0.0000562	-0.0000363	-0.00018634	
556604	-0.0000614	-0.0000568	-0.0000783	-0.0000507	

As can be seen from the mesh test graphs at Figure 8 and Figure 9, the most accurate turbulence model for the given conditions is the Transition k-kl- $\omega$ , and after 336124 nodes the solution becomes independent of the mesh, the other models show relative independence but they are less accurate, the accuracy of the Transition k-kl- $\omega$  model is shown in the  $C_d$  results, In terms of  $C_l$ , most models demonstrated a reasonable level of accuracy.

The next step is the model validation of the present work, using Eleni Douvi <sup>1</sup> as the validation for the present project, the 80 k nodes mesh was utilized to compare it to the same cell count as was used in Douvi’s study, and compared the same NACA0012 airfoil at the same Re number of  $3 \times 10^6$ , at an angle of attack of  $0^\circ$ .

**Table 2 Airfoil model validation**

	CFD current mesh (80k nodes and k-kl- $\omega$ )	Douvi (1)	Deviation %
<b>Cd</b>	0.006370985	0.00635815	0.201 %
<b>Cl</b>	-0.000173073	0	Not Applicable

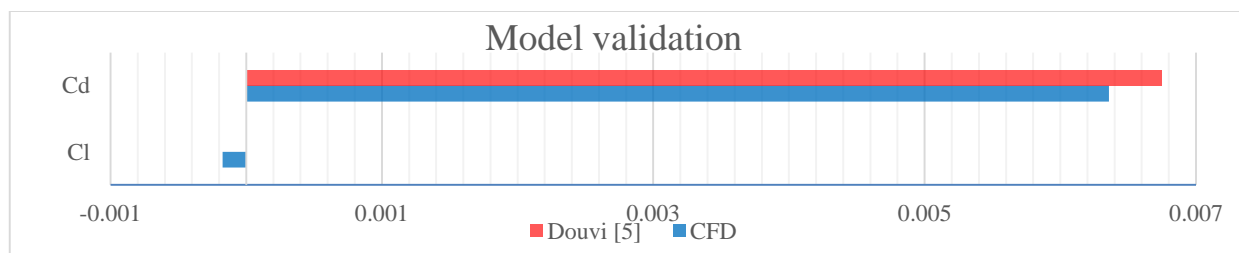


**Fig. 10. Airfoil model validation**

**Car mesh test:**

Car mesh is tested for solution independence using several mesh node resolutions and turbulence models, selected at three various speeds, 100kmph, 160kmph and 200kmph, which were chosen because they are realistic highway speeds.

The mesh test is conducted on a BMW E36 with a NACA 4412 inverted wing at an angle of attack of  $14^\circ$  as presented in Table 3.

**Table 3 BMW 3series (E36) mesh test**

Nodes	180000	255927	355447	500000	
Model	100kmph				
k kl ω	C <sub>d</sub>	0.454195	0.450342	0.450922	0.448735
	C <sub>l</sub>	-2.35805	-2.43034	-2.51799	-2.54053
	Drag (N)	422.6578	419.0728	419.6132	417.5776
	Lift (N)	-2194.32	-2261.59	-2343.16	-2364.13
	160kmph				Unstable
	C <sub>d</sub>	0.43986	0.434905	0.435619	0.433068
	C <sub>l</sub>	-2.37036	-2.40457	-2.45463	-2.4759
	Drag (N)	1047.853	1036.048	1037.75	1031.672
	Lift (N)	-5646.76	-5728.28	-5847.52	-5898.2
	200kmph				Unstable
	C <sub>d</sub>	0.432401	0.470954	0.430603	0.428–059
	C <sub>l</sub>	-2.32786	-2.55363	-2.40075	-2.41287
	Drag (n)	1609.508	1753.009	1602.813	1593.347
Lift (n)	-8664.9	-9505.24	-8936.2	-8981.32	
Spalart Allmaras	100kmph				
	C <sub>d</sub>	0.432697	0.429656	0.428051	0.426511
	C <sub>l</sub>	-3.56567	-3.54026	-3.58361	-3.55978
	Drag (N)	402.6533	399.8234	398.3297	396.8967
	Lift (N)	-3318.09	-3294.44	-3334.79	-3312.61
	160kmph				
	C <sub>d</sub>	0.42761	0.42428	0.418946	0.418019
	C <sub>l</sub>	-3.72755	-3.70285	-3.72101	-3.7048
	Drag (N)	1018.67	1010.739	998.0312	995.8191
	Lift (N)	-8879.92	-8821.09	-8864.35	-8825.73
	200kmph				
	C <sub>d</sub>	0.425626	0.422212	0.41541	0.414556
	C <sub>l</sub>	-3.80655	-3.78129	-3.79065	-3.77611
Drag (N)	1584.29	1571.581	1546.265	1543.087	
Lift (N)	-14169	-14074.9	-14109.8	-14055.7	
k-ω SST	100kmph				
	C <sub>d</sub>	0.37115	0.357593	0.357179	0.358064
	C <sub>l</sub>	-2.87933	-2.75098	-2.76362	-2.87303
	Drag (N)	345.3797	332.7639	332.3785	333.2018
	Lift (N)	-2679.4	-2559.97	-2571.73	-2673.54
	160kmph				
	C <sub>d</sub>	0.353834	0.351034	0.350595	0.344617
	C <sub>l</sub>	-2.92867	-2.90664	-2.91905	-3.00433
	Drag (N)	842.9171	836.2468	835.2017	820.9604
	Lift (N)	-6976.8	-6924.32	-6953.89	-7157.05
	200kmph				
	C <sub>d</sub>	0.350211	0.348012	0.347617	0.34306
	C <sub>l</sub>	-2.99511	-2.97821	-2.98996	-3.05896
Drag (N)	1303.575	1295.39	1293.92	1276.959	
Lift (N)	-11148.6	-11085.7	-11129.4	-11386.3	

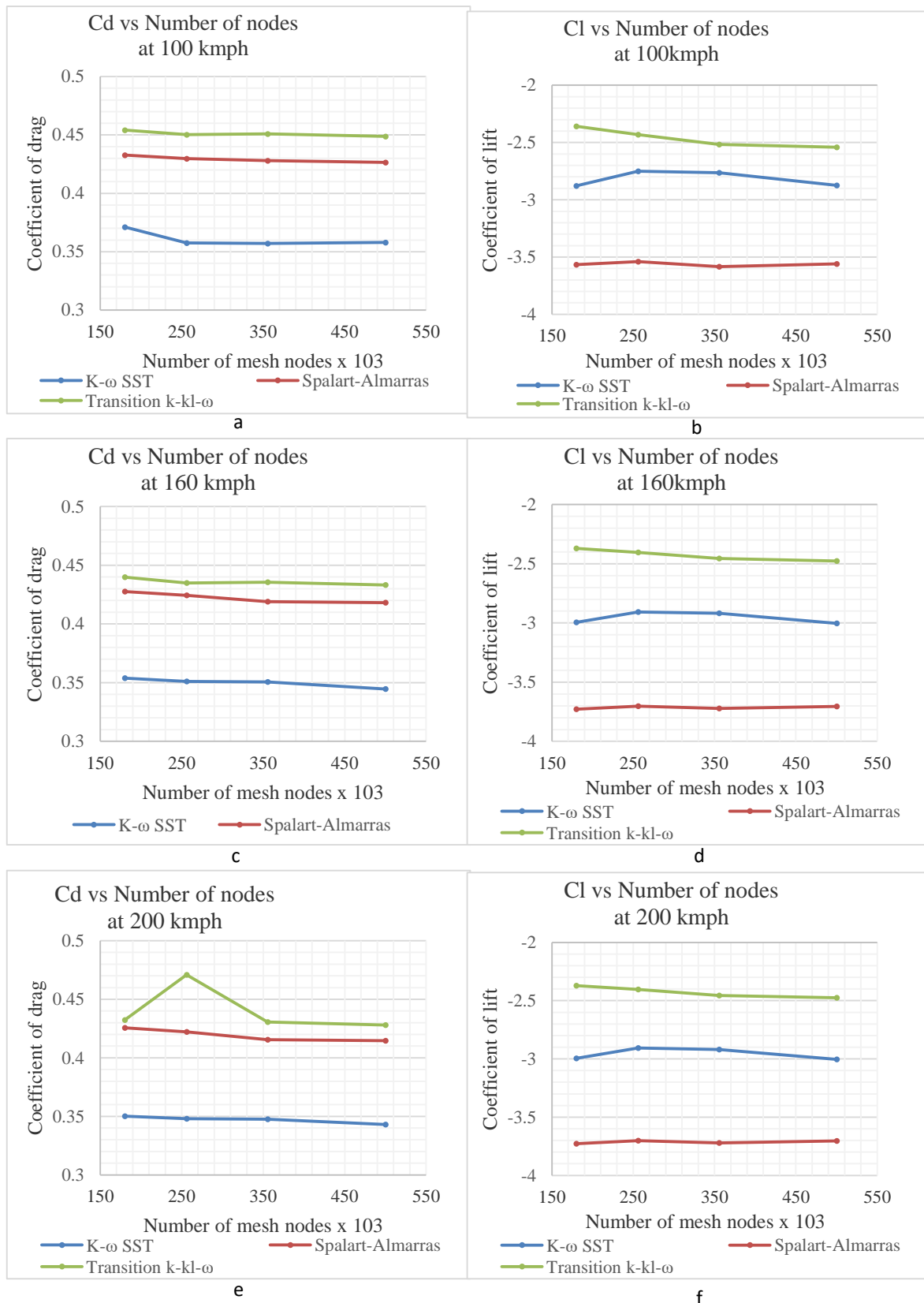
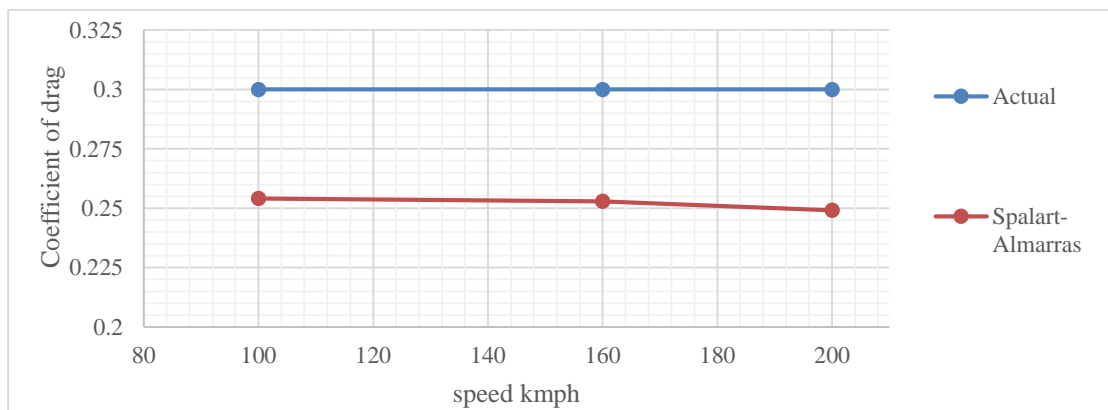


Fig. 11. a) Cd vs number of nodes at 100km/h b) Cl vs number of nodes at 100km/h c) Cd vs. number of nodes at 160km/h d) Cl vs number of nodes at 160km/h e) Cd vs number of nodes at 200km/h f) Cl vs number of nodes at 200km/h

**Table 4 BMW 3-series (E36) model validation**

Spalart Allmaras	100kmph	
	C <sub>d</sub>	0.254132
	C <sub>l</sub>	-2.0065
	Drag (N)	236.4862
	Lift (N)	-1867.18
	160kmph	
	C <sub>d</sub>	0.252933
	C <sub>l</sub>	-0.99395
	Drag (N)	602.5467
	Lift (N)	-2367.82
	200kmph	
	C <sub>d</sub>	0.249153
C <sub>l</sub>	-0.98211	
Drag (N)	927.4115	
Lift (N)	-3655.67	



**Fig. 12. BMW 3-series (E36) model**

From the mesh independence test, it can be seen that the Spalart Allmaras has shown most stability from 355k node mesh to 500k node mesh, while the k-kl- $\omega$  transition model has shown instabilities and non-converged solutions in the 500k node mesh so it was eliminated, then the selected mesh was the 355k node with the Spalart Allmaras model, the selected mesh is to be validated.

The car simulation model was validated using actual results from BMW’s service manual, the C<sub>d</sub> is stated as 0.3 for the car, our 2D result for the same mesh for the car without any wing is around 0.25, with little change across different speeds, the error percentage is 16.67%, which is very reasonable since the 2D model doesn’t account for wheels turbulence induced drag, side mirrors

and other details that affect the drag, so it is reasonable for the drag to be less than the actual value.

### 3. RESULTS AND DISCUSSION

In this section, the results are presented and discussed thoroughly, simulations are divided into airfoils simulations and car with airfoil (inverted wing). The airfoils considered in the present work are: NACA 0012, NACA 4412 and Eppler E 423

#### *Simulation of the airfoils:*

In this stage of the simulation, the performance of three airfoils was compared using the selected and validated model in the previous section, the mesh test has shown that the best suited mesh for the selected

conditions was the 355647-node mesh using the transition k-kl- $\omega$  turbulence model.

The angle of attack for all airfoils in freestream was chosen at 0 was to serve the objective of the study by highlighting the effect the difference in camber and shape of the airfoil had on its performance, as discussed in the mesh section earlier. It is worth to mention that Lift will be zero only for 0012, however, the study of the effect of angle of attack was not the objective of this study, it was to highlight the difference in performance of the airfoils

in freestream and how it is reflected in the automotive application of the airfoil in an inverted rear wing.

The simulation conditions selected are:

Reynolds number =  $3 \times 10^6$ , and AOA =  $0^\circ$

From equations 10 and 11, the Cd and Cl were calculated, and compared with experimental data (1) to evaluate the accuracy of the solution, the results are shown in Table 5, Figure 13 and Figure 14.

**Table 5 Airfoil simulation results compared with experimental data**

Airfoil		CFD results	Experimental results	Percentage error %
NACA 0012	Cd	0.00625686	0.00587	6.5%
	Cl	-0.000772	0	n/a
NACA 4412	Cd	0.006579026	0.006744	2.44%
	Cl	0.42086817	0.4129	1.9%
E 423	Cd	0.009057841	0.00915	1%
	Cl	1.1834935	1.16	2%

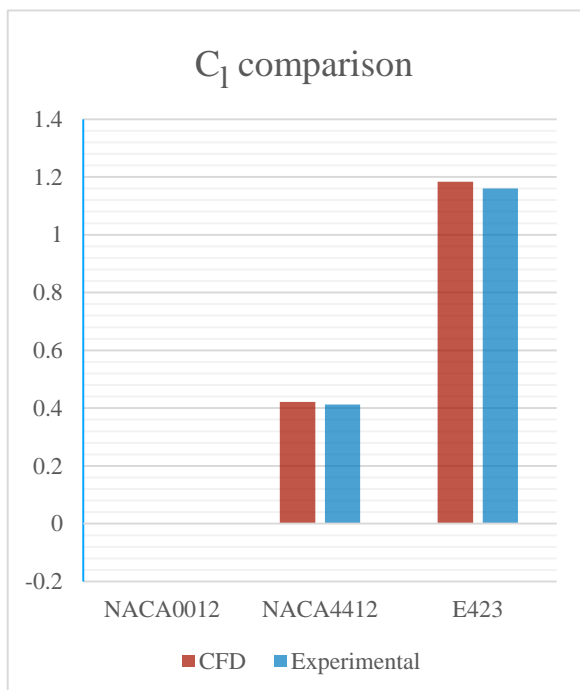


**Fig. 13. Airfoil  $C_l$  comparison**

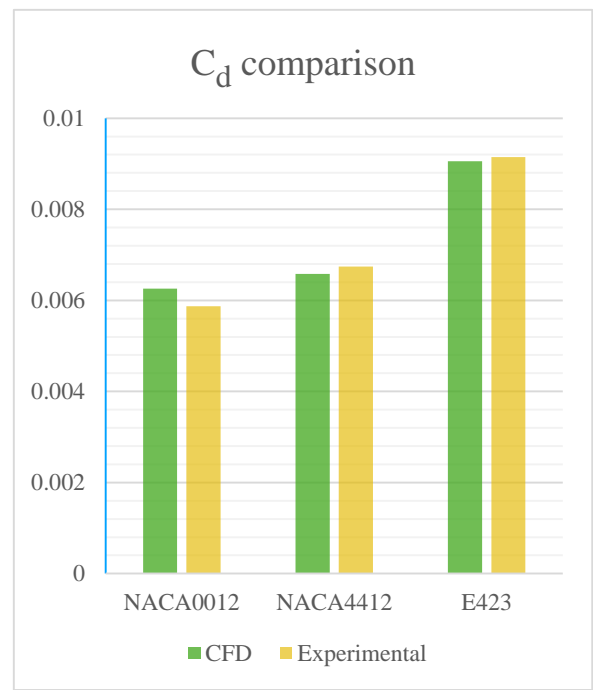


**Fig. 14. Airfoil  $C_d$  comparison**

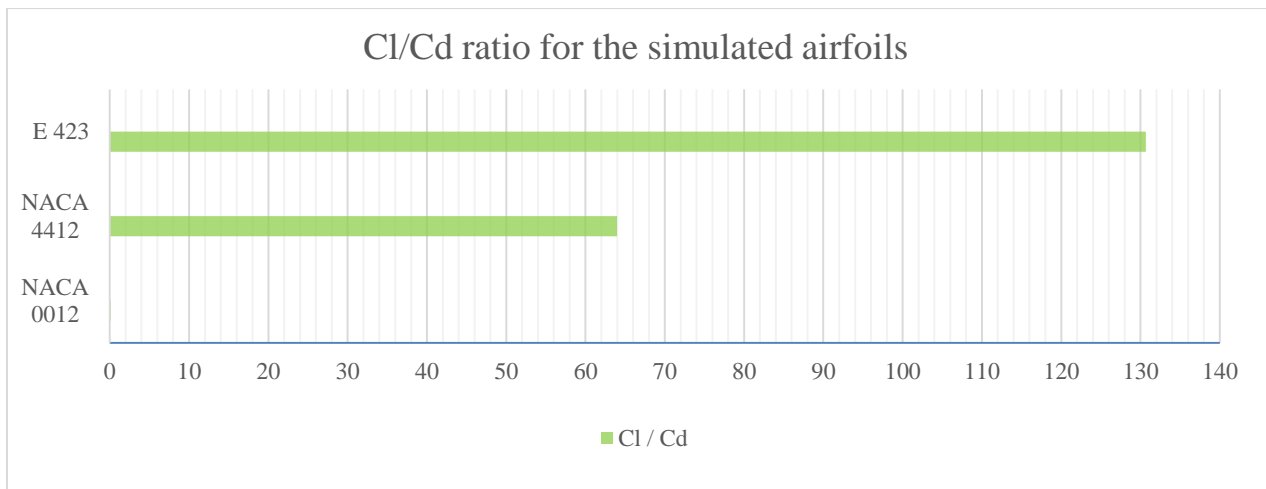


**Fig. 15. Cl/Cd ratio for the simulated airfoils**

The Cl value for the NACA0012 is very small that it can't be displayed in the graph. Given the favorable agreement displayed in the results, we proceeded with assessing the performance of each airfoil.

**Table 6 Cl/Cd for airfoils**

NACA 0012	0.12
NACA 4412	63.97
E 423	130.659

Table 6 and the Figure 15 show that at an AOA of 0° the most lift to drag ratio was generated by the Eppler E423 airfoil, followed by NACA 4412, then NACA0012 generated almost no lift at all at an AOA of zero.

The performance of the airfoils will be further evaluated when used in an application in the second stage of the present study, in such a case where the automotive application as an inverted wing mounted on a BMW 3-series (E36).

**Car simulation with airfoil (inverted wing):**

In this section, the BMW 3 series (E36) was simulated without any modifications, using the selected

mesh from the mesh test, with 355447 nodes and Spalart-Allmaras turbulence model, then the results were compared with actual Cd value in (25), a very good agreement was obtained, since the mesh is tested, one is now able to simulate the BMW 3-series (E36) with the modification of adding a rear inverted wing, the AOA of the airfoil is 14° relative to the horizontal as discussed in the mesh section earlier.

Three different airfoils were used as inverted wings, to produce a negative lift force on the wheels, commonly known as downforce, to increase traction, increase max friction force and allow for faster acceleration without wheel spin, accordingly selection of the proper airfoil for the BMW is feasible.

The freestream velocities we used in the simulation are:

1. 100kmph (27.7778m/sec)
2. 160kmph (44.4444m/sec)
3. 200kmph (55.5555m/sec)

Just like the airfoil parameters calculated in the present of the study, equations 10 and 11, the Cd and Cl for the car's body was calculated and the results are shown in Table 7

**Table 7 BMW 3-series (E36)**

	wingless	NACA4412	Eppler E423	NACA0012
100kmph				
Cd	0.254	0.429	0.435	0.4131
Cl	-2.003	-3.587	-3.8779726	-3.368
Drag (n)	236.47	400.14	404.79	384.42
Lift (n)	-1864.50	-3338.61	-3608.70	-3134.35
Moment at Rear wheel	2410.1392	3308.8741	3433.97	3200.92
160kmph				
Cd	0.249	0.419	0.429	0.407
Cl	-2.135	-3.719	-4.022	-3.514
Drag (n)	593.46	999.16	1022.20	969.859
Lift (n)	-5086.47	-8861.71	-9581.67	-8371.37
Moment at Rear wheel	6497.10	8812.37	9164.86	8562.57
200kmph				
Cd	0.247	0.415	0.426	0.404
Cl	-2.203	-3.789	-4.095	-3.588
Drag (n)	920.47264	1546.8291	1588.67	1505.96
Lift (n)	-8203.3524	-14103.952	-15245.31	-13355.38
Moment at Rear wheel	10408.47	14037.41	14607.09	13660.59

Table 7 and the graphs in figures 16 and 17 show that incorporating of the rear wing Eppler E423 exhibited the highest amount of lift force, moreover the highest drag force, followed by the NACA4412, then the NACA0012, it showed the lowest values for lift and drag. All wing modifications showed lift improvements over the unmodified BMW 3-series (E36), although lift improved as negative lift increase, it came with the penalty of drag forces increase, the evaluation for the best performance that can be gained from the wings which will be discussed next.

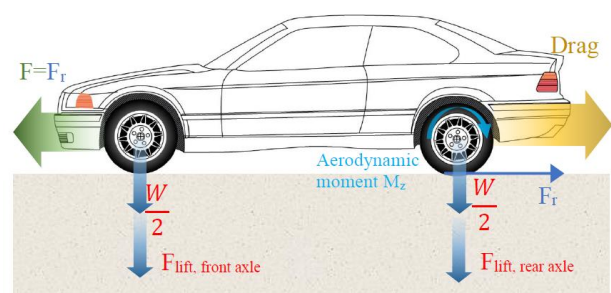


**Fig. 16 BMW E36 force and moment analysis**

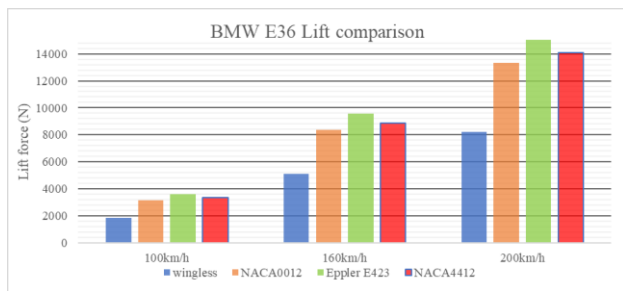


Fig. 17. BMW E36 Lift comparison

Table 7 also presents the aerodynamic moment around the center of the rear wheels due to aerodynamic forces as shown in Figure 16 above, this moment is profound to evaluate the aerodynamic balance of the car, and will aid in the calculation of the maximum acceleration attainable using the force pushing down on the rear wheels, since the car in the current study is rear wheel driven.

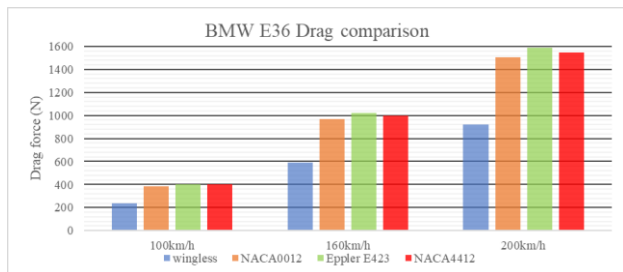


Fig. 18. BMW E36 Drag comparison

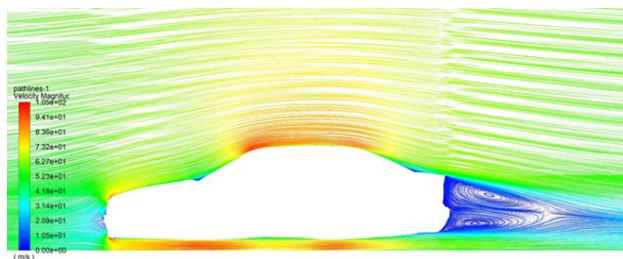


Fig. 19. BMW E36 wingless velocity lines

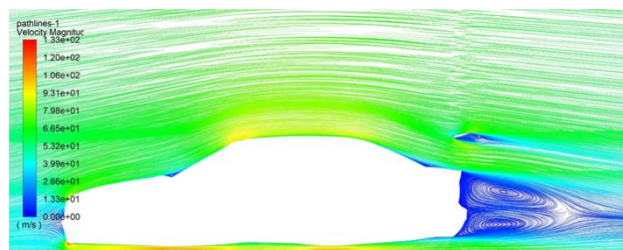


Fig. 20. BMW E36 with NACA0012 velocity lines

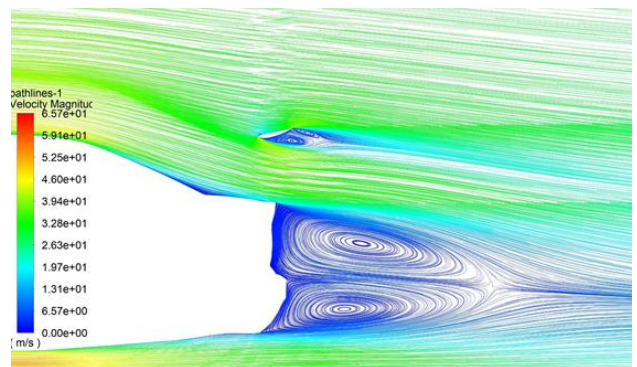


Fig. 21. BMW E36 with NACA4412 wing velocity lines wing

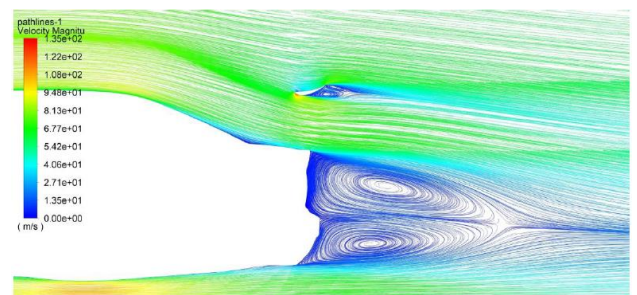


Fig. 22. BMW E36 with Eppler 423 wing velocity lines wing

Figures 19 to 22 above depict the velocity lines for BMW E36 without and with the wings used in this study. The figures illustrate the characteristics of the flow for the BMW 3-series (E36) with the addition of the different airfoils as a rear wing and show the separation zone behind the car as well as behind the rear wing.

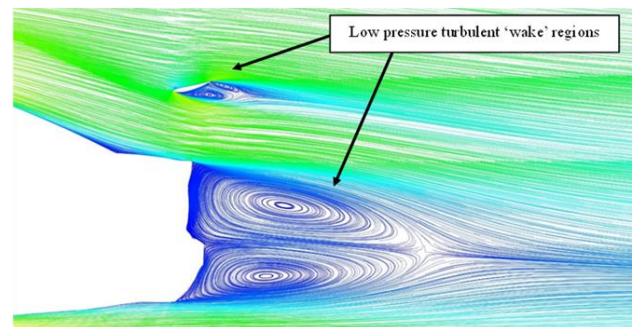


Fig. 23. Velocity Lines Showing Car Vortices and Low-Pressure Regions

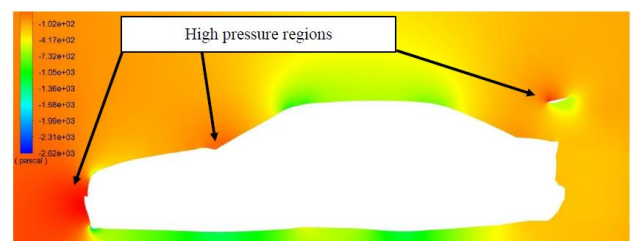


Fig. 24. Velocity Lines Showing Car Vortices and Low-Pressure Regions

The velocity lines and pressure contour depicted in the figures 23 and 24 above respectively reveal an intriguing phenomenon: how the car produces drag and lift forces, and the role of the rear inverted wing in augmenting the negative lift force, known as downforce. The pressure contours indicate that the front end of the car experiences high pressure, while pressure decreases behind it, leading to drag that opposes the car's forward motion through the air. This relationship is confirmed by the velocity lines, as pressure and velocity are inversely related. The wake area formed behind the car, where separation occurs, creates a vacuum effect that draws in air at high speeds, resulting in low pressure behind the car. Figure 23 highlights these low-pressure regions.

#### 4. CONCLUSION

The present study focused on the analysis of performance of various aerfoils and testing them in a rear wing car in a numerical study, the following findings were highlighted as:

- The NACA 0012 produced the least due to it being a symmetrical airfoil, it produced the least amount of lift making it less suitable for applications requiring significant lift. In contrast, the NACA 4412 generates higher lift and drag forces. Conversely, the Eppler E423 produces the highest lift and drag forces due to its highly cambered shape, which creates a substantial pressure differential between the upper and lower surfaces of the airfoil.
- employing the airfoil in an automotive application as an inverted wing on a BMW 3-series (E36) car, the results indicate that at a specified angle of attack (AOA) of 14 degrees for the three airfoils, the NACA0012 exhibits the lowest drag and lift forces among them. Conversely, the Eppler E423 demonstrates the highest lift-to-drag ratio. However, it's important to note that this ratio alone does not necessarily guarantee the best performance. The evaluation of performance was conducted according to predetermined criteria
- The NACA4412 has demonstrated relatively high lift and drag forces compared to both the NACA0012 and the unmodified car without wings, although these values are not as high as those produced by the Eppler E423 airfoil.
- The conclusion drawn was that the Eppler E423 inverted wing demonstrated the best performance in terms of acceleration. It exhibited the greatest increase in potential acceleration that could be applied at the wheels without causing wheel spin or power loss. However, the NACA4412 closely followed suit, showing performance very similar to the Eppler E423. Conversely, the NACA0012 performed the worst in terms of acceleration potential. Nevertheless, it's noteworthy that all airfoils provided a performance advantage over the unmodified, wingless car body.

- After thorough consideration of the studied case, which includes the car model, the airfoils utilized, and the analyzed conditions and speeds, it is concluded that incorporating the Eppler E423 airfoil as an inverted wing onto the rear of the BMW 3-series (E36) car at an angle of attack of 14 degrees represents the optimal choice in terms of achieving both performance enhancements and safety improvements.

Nonetheless, future studies should meticulously evaluate the trade-offs between drag forces, associated power consumption, and the resulting performance gains to ensure a net positive impact on overall vehicle efficiency.

#### ACKNOWLEDGMENT

We acknowledge the collaborative spirit and commitment of our team members, whose collective effort made this work possible. While this research was conducted without external funding, the encouragement and support from our colleagues were influential in our research.

#### 5. REFERENCES

1. Douvi EC, Tsavalos AI, Margaris DP. cfd calculations of the flow over a naca0012 airfoil. *Momentum*. 2010; 10:4.
2. Kevadiya M, Vaidya H. 2D analysis of NACA 4412 airfoil. *Education*. 2011;2013.
3. Reza MMS, Mahmood SA, Iqbal A, editors. Performance analysis and comparison of high lift airfoil for low speed unmanned aerial vehicle. *International Conference on Mechanical, Industrial and Energy Engineering*; 2016.
4. Panchal K. Computational Assessment of Front and Rear Wing of Amity Racing Vehicle. *SAE Technical Paper*, 2015 0148-7191.
5. Ahmed T, Amin MT, Islam SR, Ahmed S. Computational study of flow around a NACA 0012 wing flapped at different flap angles with varying Mach numbers. *Glob J Res Eng*. 2014;13(4):4-16.
6. Abobaker M, Elfaghi AM, Addeep S. Numerical Study of Wind-Tunnel Wall Effects on Lift and Drag Characteristics of NACA 0012 Airfoil. *CFD Letters*. 2020;12(11):72-82.
7. Bhatia D, Zhao Y, Yadav D, Wang J. Drag reduction using biomimetic sharkskin denticles. *Engineering, Technology and Applied Science Research*. 2021;11(5):7665-72.
8. Etaig SAM. Computation of Turbulent Buoyancy-affected Flows Relevant to Nuclear Reactor Cooling Applications: *University of Manchester*; 2007.
9. Sogukpinar H, editor the effects of NACA 0012 airfoil modification on aerodynamic performance improvement and obtaining high lift coefficient and post-stall airfoil. *AIP conference proceedings*; 2018: AIP Publishing.

10. Karim MM, Prasad B, Rahman N. Numerical simulation of free surface water wave for the flow around NACA 0015 hydrofoil using the volume of fluid (VOF) method. *Ocean engineering*. 2014; 78:89-94.
11. Azim R, Hasan M, Ali M. Numerical investigation on the delay of boundary layer separation by suction for NACA 4412. *Procedia Engineering*. 2015; 105:329-34.
12. Hossain S, Raiyan MF, Akanda MNU, Jony NH. A comparative flow analysis of NACA 6409 and NACA 4412 aerofoil. *International Journal of Research in Engineering and Technology*. 2014;3(10):342-50.
13. Singh J, Singh J, Singh A, Rana A, Dahiya A. Study of NACA 4412 and Selig 1223 airfoils through computational fluid dynamics. *SSRG International Journal of Mechanical Engineering (SSRG-IJME)–volume*. 2015;2(6):17-21.
14. Saraf AK, Singh M, Kumar A. Analysis of the Spalart-Allmaras and  $k\omega$  standard models for the simulation of the flow over a National Advisory Committee for Aeronautics (NACA) 4412 airfoil. 2012.
15. Saraf A, Nazar FA, Singh SP. Analysis of the  $k-\epsilon$  and  $k-\omega$  standard models for the simulation of the flow over a National Advisory Committee for Aeronautics (NACA) 4412 airfoil *International Journal of Scientific & Engineering Research*. *International Journal of Scientific & Engineering Research*. 2013;4(6).
16. Petinrin M, Onoja V. Computational study of aerodynamic flow over NACA 4412 airfoil. *British Journal of Applied Science & Technology*. 2017;21(3):1-11.
17. Win SY, Thianwiboon M. Parametric optimization of NACA 4412 airfoil in ground effect using full factorial design of experiment. *Engineering Journal*. 2021;25(12):9-19.
18. <BOUANCY DRIVEN.pdf>.
19. Qu Q, Jia X, Wang W, Liu P, Agarwal RK. Numerical study of the aerodynamics of a NACA 4412 airfoil in dynamic ground effect. *Aerospace Science and Technology*. 2014; 38:56-63.
20. Huminic A, Huminic G. Automotive wing with active control of flow. *UPB Scientific Bulletin, Series D: Mechanical Engineering*. 2014;76(4):231-8.
21. Bhatkar O, Prabhutendolkar N, Sakpal A, Sawant S, Sakpal O. '2D analysis of multi-element airfoil for wing. *International Research Journal of Engineering and Technology*. 2018;5(2):174-7.
22. Sreejith B, Sathyabhama A. Numerical study on effect of boundary layer trips on aerodynamic performance of E216 airfoil. *Engineering science and technology, an international journal*. 2018;21(1):77-88.
23. Guda NT, Suriseti BV, Kolla SRC, Vasamsetti S. Enhancing Aerodynamic Performance of a Hatch Back Model Passenger Car using Ansys Fluent Software.
24. Kumar VN, Narayan KL, Rao L, Ram YS, Kumar V. Investigation of Drag and Lift Forces over the Profile of Car with Rear spoiler using CFD. *International journal of advances in scientific research*. 2015;1(08):331-9.
25. Kiley D. *Driven: inside BMW, the most admired car company in the world*: John Wiley & Sons; 2004.



# Effect of Intercritical Annealing Parameters on The Hardness Property: Statistical Study Using Taguchi

Asma F. Haiba<sup>1</sup> - Farag I. Haider<sup>2\*</sup> - Mohamed Gebri<sup>2</sup> - Dawod Elabar<sup>2</sup> - Ayad O. Abdalla<sup>3</sup>

<sup>1</sup> Medical Engineering Department - College of Medical Technology-Benghazi.

<sup>2</sup> Mechanical Engineering Department - Faculty of Engineering - University of Benghazi.

<sup>3</sup> Mechanical Engineering Department - College of Mechanical Engineering Technology-Benghazi.

Received: 09 / 03 / 2024; Accepted: 14 / 05 / 2024

## ABSTRACT

Dual-phase steel is characterized by good strength and hardness with high ductility. This type of steel has a wide range of uses in the modern-day industry, especially in the automobile industry. This paper reports an experimental study of the effect of intercritical annealing parameters such as temperature and soaking time on hardness. The Taguchi method based on  $L_9$  was used with a temperature range from 750 °C to 800 °C and a soaking time range from 30 min to 60 min. All samples were treated in the furnace at a specified temperature and soaking time quenched in water. It is observed that the hardness increases with increasing the intercritical temperature and soaking time. On the other hand, temperature has a significant effect more than soaking time on the hardness.

**KEYWORDS:** Intercritical Annealing, Dual-phase Hardness, Taguchi.

## 1. INTRODUCTION

Dual-phase (DP) steels have become the preferred materials for many modern industries, particularly in the automotive sector, due to their energy-saving, lightweight, and safe properties<sup>1</sup>. This is because DP steels are composed of different phases, with martensite as the hard phase and ferrite as the ductile soft phase<sup>2</sup>. The martensite phase is dispersed within the ferrite matrix, resulting in a material that is both strong and ductile, making it ideal for applications that require high strength and good formability<sup>3,4</sup>.

DP steel possesses excellent mechanical qualities such as high tensile strength, improved formability, continuous yielding behavior, crashworthiness, high strength-ductility, and high work hardening rates, which make it a reliable and affordable material for the manufacturing sector, including welding<sup>5-8</sup>. The microstructure of DP steels is significantly influenced by heat treatment, particularly during intercritical annealing, which creates a ferrite-martensite structure<sup>9,10</sup>. The mechanical properties of DP steels are further enhanced by factors such as annealing, quenching medium, cooling rate, grain size and pattern, and the chemical composition of the parent material<sup>11</sup>. Finer grain size is preferred as it results in better mechanical properties<sup>12</sup>.

\*Correspondence: Farag I. Haider

[Farag.haider@uob.edu.ly](mailto:Farag.haider@uob.edu.ly)

While much research has been conducted on the microstructure and mechanical properties of DP steels<sup>13-16</sup>, little has been done to predict their hardenability resulting from austenite. Therefore, this study applies the Taguchi method to investigate the effect of process parameters such as temperature (T) and soaking time (ST) on the hardness property of DP steel.

## 2. METHODOLOGY

### 2.1. Material

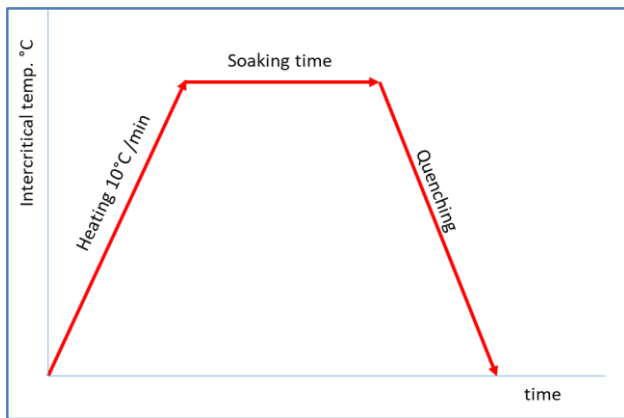
The low-carbon steel was utilized as a workpiece, which was manufactured at the Musrata Steel Factory and had a chemical composition as presented in Table 1.

Table 1. Chemical composition of the low-carbon steel

C	Si	Mn	P	Ni
0.23	0.17	0.68	0.03	0.14
Cr	Mo	Cu	Co	V
0.12	0.02	0.5	0.01	0.01

The study employed an intercritical process for the intercritical annealing of low-carbon steel, as illustrated in Figure 1. The process involved heating the steel to the intercritical temperature, holding it at that temperature for

a specific duration, and then cooling it down to room temperature using water.



**Fig. 1. Intercritical annealing procedure.**

It is important to note that the upper and lower critical temperatures (Ac1 and Ac3) of alloy steel can vary depending on its chemical composition. Andrews' empirical formula, expressed in Equations (1) and (2), provides an estimate of the approximate critical temperatures<sup>17</sup>.

$$Ac1 (C) = 723 - 10.7(\%Mn) - 16.9(\%Ni) + 29.1(\%Si) + 16.9(\%Cr) + 290(\%As) + 6.38(\%W) \quad (1)$$

$$Ac3 (C) = 910 - 203 \%C - 15.2(\%Ni) + 44.7(\%Si) + 104(\%V) + 31.5(\%Mo) + 13.1(\%W) \quad (2)$$

Based on the chemical composition of the low-carbon steel, as given in Table 1, the adjusted Ac<sub>1</sub> and Ac<sub>3</sub> temperatures can be estimated as 720°C and 870°C, respectively.

## 2.2. Taguchi method and design of experiments

### 2.2.1. Taguchi Method

During this study, two process parameters with three levels were selected as presented in Table 2. These experimental factors were used to evaluate the impact of each parameter on the hardness property of the DP steel. The L9 orthogonal array, consisting of nine experiments was chosen to determine the relationship between the input and out parameters.

Table 3 shows the results from heating the samples to a specific temperature and then holding them for the

duration of the soaking time. All heat-treated samples were then quenched in water.

**Table 2. Process Parameter and their levels**

Parameter		Level 1	Level 2	Level 3
A	Temperature (°C)	750	775	800
B	Soaking time (min)	30	45	60

### The signal-to-noise ratio (S/N)

In Taguchi analysis, the responses were converted into signal-to-noise (S/N) ratios. As the goal of this study was to maximize the response (hardness), the higher-the-better performance characteristics were utilized to calculate the S/N ratio using Equation (3)<sup>18</sup>.

$$S/N = -10 \log \left( \frac{1}{n} \sum_{i=1}^n \frac{1}{y_i^2} \right) \quad (3)$$

where n is the number of replications for each experiment and y<sub>i</sub> the result value for the i<sup>th</sup> performance characteristics.

### 2.2.2. Analysis of variance (ANOVA)

ANOVA is a statistical method used to determine the individual contributions and interactions of each parameter within an experimental design. It was employed in this study to investigate the effects of temperature and soaking time on the hardness of the low-carbon steel. ANOVA is a useful tool in determining the order of importance of the influencing parameters on the response, which helps in validating the results obtained through the Taguchi method<sup>19</sup>.

## 3. RESULTS & DISCUSSION

### 3.3. Analysis of a response (Hardness)

The experimental design and results of intercritical annealing are presented in Table 3. Each hardness value represents an average of five measurements. Experiment number 9 yielded the highest hardness value, with an HRA of 62.9, while experiment number 1 had the lowest hardness value, with an HRA of 57.4.

**Table 3. Experimental results and their S/N ratios**

Run	A Temperature (°C)	B Soaking time (min)	Average Hardness (HRA)	S/Nraios
L1	750	30	57.4	35.1782
L2	750	45	57.8	35.2386
L3	750	60	58.0	35.2686
L4	775	30	59.2	35.4464
L5	775	45	59.8	35.5340
L6	775	60	60.2	35.5919
L7	800	30	62.4	35.9037
L8	800	45	62.6	35.9315
L9	800	60	62.9	35.9730

Figure 2 displays the average hardness value for each run, as well as the hardness value of the as-received sample. It is evident that the hardness increased with all heat treatment runs when compared to the as-received hardness of 55.9 HRA. However, for runs 1, 2, and 3, when the temperature was 750°C and the soaking time was 30, 45, and 60 min, respectively, the hardness increased only slightly from 57.4 HRA to 58.0 HRA. Similarly, runs 4, 5, and 6, when the temperature was 775°C and the soaking time was 30, 45, and 60 min,

respectively, resulted in an increase in hardness from 59.2 HRA to 60.2 HRA. In contrast, the hardness increased significantly from 62.2 HRA at run 7, where the temperature was 800°C and the soaking time was 30 min, to 62.9 HRA at run 9, where the temperature was 800°C and the soaking time was 60 min. Additionally, the hardness increased noticeably with an increase in temperature from 58 HRA at a temperature of 750°C and a soaking time of 60 min to 62.9 HRA at a temperature of 800°C and a soaking time of 60 min.

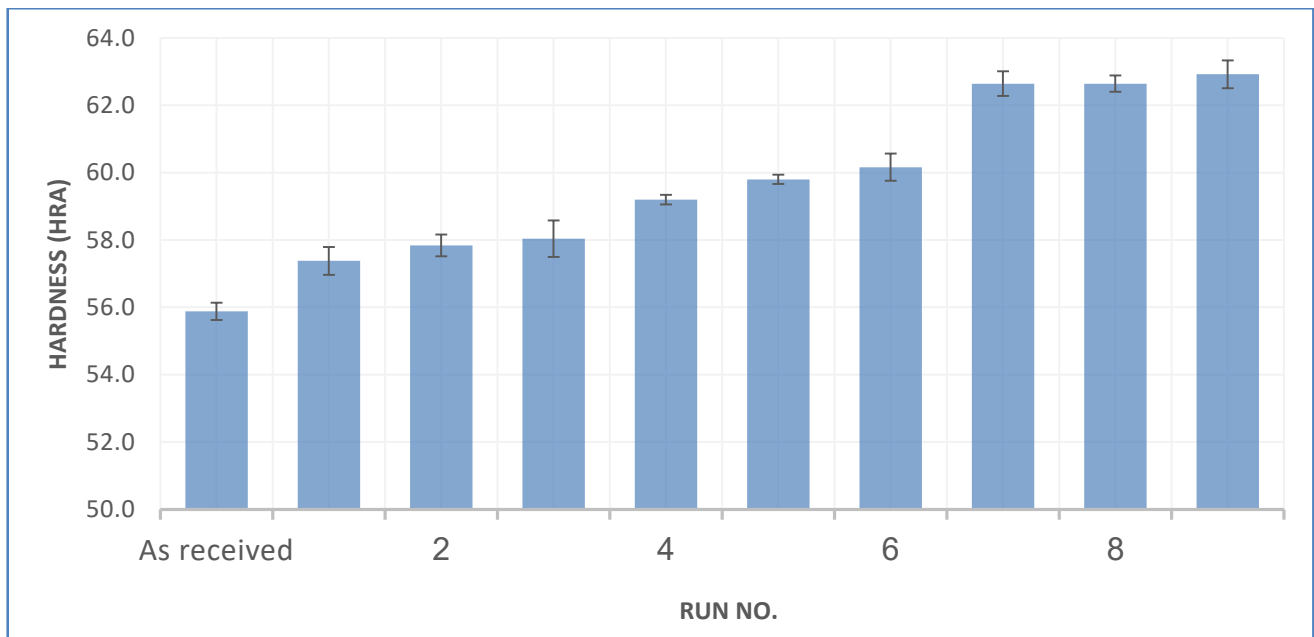


**Fig. 2. Hardness vs. runs**

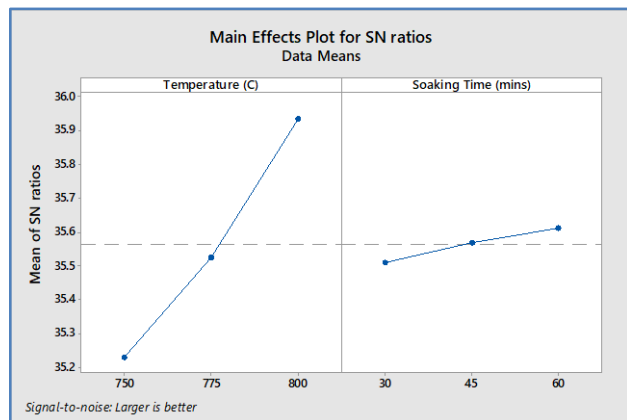
**Analysis of the signal-to-noise ratio (S/N)**

Table 4 displays the average S/N ratios and the ranking of the importance of the process parameters on the hardness value. The results indicate that the temperature had a greater impact on the hardness of the low-carbon steel than soaking time, with temperature being ranked as the more important process parameter. Both the main effect plots of the Taguchi method and the ANOVA results produced a similar ranking of the effect of the process parameters on the hardness of the low-carbon steel.

**Table 4. Response for S/N ratios larger is better (Hardness via temperature and soaking time).**

Level	Temperature (C)	Soaking Time (mins)
1	35.23	35.51
2	35.52	35.57
3	35.94	35.61
Delta	0.71	0.10
Rank	1	2

In Figure 3, the main effect of each parameter on the hardness of the low-carbon steel is depicted. When there is a small variation between the highest and lowest S/N ratios, it indicates that the parameter has a relatively low effect on the response. On the other hand, the level of the design parameter with the maximum S/N ratio indicates the optimal conditions of the system. Therefore, the process parameters that yield the maximum hardness are determined to be a temperature of 800°C and a soaking time of 60 minutes, as shown in Figure 1. This implies that the highest hardness can be achieved when the heat treatment is performed at a heating temperature of 800°C with a soaking time of 60 minutes. Thus, the optimal hardness within the operating condition range of this study can be obtained by conducting the heat treatment process under optimal working conditions.



**Fig. 3. The main effect plots for S/N ratios on hardness (Taguchi).**

**Analysis of the interaction**

As we know, when experimental designs incorporate multiple factors, the potential for each factor to interact with one or more other factors increases exponentially. Interaction refers to the effect of one factor's levels on the impact of another parameter. If the lines on an interaction plot are parallel, it indicates that there is no relationship between the inputs, whereas a deviation in the lines indicates a relationship. In Figure 4, the influence of various inputs on hardness is illustrated. Within the parameter ranges of this study, no significant interaction is observed between temperature and soaking time on hardness.

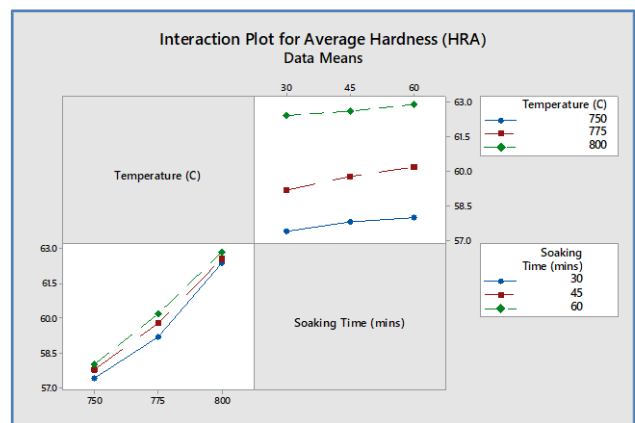


**Fig. 4. Main and interaction plots created by experimental and Taguchi-predicted data sets**

The effects of Temperature and soaking time on hardness, depending on the S/N ratio values. The values show that the temperature has more significant effect than soaking time as resulting from Table 4 which illustrated the rank of temperature is 1 and soaking time is 2. The graphical representation of S/N ratio data is given in Figure 3 and Figure 4. As per the graph, with an increase in the temperature, the value of S/N ratio for the hardness increases. This directly indicates that a high temperature results in more hardness during the intercritical annealing.

In the current study, surface hardness, is taken as response (output) while temperature and soaking time are considered as independent (input) variables. Assuming no interaction between input parameters, after performing all experiments and obtaining the output parameter, the regression model can be explicitly formulated involving the independent variables. The experimental results for average surface hardness can be migrated to a linear regression model equation as shown in Eq. (4):

$$\text{Average Hardness (HRA)} = -16.97 + 0.09800 \text{ Temperature (}^\circ\text{C)} + 0.02333 \text{ Soaking Time (mins)} \quad (4)$$

Equation 4 specifies regression model obtained for surface hardness. The R-square (coefficient of determination) which is representative for efficiency of correlated model, was found to be 98.68%. The closer the R-square value to 1.00, the effective the model is and represents the highest proportion of total variability in the response variable. The R-Sq(adj) which is 98.25%, specifies the amount of variation in the regression equation, and the R-Sq(pred) which is 97.19%, determines how accurate the regression equation predicts the response value. As the value of both R-Sq(adj) and R-Sq(pred) are very high (greater than 91%), and they are also so close to the value of R-Sq, it is confirmed that the design models fit the new experimental data very fine.

#### 4. CONCLUSION

In conclusion, this study aimed to investigate the effect of temperature and soaking time on the surface hardness of low-carbon steel through intercritical annealing. The results showed that the hardness increased with all heat treatment runs, and the highest hardness was obtained at run 9, where the temperature was 800°C and the soaking time was 60 min. The signal-to-noise ratio analysis indicated that temperature had a greater impact on hardness than soaking time. The regression model obtained for surface hardness had a high R-square value of 98.68%, indicating the effectiveness of the model in representing the total variability in the response variable. Overall, the study provides valuable insights into optimizing the heat treatment process for achieving the desired surface hardness of low-carbon steel.

#### 5. REFERENCES

- Ghosh M, Ghosh A, Roy A. Renewable and sustainable materials in automotive industry. *Encyclopedia of Renewable and Sustainable Materials*. 2020; 3: 162-179.  
<https://doi.org/10.1016/B978-0-12-803581-8.11461-4>
- Gao B, Chen X, Pan Z, Li J, Ma Y, Cao Y, Zhou, H. A high-strength heterogeneous structural dual-phase steel. *Journal of Materials Science*. 2019; 54(19): p. 12898-12910.  
<https://doi.org/10.1007/s10853-019-03785-1>
- Gebriil MA, Aldlemey MS, Haider FI. Heat Treatment Recycling of Dual Phase Region and its Effect on Hardness, Microstructure and Corrosion Rate of Medium Carbon Steel. *AMR* 2014; 909:100–4.  
<https://doi.org/10.4028/www.scientific.net/amr.909.100>.
- Kong H J, Yang T, Chen R, Jiao Z, Zhang T, Cao B. Design of ultra-strong but ductile iron-based alloys with low supersaturations. *Acta Materialia*. 2023; 256: 119000.  
<https://doi.org/10.1016/j.actamat.2023.119000>
- Bassini E, Sivo A, Ugues D. Assessment of the Hardening Behavior and Tensile Properties of a Cold-Rolled Bainitic–Ferritic Steel. *Materials*. 2021; 14(21):6662.  
<https://doi.org/10.3390/ma14216662>
- Chandiran E, Kamikawa N, Sato Y, Miyamoto G. Improvement of Strength–Ductility Balance by the Simultaneous Increase in Ferrite and Martensite Strength in Dual-Phase Steels. *Metallurgical and Materials Transactions*. 2021; 52: p. 5394-5408.  
<https://doi.org/10.1007/s11661-021-06477-1>
- Khorasani F, Jamaati R, Aval H J. On the significance of intercritical annealing time in governing mechanical properties of lean composition dual-phase steel. *Archives of Civil and Mechanical Engineering*. 2023; 23(2): p. 105.  
<https://doi.org/10.1007/s43452-023-00651-5>
- Nanda T, Singh V, Singh G, Singh M, Kumar B R. Processing routes, resulting microstructures, and strain rate dependent deformation behaviour of advanced high strength steels for automotive applications. *Archives of civil and mechanical engineering*. 2021; 21: p. 1-24.  
<https://doi.org/10.1007/s43452-020-00149-4>
- Avendano-Rodriguez D F, Rodriguez-Baracaldo R, Weber S. Damage Evolution and Microstructural Fracture Mechanisms Related to Volume Fraction and Martensite Distribution on Dual-Phase Steels. *steel research international*. 2023; 94.6: 2200460.  
<https://doi.org/10.1002/srin.202200460>
- Lavakumar A, Park M H, Gholizadeh R, Ray R K. Unique microstructure formations during low-temperature partitioning after intercritical annealing in low alloy multi-phase TRIP steel and their mechanical behavior clarified by in-situ synchrotron X-Ray diffraction. *Materials Science and Engineering*. 2023; 878: 145214.  
<https://doi.org/10.1002/srin.202200460>
- Olorundaisi E, Jamiru T, Adegbola T A. Response surface modelling and optimization of temperature and holding time on dual phase steel. *Materials Today: Proceedings*. 2021; 38: 1164-1169.  
<https://doi.org/10.1016/j.matpr.2020.07.408>
- Wei K, Hu R, Yin D, Xiao L, Pang S, Cao Y, Zhu Y. Grain size effect on tensile properties and slip systems of pure magnesium. *Acta Materialia*. 2021; 206: 116604.  
<https://doi.org/10.1016/j.actamat.2020.116604>
- Badkoobeh F, Nouri A, Hassannejad H, Mostaan H. Microstructure and mechanical properties of resistance spot welded dual-phase steels with various silicon contents. *Materials Science and Engineering*. 2020; 790: p. 139703.  
<https://doi.org/10.1016/j.msea.2020.139703>

14. He H, Forouzan F, Volpp J, Robertson SM, Vuorinen E. Microstructure and Mechanical Properties of Laser-Welded DP Steels Used in the Automotive Industry. *Materials*. 2021; 14(2):456.  
<https://doi.org/10.3390/ma14020456>
15. Kim Y, Park H K, Jung J, Asghari-Rad P, Lee S, Kim J Y. Exploration of optimal microstructure and mechanical properties in continuous microstructure space using a variational autoencoder. *Materials & Design*. 2021; 202: p. 109544.  
<https://doi.org/10.1016/j.matdes.2021.109544>
16. Mostaan H, Saeedpour P, Ahmadi H, Nouri. A Laser welding of dual-phase steels with different silicon contents: Phase evolutions, microstructural observations, mechanical properties, and fracture behavior. 2021; 811: p. 140974.  
<https://doi.org/10.1016/j.msea.2021.140974>
17. Andrews K. Empirical formulae for the calculation of some transformation temperatures. *J. Iron Steel Inst.*, 1965; p. 721-727.
18. Haider FI, Gebriil MA, Elkoum SM. Evaluation of the Performance of Cylinder Liner under Dry Reciprocating Wear Conditions. *AMM* 2013; 330:310–4.  
<https://doi.org/10.4028/www.scientific.net/AMM.330.310>.
19. Haider F I, Ani M H, Mahmood M. Modelling and Optimization of Copper Electroplating Adhesion Strength. *IOP Conference Series: Materials Science and Engineering*. 2017; Vol. 204, No. 1, p. 012017  
<https://doi.org/10.1088/1757-899X/204/1/012017>



# Detection of Autism Spectrum Disorder by A Case Study Model Using Machine Learning Techniques

## An Experimental Analysis on Child, Adolescent and Datasets

Najat S. Bousidrah<sup>1\*</sup> - Zahow M. Khamees<sup>2</sup> - Sana M. Ali<sup>1</sup>

*1 Software development - College of Information Technology - Modern University of Benghazi- Benghazi, Libya.*

*2 Information Technology - College of Information Technology - University Ajdabiya - Ajdabiya, Libya.*

Received: 20 / 03 / 2024; Accepted: 16 / 05 / 2024

### ABSTRACT

Autism Spectrum Disorder (ASD) is a lifelong neurodevelopmental disorder that affects a person's social interaction and communication skills. It is typically diagnosed in childhood but can be identified at any age. Behavioral symptoms of autism usually appear in the first two years of a child's life and continue into adulthood. Recently, there has been increased interest in using machine learning algorithms for medical diagnosis, including the diagnosis of autism spectrum disorder.

This study aimed to investigate the feasibility of using various machine learning algorithms, such as Naïve Bayes, Support Vector Machine (SVM), Random Forest, Logistic Regression, K-Nearest Neighbors (KNN), Decision Tree, and Gradient Boosting Classifier, to predict and analyze autism in children. The researchers utilized publicly available non-clinical ASD datasets for evaluation.

Different evaluation metrics, including accuracy, specificity, sensitivity, macro-average, and weighted average, were used to assess the performance of the machine learning models. The KNN-based model achieved the highest accuracy of 87.14% and outperformed the other models in terms of specificity. The Naïve Bayes model achieved an accuracy of 70.48%, while the SVM model had the highest sensitivity of 98.2%. The Decision Tree and Random Forest models achieved perfect scores of 100% in terms of macro-average, weighted average, and Mean Accuracy for all models was 85.52%.

Based on these results, the researchers concluded that the KNN-based model is the most effective for predicting and analyzing autism in children, with an accuracy of 87.14%. However, it is important to note that these findings are specific to the dataset and evaluation metrics used in the study. Further research and validation using diverse datasets are necessary to confirm the generalizability of these findings.

**KEYWORDS:** ASD Detection, Autism spectrum disorder, Classification Feature selection, Machine learning.

## 1. INTRODUCTION

The problem of autism spectrum disorder is a common issue among different age groups, and the disorder affects a person's ability to interact with others as well as learning skills; therefore, early diagnosis contributes significantly to minimizing efforts and costs associated with late detection. Thus, the availability of a user-friendly and reliable testing tool plays an important role in predicting whether someone has autism traits sufficiently to warrant further comprehensive evaluation for<sup>1,2</sup>.

This paper aims first to study the effectiveness of autism disorder diagnosis by a case study model prepared at the Autism Center in Benghazi based on some behaviors that are diagnosed through asking questions by the person caring for that individual and testing them using machine learning algorithms, knowing that before such health care, professionals could diagnose autism with standardized diagnostic tools. Secondly, they conduct interviews with the parents or caregiver to assess developmental milestones and current behavior<sup>3,4</sup>.

While diagnosticians employ standardized tools for the diagnosis of autism spectrum disorder, one of the major challenges is that using diagnostic instruments takes a lot of time to administer and interpret results<sup>5</sup>.

\*Correspondence: Najat S.Bousidrah

[naj\\_1971@yahoo.com](mailto:naj_1971@yahoo.com)

To address this issue, a machine learning model was suggested that aims to shorten the diagnosis time while increasing accuracy. The second aim of the proposed model is to establish that the case study method used for the analysis of autism based on the patient's behavior and to understand associations between the concerned input data set.

The motivation behind this study is to present a method for diagnosing the autism spectrum disorder with the help of a better and more accurate machine learning model.

The major contributions of this research work are as follows:

- This study investigates the feasibility of using various machine-learning algorithms for predicting and analyzing autism spectrum disorder in children.
- The algorithms explored include Naïve Bayes, SVM, Random Forest, Logistic Regression, KNN, Decision Tree, and Gradient Boosting Classifier.
- The research will aim to help understand how machine learning can be used to diagnose autism spectrum disorder.
- Performance evaluation metrics such as accuracy, specificity, sensitivity, overall average, and weighted average are utilized to assess the models' predictive capabilities,
- These metrics provide a comprehensive assessment of the strengths and weaknesses of the machine learning models.
- The study aims to identify the most effective model for detecting autism spectrum disorder based on the analysis of performance metrics.
- The model with the highest accuracy, specificity, sensitivity, and overall average is sought to optimize the diagnostic process and improve the accuracy of autism spectrum disorder identification.
- A feature selection technique is used to filter the dataset and identify the most suitable features for prediction, utilizing the entire dataset.
- In order to determine if the use of the balanced and scaled data technique affects the performance, we use the test data technique to test performance.
- A new model is proposed using machine learning-based on the Autism Spectrum Disorder prediction model to enhance the accuracy of the existing model, which improves the predicted autism and improves the Autism Spectrum Disorder Models.

Our paper is structured in the manner below: In the "Introduction" section, we provide an overview of our

project, followed by a "Literature Review" which is defined as a "review of literature, which has been studied and is relevant to the research paper topic. Business Model and Methodology section explains work that was performed along with methodologies followed or proposed for implementation." The Analysis describes inferences drawn from the results obtained. Lastly, the section "Conclusion" describes our conclusions.

## 2. RELATED WORK AND LITERATURE REVIEW

This section briefly presents a group of studies in which machine-learning models were built to predict autism spectrum conditions for different age groups.

Vakadkar, K et al. (2021). Researchers focused on the use of machine learning techniques for detecting Autism Spectrum Disorder (ASD) in children. It explores the application of machine learning algorithms in analyzing data related to ASD and discusses the potential of these techniques in improving early diagnosis.<sup>6</sup>

Hossain, M. D., et al. (2021). They focused on using machine learning techniques to detect autism spectrum disorder. It discusses the application of different algorithms and features in analyzing data related to autism spectrum disorder and highlights the potential of machine learning in assisting in the diagnosis of autism spectrum disorder.<sup>7</sup>

In Usta's study (2019), the main objective was to explore the use of machine learning methods for predicting short-term outcomes in individuals with Autism Spectrum Disorder (ASD). The researchers aimed to harness the power of machine learning algorithms to analyze clinical data and Provide insights into the prognosis of individuals with ASD.<sup>8</sup>

Saeed, F. (2018). The author explores the potential of machine learning algorithms, such as Support Vector Machines (SVM) and Convolutional Neural Networks (CNN), in analyzing large-scale fMRI datasets obtained from individuals with psychiatric disorders. While various psychiatric disorders are considered in the study, the principles and methodologies presented can be applied to ASD research as well.<sup>9</sup>

Thabtah's review article (2017) provides a comprehensive overview of the application of machine learning in behavioral research related to Autism Spectrum Disorder (ASD). The study highlights the use of machine learning algorithms in analyzing behavioral data, identifying patterns, and improving diagnostic accuracy in ASD research.<sup>10</sup>

In a previous study by Küpper et al. (2020), machine-learning techniques were employed to identify predictive features of Autism Spectrum Disorders (ASD) in a clinical sample of adolescents and adults. The researchers

focused on enhancing ASD detection by utilizing a specific machine-learning algorithm. They also explored the potential of the identified features to aid in the diagnostic process. The study aimed to contribute to the existing body of knowledge on ASD and improve the accuracy of ASD diagnosis through the application of machine learning methods.<sup>11</sup>

Mellema et al. (2022) conducted a study focusing on reproducible neuroimaging features for the diagnosis of ASD using machine learning. The researchers employed a variety of neuroimaging techniques and developed models that demonstrated promising results in distinguishing individuals with ASD from neurotypical individuals. The study highlights the potential of neuroimaging data in contributing to the accurate diagnosis of ASD.<sup>23</sup>

Another study by Ali et al. (2023) aimed to classify the behavioral severity of ASD using a comprehensive machine-learning framework. The researchers

incorporated various behavioral measures and developed personalized classification models. The study demonstrated the potential of machine learning techniques in providing individualized assessments of ASD severity, which can inform personalized interventions and treatments.<sup>24</sup>

Rogala et al. (2023) focused on enhancing ASD classification in children by integrating traditional statistics and classical machine learning techniques in EEG analysis. By combining features extracted from electroencephalography (EEG) data with traditional statistical approaches, the researchers achieved improved classification accuracy for ASD. The study highlights the importance of integrating different analytical approaches to enhance the diagnostic accuracy of ASD.<sup>25</sup>

In comparison with previous studies, Table 1 shows a summary of the results of our current study and their comparison with the mentioned studies:

**Table 1 summary of the results of our current study and their comparison with the mentioned studies**

Source	Objective	Algorithms	Data
Current Study	Investigate the feasibility of using various machine learning algorithms to predict and analyze autism in children.	Naïve Bayes, (SVM), Random Forest, Logistic Regression, (KNN), Decision Tree, and Gradient Boosting Classifier.	Publicly available non-clinical ASD datasets.
Mellema et al. (2022)	Diagnosis of Autism Spectrum Disorder using machine learning.	support vector machines (SVM), random forests, and neural networks.	Neuroimaging data related to Autism Spectrum Disorder, specifically functional magnetic resonance imaging (fMRI) data
Ali et al. (2023)	Personalized classification of behavioral severity of autism spectrum disorder	Support vector machines (SVM), random forests, decision trees, or deep learning approaches like neural networks.	Behavioral data collected from individuals with ASD.
Rogala et al. (2023)	Enhancing Autism Spectrum Disorder classification	traditional statistics and classical machine learning techniques	EEG data collected from children with and without ASD.

In recent years, there has been a growing interest in utilizing machine-learning techniques for the detection and diagnosis of Autism Spectrum Disorder (ASD). Several studies have explored the application of machine learning algorithms to neuroimaging data and behavioral features to improve the accuracy of ASD diagnosis.

### 3. WORKING MODEL

#### A. Research Methodology

Figure 1 demonstrates the flow of the proposed system. First, we collect case study data from a sample of public and private centers; we then clean the dataset by eliminating missing values or outliers, encode categorical features, and analyze information to obtain the most

important characteristics among all database characters that have been generated.

For the pre-processed dataset, classification algorithms which include Logistic Regression, Naïve Bayes, Support Vector Machine, and K-Nearest Neighbors Gradient Boosting Classifier Random Forest classifiers are used to predict an output label (ASD or Non-ASD).

After that, the correctness of each classifier is then analyzed and compared for comparison to its matching classifiers. The assessment of each classifier is based on a combination of various metrics, such as F1 score and exact recall values, as well as calculations using a variety of other metrics to improve the evaluation of each one. If the classifier is successful, then training accuracy will be

greater than testing accuracy. This model can then be considered the optimal model and used for further learning as well as classification. This work is coded in Python 3.

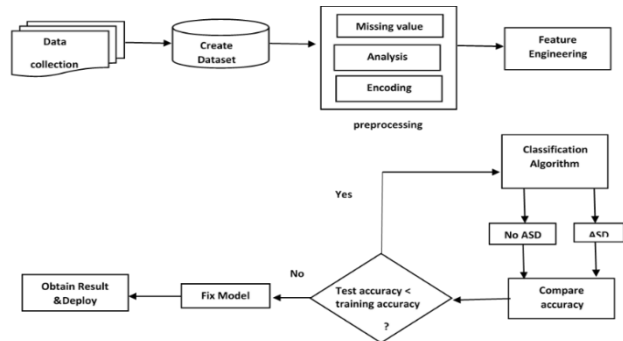


Fig. 1. Architecture of proposed system

These stages are briefly discussed in the following subsections:

**B. Data collection**

For the case study, Data used in developing the predictive model was collected from Benghazi Center for Comprehensive Rehabilitation of Autistic Children; Al-Eradah Centre for Autism and Special Needs; Nour center for autistic children with speech problems. That is composed of behavior datasets based on the AQ-10 screening tool questions <sup>12</sup>.

Certain aspects of attention to detail, switching of attention, communication skills, imagination, and social interaction are addressed by the AQ-10 screening questions. Evaluation method: For each question only one point is assigned out of 10 questions.

The user will earn either zero or one point per question depending on the answer. There are 202 cases in the dataset for individuals.

The dataset contains fourteen attributes and is a mixture of numerical and categorical data, which includes: Age, gender question 1-10 and category.

The data category includes 14 attributes used in prediction. These attributes are listed below.

Table 2: List of Attributes in the dataset

Attribute Id	Attributes Description
1	Id
2	Age
3	Sex
4-13	Based on the screening method answers of 10 questions
14	Screening score

**C. preprocessing and analysis**

Since the dataset has a small number of categorical features, it had to be pre-processed. The data set was preprocessed by applying a series of transformations before using it in the proposed model.

The raw data was cleaned by eliminating irrelevant features like the serial number and age, removing incomplete records, and handling categorical values. During the construction of the data set, which will be used in modeling, the coding was done manually. For categorical values, we transform the labels to numeric form because they need a machine-readable format. The features that include two classes (Class, q1.q10) are chosen to be encoded with a binary label.

This data set has been created in CSV format using Excel and contains thirteen attributes including 202 instances.

**Classification Algorithms**

The data was split into an 80% training set for the model and a 20% test sample to determine how effective and accurate the model is after completing the pre-processing of the data, seven classification models were applied, which are as follows: logistic regression: Naive Bayes, K-Nearest Neighbors, Random Forest Classifier Decision Tree Gradient Boosting Classifier Support Vector Machine.

We compared the accuracy and f1 score for each model along with a brief description of the classification models that we used.

**Logistic Regression Logistic Regression (LR)**

Logistic regression (LR) is regarded as a technique used by statisticians and researchers to analyze and classify data sets, with binary and proportional responses. LR has the advantage of being able to provide probabilities making it applicable to multi-class classification problems <sup>12</sup>.

**Naive Bayes (NB)**

Naive Bayes (NB) is an algorithm used for classifying both two-class and multi-class problems. It is easier to understand when explained using categorical input values.

The name "naive Bayes" or "idiot Bayes" comes from the simplification of probability calculations for each hypothesis making them computationally manageable. Calculating attribute values like  $P(d_1, d_2, d_3|h)$  are assumed to be conditionally independent given the target value and calculated as  $P(d_1|h) * P(d_2|h)$ .

Here the predictions or features are believed to be independent meaning that one function does not impact

another. There are types of NB classifiers such as Multinomial, Bernoulli and Gaussian.<sup>13,20</sup>

### **Support Vector Machine (SVM)**

The objective of the support vector machine algorithm is to find a hyperplane in an N-dimensional space (N — the number of features) that distinctly classifies the data points.

To separate the two classes of data points, many possible hyperplanes could be chosen. Our objective is to find a plane that has the maximum margin, i.e. the maximum distance between data points of both classes. Maximizing the margin distance provides some reinforcement so that future data points can be classified with more confidence.<sup>14,20</sup>

### **K-Nearest Neighbors (KNN)**

KNN classifier is to classify unlabeled observations by assigning them to the class of the most similar labeled examples. Characteristics of observations are collected for both training and test dataset.<sup>15</sup>

The intuition underlying Nearest Neighbor Classification is quite straightforward; examples are classified based on the class of their nearest neighbors. It is often useful to take more than one neighbor into account so the technique is more commonly referred to as k-Nearest Neighbor (K-NN) Classification where k nearest neighbors are used in determining the class. Since the training examples are needed at run-time, i.e. they need to be in memory at run-time, it is sometimes also called Memory-Based Classification. Because induction is delayed to run time, it is considered a Lazy Learning technique. Because classification is based directly on the training examples it is also called Example-Based Classification or Case-Based Classification.<sup>16</sup>

### **Random Forest Classifier (RFC)**

Random forest classifier is a flexible algorithm that can be used for classification, regression, and other tasks, as well. It works by creating multiple decision trees on arbitrary data points. After getting the prediction from each tree, the best solution is selected by voting.

Random forest algorithms have three main hyperparameters, which need to be set before training. These include node size, the number of trees, and the number of features sampled. Random Forest is a popular and easy-to-use machine learning algorithm that produces a great result most of the time. Random forest is used in various fields, such as healthcare to identify the correct combination of components in medicine to analyze a patient's medical history to identify diseases, and in e-commerce to determine whether a customer will like the product or not.<sup>17</sup>

### **Decision tree**

A decision tree is a supervised learning algorithm that can be used for both classification and regression tasks. A decision tree is a flow chart resembling a tree structure, where each internal node is notated by rectangles and therefore the leaf nodes are notated by ovals. This algorithmic program is commonly used as a result of the implementation is simple and easier to grasp compared to the other different classification algorithms. A decision tree starts with a root node that allows the users to take needed actions. From this node, users split each node recursively according to the decision tree learning algorithmic program. The result is a decision tree in which every branch associates an outcome. The decision tree algorithm makes decisions by recursively partitioning the data based on the feature values. It selects the best feature at each step by evaluating different criteria, such as information gain or Gini impurity, to maximize the homogeneity or purity of the resulting subsets.<sup>19</sup>

### **Gradient Boosting Classifier**

Which is a popular ensemble method used for classification tasks. Gradient Boosting is a general technique that can be applied to various types of models, including decision trees.

**Initial model:** The process begins by training an initial model, typically a decision tree, on the training data. This initial model is called the "base model" or "weak learner."

**Residual calculation:** The Gradient Boosting Classifier then calculates the residuals, which are the differences between the actual target values and the predictions made by the base model.

**Building subsequent models:** The subsequent models are built to predict the residuals of the previous model, rather than the actual target values. These models are created in an iterative manner, with each subsequent model attempting to correct the errors made by the previous model.

**Model weighting:** Each model is assigned a weight or learning rate that determines its contribution to the final prediction. The learning rate controls the step size or shrinkage of the updates made by each model. A lower learning rate generally leads to more accurate predictions but requires more iterations.<sup>21</sup>

## **4. RESULTS**

### **Dataset Analysis**

The data set collected and used here is based on a quantitative screening method for autism in children and is extracted from the case study model used in rehabilitation centers for autistic children in the city of Benghazi.

A shortened version containing a set of 10 questions was used (Table 3). The answers to these questions are mapped to binary values as the class type.

These values are determined during the data collection process by answering the questions of the case form for evaluating the child’s behavior, so that the value

of the category “Yes” is determined if the result of the answer (No) to the questions is greater than 3, meaning that there are possible features of autism spectrum disorder. Otherwise, the category value is set as “no,” meaning no ASD traits are present. We drew several graphs to get different visual views of the data set. In the first chart (Figure 2), we can see that.

**Table 3: Feature mapping for behavior screening using the case model method**

Dataset variable	Description
A1	Does your child enjoy swinging or swaying?
A2	Is your child interested in others?
A3	Does your child climb things like ladders and the like?
A4	Does your child play children’s games such as hide and seek?
A5	Does your child practice imaginative play, for example, making tea using toy cups and utensils? Or claim other things like that
A6	Does your child use his finger to point to things he wants to ask you about?
A7	Does your child use his finger to point to things he is interested in?
A8	Does your child bring you things to show you?
A9	Does your child spin around?
10	Does your child walk on his toes?

**Training and testing model**

The generated dataset was divided into two parts, one for training the dataset and the other for testing the dataset in the ratio of 80:20 respectively. For cross-validation purposes, the training data was again split into two parts. Partition of the training dataset and the other part is validation dataset in the ratio of 80:20 respectively. Figure 2 displays the final training, test, and validation sets on which classification was performed.

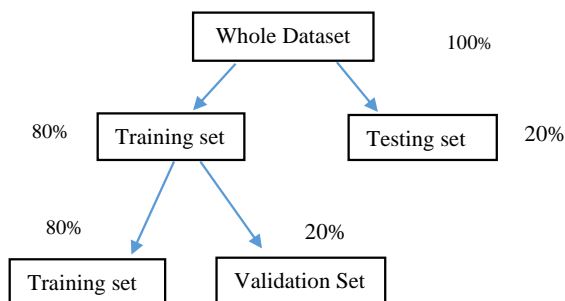


**Fig. 2. Final Training, Testing and Validation Sets**

**Exploratory Data Analysis (EDA)**

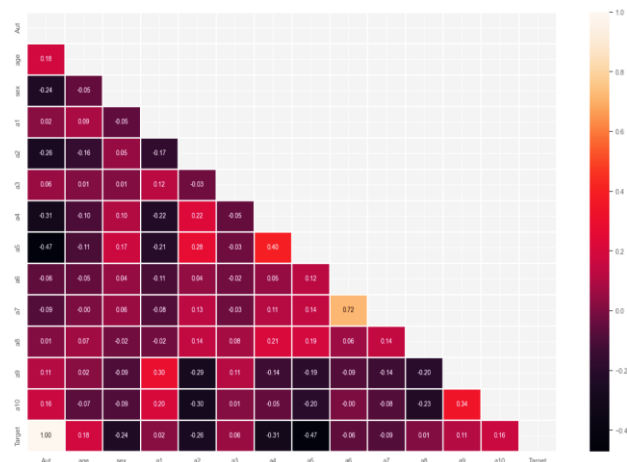


**Fig. 3. Correlation between Features and Features Using Heatmap**

**Evaluation Matrix**

Based on the provided confusion matrices, it appears that several machine learning models were used to detect autism spectrum disorder (ASD) in a case study and table 4 describe Elements of a Confusion Matrix. Here is a summary of the results in Table 4:

**Table4: Elements of a Confusion Matrix**

	Predictive ASD values	
Actual ASD values	True Positive (TP)	False Positive (FP)
	False Negative (FN)	True Negative (TN)

**Table 5 summary of the results Evaluation Matrix**

Classifier	True positive (TP)	False positive (FP)	True negative (TN)	False negative (FN)
Naive Bayes	6	1	33	2
SVM	6	1	35	0
Logistic Regression	6	1	34	1
Decision Tree	7	0	35	0
Random Forest	7	0	35	0
Gradient Boosting	7	0	34	1
K-Neighbors	5	2	34	1

In general, all the models achieved reasonably high true positive rates, indicating that they were able to correctly identify individuals with ASD. The true negative rates were also consistently high, suggesting that the models were effective in identifying individuals without ASD.

Among the models, Decision Tree, Random Forest, performed particularly well, achieving a perfect true positive rate and true negative rate. K-Neighbors had a slightly lower true positive rate but still performed well overall.

It's important to note that the performance of these models may vary depending on the specific dataset and the features used. Additionally, other evaluation metrics such as precision, recall, and F1 score can provide a more comprehensive assessment of the models' performance.

**Comparison of Classification Models**

All the algorithms that have been applied have shown high accuracy ranging from 93% to 100%. This indicates their ability to accurately distinguish between individuals with autism and those without.

Accuracy, recall, and F1 measure: Analyzing the accuracy, recall, and F1 measure for each class (0 and 1) provides valuable insights into the algorithms' performance. For class 0, the accuracy ranged from 75% to 100%, indicating their ability to correctly identify actual non-autism cases. The recall for class 0 ranged from 57% to 86%, highlighting the algorithms' ability to correctly identify non-autism cases out of the total

number of non-autism cases. For class 1, both the accuracy and recall were consistently high, ranging from 92% to 100%, indicating the algorithms' ability to correctly identify actual autism cases and recall them from the total number of autism cases.

F1 measure and accuracy: The F1 measure takes both precision and recall into account and provides a single measure to evaluate the algorithms' overall performance. The F1 measure values for most algorithms were high, ranging from 80% to 100%, indicating a good balance between precision and recall. The overall accuracy of the algorithms ranged from 93% to 100%, further confirming their effectiveness in detecting autism.

Algorithm comparison: Compare the performance of different algorithms and highlight their strengths and weaknesses. For example, the decision tree achieved perfect accuracy, recall, and F1 measure for both classes, indicating its excellent performance. On the other hand, K-Neighbors showed relatively lower recall for class 0, suggesting a potential for improvement in identifying non-autism cases. When choosing the best model Based on the results, the best algorithms for autism detection can be discussed. Considering factors such as accuracy, recall, and F1 measure to determine the most suitable algorithm for our dataset. It is important to note the suitability of algorithms based on the given dataset and highlight the considerations to be taken into account when choosing the best model.

Based on the data used, it appears that all the algorithms used (Naive Bayes, SVM, Logistic Regression, Decision Tree, Random Forest, Gradient Boosting, K-Neighbors) have achieved excellent performance in detecting autism in children. All the algorithms achieved an accuracy of 100% or close to it and gave accuracy, recall, and F1 measure values close to 1 for both autism and non-autism groups. After this comparison, we will design the system using the KNN algorithm as an experiment, and we will see all the comparison details in Table 6, Table 7 and Figure 3 describe all the performance values obtained for the algorithms used.

**Table 6 Comparison of Classification Models with Training Set**

Model	Training Set			
	precision	recall	f1-score	support
Naive Bayes	0.75	0.86	0.80	7
SVM	1.00	0.86	0.92	7
Logistic Regression	0.86	0.86	0.86	7
Decision Tree	1.00	1.00	1.00	7
Random Forest	1.00	1.00	1.00	7
Gradient Boosting	0.88	1.00	0.93	7
K-Neighbors	0.83	0.71	0.77	7

**Table 7 Comparison of Classification Models with Test set**

Model	Test Set			
	precision	recall	f1-score	support
Naive Bayes	0.97	0.94	0.96	35
SVM	0.97	1.00	0.99	35
Logistic Regression	0.97	0.97	0.97	35
Decision Tree	1.00	1.00	1.00	35
Random Forest	1.00	1.00	1.00	35
Gradient Boosting	1.00	0.97	0.99	35
K-Neighbors	0.94	0.97	0.96	35

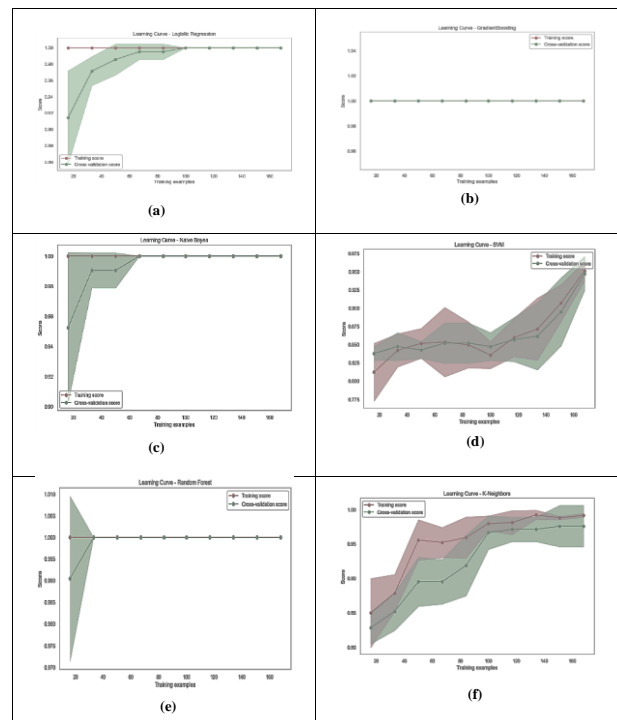


**Fig. 4. Learning Curve of (a) Logistic Regression; (b) Gradient Boosting; (c) Naïve Bayes; (d) SVM; (e) Random Forest; (f) Decision Tree; (g) KNN; for children’s dataset.**

Two metrics were used to compare the performance of the algorithms: the macro average and the weighted average.

**1. Macro Average:**

$$\text{Macro Average Precision} = \frac{(\text{Precision}_{\text{class}_0} + \text{Precision}_{\text{class}_1} + \dots)}{\text{Number\_of\_classes}} \tag{1}$$

$$\text{Recall} = \frac{(\text{Recall}_{\text{class}_0} + \text{Recall}_{\text{class}_1} + \dots)}{\text{Number\_of\_classes}} \tag{2}$$

$$\text{F1 – score} = \frac{(\text{F1\_score}_{\text{class}_0} + \text{F1\_score}_{\text{class}_1} + \dots)}{\text{Number\_of\_classes}} \tag{3}$$

**2. Weighted Average:**

$$\text{Weighted Average Precision} = \frac{(\text{Precision}_{\text{class}_0} * \text{Support}_{\text{class}_0} + \text{Precision}_{\text{class}_1} * \text{Support}_{\text{class}_1} + \dots)}{\text{Total\_support}} \tag{4}$$

$$\text{Weighted Average Recall} = \frac{(\text{Recall}_{\text{class}_0} * \text{Support}_{\text{class}_0} + \text{Recall}_{\text{class}_1} * \text{Support}_{\text{class}_1} + \dots)}{\text{Total\_support}} \tag{5}$$

$$Weighted\ Average\ F1 - score = \frac{(F1\_score\_class\_0 * Support\_class\_0 + F1\_score\_class\_1 * Support\_class\_1 + \dots)}{Total\_support}$$

(6)

In general, most models achieved high accuracy and good performance in terms of precision, recall, and F1 score. Decision Tree, Random Forest, achieved perfect scores in all metrics, indicating excellent performance. SVM, Gradient Boosting, and logistic regression also achieved high scores.

### Designing a system to detect autism

After evaluating the 12 algorithms that were used and ensuring the performance of each algorithm, a decision can be made regarding the suitable algorithm for use in

the user interface as an application using the TKinter library. This library is provided by the Python programming language and contains tools that assist in designing the system that includes the autism detection method for children. The chosen algorithm for this small system is K-Nearest Neighbors (KNN).

### Testing and experimental

In this paragraph, outlier values will be entered into the user interface to ensure the accuracy of the specified algorithm, and we can also replace the algorithm with another after ensuring that most of the algorithms have achieved excellent success. We can see the test in Figures 5.

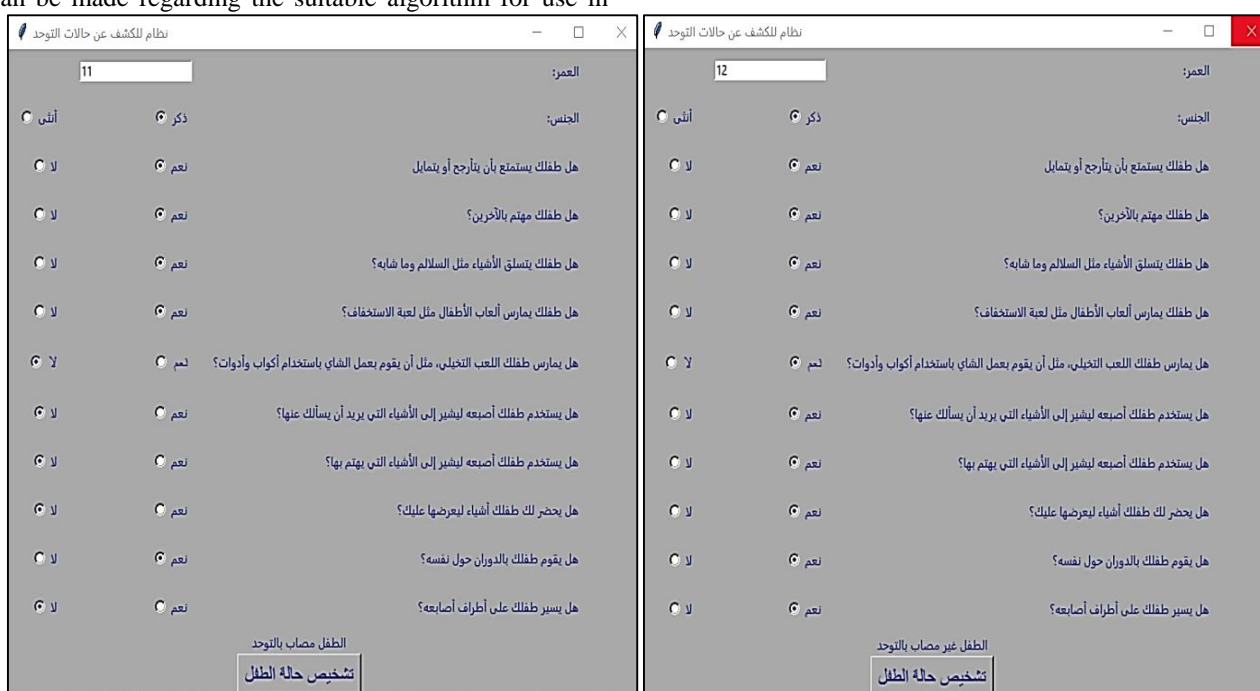


Fig. 5. test 1 model on the user interface and test 2 model on the user interface

## 5. DISCUSSION

The accuracy of a trained model can be evaluated by using the confusion matrix and classification report, which measure specificity, sensitivity, and accuracy. These metrics provide an assessment of how well the model performs.

### Performance Evaluation metrics

Evaluating the performance of a classification model is crucial to assess its effectiveness in achieving the desired objectives. Performance evaluation metrics are employed to measure the model's performance on the test dataset. It is important to select appropriate metrics to evaluate the model's performance, including the confusion matrix, accuracy, specificity, sensitivity, and others. These performance metrics are calculated using

specific formulas to provide quantitative measures of the model's performance.

$$Specificity = \frac{TN}{(TN+TP)} \tag{7}$$

$$True\ Positive\ Rate\ or\ Sensitivity = \frac{TP}{(TP+FN)} \tag{8}$$

$$Accuracy = \frac{TP+TN}{(TN+TP+FP+FN)} \tag{9}$$

Precision (Prec) is named the division of the examples, which are actually positive among all the examples that we predicted as positive:

$$Precision = \frac{TP}{(TP+FP)} \tag{10}$$

$$Negative\ predictive\ value(NPV) = \frac{TN}{(TN+FN)} \tag{11}$$

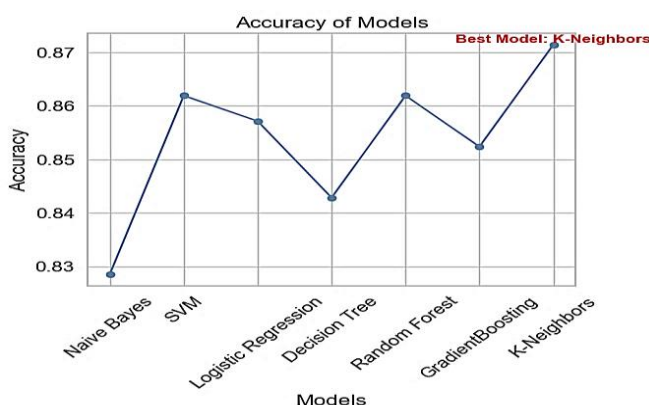
F1 score F1 score is defined as the harmonic mean between precision and sensitivity:

$$F1\ score = \frac{2TP}{(2TP+FP+FN)} \tag{12}$$

The experimental results for different machine learning algorithms were obtained using pediatric ASD screening data. All 12 features were selected to assess the privacy, sensitivity, and accuracy of the predictive model. The Naïve Bayes Gaussian NB algorithm was implemented for this purpose. Additionally, the SVM algorithm was applied, and for the KNN algorithm, N folds were set to 5. When calculating the performance metrics of the algorithms, a specific metric was used Scaler as a standard measure for data normalization. For all the models employed, detailed performance metrics are presented for each of the three datasets.

*The results of the machine learning models for ASD screening data are as follows:*

- Naive Bayes achieved an accuracy of 82.86%, with good sensitivity and overall accuracy.
- SVM had high recall and sensitivity but low specificity.
- Logistic Regression performed well in terms of accuracy and sensitivity.
- The Decision Tree had good accuracy and sensitivity.
- Random Forest performed well in terms of accuracy and sensitivity.
- Gradient Boosting showed good overall performance in accuracy and sensitivity. Figure 5 describes the best performance values obtained for the algorithms used.



(a)

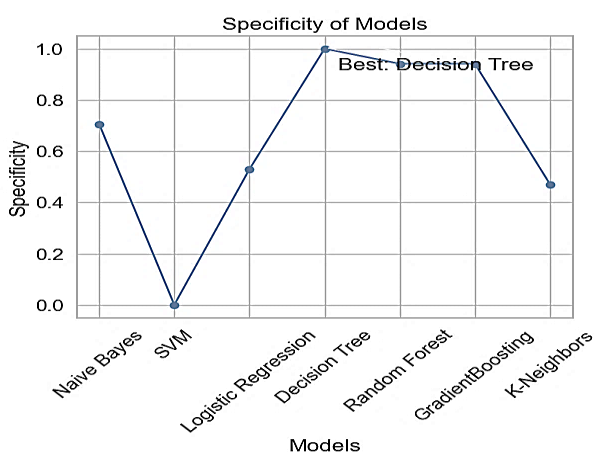
- K-Neighbors achieved high accuracy and sensitivity.

Figure 6 describes all the performance values obtained for the algorithms used.

These findings suggest that different machine learning models have varying performances on ASD screening data. Models like SVM and K-Neighbors have high recall and sensitivity, making them effective in identifying positive cases. While other models showed a trade-off between sensitivity and specificity. Based on the specific requirements and priorities of the application, K-Neighbors could be considered a suitable model for ASD screening. The Overall Performance measures of all machine learning classifiers with all datasets have been shown below in detail:

**Table 8: Overall results of autism spectrum disorder screening data for children**

Classifier	Specificity	Sensitivity	Accuracy	Recall
SVM	0.37619	0.954603	0.861905	0.954603
K-Neighbors	0.495238	0.943492	0.871429	0.943492
Random Forest	0.438095	0.943175	0.861905	0.943175
Logistic Regression	0.404762	0.942857	0.857143	0.942857
Gradient Boosting	0.438095	0.931905	0.852381	0.931905
Decision Tree	0.466667	0.914921	0.842857	0.914921
Naive Bayes	0.704762	0.85254	0.828571	0.852540



(b)

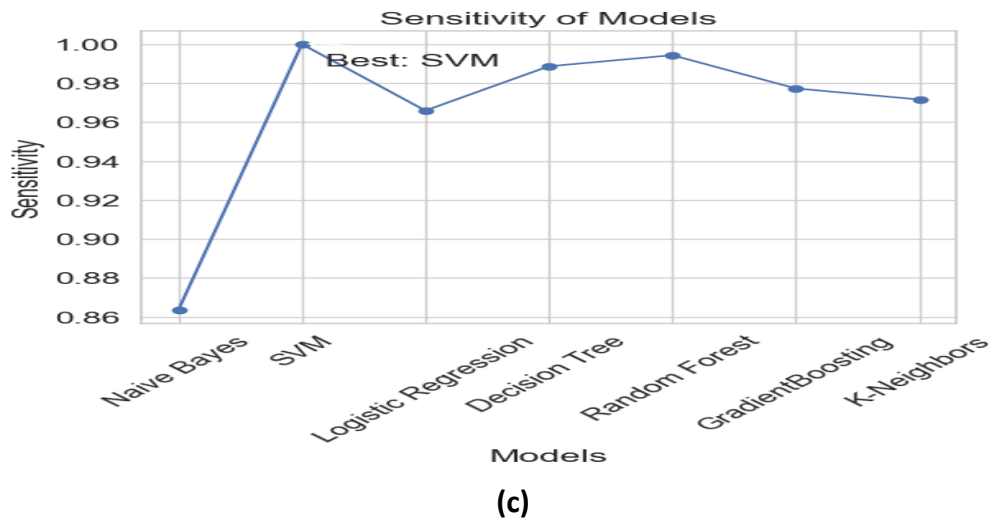


Fig. 6. (a) Learning Curve of best Accuracy of Model; (b) Learning Curve of best Specificity of Model; (c) Learning Curve of best sensitivity Of Model.

Evaluation of different machine learning models on an autism spectrum disorder dataset observed accuracy in the range (82.857 to 87.143%) on the original dataset. The K-NN classifier with K=5 produced the highest accuracy of 87.143% and Figure 7 describes the performance values obtained for the algorithms used

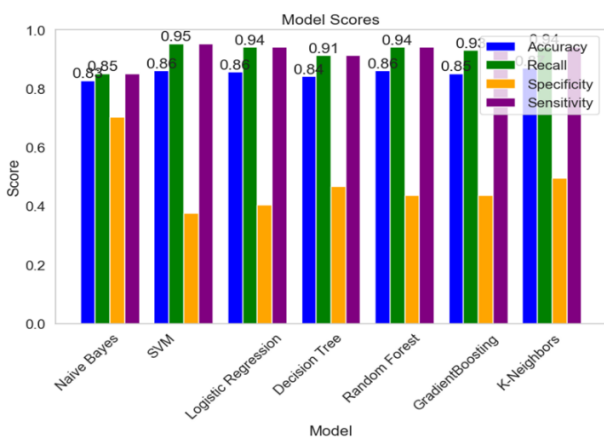


Fig. 7. The Overall Performance measures of all machine learning classifiers.

**Feature Selection**

Most models provide a way to return the importance of features or parameters so that we can get an idea of what are considered the most important features in our data set. SVC, Linear SVC and KNN are the ones that don't have it. But in this paper, we will not discuss choosing the best features. Just look at them and have the algorithms choose the features that have the most impact on detecting the target.

We will see if we can find anything from the other models' preferences. Based on the feature importance calculated by different models, we can summarize the results as follows:

The logistic regression model considers the features 'age', 'sex', 'a1', 'a2', 'a4', 'a5', 'a6', 'a8', and 'a10' to be important in predicting the target variable. Among these features, 'age' and 'sex' have relatively higher importance.

The decision tree model identifies 'a5' as the most important feature, followed by 'a1', 'age', 'a4', 'a2', 'a3', 'a8', 'a6', 'sex', and 'a7'.

The random forest model ranks the features based on their importance. 'a5' is considered the most important feature, followed by 'a1', 'age', 'a4', 'a2', 'a3', 'a8', 'a6', 'sex', and 'a7'.

The gradient boosting model also ranks the features based on their importance. 'a5' is considered the most important feature, followed by 'a1', 'age', 'a4', 'a2', 'a3', 'a8', 'a6', 'sex', and 'a7' all datasets below are detailed in figure 7.

These results provide insights into which features are considered important by each model. It's important to note that the importance of features can vary between models, and different models may have different criteria for determining feature importance. The importance of features of all machine learning classifiers with all datasets below is detailed in Table 8 except Algorithms (SVM, Naive Bayes, K-Neighbors) do not have this feature.

**Table 9** the importance of features of all machine learning classifiers

Feature	Logistic Regression	Decision Tree	Random Forest	Gradient Boosting
Age	0.388826	0.258788	0.255564	0.230074
Sex	0.508803	0.090916	0.090208	0.106742
a1	0.615685	0.055460	0.083204	0.059406
a2	0.696871	0.030778	0.061583	0.012336
a3	0.374806	0.059377	0.051869	0.027684
a4	0.553651	0.166304	0.060354	0.107492
a5	1.320247	0.234783	0.191457	0.319309
a6	0.289054	0.042319	0.056039	0.015947
a7	0.144882	0.023083	0.024820	0.045522
a8	0.798879	0.015109	0.045901	0.072265
a9	0.025382	0.023083	0.025065	0.000780
a10	0.516303	0.000000	0.053936	0.002442

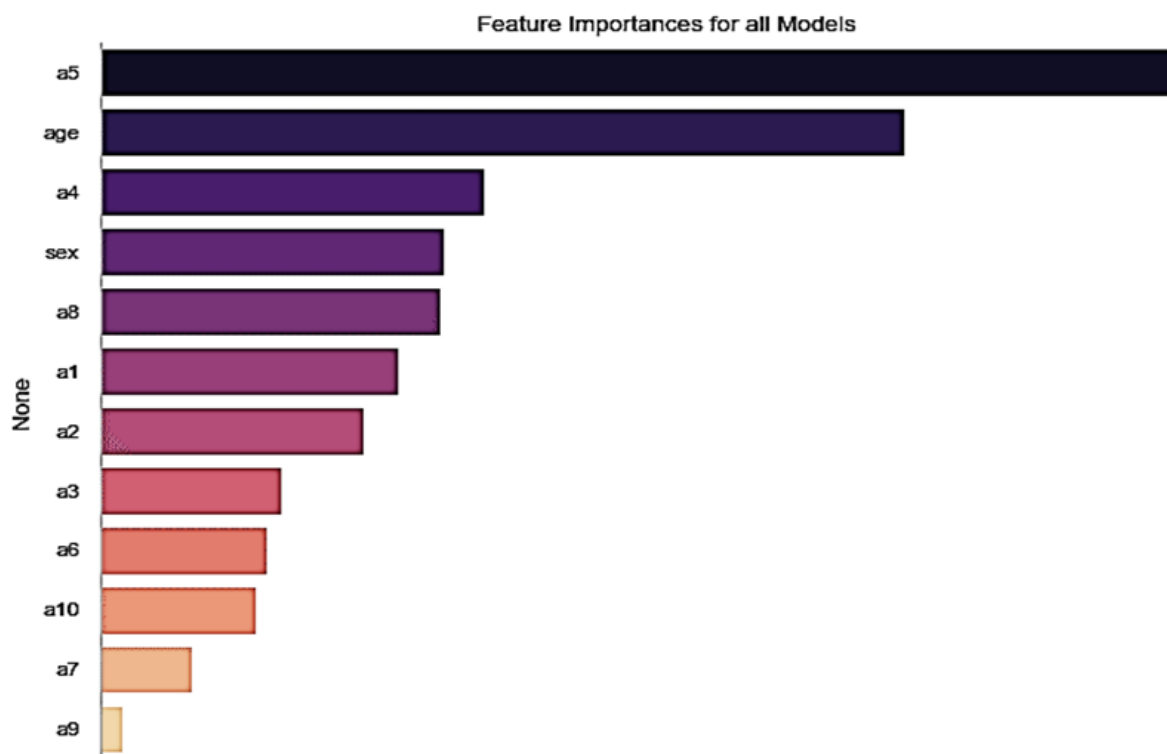


**Fig. 9.** Feature importance for all Models.

## 6. CONCLUSION

This study presents a machine learning framework designed to detect autism spectrum disorder (ASD) in individuals from young child age groups. The results demonstrate the effectiveness of machine learning techniques as valuable tools to accurately identify cases of autism spectrum disorder. The predictive models proposed in this study could serve as alternative or supportive tools for healthcare professionals in screening children for ASD.

The experimental analysis conducted in this research provides valuable insights for healthcare practitioners, helping them consider the most significant features when screening for ASD cases. However, it is important to acknowledge the limitation of this study, which is the insufficient amount of data to develop a generalized model covering all stages of ASD. A large dataset is crucial for constructing an appropriate model, which was lacking in the dataset used for this analysis.

However, this research has contributed to the development of an automated model that can help medical professionals diagnose autism in children. In future studies, the possibility of using a larger dataset to improve generalizability will be explored. The goal is to collect a more comprehensive data set specifically related to autism spectrum disorder, allowing the construction of a prediction model applicable to individuals of any age. This will enhance the detection of autism spectrum disorder and facilitate better recognition of other neurodevelopmental disorders.

Additionally, the study focused on the use of machine learning algorithms for the prediction and analysis of autism. Future research could explore the integration of other data sources, such as genetic and neuroimaging data, to improve the accuracy and understanding of the underlying mechanisms of ASD.

Furthermore, the study evaluated the performance of different machine-learning models using specific evaluation metrics. It would be valuable to compare the results with other established diagnostic methods, such as clinical assessments and behavioral observations, to assess the clinical utility and potential limitations of machine learning approaches in real-world settings.

## 7. ACKNOWLEDGMENT

We extend our thanks and appreciation to Dr. Ahmed Al-Awjali and Dr. Walid Al-Bariki for the valuable information that we benefited from completing this paper, and thanks to the Benghazi Autism Center, the Al-Eradah Center, the Al-Noor Center, and the Nusseibeh Center for their cooperation in providing the data required to form the database that was used during this paper.

## 8. REFERENCES

1. Raj S, Masood S. Analysis and Detection of Autism spectrum Disorder Using machine learning Techniques. *Procedia Computer Science*. (2020); 167: 994-1004  
<https://doi.org/10.1016/j.procs.2020.03.399>
2. Omar K S, Mondal P, Islam M N. A Machine Learning Approach to Predict Autism Spectrum Disorder. *International Conference on Electrical, Computer and Communication Engineering*. 2019  
<https://doi.org/10.1109/ECACE.2019.8679454>
3. Rahman M M, Usman O L, Muniyandi R C, Sahran S, Mohamed S, Razak R A. A Review of Machine Learning Methods of Feature Selection and Classification for Autism Spectrum Disorder *MDPI journals*. 2020; 10(12): 949.  
<https://doi.org/10.3390/brainsci10120949>
4. Wiggins L D, Reynolds A, Rice C E, Moody E J, Bernal P, Blaskey L, Rosenberg S A, Lee L, Levy S E. Using standardized diagnostic instruments to classify children with autism in the study to explore early development. *Journal of Autism and Developmental Disorders*. 2015; 45: 1271-1280.  
<https://doi.org/10.1007/s10803-014-2287-3>
5. Lai M C, Lombardo M V, Baron-Cohen S. Autism. *National library of medicine*. 2014; 383(9920):896-910  
[https://doi.org/10.1016/S0140-6736\(13\)61539-1](https://doi.org/10.1016/S0140-6736(13)61539-1)
6. Vakadkar K, Purkayastha D , Krishnan D. Detection of Autism Spectrum Disorder in Children Using Machine Learning Techniques . *SN Computer Science*. 2021; 2(386)  
<https://doi.org/10.1007/s42979-021-00776-5>
7. Hossain M D, Kabir M A, Anwar A, Islam M Z. Detecting autism spectrum disorder using machine learning techniques. *Health Information Science and Systems*. 2021; 9(17)  
<https://doi.org/10.1007/s13755-021-00145-9>
8. Usta M B, Karabekiroglu K, Sahin B, Aydin M , Bozkurt A. Use of machine learning methods in prediction of short-term outcome in autism spectrum disorders. *Psychiatry And Clinical Psychopharmacology*. 2018; 29(3):320-325  
<https://doi.org/10.1080/24750573.2018.1545334>
9. Saeed F. Towards quantifying psychiatric diagnosis using machine learning algorithms and big fMRI data. *Big Data Analytics* .2018;3(7)  
<https://doi.org/10.1186/s41044-018-0033-0>
10. Thabtah F. Machine learning in autistic spectrum disorder behavioral research: A review and ways forward. *Informatics For Health & Social Care*. 2018; 44(3):278-297  
<https://doi.org/10.1080/17538157.2017.1399132>

11. Küpper C, Stroth S, Wolff N, Hauck F, Kliewer N, Hansjosten T S, Becker I K, Poustka L, Roessner V, Schultebrucks K, Roepke S. Identifying predictive features of autism spectrum disorders in a clinical sample of adolescents and adults using machine learning. *Scientific Reports*. 2020; 10(1)  
<https://doi.org/10.1038/s41598-020-61607-w>
12. Maalouf M. Logistic Regression in Data Analysis: An Overview. *Int. J. Data Analysis Techniques and Strategies*. 2009 ;3(3): 281–299  
<http://dx.doi.org/10.1504/IJDATS.2011.041335>
13. Brownlee J. Naive Bayes for Machine Learning. *Machine Learning Mastery*. 2020 Naive Bayes for Machine Learning - MachineLearningMastery.com
14. Gandhi R. Support Vector Machine Introduction to Machine Learning Algorithms by Towards Data Science. *Towards Data Science*. 2018 Support Vector Machine — Introduction to Machine Learning Algorithms | by Rohith Gandhi | Towards Data Science
15. Zhang Z. Introduction to machine learning: K-nearest neighbors. *Annals of Translational Medicine*. 2016; 4(11)  
<http://dx.doi.org/10.21037/atm.2016.03.37>
16. Cunningham P, Delany S J. k-Nearest Neighbour Classifiers Technical. *ACM Computing Surveys* .2021; 54(6):1-25  
<https://doi.org/10.1145/3459665>
17. Reinstein I. Algorithms, CART, Decision Trees, Ensemble Methods, Explained, *Machine Learning, random forests algorithm, Salford Systems. KDnuggets* .2017 Random Forests®, Explained - KDnuggets
18. Azmi S S, Baliga S. An overview of boosting decision tree algorithms utilizing. *International Research Journal of Engineering and Technology (IRJET)* .2020 ;7(5): 6867-6870  
<https://www.irjet.net/archives/V7/i5/IRJET-V7I51293.pdf>
19. Mythili M S, Shanavas A M. A novel approach to predict the learning skills of autistic children using SVM and decision tree. *International Journal of Computer Science and Information Technologies*. 2014; 5(6): 7288-7291  
<http://www.ijcsit.com/docs/Volume%205/vol5issue06/ijcsit2014050683.pdf>
20. Sujatha R, Aarthy S L, Chatterjee J, Alaboudi A, Jhanjhi N Z. A machine learning way to classify autism spectrum disorder. *International Journal of Emerging Technologies in learning (iJET)*. 2021;16(6): 182-200  
<https://doi.org/10.3991/ijet.v16i06.19559>
21. Ferreira A J, Figueiredo M A. Boosting algorithms: A review of methods, theory, and applications. Springer, New York, NY. 2012;  
[https://doi.org/10.1007/978-1-4419-9326-7\\_2](https://doi.org/10.1007/978-1-4419-9326-7_2)
22. Qureshi M S, Qureshi M B, Asghar J, Alam F, Aljarbouh A. Prediction and Analysis of Autism Spectrum Disorder Using Machine Learning Techniques. *Journal of health care engineering*. 2023;12(10):9815989  
<https://doi.org/10.1155/2023/9815989>
23. Mellema C J, Nguyen K P, Treacher A, Montillo A. Reproducible neuroimaging features for Diagnosis of autism spectrum disorder with machine learning. *Scientific reports*. 2022; 12(1): 3057  
<https://doi.org/10.1038/s41598-022-06459-2>
24. Ali MT, Gebreil A, ElNakieb, Y, Elnakib A, Shalaby A, Mahmoud A, Sleman A, Giridharan G A, Barnes G, Elbaz A S. A personalized classification of behavioral severity of autism spectrum disorder using a comprehensive machine-learning framework. *Scientific reports*. 2023 ; 13(1): 17048  
<https://doi.org/10.1038/s41598-023-43478-z>
25. Rogala J, Żygierewicz J, Malinowska U, Cygan H, Stawicka E, Kobus A, Vanrumste B. Enhancing autism spectrum disorder classification in children through the integration of traditional statistics and classical machine learning techniques in EEG analysis. *Scientific Reports*. 2023. 13(1): 21748  
<https://doi.org/10.1038/s41598-023-49048-7>



## On Convergent Filters in Soft Topological Spaces

Rukaia Mahmoud Mohammed Rashed <sup>1\*</sup>

*1 Department of Mathematics - Faculty of Education - Al-Zawia University.*

Received: 07 / 03 / 2024; Accepted: 26 / 05 / 2024

### ABSTRACT

This study explains the concept of soft topological spaces in the view soft filters, studying the properties of soft filters in soft topological spaces. The study aims to contribute to the development of soft mathematical concepts and structures, building on the foundations of soft set theory. During the study, we found a relation between the concepts  $\tau$ -convergence and  $\tau$ -Hausdorff soft topological spaces.

**KEYWORDS:** Soft Set, Soft Topological Space, Soft Filter, Soft Ultrafilter,  $\tau$ -Converges,  $\tau$ -Hausdorff.

### 1. INTRODUCTION

Classical tools of Mathematics <sup>19</sup> cannot solve the problems, which are vague rather than precise. To overcome these difficulties Molodtsov <sup>16</sup> initiated the concept of soft set theory which doesn't require the specification of parameters. He applied soft set theory successfully in smoothness of functions, game theory, and operation research and so on. Thereafter so many research works <sup>5</sup> have been done on this concept in different disciplines of Mathematics.

Research on soft sets-based decision-making has received much attention in recent years. Later, in 2003, Maji et al. <sup>14,15</sup> made a theoretical study on soft set theory. They introduced several operations on soft sets and applied soft sets to decision-making problems.

Kharal and Ahmed <sup>8</sup> defined soft mappings. In 2011, Shabir and Naz <sup>17</sup> came up with an idea of soft topological spaces.

Later some researchers <sup>2, 19, 4</sup> and <sup>18</sup> studied on soft topological spaces. The definition of filter and ultrafilter given here are those of Sharma <sup>7</sup>.

In our present work, we have introduced the concept of soft topological spaces in the view of soft filters. We also discuss some of the properties of soft filters in soft topological spaces.

The researcher in this study adopted a theoretical approach, building on the foundations of soft set theory and its applications in topology. The research involves a comprehensive review of existing literature on soft sets, soft topology, and their applications, where he explained the concept of soft filters is defined as a collection of soft sets that satisfy certain properties, including being closed under finite intersections and the superset operation. Soft topology is an extension of classical topology, where soft sets are used to define soft open sets. The study of soft filters and soft topology has many applications, including decision-making and data analysis, the study aims to contribute to the development of soft mathematical concepts and structures, which can have applications in various fields, including fuzzy mathematics, also aims to:

1. Investigate the concept of soft topological spaces in the context of soft filters.
2. Examine the properties of soft filters in soft topological spaces.
3. Study the relationship between soft filters and  $\tau$ -convergent and  $\tau$ -Hausdorff soft topological spaces.
4. Contribute to the development of soft mathematical concepts and structures based on soft set theory.

### 2. PRELIMINARIES

**Definition 2.1** <sup>6</sup> A soft set  $F_A$  over  $X$  is a set defined by the function  $f_A$  representing a mapping  $f_A: A \rightarrow P(X)$  such that  $f_A = \emptyset$  if  $x \notin A$ . Here,  $f_A$  is called the approximate function of the soft set  $F_A$ . A soft set over  $X$  can be represented by the set of ordered pairs

$$F_A = \{(x, f_A): x \in A, f_A(x) \in P(X)\}.$$

**Definition 2.2** <sup>2</sup> Let  $F_A$  and  $G_A$  be two soft sets over  $X$ . The parallel product of  $F_A$  and  $G_A$  is defined as  $F_A \tilde{\times} G_A = (F \tilde{\times} G)_A$ , where  $(F \tilde{\times} G)_{(\alpha)} =$

\*Correspondence: Rukaia Mahmoud Mohammed Rashed

[r.rasheed@zu.edu.ly](mailto:r.rasheed@zu.edu.ly)

$F(\alpha) \tilde{\times} G(\alpha), \forall \alpha \in A \subseteq E$ . It is clear that  $(F \tilde{\times} G)_A$  is a soft set over  $X \tilde{\times} X$ .

**Definition 2.3**<sup>17</sup> Let  $\tau$  be the collection of soft sets over  $X$ , then  $\tau$  is said to be a soft topology on  $X$  if:

1.  $\emptyset, X$  are belong to  $\tau$ .
2. The union of any number of soft sets in  $\tau$  belong to  $\tau$ .
3. The intersection of any two soft sets in  $\tau$  belong to  $\tau$ .

In this case, the triplet  $(X, \tau, A)$  is called soft topological space over  $X$ , and any member of  $\tau$  is known as soft open set in  $X$ . The complement of a soft open set is called soft closed set over  $X$ .

**Definition 2.4**<sup>9</sup> A crisp element  $x \in X$  is said to be in the soft set  $F_A$  over  $X$ , denoted by  $x \in X$  iff  $x \in F(\alpha), \forall \alpha \in A$ .

**Definition 2.5**<sup>9</sup> A soft set  $F_A$  is said to be  $\tau$ -soft neighborhood of an element  $x \in X$  if there exist  $G_A \in \tau$  such that  $x \in G_A \subseteq F_A$ .

**Definition 2.6**<sup>10,11</sup> Let  $(X, \tau, A)$  and  $(Y, \sigma, A)$  be two soft topological spaces. The mapping  $f: (X, \tau, A) \rightarrow (Y, \sigma, A)$  is said to be:

1. Soft continuous if  $f^{-1}(F_A) \in \tau, \forall F_A \in \sigma$ .
2. Soft home morphism if  $f$  is bijective and  $f, f^{-1}$  are soft continuous.
3. Soft open if  $F_A \in \tau \Rightarrow f[F_A] \in \sigma$ .
4. Soft closed if  $F_A$  is soft closed in  $(X, \tau, A) \Rightarrow f[F_A]$  is soft closed in  $(Y, \sigma, A)$ .

**Definition 2.7**<sup>3</sup> Let  $(X, \tau, A), (Y, \sigma, A)$  and  $(Z, \omega, A)$  be two soft topological spaces. If  $f: (X, \tau, A) \rightarrow (Y, \sigma, A)$  &  $g: (Y, \sigma, A) \rightarrow (Z, \omega, A)$  are soft continuous and  $f(X) \subseteq Y$ , then the mapping  $gf: (X, \tau, A) \rightarrow (Z, \omega, A)$  is soft.

**Definition 2.8**<sup>10</sup> Let  $\tau$  be a soft topology on  $X$ . Then a soft set  $F_A$  is said to be  $\tau$ -soft neighborhood (shortly soft nbh) of the element  $E_\alpha^X$  if there exist a soft set  $G_A \in \tau$  such that  $E_\alpha^X \in G_A \subseteq F_A$ . The soft nbh system of a soft element  $E_\alpha^X$  in  $(X, \tau, A)$  is denoted by  $N_\tau(E_\alpha^X)$ .

**Definition 2.9**<sup>9</sup> Let  $(X, \tau, A)$  be a soft topological space. A subcollection  $\beta$  of  $\tau$  is said to be an open base of  $\tau$  if every member of  $\tau$  can be expressed as the union of some member of  $\beta$ .

**Definition 2.10**<sup>10</sup> The soft topology in  $X \times Y$  induced by the open base  $\beta = \{F_A \times G_A: F_A \in \tau, G_A \in \sigma\}$  is said to be the product soft topology of the soft topologies  $\tau$  &  $\sigma$  it is denoted by  $\tau \times \sigma$ . The soft topological space  $(X \times Y, \tau \times \sigma, A)$  is said to be the soft topological product of soft topological space  $(X, \tau, A)$  and  $(Y, \sigma, A)$ .

**Definition 2.11**<sup>3</sup> A collection  $\mathfrak{B}$  of soft neighborhoods of a soft element  $E_\alpha^X, \forall \alpha \in A$  is said to be fundamental soft neighborhood system or soft neighborhood base of  $E_\alpha^X$  if for any soft neighborhood  $N_A$  of  $E_\alpha^X, \exists H_A \in \mathfrak{B}$  such that  $H_A \subseteq N_A$ .

**Definition 2.12**<sup>13</sup> Let  $(X, \tau, A)$  be a soft topological space. Then  $\mathcal{F}$  is called a soft filter on  $X$  if  $\mathcal{F}$  satisfies the following properties:

1.  $\emptyset \notin \mathcal{F}$ .
2.  $\forall F_A, G_B \in \mathcal{F}, F_A \cap G_B \in \mathcal{F}$ .
3.  $\forall F_A \in \mathcal{F} \& F_A \subseteq G_B, G_B \in \mathcal{F}$ .

**Definition 2.13**<sup>13</sup> A soft filter  $\mathcal{F}$  in a topological space  $X$  is said to converges to a soft point  $x_\lambda \in X$  if every soft neighborhood of  $x_\lambda$  belongs to  $\mathcal{F}$  for each  $\lambda \in A$ .

**Theorem 2.1**<sup>13</sup> Let  $(X, \tau, A)$  be a soft filter of a soft topological Hausdorff space  $X$ , if  $\mathcal{F}$  converges to  $x(\lambda) \in X$  also to  $y(\lambda) \in X$ , for each  $\lambda \in A$  then  $x = y$ .

**Theorem 2.2**<sup>13</sup> Let  $\mathcal{F}$  be a soft filter of a soft topological space and let  $F_A \subseteq X$ . Then  $x_\lambda \in \overline{F_A}$  iff there exist a soft filter  $\mathcal{F}$  of subsets of  $X$  such that  $F_A \in \mathcal{F}$  and  $\mathcal{F}$  converges to  $x_\lambda, \forall \lambda \in A$ .

**Definition 2.14**<sup>12</sup> Let  $(X, \tau, A)$  be a soft topological space. A filter  $\mathcal{F}$  on  $X$  is said to be  $\tau$ -convergent to a point  $x \in X$  if every  $\tau$ -neighborhood  $N_A$  of  $x$  is a subset of  $\mathcal{F}$ . We say that  $x$  is a  $\tau$ -limit point of  $\mathcal{F}$ .

**Example 2.1** Let  $(X, \tau, A)$  be a soft topological space,  $X = \{1,2,3\}$  &  $A = \{\{1\}, \{1,2\}, \{1,2,3\}\}$ , and let  $\mathcal{F} = \{\emptyset, \{1\}, \{1,2\}, \{1,2,3\}\}$  be a filter on  $X$ , then the  $\tau$ -nbh are as follows:  $\tau\text{-cl}(\{2\}) = \{1,2\} \in \mathcal{F}, \tau\text{-cl}(\{1,2\}) = \{1,2\} \in \mathcal{F}$  &  $\tau\text{-cl}(\{2,3\}) = \{1,2,3\} \in \mathcal{F} \Rightarrow$  since all  $\tau$ -closure of  $\tau$ -nbh of  $x = 2$  belong to  $\mathcal{F}$ , then every  $\tau$ -nbh  $N_A$  of  $x = 2$  has a  $\tau$ -closure ( $\tau\text{-cl}(N_A)$ ) belong to  $\mathcal{F}, \Rightarrow x = 2$  is a  $\tau$ -limit point of the filter  $\mathcal{F}$ , and  $\mathcal{F}$  converges to  $x = 2$ .

**Definition 2.15**<sup>12</sup> Let  $(X, \tau, A)$  be a soft topological space. A filter base  $\mathcal{G}$  on  $X$  is said to be  $\tau$ -converges to a point  $x \in X$ , if the filter whose base is  $\mathcal{G}^*$  to a point  $x$ , we say that  $x$  is a  $\tau$ -limit point of  $\mathcal{G}$ .

### 3. SOFT FILTERS IN SOFT TOPOLOGICAL SPACES

**Proposition 3.1**<sup>1</sup> Let  $(X, \tau, A)$  be a soft topological space and  $\mathcal{F}$  be a filter on  $X$  then the following statement are equivalent:

1.  $\mathcal{F}$  is  $\tau$ -converges to a point  $x \in X$ .
2.  $\mathcal{F}$  is finer than the collection  $\Omega = \{\tau\text{-cl}(N_A): N_A \text{ is } \tau\text{-nbh of } x\}$ .

3. For every  $\tau$ -nbh  $N_A$  of  $x$ , there is  $F \in \mathcal{F}$  such that  $F \subset \tau - cl(N_A)$ .

**Corollary 3.1** Let  $(X, \tau, A)$  be a soft topological space. Then the  $\tau$ -nbh filter of a point  $x \in X$  is  $\tau$ -converges to  $x$ .

**Proof** Let  $N_A$  be a  $\tau$ -nbh of  $x$ . By definition of a  $\tau$ -nbh, there exists a set  $V$  in  $A$  such that  $x \in V$  &  $V \subseteq N_A$ . Now, consider the  $\tau$ -nbh filter of  $x$ , denoted by  $F_\tau(x)$ . Since  $V \in A$  &  $x \in V$ , we have  $V \in F_\tau(x)$ . Since  $V \subseteq N_A$ , we conclude that  $F_\tau(x)$  is  $\tau$ -converges to  $x$ .

**Proposition 3.2** Let  $(X, \tau, A)$  be a soft topological space, let  $\tau$  be an indiscrete topology on  $X$ . Then every filter on  $X$  is  $\tau$ -converges to a point  $x \in X$ .

**Proof** Suppose that  $\mathcal{F}$  is an arbitrary filter on  $X$ . Since the only open sets in  $\tau$  are  $X$  and the empty set. So, we have two cases:

1. If  $\mathcal{F}$  contains the empty set, then the filter  $\mathcal{F}$  is trivial and we can say that it  $\tau$ -converges to every point in  $X$ .
2. If  $\mathcal{F}$  does not contains the empty set, then  $\mathcal{F}$  contains  $X$ . Since  $X$  is the only non-empty open set in  $\tau$ , every subset of  $X$  is a  $\tau$ -nbh of every point in  $X$ . Therefore,  $\mathcal{F}$  is  $\tau$ -converges to every point  $x$  in  $X$ .

**Proposition 3.3** Let  $(X, \tau, A)$  be a soft topological space. If a filter  $\mathcal{F}$  on  $X$  is  $\tau$ -converges to a point  $x$  in  $X$ , then every filter  $\mathcal{G}$  is finer than  $\mathcal{F}$  also  $\tau$ -converges to a point  $x$ .

**Proof** To prove this, assume that  $\mathcal{F}$  is  $\tau$ -converges to  $x$  in  $X$ , this means that for every  $\tau$ -nbh  $N_A$  of  $x$ , there exists a set  $A$  in  $\mathcal{F}$  such that  $A \subseteq N_A$ . Now, consider a filter  $\mathcal{G}$  that is finer than  $\mathcal{F}$ , this means that every set in  $\mathcal{G}$  is also a set in  $\mathcal{F}$ . Let take a  $\tau$ -nbh  $N_A$  of  $x$ . Since  $\mathcal{F}$  is  $\tau$ -converges to  $x$ , there exist a set  $A$  in  $\mathcal{F}$  such that  $A \subseteq N_A$ . Since  $\mathcal{G}$  is finer than  $\mathcal{F}$ ,  $A$  is also in  $\mathcal{G}$ . Therefore, we have  $A \subseteq N_A$  for every  $\tau$ -nbh  $N_A$  of  $x$ , and every set  $A$  in  $\mathcal{G}$ . This implies that  $\mathcal{G}$  is  $\tau$ -converges to  $x$  in  $X$ .

**Proposition 3.4** Let  $\Omega$  be the collection of all filters on a soft topological space  $(X, \tau, A)$  which is  $\tau$ -converges to the same point  $x$  in  $X$ . Then the intersection of all filters in  $\Omega$  also  $\tau$ -converges to a point  $x$ .

**Proof** Assume that  $\Omega$  is the collection of all filters on a soft topological space  $(X, \tau, A)$  which  $\tau$ -converges to the same point  $x$  in  $X$ . Now, let  $\mathcal{F}$  be the intersection of all filters in  $\Omega$ . By the definition of  $\tau$ -converges, a filter  $\mathcal{F}$  is converges to  $x$  if for every  $\tau$ -open set  $U$  containing  $x$ , there exists a set  $A$  in  $\mathcal{F}$  such that for every element  $y$  in  $A$ ,  $(x, y)$  is in  $\tau(U)$ . Let  $U$  be a  $\tau$ -open set containing  $x$ , and since  $\mathcal{F}$  is the intersection of all filters in  $\Omega$ , it means that for every filter  $\mathcal{G}$  in  $\Omega$ ,  $U$  is in  $\mathcal{G}$ . Therefore,  $U$  is also in  $\mathcal{F}$ . Now  $y$  any element in  $\mathcal{F}$ , and since  $\mathcal{F}$  is a filter, it means that it contains the intersection of any two sets in  $\mathcal{F}$ . Thus, if  $A$  is any set in  $\mathcal{F}$ , then  $y$  is also in  $A$ . This

implies that  $(x, y)$  is in  $\tau(U)$ , as  $U$  is a  $\tau$ -open set containing  $x$ . Therefore, for any  $\tau$ -open set  $U$  containing  $x$ , there exists a set  $A$  in  $\mathcal{F}$  such that for every element  $y$  in  $A$ ,  $(x, y)$  is in  $\tau(U)$ . This fulfills the definition of  $\tau$ -converges, Then the intersection of all filters in  $\Omega$  also  $\tau$ -converges to a point  $x$ .

**Proposition 3.5** Let  $(X, \tau, A)$  be a soft topological space. A filter  $\mathcal{F}$  on  $X$  is  $\tau$ -converges to a point  $x$  in  $X$  if and only if every ultrafilter containing  $\mathcal{F}$  is  $\tau$ -converges to a point  $x$ .

**Proof** Suppose that  $\mathcal{F}$  does not  $\tau$ -converges to  $x$ . This means that there exists a  $\tau$ -open set  $U$  containing  $x$  such that for every set  $A$  in  $\mathcal{F}$ , there exists an element  $y$  in  $A$  such that  $(x, y)$  is not in  $\tau(U)$ . Now, consider the collection  $\Omega$  of all ultrafilters containing  $\mathcal{F}$ , and since every ultrafilter containing  $\mathcal{F}$  is  $\tau$ -converges to  $x$ , it follows that for every  $\tau$ -open set  $U$  containing  $x$ , there exist a set  $A$  in every ultrafilter  $\mathcal{H}$  in  $\Omega$  such that for every element  $y$  in  $A$ ,  $(x, y)$  is in  $\tau(U)$ . However, we have found a  $\tau$ -open set  $U$  containing  $x$  such that for every set  $A$  in  $\mathcal{F}$ , there exists an element  $y$  in  $A$  such that  $(x, y)$  is not in  $\tau(U)$ . This implies that there exists at least one ultrafilter in  $\Omega$  (specifically, the one containing the sets that do not satisfy the  $\tau$ -convergence condition) that does not  $\tau$ -converge to  $x$ . This contradicts our assumption that every ultrafilter containing  $\mathcal{F}$  is  $\tau$ -converges to  $x$ . Therefore, if every ultrafilter containing  $\mathcal{F}$  is  $\tau$ -converges to  $x$ , then  $\mathcal{F}$  must indeed  $\tau$ -converge to  $x$ .

**Example 3.1** Let  $(X, \tau, A)$  be a soft topological space where  $X = \{1,2,3\}$  &  $A = \{\{1\}, \{1,2\}, \{1,2,3\}\}$ , and let  $\mathcal{F} = \{\emptyset, \{1\}, \{1,2\}, \{1,2,3\}\}$  be a filter on  $X$ , if  $x = 2 \Rightarrow$  the  $\tau$ -nbh are as follows: for  $\{2\} \Rightarrow \{2\} \in \mathcal{F}$ , for  $\{1,2\} \Rightarrow \{1,2\} \in \mathcal{F}$ , for  $\{2,3\} \Rightarrow \{1,2,3\} \in \mathcal{F}$ . Since all  $\tau$ -nbh of  $x = 2$  belong to  $\mathcal{F} \Rightarrow \mathcal{F}$  is  $\tau$ -converges to  $x = 2$ . Suppose that  $\mathcal{H}$  is an ultrafilter containing  $\mathcal{F} \Rightarrow \mathcal{H} = \{\emptyset, \{1,2,3\}\}$ . For the ultrafilter  $\mathcal{H}$  is  $\tau$ -converges to a point  $x$ , for the same point  $x = 2 \Rightarrow$  for  $\{2\} \Rightarrow \{2\} \in \mathcal{H}$ , for  $\{1,2\} \Rightarrow \{1,2\} \notin \mathcal{H}$ , for  $\{2,3\} \Rightarrow \{1,2,3\} \in \mathcal{H}$ . Since there exist a  $\tau$ -nbh  $\{1,2\} \notin \mathcal{H} \Rightarrow \mathcal{H}$  does not  $\tau$ -converge to  $x = 2$ .

**Definition 3.1** A soft topological space  $(X, \tau, A)$  is said to be  $\tau$ -Hausdorff if for every two distinct points  $x$  &  $y$  in  $X$ , there exist two  $\tau$ -open sets  $U$  &  $V$  such that  $\tau-cl(U) \cap \tau-cl(V) = \emptyset$ .

**Proposition 3.6** If a soft topological space  $(X, \tau, A)$  is  $\tau$ -Hausdorff, then every  $\tau$ -converges filter on  $X$  has a unique  $\tau$ -limit point.

**Proof** Suppose that  $(X, \tau, A)$  is a  $\tau$ -Hausdorff soft topological space, and let  $\mathcal{F}$  be a  $\tau$ -convergent filter on  $X$ . Assume, for contradiction, that  $\mathcal{F}$  has more than one  $\tau$ -limit point and let  $x, y$  be two distinct  $\tau$ -limit point in  $\mathcal{F}$ , then by definition of a  $\tau$ -Hausdorff space, there exist two

$\tau$ -open sets  $U$  &  $V$  such that  $x \in U, y \in V$  &  $\tau-cl(U) \cap \tau-cl(V) = \emptyset$ . Since  $\mathcal{F}$  is a  $\tau$ -convergent filter, for any  $\tau$ -open set containing  $x$ , (in this case  $U$ ), there exists an element  $z$  in  $\mathcal{F}$  such that  $z \in U$ . Similarly, there exists an element  $s$  in  $\mathcal{F}$  such that  $s \in V$ . Now, consider the set  $W = U \cap V$ . Since  $\tau-cl(U) \cap \tau-cl(V) = \emptyset$ , it follows that the  $\tau-cl(W) \cap \mathcal{F} = \emptyset$ . However, this contradicts the assumption that  $x$  &  $y$  are  $\tau$ -limit points in  $\mathcal{F}$ , as  $W$  is a  $\tau$ -open set containing both  $x$  &  $y$ , and there is no element in  $\mathcal{F}$  contained in  $W$ . Therefore, our assumption that  $\mathcal{F}$  has more than one  $\tau$ -limit point is false. This implies that  $\mathcal{F}$  has a unique  $\tau$ -limit point.

**Definition 3.2** Let  $(X, \tau, A)$  a soft topological space, A filter (filter base)  $\mathcal{G}$  on a set  $X$  is said to be  $\tau$ -accumulates at a point  $x \in X$  if every  $\tau$ - $nbh N_A$  of  $x$ , and every  $F \in \mathcal{F}$ , the intersection  $\tau-cl(N_A) \cap F \neq \emptyset$ . We say that  $x$  is a  $\tau$ -cluster point of  $\mathcal{F}$ .

**Proposition 3.7** Let  $(X, \tau, A)$  be a soft topological space and let  $\mathcal{F}$  be a filter on  $X$ . If a point  $x \in X$  is  $\tau$ -limit point of  $\mathcal{F}$ , then it is  $\tau$ -cluster point of  $\mathcal{F}$ .

**Proof** Suppose that a point  $x$  is a  $\tau$ -limit point of  $\mathcal{F}$ , i.e., for every  $\tau$ - $nbh N_A$  of  $x, N_A \cap \mathcal{F} \neq \emptyset$ . Let  $W$  be any  $\tau$ - $nbh$  of  $x$ , then by definition of  $\tau$ -cluster point, for every  $\tau$ - $nbh N_A$  of  $x$ ,

$N_A \cap \mathcal{F} \neq \emptyset$ . Since  $\tau$ - $nbh N_A$  of  $x$ , and since  $x$  is a  $\tau$ -limit point of  $\mathcal{F}$ . Then  $N_A \cap \mathcal{F} \neq \emptyset$ . Now, consider the intersection  $(N_A \cap W) \cap \mathcal{F} \neq \emptyset$ . Since  $N_A \cap \mathcal{F} \neq \emptyset, N_A \cap W \neq \emptyset$ , we have  $(N_A \cap W) \cap \mathcal{F} \neq \emptyset$ . Thus,  $X$  is a  $\tau$ -cluster point of  $\mathcal{F}$ .

**Proposition 3.8** Let  $(X, \tau, A)$  be a soft topological space. If a filter base  $\mathcal{G}$  on  $X$  is  $\tau$ -converges to  $x \in X$ , then it is  $\tau$ -accumulates at  $x \in X$  and in a  $\tau$ -Hausdorff space, at no point other than  $x$ .

**Proof** Assume a filter  $\mathcal{G}$  on  $X$   $\tau$ -converges to  $x$ . This means that every  $\tau$ - $nbh N_A$  of  $x, N_A \in \mathcal{G}$ . Since  $\mathcal{G}$  is  $\tau$ -converges to  $x$ , we have  $N_A \in \mathcal{G}$  for every  $\tau$ - $nbh N_A$  of  $x$ . Therefore,  $N_A \cap \mathcal{G} \neq \emptyset$ , as  $N_A$  it self is in  $\mathcal{G}$ . Now, let  $y$  be a point in  $X$  other than  $x$ . We need to show that  $\mathcal{G}$  does not  $\tau$ -accumulate at  $y$ . Since  $X$  is a  $\tau$ -Hausdorff space, then there exists disjoint  $\tau$ - $nbh N_A$  &  $M_A$  of  $x$  &  $y$ , respectively. Since  $\mathcal{G}$   $\tau$ -converges to  $x$ , we know that  $N_A \in \mathcal{G}$ . However, since  $N_A$  &  $M_A$  are disjoint,  $N_A \cap M_A = \emptyset$ , which implies that  $N_A \cap (M_A \cap \mathcal{G}) = \emptyset$ . Therefore,  $\mathcal{G}$  does not  $\tau$ -accumulate at  $y$  in a  $\tau$ -Hausdorff space.

**Proposition 3.9** Let  $(X, \tau, A)$  be a soft topological space and let  $\mathcal{F}$  is subordinate to  $\mathcal{G}$ , if  $\mathcal{G}$  is  $\tau$ -converges to  $x \in X$ , then  $\mathcal{F}$  is  $\tau$ -converges to  $x$ .

**Proof** By definition of  $\tau$ -convergence, we know that for any  $nbh N_A$  of  $x$  in  $A, \mathcal{G}$  eventually enters  $N_A$  with respect to  $\tau$ . That is, there exist some index  $n$  such that

for all  $k \geq n, \mathcal{G}(k) \in N_A$ . Now, since  $\mathcal{F}$  is subordinate to  $\mathcal{G}$ , it follows that for every all  $k \geq n, \mathcal{F}(k) \subseteq \mathcal{G}(k)$ . Therefore,  $\mathcal{F}(k)$  is also in  $N_A$  for all  $k \geq n$ . Thus, we have shown that for every  $nbh N_A$  of  $x, \mathcal{F}$  eventually enters  $N_A$  with respect to  $\tau$ . Therefore,  $\mathcal{F}$  is  $\tau$ -converges to  $x$  in the soft topological space  $(X, \tau, A)$ .

**Proposition 3.10** Let  $(X, \tau, A)$  be a soft topological space and let  $\mathcal{F}$  is subordinate to  $\mathcal{G}$ , if  $\mathcal{F}$  is  $\tau$ -accumulates at  $x \in X$ , then  $\mathcal{G}$  is  $\tau$ -accumulates at  $x$ .

**Proof** By definition of  $\tau$ -accumulation, we know that for any  $nbh N_A$  of  $x$  in  $A, \mathcal{G}$  intersects  $N_A$  with respect to  $\tau$  at infinitely many indices. That is, there exist infinitely many indices  $k$  such that  $\mathcal{G}(k) \in N_A$ . Now, since  $\mathcal{F}$  is subordinate to  $\mathcal{G}$ , it follows that for every  $k, \mathcal{F}(k) \subseteq \mathcal{G}(k) \in N_A$  for those same indices. Thus, we have show that for every  $nbh N_A$  of  $x, \mathcal{F}$  intersects  $N_A$  with respect to  $\tau$  at infinitely many indices. Therefore,  $\mathcal{F}$  is  $\tau$ -accumulates at  $x$  in the soft topological space  $(X, \tau, A)$ .

**Definition 3.3** Let  $\mathcal{F}$  &  $\mathcal{G}$  be two soft filters in soft topological space  $(X, \tau, A)$ , we say that  $\mathcal{F}$  is finer than  $\mathcal{G}$  or  $\mathcal{G}$  is coarser than  $\mathcal{F}$  if  $\mathcal{G} \subset \mathcal{F}$ . If  $\mathcal{F} \neq \mathcal{G}$ , then we say that  $\mathcal{F}$  is strictly finer than  $\mathcal{G}$  or  $\mathcal{G}$  is strictly coarser than  $\mathcal{F}$ .

**Proposition 3.11** Let  $(\mathcal{F}_i)_{i \in I}$  be any non-empty family of soft filters on  $X$ . Then  $\mathcal{F} = \bigcap_{i \in I} \mathcal{F}_i$  is a soft filter on  $X$ .

**Proof** Let  $(\mathcal{F}_i)_{i \in I}$  be any non-empty collection of soft filters on  $X$ . Let  $\mathcal{F}$  be the intersection of all elements in  $\mathcal{F}_i$  i.e.,  $\mathcal{F} = \bigcap \{A : A \in \mathcal{F}_i\} = \bigcap_{i \in I} \mathcal{F}_i$ . Since  $\mathcal{F}_i$  is non-empty,  $\mathcal{F}$  is guaranteed to exist. To do this, we need to verify the following properties:  
 1-  $\mathcal{F}$  is non-empty: since  $\mathcal{F}_i$  is non-empty, each element in  $\mathcal{F}_i$  is non-empty. So, the intersection  $\mathcal{F}$  will also be non-empty.  
 2-  $\mathcal{F}$  is upward closed: let  $A \in \mathcal{F}$  &  $A \subseteq B$ , since each element in  $\mathcal{F}_i$  is upward closed we have  $B \in A$  for all  $A \in \mathcal{F}_i$ . So,  $B \in \mathcal{F}$ .  
 3-  $\mathcal{F}$  is closed under finite intersection: Let  $A, B \in \mathcal{F}$ . Then  $A, B \in \mathcal{F}_i$ . Since each element in  $\mathcal{F}_i$  is closed under finite intersection, we have  $A \cap B \in \mathcal{F}_i$ . Therefore,  $A \cap B \in \mathcal{F}$ .  
 4- As  $\mathcal{F}$  satisfies all the properties of soft filter,  $\mathcal{F}$  is indeed a soft filter on  $X$ .

**Remark 3.1** The soft filter induced by the single set  $X$ , is the smallest element of the order set of all soft filters on  $X$ .

**Theorem 3.1** Let  $A$  be a set in  $X$ . Then there exists a soft filter on  $X$  containing  $A$  if for any given finite subset  $\{S_1, S_2, \dots, S_n\}$  of  $A$ , the intersection  $\bigcap_{i \in I} S_i \neq \emptyset$ . In fact  $\mathcal{F}_A$  is the coarsest soft filter containing  $A$ .

**Proof** Suppose that there exists a soft filter  $\mathcal{F}_A$  on  $X$  containing  $A$ . Let  $B$  be the set of all finite intersections of members of  $A$ . Then by conditions of soft filter we have

$B \subseteq \mathcal{F}_A$  &  $\mathcal{F}_A \neq \emptyset$ . Suppose that  $\mathcal{F}_A = \{A \in \mathcal{F}^X : A \text{ contains a member of } B\}$ , where  $B$  is the family of finite intersections of  $A$ . Then  $\mathcal{F}(A)$  satisfies the conditions,  $\Rightarrow \mathcal{F}(A)$  is generated by  $A$ .

**Corollary 3.2** Let  $\mathcal{F}$  be a soft filter in a set  $X$ , and  $A \subseteq X$ . Then, there is a soft filter  $\mathcal{F}'$  which is finer than  $\mathcal{F}$ , and such that  $A \in \mathcal{F}'$  iff  $A \cup U = \emptyset$  for each  $U \in \mathcal{F}$ .

**Proof**  $\Rightarrow$  Assume that  $A \subseteq \mathcal{F}'$ , where  $\mathcal{F}'$  is a soft filter finer than  $\mathcal{F}$ . i.e. that  $\mathcal{F}'$  satisfies the three conditions for being a soft filter, we can consider an arbitrary  $U$  in  $\mathcal{F}$ . Since  $\mathcal{F}'$  is finer than  $\mathcal{F}$ , we know that  $U$  is a subset of  $\mathcal{F}'$ . Therefore, the intersection of  $A$  &  $U$  is non-empty, as  $A$  is a subset of  $\mathcal{F}'$ .  $\Leftarrow$  Conversely,  $A \cap U \neq \emptyset$  is non-empty for every  $U$  in  $\mathcal{F}$ . We want to show that there exists a soft filter  $\mathcal{F}'$  that finer than  $\mathcal{F}$ , and such that  $A$  is a subset of  $\mathcal{F}'$ . To construct such an  $\mathcal{F}'$ , we define the family of subsets  $\mathcal{R}$  of  $X$  as follows:

$\mathcal{R} = \{V \subseteq X, V \cap A \neq \emptyset \text{ for every } U \text{ in } \mathcal{F}\}$  we will show that  $\mathcal{R}$  is a soft filter finer than  $\mathcal{F}$ , and  $A$  is a subset of  $\mathcal{R}$ .

\*  $\mathcal{R} \neq \emptyset$ , since  $A \cap U \neq \emptyset, \forall U \in \mathcal{F}$ , we have that  $X$  is in  $\mathcal{R}$ .

\*  $\mathcal{R}$  closed, let  $V \subseteq X$ , such that  $V$  in  $\mathcal{R}$ , and let  $W$  be a subset of  $X$  such that  $V$  is a subset of  $W$ . We want to show that  $W$  is in  $\mathcal{R}$ . For every  $U$  in  $\mathcal{F}$   $A \cap U \neq \emptyset$ . Since  $V \subseteq W, A \cap V \subseteq A \cap W$ . Thus,  $A \cap W \neq \emptyset, \forall U \in \mathcal{F} \xrightarrow{\text{yields}} W \in \mathcal{R}$ .

\* Let  $V_1 \& V_2 \subseteq X \ni V_1 \& V_2 \in \mathcal{R}$ . We want to show that  $V_1 \cap V_2 \neq \emptyset$ . Since  $V_1 \& V_2 \in \mathcal{R} \xrightarrow{\text{yields}} A \cap V_1 \neq \emptyset \& A \cap V_2 \neq \emptyset$ . Therefore, the  $A \cap (V_1 \cap V_2) \neq \emptyset, \forall U$  in  $\mathcal{F}$ , which means that  $V_1 \cap V_2 \in \mathcal{R}$

**Corollary 3.3** a set  $F$  of a soft filter on a non-empty set  $X$ , has a least upper bound in the set of all soft filters on  $X$ , if for all finite sequence  $(\mathcal{F}_i)_{i \in I}, 0 \leq i \leq n$  of elements of  $F$  and all  $A_i \in \mathcal{F}_i, 1 \leq i \leq n, \bigcap_{i=1}^n A_i \neq \emptyset$ .

Note that the above corollary is not true in general case.

**Example 3.2** Let  $X \neq \emptyset$  &  $\mathcal{F}$  be a soft filter such that  $\mathcal{F} = \{A, B\}$ , where  $A \& B \subseteq X$ . Suppose that  $A \cap B \neq \emptyset$ . In this case, we can see that there is no soft filter  $\mathcal{F}'$  in  $\mathcal{F}$  that is a subset of every upper bound of  $\mathcal{Q}$ . Then any upper bound of  $\mathcal{Q}$  must be contain both  $A$  &  $B$  but there is no soft filter contain  $A$  &  $B$ .

**Theorem 3.2** Let  $\beta$  be a set of  $X$ . Then the set of  $X$  containing an element of  $\beta$  is a soft filter on  $X$  if  $\beta$  possesses the following conditions:  
 1-  $\beta_1$ : The intersection of two members of  $\beta$  contain a member of  $\beta$ .  
 2-  $\beta_2$ :  $\beta \neq \emptyset, \emptyset \notin \beta$ .

**Proof** Let  $X$ , be a non-empty and  $\mathcal{G} \subseteq X$ . We need to show that  $\mathcal{G}$  satisfies the properties of a soft filter:

1.  $\mathcal{G}$  is non-empty: since  $\beta$  is non-empty, there exists at least one subset  $A$  in  $\beta$ . Since  $A$  is a non-empty subset of  $X$ , it must contain at least one element. Therefore,  $\mathcal{G}$  is non-empty.
2. Any subset of  $X$  that contains an element of  $\mathcal{G}$  is also an element of  $\mathcal{G}$ : let  $B$  be a subset of  $X$  that contains an element of  $\mathcal{G}$ . This means that there exists an element  $G$  in  $\beta$  such that  $G$  is a subset of  $B$ . Since  $G$  is a member of  $\beta$ , it satisfies the conditions of  $\beta$ . Therefore,  $B$  also contains at least one element of  $\beta$ , making it a member of  $\mathcal{G}$ .
3. The intersection of any two members of  $\mathcal{G}$  is also a member of  $\mathcal{G}$ : let  $D \& E$  be two members of  $\mathcal{G}$ . This means that there exist elements  $N \& M$  in  $\beta$  such that  $N \cap D \& M \subseteq E$ . Since  $\beta$  satisfies the condition that the intersection of any two members contains a member of  $\beta$ , the intersection of  $N \& M$  is a non-empty subset of  $X$ . Let us call this intersection  $H$ . Since  $H$  is a non-empty subset of  $X$ , &  $H$  is contained in both  $D \& E$ , then  $H$  is an element of  $\mathcal{G}$ . Therefore,  $\mathcal{G}$  satisfies all the properties of a soft filter on  $X$ .

**Definition 3.4** Let  $A \& B$  be two sets on  $X$  satisfying conditions  $\beta_1 \& \beta_2$ . We call them base of soft filters they generate. We consider two bases equivalent, if they generate the same soft filter.

**Remark 3.2** Let  $A$  be a subset of soft filter  $\mathcal{F}$ . Then the set  $\beta$  of finite intersections of members of  $A$  is a base of soft filter  $\mathcal{F}$ .

**Proposition 3.12** A subset  $\beta$  of a soft filter  $\mathcal{F}$  on  $X$  is a base of  $\mathcal{F}$  if every member of  $\mathcal{F}$  contains a member of  $\beta$ .

**Proof** Let  $\mathcal{F}$  be a soft filter on a set  $X$ , and let  $\beta$  be a subset of  $\mathcal{F}$ . To prove this, we need to show two conditions:

1. Every member of  $\beta$  is also a member of  $\mathcal{F}$ : since  $\beta$  is a subset of  $\mathcal{F}$ , every member of  $\beta$  is also a member of  $\mathcal{F}$ . This ensures that the members of  $\beta$  are contained in  $\mathcal{F}$ .
2. For every element  $A$  in  $\mathcal{F}$ , there exists an element  $B$  in  $\beta$  such that  $B$  is contained in  $A$ : given any element  $A$  in  $\mathcal{F}$ . We know that  $A$  is a member of  $\mathcal{F}$  and thus, by the given condition,  $A$  contains a member of  $\beta$ . Let denote this member as  $B$ . Since  $B$  is a member of  $\beta$  and  $\beta$  is a subset of  $\mathcal{F}$ ,  $B$  is also a member of  $\mathcal{F}$ . Moreover, since  $A$  contains  $B$ , it follows that  $B$  is contained in  $A$ . Therefore, for every element  $A$  in  $\mathcal{F}$ , there exists an element  $B$  in  $\beta$  such that  $B$  is contained in  $A$ . By satisfying both conditions, we can conclude that  $\beta$  is indeed a base of the soft filter  $\mathcal{F}$ .

**Proposition 3.14** On a set  $X$ , a soft filter  $\mathcal{F}$  with base  $\beta$  is a finer than a soft filter with base  $\beta$  if every member of  $\beta$  contains a member of  $\beta$ .

**Proof** Let us consider an element  $x$  in  $\mathcal{F}$ . By definition of a soft filter with base  $\beta$ , there exists a member  $y$  in  $\beta$  such that  $y$  is a subset of  $x$ . Now, since every member of  $\beta$  contains a member of  $\beta$ , there exists a member  $z$  in  $\beta$  such that  $z$  is a subset of  $y$ . Since  $y$  is a subset of  $x$  and  $z$  is a subset of  $y$ , it follows that  $z$  is a subset of  $x$ . Hence, every element in  $\mathcal{F}$  is also in  $\mathcal{F}$ , which implies that  $\mathcal{F}$  with base  $\beta$  is finer than  $\mathcal{F}$  with base  $\beta$ .

**Proposition 3.15** Two soft filter bases  $\beta$  and  $\beta$  on a set  $X$  are equivalent if every member of  $\beta$  contains a member of  $\beta$  and every member of  $\beta$  contains a member of  $\beta$ .

**Proof** Let us consider an element  $x$  in the soft filter  $\mathcal{F}$  with base  $\beta$ . By definition of a soft filter with base  $\beta$ , there exists a member  $y$  in  $\beta$  such that  $y$  is a subset of  $x$ . Since every member of  $\beta$  contains a member of with base  $\beta$ , there exists a member  $z$  in  $\beta$  such that  $z$  is a subset of  $y$ . Now, let us consider an element  $x$  in the soft filter  $\mathcal{F}$  with base  $\beta$ . By definition of a soft filter with base  $\beta$ , there exists a member  $y$  in  $\beta$  such that  $y$  is a subset of  $x$ . Since every member of  $\beta$  contains a member of  $\beta$ , there exists a member  $z$  in  $\beta$  such that  $z$  is a subset of  $y$ . From the above, we can conclude that for every element in  $\mathcal{F}$  there exists an element in  $\mathcal{F}$  that is a subset of it, and for every element in  $\mathcal{F}$ , there exists an element in  $\mathcal{F}$  that is a subset of it. Therefore, the soft filters with bases  $\beta$  and  $\beta$  are equivalent.

#### 4. SOFT ULTRAFILTER

**Definition 4.1** A soft ultrafilter on a set  $X$ , is a soft filter  $\mathcal{F}$  such that for any soft filter  $\mathcal{F}$  on  $X$ , if  $\mathcal{F}$  is strictly finer than  $\mathcal{F}$ , then  $\mathcal{F} = \mathcal{F}$ .

**Definition 4.2** A soft ultrafilter on a set  $X$ , is a soft filter  $\mathcal{F}$  such that there is no soft filter on  $X$  which is strictly finer than  $\mathcal{F}$ .

**Theorem 4.1** Let  $\mathcal{F}$  be any soft ultrafilter on a set  $X$ , then there exists a soft ultrafilter other than  $\mathcal{F}$ .

**Proof** Assume that  $\mathcal{F}$  is a soft ultrafilter on  $X$ . Let  $\mathcal{F}$  be the all subsets  $A$  of  $X$  such that  $A^c$  is in  $\mathcal{F}$ , then there exists a non-empty set  $G$ , which is a complement of the empty set, i.e.,  $X \in \mathcal{F}$ . Now, we will show that  $\mathcal{F}$  satisfies the three conditions required for a soft filter to an ultrafilter: finiteness, upward closure and downward closure.

**Condition 1:** Since,  $\mathcal{F}$  is a soft ultrafilter,  $\mathcal{F}$  does not contain the empty set, and it is closed under finite intersections and supersets. Let us assume that there

exists a finite collection  $\Omega$  of subsets of  $X$  such that each element in  $\Omega$  or their complements is not in  $\mathcal{F}$ . We can consider the intersection of all sets in  $\Omega$ , denoted as  $A = \bigcap(\Omega)$ . Since  $\Omega$  is a finite collection,  $A$  is a finite intersection of subsets of  $X$ . If  $A$  is in  $\mathcal{F}$ , then  $A^c$  is also in  $\mathcal{F}$  (as  $\mathcal{F}$  is an ultrafilter). Since each set in  $\Omega$  or their complements is not in  $\mathcal{F}$ ,  $A$  or  $A^c$  is not in  $\mathcal{F}$ , leading to a contradiction. Therefore, the assumption that such a finite collection  $\Omega$  exists is false, and  $\mathcal{F}$  satisfies the finiteness condition.

**Condition 2:** Let  $A$  be a subset of  $X$  such that  $A$  is in  $\mathcal{F}$  and  $B$  is a subset of  $X$  such that  $B$  is a superset of  $A$ . Since  $A$  is in  $\mathcal{F}$ ,  $A^c$  is in  $\mathcal{F}$  (by definition of  $\mathcal{F}$ ). Since  $B$  is a superset of  $A$ ,  $B^c$  is a subset of  $A^c$ , by the upward closure property of  $\mathcal{F}$  (as it is an ultrafilter), if  $A^c$  is in  $\mathcal{F}$ , then  $B^c$  is also in  $\mathcal{F}$ . Therefore,  $B$  is in  $\mathcal{F}$ , satisfying the upward closure condition.

**Condition 3:** Let  $A$  be a subset of  $X$  such that  $A$  is in  $\mathcal{F}$  and  $B$  is a subset of  $X$  such that  $B$  is a subset of  $A$ . Since  $A$  is in  $\mathcal{F}$ ,  $A^c$  is in  $\mathcal{F}$  (by definition of  $\mathcal{F}$ ). By the downward closure property of  $\mathcal{F}$  (as it is ultrafilter) if  $A^c$  is in  $\mathcal{F}$ , then  $B^c$  is also in  $\mathcal{F}$ . Therefore,  $B$  is in  $\mathcal{F}$ , satisfying the downward closure condition. From conditions 1, 2&3, we conclude that  $\mathcal{F}$  is a soft filter on  $X$ .

Now, let us verify that  $\mathcal{F}$  is an ultrafilter.  $\mathcal{F}$  does not contain the empty set because  $X$  is not in  $\mathcal{F}$ ,  $\mathcal{F}$  is proper because it contains all complements of sets in  $\mathcal{F}$ . Since  $\mathcal{F}$  satisfies the definition of a soft ultrafilter, it is an ultrafilter. As we have constructed a soft ultrafilter  $\mathcal{F}$  other than  $\mathcal{F}$ .

**Example 4.1** Let  $X = \{1,2,3,4\}$  and the soft filters  $\mathcal{F} = \{\emptyset, X, \{1,2\}, \{1,3\}, \{2,4\}, \{3,4\}\}$ , and  $\mathcal{F} = \{\emptyset, X, \{1,2\}, \{3,4\}\}$ , we note that every element of  $\mathcal{F}$  is also an element of  $\mathcal{F}$ , but  $\mathcal{F}$  strictly contains a subset of  $\mathcal{F}$ . Therefore,  $\mathcal{F}$  is a soft filter that is finer than  $\mathcal{F}$ .

**Proposition 4.1** Let  $\mathcal{F}$  be a soft ultrafilter on a set  $X$ . If  $A$  &  $B$  are two soft subsets, such  $A \cup B \in \mathcal{F}$ , then  $A \in \mathcal{F}$  or  $B \in \mathcal{F}$ .

**Proof** Suppose  $\mathcal{F}$  is a soft ultrafilter on  $X$ , and let  $A$  &  $B$  be two soft subsets of  $X$  such  $A \cup B \in \mathcal{F}$ , we will show that either  $A \in \mathcal{F}$  or  $B \in \mathcal{F}$ .

Case 1:  $A \cup B \in \mathcal{F}$  & neither  $A$  nor  $B \in \mathcal{F}$  leads to a contradiction because  $\mathcal{F}$  is a soft ultrafilter, and by definition it is closed under finite intersections. Let us consider that the intersection of the complements of  $A$  &  $B$  denoted as  $A^c$  &  $B^c$ , respectively. Since neither  $A$  nor  $B \in \mathcal{F}$ , it follows that  $A^c$  &  $B^c$  are not in  $\mathcal{F}$ . According to the definition of a soft ultrafilter, if  $\mathcal{F}$  is closed under finite intersections, that the intersection of  $A^c$  &  $B^c$  denoted as  $A^c \cap B^c = (A \cup B)^c$ , must also be

in  $\mathcal{F}$ . Since the empty set does not belong to  $\mathcal{F}$  (as  $\mathcal{F}$  is proper), this leads to a contradiction. Therefore, our assumption that neither  $A \in \mathcal{F}$  nor  $B \in \mathcal{F}$  must be incorrect.

Case 2: Either  $A \in \mathcal{F}$  nor  $B \in \mathcal{F}$ . Assuming  $A \cup B \in \mathcal{F}$  and either  $A \in \mathcal{F}$  nor  $B \in \mathcal{F}$  holds true based on the logical negation of case 1. In other words, if neither  $A \in \mathcal{F}$  nor  $B \in \mathcal{F}$ , so  $A^c \cap B^c$  would belong to  $\mathcal{F}$ , leading to a contradiction. Hence,  $A \in \mathcal{F}$  or  $B \in \mathcal{F}$ .

**Corollary 4.1** Let  $\mathcal{F}$  be a soft ultrafilter on a set  $X$ , and let  $(F_i)_{i \in I}$  be a finite sequence of soft sets in  $X$ , if  $\bigcup_{i \in I} F_i \in \mathcal{F}$ , then at least one of the  $F_i \in \mathcal{F}$ .

**Proof** Suppose that  $\mathcal{F}$  is a soft ultrafilter on  $X$ , let  $F_i$  be a finite sequence of soft sets in  $X$ . Suppose that  $\bigcup_{i \in I} F_i \in \mathcal{F}$ . Suppose that none of the sets in  $F_i$  belong to  $\mathcal{F}$ . Since none of the sets in  $F_i \in \mathcal{F}$ , their complements  $(F_i)^c$  must be belong to  $\mathcal{F}$ . By the definition of soft ultrafilter, if  $\mathcal{F}$  is closed under finite intersections, then the intersection of the complements of the sets in  $F_i$ , denoted by  $\bigcap (F_i)^c$  must also belong to  $\mathcal{F}$ . However,  $\bigcap (F_i)^c = (\bigcup F_i)^c$  which is the complement of the union of all the sets in  $F_i$ . Since we assumed that  $\bigcup F_i \in \mathcal{F}$ , it follows that  $(\bigcup_{i \in I} F_i)^c$  does not belong to  $\mathcal{F}$ . This contradicts the fact that  $\bigcap (F_i)^c$  must also belong to  $\mathcal{F}$ . Therefore, our assumption that none of the sets in  $F_i$  belong to  $\mathcal{F}$  must be incorrect, Hence at least one of the sets in  $F_i$  belong to  $\mathcal{F}$ , as stated in the theorem.

**Definition 4.3** Let  $A$  be a soft set in a set  $X$ . If  $U$  is any soft set in  $X$ , then the soft set  $A \cap U$  is called trace of  $U$  on  $A$ , and it is denoted by  $U_A$ . For all soft sets  $U$  &  $V$  in  $X$ , we have  $(U \cap V)_A = U_A \cap V_A$ .

**Definition 4.4** Let  $A$  be a soft set in a set  $X$ . Then the set  $\Lambda_A$  of traces  $A \in \mathcal{F}^X$  of member of  $\Lambda$  is called the trace of  $\Lambda$  on  $A$ .

**Definition 4.5** Let  $A$  be a soft set in a set  $X$ , and let  $\Lambda$  be any soft set in  $X$ . The set of traces denoted by  $\Lambda_A$ , consists of all members of  $\Lambda$  for which the intersection with  $A$  is non-empty. In other words,  $\Lambda_A$  is the set of all elements in  $\Lambda$  that have a non-empty intersection with  $A$ .

**Definition 4.6** Let  $\mathcal{F}$  be a soft filter on a set  $X$ , and  $A \in \mathcal{F}^X$ . If  $\mathcal{F}_A$  is trace of  $\mathcal{F}$  on  $A$ , then  $\mathcal{F}_A$  is said to be induced by  $\mathcal{F}$  &  $A$ . Note that: the trace of a soft filter  $\mathcal{F}$  on  $A$  is the set of all elements  $x \in X$  such that every soft set  $U \in \mathcal{F}$  contains  $x$  whenever it contains  $A$ . Mathematically, it can be written as  $\mathcal{F}_A = \{x \in X: \forall U \in \mathcal{F}, A \subseteq U \xrightarrow{yields} x \in U\}$ .

**Proposition 4.2** Let  $\mathcal{F}$  be a soft filter on a set  $X$  inducing a soft filter  $\mathcal{G}_A$  on  $A \in \mathcal{F}^X$ , then the trace  $\beta_A$  on  $A$  of a base  $\beta$  of  $\mathcal{F}$  is a base of  $\mathcal{G}_A$ .

**Example 4.2** Let  $X = \{1,2,3\}, \mathcal{F} = \{\emptyset, X, \{1,2\}, \{1,3\}, \{2,3\}\}$ , &  $A = \{1,2\}$ , then the soft filter induced on  $A$  by  $\mathcal{F}$  is  $\mathcal{G}_A = \{\emptyset, X, \{1,2\}\}$ . Now take a base for  $\mathcal{F}$  as  $\beta = \{\{1,2\}, \{2,3\}\}$  and the trace of  $\beta$  is  $\beta_A = \{\{1,2\} \cap A, \{2,3\} \cap A\} = \{\{1,2\}, \{2\}\}$ . If we examine  $\mathcal{G}_A$  the soft filter induced on  $A$ , the trace  $\beta_A = \{\{1,2\}\}$  is not a base for  $\mathcal{G}_A$  under  $A$  since it does not satisfy the properties of being non-empty sets, and closed under finite intersection.

## 5. CONCLUSION

The study highlights the significance of soft topological spaces in dealing with uncertainty and their potential applications in various fields. The results of this research demonstrate the importance of soft filters in soft topological spaces and their research demonstrates the relationship with  $\tau$ -convergent and  $\tau$ -Hausdorff soft topological spaces. The findings of this study open up avenues for further research on soft topological spaces and their connections with other topological spaces. The most important expected outcomes of this study are the following:

1. A deeper understanding of soft topological spaces and their properties.
2. Insights into the relationship between soft filters and  $\tau$ -convergent and  $\tau$ -Hausdorff soft topological spaces.
3. Contributions to the development of soft mathematical concepts and structures.
4. Identification of potential applications of soft topological spaces in various fields.

## 6. REFERENCES

1. Al-Fatlawee I J. On  $\theta$ -convergent filters in Bi-topological spaces. University of Al-Qadisiya: College of Computer Sciences and Mathematics, Department of Mathematics; 2017.
2. Aygunoglu A, Aygun H. Some notes on soft topological spaces. Neural Computers and Applications 2012; 21:113-119.  
<https://link.springer.com/article/10.1007/s00521-011-0722-3>
3. Chiney M, Samanta SK. Vector soft topology. Ann. Fuzzy Math. Inform. 2015 Jul;10(1):45-64.
4. Cagman N, Karatas S, Enginoglu S. Soft topology. Computers and Mathematics with Applications 2011; 62:351-358.  
<https://doi.org/10.1016/j.camwa.2011.05.016>
5. Das S, Samanta S K. Soft real sets, soft real numbers and their properties, Journal of Fuzzy Mathematics 2012;20:551-576.

6. Das S, Majumdar P, Samanta S K. On soft linear spaces and soft normed linear spaces. *Ann. Fuzzy Mathematics Information* 2015; (9):91-109.
7. Sharma J N. *Topology*. Published by Krishna Pracushna, Mandir and printed at Mano; 1977.
8. Kharal A, Ahmad B. Mappings on soft classes. *New Mathematics Nat. Computer* 2011;7(3): 471- 481.  
<https://doi.org/10.1142/S1793005711002025>
9. Nazmul S. K, Samanta S K. Group Soft Topology. *Journal of Fuzzy Mathematics* 2014; 22:435-450.
10. Nazmul S K, Samanta S K. Some properties of soft topologies and group soft topologies. *Annals of Fuzzy Mathematics and Information* 2014; 8(4):645-661.
11. Ozturk T Y, Bayramov S. Soft mapping spaces. *The Scientific World Journal*, Article ID 307292, 2014; (8).  
<https://doi.org/10.1155/2014/307292>
12. Martin M K. On 3-topological version of  $\theta$ -regularity. *Hindawi Publishing Corp International Journal Mathematics Sciences* 1988; 23(6):393-398.
13. Sheik John M, Suraiya Begum M. Soft topological vector spaces in the view of soft filters. *Global Journal of Pure and Applied Mathematics* 2017;13(7):4075-4085.  
<http://www.ripublication.com/gjpam.htm>
14. Maji P K, Biswas R, Roy A R. An application of soft sets in a decision-making problem. *Computers and Mathematics with Applications* 2002; 44:1077-1083.  
[https://doi.org/10.1016/S0898-1221\(02\)00216-X](https://doi.org/10.1016/S0898-1221(02)00216-X)
15. Maji P K, Biswas R, Roy A R. Soft set theory. *Computers and Mathematics with Applications* 2003;45(4-5):555-562.  
[https://doi.org/10.1016/S0898-1221\(03\)00016-6](https://doi.org/10.1016/S0898-1221(03)00016-6)
16. Molodtsov D. Soft set theory-first results. *Computers and Mathematics with Applications* 1999;37(4-5):19-31.  
[https://doi.org/10.1016/S0898-1221\(99\)00056-5](https://doi.org/10.1016/S0898-1221(99)00056-5)
17. Shabir M, Naz M. On soft topological spaces, *Computers and Mathematics with Applications* 2011;61(17):1786-1799.  
<https://doi.org/10.1016/j.camwa.2011.02.006>
18. Hussain S, Ahmad B. Some properties of soft topological spaces. *Computers and Mathematics with Applications* 2011;62(11):4058-4067.  
<https://doi.org/10.1016/j.camwa.2011.09.051>
19. Zadeh L A. Fuzzy sets. *Information control* 1965;(8):338-353.  
[http://dx.doi.org/10.1016/S0019-9958\(65\)90241-X](http://dx.doi.org/10.1016/S0019-9958(65)90241-X)

مجلة جامعة بنغازي العلمية

# Medical Sciences



SJUOB



## Knowledge, Attitude, and Practices Regarding Safe and Hygienic Food among Food Handlers in some Benghazi Hospitals

Sara Ahmed Elsherif <sup>1\*</sup> - Aya Abdallah Mohammed <sup>1</sup> - Budor Omar Mansor <sup>1</sup> - Manar Wanis Elbarghathi <sup>1</sup> - Najwa Faraj Elmodabel <sup>1</sup>.

*1 Nutrition department - Public Health - University Of Benghazi.*

Received: 19 / 02 / 2024; Accepted: 09 / 05 / 2024

### ABSTRACT

**Background:** In the healthcare sector, hospitals play a pivotal role in patient care, with food services being a vital component.

**Aim:** This study focused on the knowledge, attitudes, and practices (KAP) of food handlers in some hospitals in Benghazi, Libya, who are instrumental in preventing foodborne illnesses through proper food safety and hygiene.

**Methods:** A descriptive study of a cross-sectional design was conducted in Benghazi, the research assessed 70 food handlers from Benghazi Medical Center, Benghazi Children's Hospital, and Dar-Alshifa Hospital, aged 18 to 48 years. Data was collected via interviews using a questionnaire covering socio-demographic information and KAP-related questions.

**Results:** The participants, encompassing various roles such as waiters, cooks, nutritionists, and cleaners, mostly had 1-5 years of experience, with 58.6% having undergone prior training. Despite a generally positive attitude towards food safety, the study uncovered a deficiency in food hygiene knowledge. However, practices for periodic analysis were commendably executed. Further scrutiny indicated that knowledge levels regarding hygiene and sanitation did not significantly differ among food handlers based on age, gender, occupation, education, experience, training, or hospital type.

**Conclusion:** The findings suggest that while the attitude towards food safety is commendable, there is an imperative need to enhance the food handlers' knowledge of hygiene. This improvement is crucial for ensuring the implementation of safe and hygienic food handling practices within hospital settings, thereby safeguarding patient health against foodborne diseases.

**KEYWORDS:** Food Safety, Food Hygiene, Food Safety Knowledge, Attitude, Practice, Food Handlers.

### 1. INTRODUCTION

Food hygiene is a set of practices and conditions that are necessary to ensure food safety throughout the entire food supply chain from production to consumption. Food contamination can occur at any stage of the process, including during slaughter or harvesting, processing, storage, distribution, transportation, preparation, and handling <sup>1</sup>.

Food handlers are individuals who handle unpackaged food and beverages and are involved in various activities such as preparation, manufacturing, serving, testing, and packaging of food and beverages. Food handlers must use appropriate hygiene measures when handling food to prevent the spread of foodborne illnesses <sup>2</sup>.

Food handlers play a crucial role in the transmission of foodborne pathogens, particularly through contaminated food and from raw meat to prepared-to-consume meals. Food handlers can carry human-specific foodborne pathogens such as Hepatitis A, noroviruses, Salmonella, Staphylococcus aureus, and Shigella species on their fingers, cuts, sores, mouth, skin, and hair, which can then be transmitted to food <sup>3</sup>.

Data indicates that foodborne illnesses are prevalent worldwide. However, due to limitations in surveillance systems, only a small proportion of actual cases are reported. Estimates suggest that approximately 600 million people worldwide fall ill from consuming contaminated food annually, with diarrheal diseases being the most common form of these illnesses. It has been reported that foodborne illnesses cause up to 70% of diarrheal sickness in developing countries. This is due in part to a lack of personal hygiene and food safety measures among food handlers <sup>4</sup>.

Hospital food hygiene is critical in ensuring the health of patients. Studies have shown that incorrect practices and lack of knowledge among food handlers are contributing

\*Correspondence: Sara Ahmed Elsherif.

[sara.elsherif@uob.edu.ly](mailto:sara.elsherif@uob.edu.ly)

factors to foodborne illnesses, which remain a common problem in healthcare settings. Food poisoning is a condition caused by the ingestion of food contaminated with pathogenic microorganisms or toxins produced by such microorganisms in sufficient amounts to cause pathological conditions. Studies have linked lack of knowledge and poor handling of food as a major cause of food poisoning; The knowledge, attitudes, and practices (KAP) of food handlers have been identified as having a significant impact on the incidence of food poisoning <sup>5,6,7,8</sup>.

A cross-sectional study was conducted between January and June 2020 to assess the food safety knowledge (FSK) of food handlers (FHs) in hospitals' food services in Amman, Jordan. The study included 264 FH participants and found that the overall FSK was moderate. The study recommends additional food safety training in specific areas, including food handling operations and foodborne pathogens <sup>4</sup>.

a cross-sectional study conducted at a psychiatric hospital in Magelang, Central Java Province, Indonesia, the researchers investigated the knowledge, attitude, and practice of hygiene and sanitation among 37 food handlers. The findings revealed that while knowledge and attitude were generally positive (with 89% having good knowledge and 84% exhibiting a positive attitude), more than one-third (38%) of food handlers had poor hygiene and sanitation practices. Surprisingly, there were no significant correlations between knowledge, attitude, and practice, indicating that knowledge did not necessarily translate into better practices. Additionally, the majority (73%) of food handlers had never received formal training related to hygiene and sanitation, which significantly impacted their practices. In conclusion, addressing this gap between knowledge and practice is crucial for improving food safety among hospital food-handlers <sup>9</sup>.

A cross-sectional descriptive study was conducted in governmental hospitals affiliated with Daqahlia Governorate, Egypt, to assess the knowledge, attitude, and practices of food handlers regarding safe and hygienic food in Egyptian government hospitals. The study involved 542 food handlers, and the findings showed that the overall knowledge, attitude, and practices of food handlers were less than half of what they should be. Based on the findings of the study, there was a strong correlation between food handlers' knowledge, attitude, and practices, which suggests that improving one of these factors may lead to improvements in the others. Therefore, the study recommends that educational and training programs be implemented to improve food handlers' knowledge, attitudes, and practices. To achieve this goal, the study suggests that community health nurses use a variety of teaching methods and modes to ensure that the training is effective <sup>10</sup>.

Hospitals serve a significant population, including patients, doctors, nurses, and visitors, and the hospital

kitchen produces a large amount of ready-to-eat food that is particularly susceptible to contamination. Thus, food handlers play a critical role in preventing food poisoning and promoting food safety. They must ensure that food preparation, processing, and serving meet hygienic standards. However, it is essential to acknowledge that food handlers may carry various foodborne pathogens, which can pose health risks to others.

The purpose of this research was to evaluate the knowledge, attitude, and practice of hospital food handlers about safe and hygienic food; it also aimed to explore the potential association between the hospital category and the employees' knowledge as well as to explore if individual characteristics influence their awareness about food safety.

## 2. METHODOLOGY:

### *Designs:*

A cross-sectional descriptive study was utilized to conduct this study.

### *Setting:*

The study was carried out at Benghazi Medical Center (BMC), Benghazi Children's Hospital, and Dar-Alshifa Hospital.

### *Study Period:*

The Data of the study was collected between February 2023 and June 2023.

### *Study Participants:*

All food handlers who worked at the three hospitals, including cooks, cleaners, waiters, and nutritionists, were recruited for the study. The study involved 70 food handlers who were available during data collection and willing to participate in the study.

### *Study tools and methods of data collection:*

To assess the knowledge, attitude, and practices of food handlers in food preparation and safety, direct face-to-face interviews were conducted. A self-administered questionnaire for this study was prepared based on the questionnaires used in studies undertaken in Italy, and Turkey<sup>(24,22)</sup>; consisting of 25 multiple-choice questions, which were divided into four sections. The first section of the questionnaire comprised seven questions that focused on the demographic information of the participants, including gender, age, type of employment, educational level, number of years of service, previous training, and hospital sector. The second section of the questionnaire was designed to test the participants' knowledge of food safety in hospital kitchens, and it included nine questions. The third section focused on the attitudes of food handlers toward food safety. Finally, the fourth section assessed the practices of food handlers related to food safety, and it included six questions

### *Statistical Analysis:*

The gathered data were organized, encoded, and processed using IBM SPSS Statistics for Windows, Version 21. Descriptive statistical measures such as frequency and percentage were computed for all pertinent variables. Additionally, the chi-square test was employed to assess the statistical significance of relationships between various variables, with a threshold for significance set at ( $P < 0.05$ ).

**Ethical consideration:**

Before conducting the study, ethical approval was obtained from the Faculty of Public Health, Benghazi Medical Centre, Dar-Alshifa, and Benghazi Children’s Hospital. In addition, informed consent was obtained from food handlers before administering the questionnaires.

**3. RESULTS**

**Demographic Characteristics**

In this study, participants were 70 food handlers from three hospitals in Benghazi. Specifically, there were 24 from Dar-Alshifa, 27 from Benghazi Medical Centers, and 19 from Benghazi Children’s Hospital. The gender distribution among the surveyed food handlers was 39 males and 31 females. The participants held various occupations: 24 were waiters, 23 were cooks, 9 were nutritionists, and 14 were cleaners. The age range of the participants was 18 to >48 years, with the majority falling between 18 and 38 years, followed by those aged between 38 and 48. In terms of education, 34.3% (n=24) had less than a high school education, 42.9% (n=30) held a high school certificate, and 22.9% (n=16) were BSc certified. Their employment experience varied from 1 to 20 years, with the majority having 1 to 5 years of experience. Additionally, 58.6% of the participants received previous training, and most of them worked in the public sector (66%), (see Table 1).

Table 1 provides details of the demographic profile for each hospital included in the study. The BMC had the largest number of participants (n=27), followed by Dar Al Shifa (n=24). The pediatric hospital had 19 participants. Notably, Dar-Alshifa is the only private-sector hospital in this study. The highest age group of employees who participated in the study were aged 38-48 years for BMC, 28-38 years for the Benghazi Children’s Hospital, and 18-28 years for Dar Al Shifa, constituting 37.3%, 36.8%, and 37.5%, respectively. The table also reveals that 55.6%, 75.9%, and 54.2% of the participants in BMC, Benghazi Children’s Hospital, and Dar Al Shifa hospitals were male. Among the food handlers, 51.9% worked as waiters in BMC, 36.8% worked as cleaners in Benghazi Children’s Hospital, and 41.7% worked as cooks in Dar-Alshifa.

Regarding education, 48.1% of participants in BMC had a secondary degree, 42.1% had a basic degree in pediatric hospital employment, and 45.8% had a secondary degree of employment in Dar-Alshifa. According to (Table 1) Examining employment experience, 40.7% of BMC participants had 6-10 years of experience, whereas 63.2% and 62.5% of those in the Benghazi Children’s Hospital and Dar-Alshifa Hospital, respectively, had 1-5 years of experience. Additionally, 51.9%, 36.8%, and 83.3% of food handlers received training in BMC, Pediatric, and Dar-Alshif Hospital, respectively.

**Table 1. Sociodemographic & Setting States Overview (n=70)**

	Hospitals No (%)			Total No (%)	
	Dar-Alshifa	BMC	Benghazi Children’s		
<b>Sample size</b>	24 (34.3)	27 (38.6)	19 (27.1)	70 (100)	
<b>Variables</b>					
<b>Age</b>	<b>18 - 28</b>	9 (37.5)	5 (18.5)	8 (42.1)	22 (31.4)
	<b>28 - 38</b>	6 (25.0)	9 (33.3)	7 (36.8)	22 (31.4)
	<b>38 - 48</b>	5 (20.8)	10 (37.0)	3 (15.8)	18 (25.7)
	<b>&gt;48</b>	4 (16.7)	3 (11.1)	1 (5.3)	8 (11.4)
<b>Sex</b>	<b>Male</b>	13 (54.2)	15 (55.6)	11 (57.9)	39 (55.7)
	<b>female</b>	11 (45.8)	12 (44.4)	8 (42.1)	31(44.3)
<b>Occupation</b>	<b>cooker</b>	10 (41.7)	7 (25.9)	6 (31.6)	23 (32.9)
	<b>cleaner</b>	5 (20.8)	2 (7.4)	7 (36.8)	14 (20.0)
	<b>Waiter</b>	5 (20.8)	14 (51.9)	5 (26.3)	24 (34.3)
	<b>Nutritionist</b>	4 (16.7)	4 (14.8)	1 (5.3)	9 (12.9)
<b>Education</b>	<b>Basic</b>	7 (29.2)	9 (33.3)	8 (42.1)	24 (34.3)
	<b>Secondary</b>	11 (45.8)	13 (48.1)	6 (31.6)	30 (42.9)
	<b>Higher</b>	6 (25.0)	5 (18.5)	5 (26.3)	16 (22.9)
<b>Years of experience</b>	<b>1 – 5</b>	15 (62.5)	7 (25.9)	12 (63.2)	34 (48.6)
	<b>6 - 10</b>	2 (8.3)	11 (40.7)	5 (26.3)	18 (25.7)
	<b>11 - 15</b>	5 (20.8)	7 (25.9)	1 (5.3)	13 (18.6)
	<b>16 - 20</b>	2 (8.3)	2 (7.4)	1 (5.3)	5 (7.1)
<b>Previous training</b>	<b>No</b>	4 (16.7)	13 (48.1)	12 (63.2)	29 (41.4)
	<b>Yes</b>	20 (83.3)	14 (51.9)	7 (36.8)	41(58.6)
<b>Hospital sector</b>	<b>Public</b>	-	27 (100)	19 (100)	46 (66)
	<b>Private</b>	24 (100)	-	-	24 (34)

**Respondent's Food Safety Knowledge**

Table 2 indicates that the majority of food handlers in the study had knowledge about the preparation of food in advance and how it can contribute to food poisoning and contamination, as well as the importance of wearing gloves (with 100% correct answers) in all three hospitals. Additionally, 86.4% of food handlers knew about proper cleaning, and 72.8% knew about detergent use.

In terms of foodborne disease transmission, the study found that 50% of food handlers in Dar-Alshifa and 40.7% in BMC were incorrect in believing that hepatitis B could be transmitted through food. However, in Benghazi Children's Hospital, 73.7% of respondents correctly recognized that hepatitis B can indeed be transmitted via food.

Additionally, 54.2%, 40.7%, and 73.7% of food handlers in Dar-Alshifa, BMC, and Benghazi Children's Hospital, respectively, were aware that cholera can also be transmitted through food. Notably, the highest percentage

of correct responses regarding food items associated with the transmission of *Vibrio cholera* was observed across all three hospitals (as indicated in Table 2).

This table presents the knowledge of food handlers regarding temperature and its impact on food safety (Table 2).

Among the participants at Dar-Alshifa, 45.8% correctly identified the appropriate refrigerator temperature as 8°C. In BMC, 40.7% of participants answered incorrectly or were unsure, while in Benghazi Children's Hospital, 68.4% of respondents provided the correct answer. However, across all three hospitals, most participants were unaware that cold ready-to-eat foods should be maintained at -11°C.

Additionally, food items associated with the transmission of *Vibrio cholera* were correctly identified by 50% of Dar-Alshifa participants, 48.1% of BMC participants, and 73.7% of Benghazi Children's Hospital respondents.

**Table 2. Assessment of Food Handlers' Safety Awareness**

Statements	Hospitals			
		Dar-Alshifa	BMC	Benghazi Children's Hospital
		N (%)	N (%)	N (%)
Preparation of food in advance is likely to contribute to food poisoning	Correct	21 (87.5)	18 (66.7)	19 (100)
	Incorrect	3 (12.5)	9 (33.3)	
	I don't know			
	<b>Total</b>	<b>24</b>	<b>27</b>	<b>19</b>
Reheating food is likely to contribute to food contamination	Correct	15 (62.5)	17 (63.0)	16 (84.2)
	Incorrect	6 (25.0)	10 (37.0)	3 (15.8)
	I don't know	3 (12.5)		
	<b>Total</b>	<b>24</b>	<b>27</b>	<b>19</b>
Wearing gloves while handling food minimizes the risk of transmitting the infection to food-service staff	Correct	24(100%)	27 (100)	19 (100)
	Incorrect			
	I don't know			
	<b>Total</b>	<b>24</b>	<b>27</b>	<b>19</b>
The correct temperature for a refrigerator is (8°C)	Correct	11 (45.8)	5 (18.5)	13 (68.4)
	Incorrect	7 (29.2)	11 (40.7)	4 (21.1)
	I don't know	6 (25.0)	11(40.7)	2 (10.5)
	<b>Total</b>	<b>24</b>	<b>27</b>	<b>19</b>
Hot ready to eat foods should be maintained at (40°C)	Correct	10 (41.7)	10 (37.0)	10 (52.6)
	Incorrect	10 (41.7)	11 (70.7)	4 (21.1)
	I don't know	4 (16.7)	6 (22.2)	5 (26.3)
	<b>Total</b>	<b>24</b>	<b>27</b>	<b>19</b>
Cold ready to eat foods should be maintained at (-11°C)	Correct	4 (16.7)	7 (25.9)	4 (21.1)
	Incorrect	17 (70.8)	13 (48.1)	11 (57.9)
	I don't know	3 (12.5)	7 (25.9)	4 (21.1)
	<b>Total</b>	<b>24</b>	<b>27</b>	<b>19</b>
Hepatitis B can be transmitted by food	Correct	9 (37.5)	8 (29.6)	14 (73.7)
	Incorrect	12 (50.0)	11 (40.7)	4 (21.1)
	I don't know	3 (12.5)	8 (29.6)	1 (5.3)
	<b>Total</b>	<b>24</b>	<b>27</b>	<b>19</b>
Cholera can be transmitted by food	Correct	13 (54.2)	11 (40.7)	14 (73.7)
	Incorrect	2 (8.3)	7 (25.9)	4 (21.1)
	I don't know	9 (37.5)	9 (33.3)	1 (5.3)
	<b>Total</b>	<b>24</b>	<b>27</b>	<b>19</b>
Food items associated with the transmission of <i>Vibrio cholera</i>	Correct	12 (50.0)	13(48.1)	14 (73.7)
	Incorrect	2 (8.3)	5 (18.5)	4 (21.1)
	I don't know	10 (41.7)	9 (33.3)	1 (5.3)
	<b>Total</b>	<b>24</b>	<b>27</b>	<b>19</b>

Table (3) conducted a chi-square test of independence P-value in the table indicates whether there is a statistically significant difference in knowledge levels across different hospitals. The test did not find a statistically significant difference in

knowledge levels across the different hospitals. In other words, the type or name of the hospital does not seem to affect the knowledge levels of the employees.

**Table 3. Hospital Knowledge Comparison Overview**

Hospitals	Classification of knowledge			Total	P –value
	Poor knowledge	Moderate knowledge	Good knowledge		
Dar-alshifa	10	13	1	24	0.221
	41.7%	54.2%	4.2%	100.0%	
BMC	10	15	2	27	
	37.0%	55.6%	7.4%	100.0%	
Benghazi Children’s Hospital	3	16	0	19	
	15.8%	84.2%	0.0%	100.0%	
Total	23	44	3	70	
	32.9%	62.9%	4.3%	100.0%	

\* (significant at p-value< 0.05).

**Food Safety Attitudes Of Food Handlers**

Table (4) regarding the attitudes of food handlers toward the prevention and control of foodborne diseases; The study examined the attitudes of food handlers across three hospitals concerning food safety practices. Notably, all respondents unanimously agreed that raw foods should be kept separate from cooked foods, demonstrating a 100% consensus on this crucial practice. Additionally, the majority of food handlers concurred that defrosted

food should not be refrozen. The agreement rates varied across hospitals: 70.8% in Dar-Alshifa, 74.1% in BMC, and a higher 84.2% in the Benghazi Children’s Hospital. Furthermore, findings emphasized the importance of hygiene: food handlers with abrasions or cuts on their fingers or hands should avoid touching unwrapped foods. Compliance rates were 83.3% in Dar-Alshifa, 96.3% in BMC, and a perfect 100% in Benghazi Children’s Hospital.

**Table 4. Food Safety Attitudes Among Handlers**

Respondent's food safety attitudes	Answer	Hospitals		
		Dar-Alshifa	BMC	Benghazi Children’s Hospital
		N (%)	N (%)	N (%)
Raw foods should be kept separate from cooked foods	No			
	Yes	24 (100)	27 (100)	19 (100)
	Uncertain			
<b>Total</b>		24	27	19
Defrosted food should not be refrozen	No	5 (20.8)	4 (14.8)	3 (15.8)
	Yes	17 (70.8)	20 (74.1)	16 (84.2)
	Uncertain	2 (8.3)	3 (11.1)	
<b>Total</b>		24	27	19
Food service staff with abrasions or cuts on their hands should not touch unwrapped food	No	4 (16.7)		
	Yes	20 (83.3)	26 (96.3)	19 (100)
	Uncertain		1 (3.7)	
<b>Total</b>		24	27	

**Food Safety Practices**

The study on self-reported hygienic practices among participants in three hospitals revealed several noteworthy trends. Firstly, most participants in these hospitals diligently wash their hands before and after handling unwrapped raw and cooked food, emphasizing the importance of this practice for preventing cross-contamination and maintaining food safety. Additionally, a significant number of food handlers in all three hospitals use separate kitchen utensils when preparing cooked and raw food, minimizing the risk of transferring harmful microorganisms between different food items.

However, when it comes to the practice of thawing frozen food at room temperature, there are variations across hospitals.

At Dar-Alshifa, 41.7% of food handlers reported always following this method.

In contrast, at BMC, the percentage was higher, with 74.1% answering always, while in Benghazi Children’s Hospital, 52.6% responded similarly. These findings underscore the need for consistent adherence to hygienic practices among food handlers, ensuring the well-being of both patients and staff see Table (5).

**Table 5. Food Safety Practices Among Handlers**

Respondent's food safety practices	Hospitals			
	Answer	Dar-Alshifa	BMC	Benghazi Children’s Hospital
		N (%)	N (%)	N (%)
Do you wash your hands before touching unwrapped raw food?	Always	23 (95.8)	19 (70.4)	19 (100)
	Often	1 (4.2)	5 (18.5)	
	Occasionally		3 (11.1)	
Total		24	27	19
Do you wash your hands after touching unwrapped raw food?	Always	22 (91.7)	20 (74.1)	18 (94.7)
	Often	1 (4.2)	4 (14.8)	1 (5.3)
	Occasionally	1 (4.2)	3 (11.1)	
Total			27	19
Do you wash your hands before touching unwrapped cooked food?	Always	22 (91.7)	19 (70.4)	18 (94.7)
	Often	1 (4.2)	5 (18.5)	1 (5.3)
	Occasionally	1 (4.2)	3 (11.1)	
Total		24	27	19
Do you wash your hands after touching unwrapped cooked food?	Always	22 (91.7)	18 (66.7)	18 (94.7)
	Often	1 (4.2)	5 (18.5)	1 (5.3)
	Occasionally	1 (4.2)	4 (14.8)	
Total		24	27	19
Do you use separate kitchen utensils to prepare cooked and raw food?	Always	19 (79.2)	17 (63.0)	14 (73.7)
	Often	5 (20.8)	7 (25.9)	5 (26.3)
	Occasionally		3 (11.1)	
Total		24	27	19
Do you thaw frozen food at room temperature?	Always	10 (41.7)	20 (74.1)	10 (52.6)
	Often	10 (41.7)	4 (14.8)	9 (47.4)
	Occasionally	2 (8.3)	3 (11.1)	
	No answer	2 (8.3)		
Total		24	27	9

**Individual Characteristics and Knowledge of Hygiene and Sanitation**

During the interview, several participants highlighted that individual characteristics could be linked to one’s hygiene knowledge. Subsequently, a more detailed analysis was conducted to explore the relationship between these individual traits

and the knowledge levels of food handlers. The findings summarized in Table 6 indicate that there is no significant difference in hygiene and sanitation knowledge across various individual characteristics, including (age, sex, occupation, education, years of experience, previous training, and hospital sector).

**Table 6. Individual Variability in Hygiene & Sanitation Knowledge**

Individual characteristic		Poor knowledge	Moderate knowledge	Good knowledge	Total	P-value
		No	No	No	No	
Age	18-28	7	14	1	22	0.579
	28-38	4	17	1	22	
	38-48	8	9	1	18	
	>48	4	4	0	8	
Sex	Male	13	24	2	39	0.916
	Female	10	20	1	31	
Occupation	cooker	7	15	1	21	0.656
	cleaner	5	9	0	14	
	Waiter	10	13	1	24	
	Nutritionist	1	7	1	9	
Education	Basic	8	13	2	23	0.117
	Secondary	15	17	12	44	
	Higher	1	0	2	3	
Years of experience	1 – 5	13	20	1	34	0.205
	6 - 10	5	13	0	18	
	11 - 15	2	9	2	13	
	16 - 20	3	2	0	5	
Previous training	Yes	15	24	2	41	0.672
	No	8	20	1	29	
Hospital sector	Public	13	34	2	49	0.211
	Private	10	10	1	21	

#### 4. DISCUSSION

The frequency of food poisoning outbreaks and related concerns is increasing, leading to demands for improved hygiene and quality practices. The European Commission has recognized the importance of limiting food poisoning outbreaks, particularly due to the rise in meals consumed outside the home and the availability of pre-prepared meals. This changing consumer behavior highlights the need for more effective food hygiene controls.<sup>10,11</sup>

According to statistics, caterers are responsible for the majority of food poisoning outbreaks compared to any other food industry, accounting for 70% of all bacterial food poisoning incidents. Inadequate time and temperature management of food accounts for 70% of food poisoning outbreaks, while cross-contamination is responsible for the remaining 30%<sup>8</sup>.

Indeed, the study aimed to assess the knowledge, attitudes, and practices of food handlers concerning safe and hygienic food preparation in Benghazi Medical Center, Dar-Alshifa, and Benghazi Children's Hospital.

Previous studies have suggested that inadequate knowledge of food safety can result in poor hygienic practices among food handlers<sup>12,13</sup>. However, Clayton *et al.*,<sup>14</sup> reported that 63% of food handlers demonstrated knowledge of food safety but did not exhibit a corresponding positive behavior towards food safety and hygiene practices. This finding contrasts with the present study, which showed good practice among food handlers despite moderate knowledge of food safety.

In a study conducted by Akabanda *et al.*,<sup>15</sup> the majority of food handlers demonstrated knowledge of the importance of general sanitary practices, such as wearing gloves (77.9% correct answers). This finding is consistent with the present study which also reported a high level of knowledge (100%) and another study conducted in Al Madinah Hospitals in Saudi Arabia which also found that all food handlers demonstrated knowledge regarding the importance of sanitary practices.

Food composition varies, and as a result, a single cooking temperature cannot ensure both the desired culinary quality and safety for all types of food. To inactivate pathogenic vegetative bacteria, different combinations of time and temperature are required; Temperature treatment is often the critical control point in the food production process, and a lack of understanding of temperature-related issues could significantly hinder the effective implementation of Hazard Analysis and Critical Control Points (HACCP)<sup>17</sup>.

According to the present study, a lack of knowledge existed among food handlers regarding acceptable refrigerator temperature ranges and the critical temperatures of hot ready-to-eat foods in Benghazi Children's Hospital (68.4%, 52.6%) and Dar-Alshifa hospitals (41.8%, 45.7%), as a significant proportion of food handlers provided incorrect answers; Similar findings have been reported in other studies. For instance, in a study conducted by (Baş M *et al.*, 2006) in Turkey, only 42% of food handlers knew the correct temperature for food storage. In addition, a study by (Walker *et al.*, 2003); found that less than half of the 444 food handlers surveyed knew the correct temperature of hot food holding.<sup>17,18</sup> Both the studies by Baş *et al.* in Turkey and Walker *et al.* reported a lack of knowledge regarding critical temperatures among food handlers, which is consistent with the findings of the present study conducted in Benghazi Children's Hospital and Dar-Alshifa hospitals; These studies highlight the importance of

improving food safety knowledge among food handlers to ensure the proper handling and preparation of food.

In a study conducted in a hospital in Turkey, 93.2% of food handlers considered that reheating food might contribute to food contamination, This finding corresponds to the result of the present study conducted in Benghazi Children's Hospital, where 84.2% of food handlers held the same belief<sup>19</sup>. These findings suggest that food handlers have an understanding of the risks associated with improper food handling practices, such as reheating, but further education and training may be necessary to ensure that food safety protocols are followed correctly.

The transmission of Hepatitis B, primarily through blood and body fluids rather than food, is a fact grasped by nearly half (50%) of the food handlers in Dar-Alshifa. Similarly, 40.7% of their counterparts at BMC are also aware of this truth. Intriguingly, these findings echo a prior study conducted in Turkish hospitals, where up to 41.1% of food handlers held the correct understanding of this matter<sup>19</sup>. This thread of knowledge, weaving its way through different cultures and countries, underscores the importance of accurate health awareness in the global community.

The majority of the food handlers in Dar-Alshifa, BMC Center, and Benghazi Children's Hospital (54.2%, 40.7, and 73.7%, respectively) knew that food could be a mode of cholera transmission. This finding is in line with a study in Turkey that reported a 64.4% rate of correct knowledge about food-borne cholera. The same study in Turkey also revealed that the percentage of food handlers who had good knowledge scores on hygiene and sanitation was 89.19%. This differed from the knowledge level of this study, which was only fair and had a low percentage of good knowledge<sup>19</sup>.

The findings of a study conducted in Pakistan were similar to this study's results regarding knowledge and attitudes but differed in practices<sup>20</sup>.

According to a report from Ghana, 96% of uncooked food was separated from cooked food, which is consistent with the current study. However, the current study had higher rates of separation in three hospitals (Dar-Alshifa, BMC Hospital, and Benghazi Children's Hospital), where 100% of food handlers followed this practice. The Ghana report also showed that 87.2% of food handlers agreed with the current study that unwrapped food should not be touched by staff with abrasions or cuts on their hands. However, Contrary to the current study, the Ghana study reported that only 30% of food handlers supported the idea that defrosted food should not be refrozen. Meanwhile, in Dar-Alshifa, BMC, and Children's Hospitals, (70.8%, 74.1%, and 84.2%) of food handlers, respectively, agreed with this statement<sup>15</sup>.

A study in a Brazilian hospital found that 41.0% of food handlers thawed frozen food at room temperature. This practice aligns with a recent study conducted at Dar-Alshifa Hospital, BMC, and Benghazi Children's Hospital, where 41.7%, 74.1%, and 52.6% of food handlers, respectively, consistently thawed frozen food at room temperature<sup>21</sup>.

A study conducted in a military hospital reported the food handling practices of food handlers, where almost all staff (94.5%) reported that they always wash their hands before preparing food. This finding is consistent with the results of the cur-

rent study, in Dar-Alshifa, BMC, and Benghazi Children's Hospital which reported rates of 95.8%, 70.4%, and 100%, respectively <sup>22</sup>.

There was no significant association ( $p > 0.05$ ) between having food hygiene/safety training and food knowledge in this study. However, a study conducted in Al-Madinah hospitals in Saudi Arabia found a significant association between respondents' training and food safety knowledge ( $p < 0.05$ ). al-Madinah hospital study reported a significant association between food safety knowledge and participant education level, which disagrees with the results of this study. However, this study's findings were consistent with the Al-Madinah hospital study regarding the association between food safety knowledge and years of experience. This study found no significant association ( $p \geq 0.05$ ) between years of experience in food service and food safety knowledge. This may be due to the advanced training tools that new staff are equipped with, which enable them to have better food safety knowledge regardless of their experience in the field <sup>23</sup>.

## 5. CONCLUSION:

Food handlers working in hospital food services had low to moderate levels of food safety knowledge, despite having satisfactory attitudes and practices. The study also revealed that there were no significant differences in knowledge levels among employees in the three hospitals, regardless of the type or name of the hospital. After examining different individual characteristics such as age, sex, occupation, education, years of experience, previous training, and hospital sector, it was concluded that there were no significant differences in hygiene and sanitation knowledge between different groups of food handlers.

To enhance food safety, it's crucial to conduct more research to improve food handlers' knowledge. Health awareness programs for producers and consumers, hygienic practices during food production, and regular training for food handlers are all recommended.

## 6. LIMITATIONS OF THE STUDY

One of the limitations of this study is that not all hospitals had kitchens to meet the needs of patients. Additionally, some hospitals refused to participate in the study, which limited the number of participants that could be included and may have impacted the generalizability of the findings.

## 7. ACKNOWLEDGMENT:

The authors of this study would like to express their gratitude to all of the hospitals and participants who took part in the research.

## 8. REFERENCES:

1. Kamboj, S., Gupta, N., Bandral, J. D., Gandotra, G., & Anjum, N. (2020). Food safety and hygiene: A review. *International Journal of Chemical Studies*, 8(2), 358-368.  
DOI: [10.22271/chemi.2020.v8.i2f.8794](https://doi.org/10.22271/chemi.2020.v8.i2f.8794)
2. Ifeadike, C. O., Ironkwe, O. C., Adogu, P. O., & Nnebue, C. C. (2014). Assessment of the food hygiene practices of food handlers in the Federal Capital Territory of Nigeria. *Tropical Journal of Medical Research*, 17(1), 10.  
DOI: [10.4103/1119-0388.130175](https://doi.org/10.4103/1119-0388.130175)
3. Todd, E. C., Michaels, B. S., Greig, J. D., Smith, D., Holah, J., & Bartleson, C. A. (2010). Outbreaks where food workers have been implicated in the spread of foodborne disease. Part 7. Barriers to reduce contamination of food by workers. *Journal of Food Protection*, 73(8), 1552-1565.  
DOI: [10.4315/0362-028x-71.11.2339](https://doi.org/10.4315/0362-028x-71.11.2339)
4. Abdelhakeem, A. A., Feyza, B., & Hekmat, A. A. (2021). Food Safety Knowledge among Food Handlers in Hospitals of Jordan. *Food Science and Technology*, 9(2), 17-30.  
DOI: [10.13189/fst.2021.090201](https://doi.org/10.13189/fst.2021.090201)
5. Lestantyo, D., Husodo, A. H., Irvati, S., & Shaluhyah, Z. (2017). Safe food handling knowledge, attitude and practice of food handlers in hospital kitchen. *International Journal of Public Health Science*, 6(4), 324-330.  
DOI: [10.11591/ijphs.v6i4](https://doi.org/10.11591/ijphs.v6i4)
6. Garcia, P. P., de Cássia Akutsu, R., Savio, K. E., Camargo, E. B., & Silva, I. C. (2015). The efficacy of food handler training: The transtheoretical model in Focus, Brazil, 2013. *Journal of Safety Studies*, 1(2).  
DOI: [10.5296/jss.v1i2.8618](https://doi.org/10.5296/jss.v1i2.8618)
7. Mukhopadhyay, P., Joardar, G. K., Bag, K., Samanta, A., Sain, S., & Koley, S. (2012). Identifying key risk behaviors regarding personal hygiene and food safety practices of food handlers working in eating establishments located within a hospital campus in Kolkata. *Al Ameen Journal of Medical Sciences*, 5(1), 21-28.
8. Da Cunha, D. T., Stedefeldt, E., & De Rosso, V. V. (2014). The role of theoretical food safety training on Brazilian food handlers' knowledge, attitude, and practice. *Food Control*, 43, 167-174.  
DOI: [10.1016/j.foodcont.2014.03.012](https://doi.org/10.1016/j.foodcont.2014.03.012)
9. Palupi, I. R., Fitasari, R. P., & Utami, F. A. (2020). Knowledge, attitude, and practice of hygiene and sanitation among food-handlers in a psychiatric hospital in Indonesia—a mixed method study. *Journal of Preventive Medicine and Hygiene*, 61(4), E642.  
DOI: [10.15167/2421-4248/jpmh2020.61.4.1526](https://doi.org/10.15167/2421-4248/jpmh2020.61.4.1526)

10. Megahed Ibrahim, A., EltabeySobeh, D., & Hafez, E. E. (2022). Food handlers' knowledge, attitude, and practices about safe and hygienic food in Egyptian government hospitals. *Egyptian Journal of Health Care*, 13(2), 1577-1585.  
DOI: [10.21608/EJHC.2022.246620](https://doi.org/10.21608/EJHC.2022.246620)
11. Faour-Klingbeil, D., & Todd, C. D. (2020). Prevention and control of foodborne diseases in Middle-East North African countries: Review of national control systems. *International Journal of Environmental Research and Public Health*, 17(1), 70.  
DOI: [10.3390/ijerph17010070](https://doi.org/10.3390/ijerph17010070)
12. Çakıroğlu, F. P., & Uçar, A. (2008). Employees' perception of hygiene in the catering industry in Ankara (Turkey). *Food Control*, 19(1), 9–15.  
DOI: [10.1016/j.foodcont.2007.01.001](https://doi.org/10.1016/j.foodcont.2007.01.001)
13. Lambiri, M., Mavridou, A., & Papadakis, J. (1995). The application of hazard analysis critical control point (HACCP) in a flight catering establishment improved the bacteriological quality of meals. *Journal of the Royal Society for the Promotion of Health*, 115(1), 26–30.  
DOI: [10.1177/146642409511500109](https://doi.org/10.1177/146642409511500109)
14. Clayton, D. A., Griffith, C. J., Price, P., & Peters, A. C. (2002). Food handlers' beliefs and self-reported practices. *International Journal of Environmental Health Research*, 12(1), 25–39.  
DOI: [10.1080/09603120120110031](https://doi.org/10.1080/09603120120110031)
15. Akabanda, F., Hlortsi, E. H., & Owusu-Kwarteng, J. (2017). Food safety knowledge, attitudes and practices of institutional food-handlers in Ghana. *BMC Public Health*, 17(1), 1-9.  
DOI: [10.1186/s12889-016-3986-9](https://doi.org/10.1186/s12889-016-3986-9)
16. Schmid, T. R., & Rodrick, G. E. (2003). *Food safety handbook*. John Wiley & Sons.
17. Walker, E., Pritchard, C., & Forsythe, S. (2003). Hazard analysis critical control point and prerequisite programme implementation in small and medium size food businesses. *Food Control*, 14(3), 169-174.  
DOI: [10.1016/S0956-7135\(02\)00061-0](https://doi.org/10.1016/S0956-7135(02)00061-0)
18. Baş, M., Ersun, A. Ş., & Kıvanç, G. (2006). The evaluation of food hygiene knowledge, attitudes, and practices of food handlers' in food businesses in Turkey. *Food Control*, 17(4), 317-322.  
DOI: [10.1016/j.foodcont.2004.11.006](https://doi.org/10.1016/j.foodcont.2004.11.006)
19. Tokuç, B., Ekuklu, G., Berberoğlu, U., Bilge, E., & Dedeler, H. (2009). Knowledge, attitudes and self-reported practices of food service staff regarding food hygiene in Edirne, Turkey. *Food control*, 20(6), 565-568.  
DOI: [10.1016/j.foodcont.2008.08.013](https://doi.org/10.1016/j.foodcont.2008.08.013)
20. Khan, M. J., Naeemullah, N. K., Wazir, A. K., Iqbal, A., Ishtiaq, M., Khan, S. A., & Ali, J. (2022). Knowledge Attitude and Practice of Food Handlers Regarding Food Safety Practices District Kohat Khyber Pakhtunkhwa Pakistan. *Pakistan Journal of Medical & Health Sciences*, 16(07), 831-831.  
DOI: [10.53350/pjmhs22167831](https://doi.org/10.53350/pjmhs22167831)
21. Soares, L. S., Almeida, R. C., Cerqueira, E. S., Carvalho, J. S., & Nunes, I. L. (2012). Knowledge, attitudes and practices in food safety and the presence of coagulase-positive staphylococci on hands of food handlers in the schools of Camaçari, Brazil. *Food control*, 27(1), 206-213.  
DOI: [10.1016/j.foodcont.2012.03.016](https://doi.org/10.1016/j.foodcont.2012.03.016)
22. Sharif, L., Obaidat, M. M., & Al-Dalalah, M. R. (2013). Food hygiene knowledge, attitudes and practices of the food handlers in the military hospitals. *Food and Nutrition Sciences*, 4(03), 245.  
DOI: [10.4236/fns.2013.43033](https://doi.org/10.4236/fns.2013.43033)
24. Alqurashi, N. A., Priyadarshini, A., & Jaiswal, A. K. (2019). Evaluating food safety knowledge and practices among foodservice staff in Al Madinah Hospitals, Saudi Arabia. *Safety*, 5(1), 9.  
DOI: [10.3390/safety5010009](https://doi.org/10.3390/safety5010009)
25. Angelillo, I. F., Viggiani, N. M., Greco, R. M., & Rito, D. (2001). HACCP and food hygiene in hospitals knowledge, attitudes, and practices of food-services staff in Calabria, Italy. *Infection Control & Hospital Epidemiology*, 22(6), 363-369.  
DOI: [10.1086/501914](https://doi.org/10.1086/501914)



## Exploring Smell Loss Patterns and Recovery Factors Among Covid-19 Patients in Benghazi, Libya

Balgeis Elfallah<sup>1\*</sup>.

*1 Department of Surgery (Otolaryngology)- Faculty of Medicine - University of Benghazi.*

Received: 28 / 03 / 2024; Accepted: 14 / 05 / 2024

### ABSTRACT

**Objective:** The main objective of this research is to investigate the recovery patterns and the demographic factors that affect patients with loss of smell post-COVID-19 disease in Benghazi, Libya. Besides, to examine whether the patient's responses statistically differ according to several variables, including severity of smell loss, gender, and age.

**Method:** This research adopts a cross-sectional design to capture a snapshot of patient experiences during the COVID-19 pandemic in Benghazi. A structured questionnaire is used for data collection. The research collects 96 valid questionnaires over the period from November 2023 to February 2024 from (1) the Speciality Surgical Center; and (2) the Al-Rowad Specialised Center. Then, the research employed descriptive analysis, the One-sample Wilcoxon Signed rank, the Spearman correlation test, and the Independent Samples Kruskal-Wallis test.

**Results:** 16 (17%) participants suffered from a mild loss of smell, 30 (31%) participants suffered a moderate loss of smell, and 50 (52%) participants suffered a severe loss of smell. Only 26 (27%) participants reported that it was gradual onset while 70 (73%) reported the opposite. Regarding the recovery pattern, 54 (56%) participants had complete recovery of loss of smell, while 18 (19%) had partial recovery, and 24 (25%) had no recovery, where 46 out of 54 participants completely recovered in the first month, and only 8 participants recovered after 60 days. There is a weakly significant relationship between the smell loss severity and recovery period. Also, there are no statistically significant differences between groups of varying smell loss severity (mild, moderate, or severe) in different genders, smell recovery periods, or age (all p-values > 0.05).

**Conclusion:** It can be concluded that, although the infection with COVID-19 among the participants was generally of moderate severity, the condition of the loss of the olfactory sense was severe and occurred suddenly, but at the same time, the largest percentage of participants recovered completely from it within the first two weeks of infection. However, it cannot be relied on smell loss as an early indicator of COVID-19 infection.

**KEYWORDS:** COVID-19, Recovery patterns, Recovery Period, Smell loss.

### 1. INTRODUCTION

The COVID-19 pandemic, which is attributed to the SARS-CoV-2 virus, has presented a wide range of clinical manifestations. These include fever, cough, mild to severe respiratory symptoms, and, a significant incidence of smell loss (anosmia)<sup>1</sup>. Beyond just respiratory discomfort, the prevalence of anosmia, hyposmia, or other olfactory abnormalities in COVID-19 patients has been extensively observed in a variety of geographical areas<sup>2</sup>. Recent international investigations have highlighted the strong link between COVID-19 disease and smell loss. Anosmia was reported to be a presenting symptom in 73.6% of patients diagnosed with COVID-19 disease in an early study published in JAMA Otolaryngology-Head & Neck Surgery<sup>1</sup>. There is a need to look into smell loss as this startling number highlights a major COVID-19 indicator.

\*Correspondence: Balgeis Elfallah.

[balgeis.elfallah@uob.edu.ly](mailto:balgeis.elfallah@uob.edu.ly)

The role of smell loss in the pathophysiology of COVID-19 disease has generated interest among researchers. Various studies have put forth explanations for why olfactory dysfunction occurs in COVID-19 disease, including invasion by the virus into the olfactory system tissues, immune responses, or neurological effects<sup>3,4</sup>. The distinct appearance of this symptom or its early manifestation emphasises its importance, as a sign for diagnosis and forecasting in the field. Studies from around the world have shed light on the link between COVID-19 disease and loss of smell.

Buzgeia et al. found that for longer than two months, loss of smell, among other symptoms, is the most prevalent and enduring symptom in patients in Libya<sup>5</sup>. Given the Libyan population's distinctive genetic, environmental, and sociocultural characteristics, a targeted study of smell loss post-COVID-19 disease is warranted. In the context of COVID-19 patients in Libya, the frequency, duration, and clinical features of olfactory impairment are yet unknown and require further investigation and examination. To the

best of the researcher's knowledge, no study has been done in Libya to investigate the recovery of the loss of smell post-COVID-19. Thus, the main objective of this research is to examine the recovery process and the demographics that influence patients in Benghazi, Libya, who have lost their sense of smell after getting COVID-19 disease, as well as the course of smell recovery. Additionally, to investigate if there are statistically significant differences in the respondents' answers based on age, gender, and the extent of smell loss.

## 2. MATERIAL AND METHODS

This research adopts a cross-sectional design to capture a snapshot of patient experiences during the COVID-19 pandemic in Libya. A questionnaire with three sections is used for data collection. These sections are (1) demographic characteristics of the participants; (2) clinical characteristics related to COVID-19 disease for the participants; and (3) a five-point Likert scale for six questions, where 1 is for “strongly disagree” and 5 is for “strongly disagree.” Data was exclusively collected from participants diagnosed with COVID-19 disease, who lost their sense of smell, whether they recovered from it or not.

The structured questionnaire is administered to participants, ensuring informed consent and anonymity. This research adheres to ethical guidelines, which include maintaining confidentiality, ensuring voluntary participation, and obtaining informed consent from participants. The questionnaire was distributed from November 2023 to February 2024 at (1) the Speciality Surgical Center, which is a government teaching centre for Urology and ENT in Benghazi; and (2) the Al-Rowad Specialized Center, which is a private centre in Benghazi for ENT and speech therapy. This research received the approval to distribute the questionnaire from the two centres. The researcher received 113 questionnaires, 17 of them were excluded because of incomplete data. Thus, the data from 96 questionnaires was entered into the Statistical Package for Social Sciences (IBM SPSS 25) program for scanning and purification before the analysis was conducted.

After introducing the demographic and clinical characteristics of the participants, this researcher employed Cronbach's alpha test to examine the reliability of the responses as well as the Kolmogorov-Smirnov test to investigate the normality of the respondent answers. Then, the descriptive analysis was conducted by using the minimum, maximum, mean, median, and standard deviation of the answer's value. After the descriptive analysis is done, the nonparametric tests are conducted. In detail, the researcher applied the One-sample Wilcoxon Signed rank test to determine if there is a significant difference between the median of the answers in the Likert-scale score and a hypothesised median value (which

is equal to 3). Besides, this research applied the Spearman correlation test to investigate the relationship between the severity of the smell loss and the recovery period. Finally, the Independent Samples Kruskal-Wallis test is applied to investigate whether there are statistically significant differences in respondents based on various factors, such as smell loss severity, gender, and age. The significant level of the tests above is at 0.05.

## 3. RESULTS

The results in Table 1 below show that the total number of participants in the study was 96; sixty-three (66%) were females and thirty-three (34%) were males. In terms of age, the majority are between 20 and 60 years old (86%), but the highest percentage remains between the ages of 40 and 60. Any participant aged less than 18 is excluded. Besides, only 8 (8%) participants are smokers, compared to 88 (92%) who are not. Regarding chronic diseases, more than half of the participants had chronic diseases (59%); the most common diseases are chronic sinusitis and allergic rhinitis, however, 41% of the participants have no medical history.

Since this research relies heavily on data that may last up to four years, participants in the study may not be accurately aware of the severity of infection with COVID-19 disease, especially since it was a new disease at the time. Thus, the severity of the infection in this research was characterised as follows: (1) participants who had home treatment are considered to have a mild disease; (2) participants who were treated at an outpatient department are considered to have a moderate disease, and (3) participants who were admitted to the hospital are considered to have a severe disease. It is worth noting that any participants admitted to the ICU are excluded since they might be unreliable. Thus, the results in the table indicate that 22 (23%) of the participants had a mild disease. 41 (43%) had a moderate disease and 33 (34%) had a severe disease. Thus, most of the participants had a moderate COVID-19 disease. Concerning the severity of the loss of smell, it was found that 16 (17%) participants suffered from a mild loss of smell, 30 (31%) participants suffered a moderate loss of smell, and 50 (52%) participants suffered a severe loss of smell. Also, the participants of the questionnaire answered the question about whether the onset of smell loss was sudden or gradual, 26 (27%) participants reported that it was a gradual onset while 70 (73%) reported the opposite. The table also indicates that 54 (56%) participants had complete recovery of loss of smell, while 18 (19%) had partial recovery, and 24 (25%) had no recovery. Lastly, there is a general trend in the responses that they are against considering loss of smell as an early indicator of infection with COVID-19 disease. The number of non-agrees reached 49 (51%) participants vs. 21 (22%) who agreed, while the other 26 (27%) partially agreed

**Table1. Demographic and Clinical Characteristics of the Participants**

Participants Demographic Characteristics		No.	(%)
Gender			
	Male	33	34%
	Female	63	66%
Age			
	More than 60 years	3	3%
	More than 40 and less than 60 years	44	46%
	Between 20 and 40 years	38	40%
	Less than 20 years	11	11%
Smoking			
	Yes	8	8%
	No	88	92%
Chronic Diseases			
	Chronic sinusitis	12	13%
	Hypertension	4	4%
	Hypertension, Diabetes	2	2%
	Hypertension, Chronic sinusitis	2	2%
	Diabetes	3	3%
	Allergic rhinitis	12	13%
	Allergic rhinitis, Chronic sinusitis	11	11%
	Allergic rhinitis, Hypertension	2	2%
	Allergic rhinitis, Hypertension, Chronic sinusitis	2	2%
	Others	7	7%
	No medical history	39	41%
Participants Clinical Characteristics		No.	(%)
COVID-19 severity			
	Mild (Home Treatment)	22	23%
	Moderate (Out-patient)	41	43%
	Severe (Hospital Admission)	33	34%
Severity of Smell Loss:			
	Mild	16	17%
	Moderate	30	31%
	Severe	50	52%
Smell loss was:			
	Gradually	26	27%
	Suddenly	70	73%
Recovery of smell loss:			
	Yes	54	56%
	Partially	18	19%
	No	24	25%
Loss of smell as an indicator of infection with COVID-19 disease?			
	Agree	21	22%
	Partially	26	27%
	Disagree	49	51%

Figure 1 below illustrates the recovery period for the 54 participants who have completely recovered from the loss of smell. The results indicate that the day’s range for recovery was between 2 and 70 days, with a mean of 24.3 days and a median of 14.5 days. It is also noted that the majority of the participants recovered on the 7<sup>th</sup>, 14<sup>th</sup>, and 30<sup>th</sup> days, with 14 participants, 8 participants, and 9 participants, respectively. Hence, there was a noticeable improvement in the recovery from loss of smell in the first 14 days after the diagnosis. In the first month, 46 out of 54 participants completely recovered, and only 8 participants recovered after 60 days.

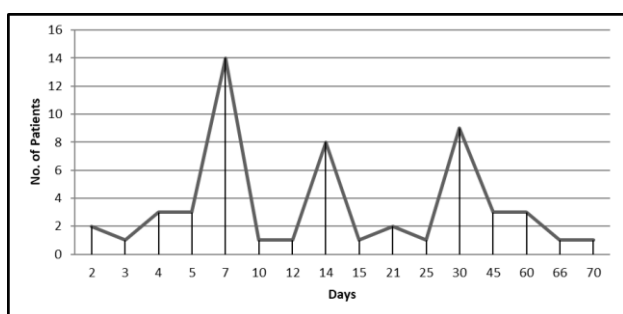


**Fig. 1. Recovery Period of Smell Loss**

Furthermore, to ensure that participants do not lose interest in their answers, this research also applied the 5-

Likert scale. Table 2 below presents the six questions and the total answers of the 96 participants. The results of the table indicate that in question 1, 57 (59%) participants either did not experience runny noses during COVID-19 disease or only had mild symptoms. On the other hand, only 7 (7%) participants had a severe to very severe runny nose. In the same vein in question 2, 47 (49%) participants either had no or very mild nasal congestion during COVID-19 disease, while more than half of the participants 49 (51%) had between moderate and severe congestion (28, 21 participants, respectively). For the change of sense of smell for regular odours during COVID-19 disease in question 3, the responses were close where 41 (43%) participants had no change or had minimal change whereas 35 (36%) participants had severe change. After recovery from COVID-19 disease, 25 (26%) participants had a strong sense of smell, 29 (30%) participants had a moderate sense of smell and 42 (44%) participants had a weak sense of smell. Upon the return of sense of smell in question 5, 66 (69%) participants still could not distinguish some smells while 30 (31%) participants did not suffer from this issue. Lastly, in question 6 regarding whether the use of the loss of smell as an early indicator of infection with COVID-19 disease, most of the participants either disagreed or slightly agreed (49 participants) compared with 21 participants who agreed and strongly agreed.

**Table 2. Total Answers of the 96 Participants for the 5-Likert Scale**

No.	Questions	1	2	3	4	5
		(Strongly Disagree)				(Strongly Agree)
Q1	Did you experience a runny nose during your COVID-19 disease?	40	17	32	5	2
Q2	Did you suffer from nasal congestion during your COVID-19 disease?	28	19	28	17	4
Q3	Did you notice a change in your sense of smell for regular odours during your COVID-19 disease?	26	15	20	24	11
Q4	Was your sense of smell back to normal after recovery from COVID-19 disease?	24	18	29	20	5
Q5	Upon the return of your sense of smell, are there still some smells you cannot distinguish?"	17	13	24	20	22
Q6	Do you think that losing the sense of smell may be used as an early indicator of infection with COVID-19 disease?	31	18	26	13	8

To test the reliability of the responses on the 5-Likert scale, this study employs Cronbach's alpha test. The results show that the alpha value of this research is equal to 0.645. If the alpha value is between 0.64 and 0.85, the questionnaire respondents are considered adequate<sup>6</sup>. Thus, the results of this research are satisfactory. Furthermore, to examine whether the answers to the 5-Likert scale are

normally distributed or not, this research applies the Kolmogorov-Smirnov test. The results of the Kolmogorov-Smirnov test are presented in Table 3. The result of the table indicates that all answers for the 96 participants on the 5-Likert scale are not normally distributed.

**Table 3. Normally Distributed Test Results**

No.	Questions	Statistic	df.	Sig.
1	Did you experience a runny nose during your COVID-19 disease?	0.260	96	0.00*
2	Did you suffer from nasal congestion during your COVID-19 disease?	0.182	96	0.00*
3	Did you notice a change in your sense of smell for regular odours during your COVID-19 disease?	0.175	96	0.00*
4	Was your sense of smell back to normal after recovery from COVID-19 disease?	0.184	96	0.00*
5	Upon the return of your sense of smell, are there still some smells you cannot distinguish?	0.159	96	0.00*
6	Do you think that losing the sense of smell may be used as an early indicator of infection with COVID-19 disease?	0.194	96	0.00*

\* Significant at a level of 0.05

Since the answers are not normally distributed, this research applies the non-parametric test, namely the One-Sample Wilcoxon Signed Rank and Independent Samples Kruskal-Wallis tests. The results of the descriptive analysis as well as the One Sample Wilcoxon Signed Rank of the respondents are presented in Table 4. The range of answers to all questions is between 1 (min) and 5 (max), and the standard deviation is between 1.073 and 1.386. The median value in the first two questions is equal to 2 (mean=2.08) and 3 (mean=2.48), respectively, with a p-value equal to 0.00. Thus, the participants significantly disagree that they experience a runny nose during the COVID-19 disease, while their opinion about whether they suffer from nasal congestion during your COVID-19 disease is significantly neutral. The responses of the participants are also neutral regarding whether they noticed a change in their sense of smell for regular odours during their COVID-19 disease, but statistically insignificant (p-value=0.065). Thus, there is no difference

between the median of the answers and the hypothesised median value of 3.

After recovery from COVID-19 disease, as the median is equal to 3, the strength of the sense of smell is significantly neutral(p-value=0.002). However, some participants regained their sense of smell as normal as it was before having the disease, and others reported that their sense of smell was not as normal as before the disease. Yet, according to the answers to question 5, the results are statistically significant (p-value=0.00) that they could distinguish between different odours upon returning their sense of smell. After asking the participants whether losing the sense of smell may be used as an early indicator of infection with COVID-19 disease, the responses significantly disagreed (p-value=0.00). It is worth noting that this question (No. 6) was also asked in this research among the questions related to COVID-19 disease (section 2).

**Table 4. Descriptive Analysis**

No.	Questions	Min	Max	Std. Deviation	Mean	Median	P-value (5%)
1	Did you experience a runny nose during your COVID-19 disease?	1	5	1.073	2.08	2	0.00*
2	Did you suffer from nasal congestion during your COVID-19 disease?	1	5	1.205	2.48	3	0.00*
3	Did you notice a change in your sense of smell for regular odours during your COVID-19 disease?	1	5	1.386	2.78	3	0.065
4	Was your sense of smell back to normal after recovery from COVID-19 disease?	1	5	1.216	2.63	3	0.002*
5	Upon the return of your sense of smell, are there still some smells you cannot distinguish?	1	5	1.172	1.88	1	0.00*
6	Do you think that losing the sense of smell may be used as an early indicator of infection with COVID-19 disease?	1	5	1.294	2.45	2	0.00*

\*Significant at a level of 0.05

This research also investigates the relationship between the smell loss severity and the period of the smell loss recovery. It is evident from the results in Table 5 that there is a statistically significant relationship between the severity of the smell loss and the period of the smell loss

recovery (p-value=0.008). The correlation is considered weak if the value falls between 0.20 and 0.39<sup>7</sup>, and hence, the relationship between the smell loss severity and the period of the smell loss recovery is weak, as the value coefficient is equal to 0.356.

**Table 5. Relationship between the Smell Loss Severity and Smell Loss Recovery Period**

Spearman Correlation Test		Smell Loss Severity	Smell Loss Recovery Period
Smell loss severity	Correlation Coefficient	1.000	0.356*
	Sig. (2-tailed)	.	0.008

\*Significant at the 0.05 level (2-tailed).

The results of whether there are differences in the answers related to smell loss severity on the one hand and between gender, smell loss recovery patterns, and smell loss recovery period on the other hand are shown, respectively, in Panels (a) through (c) in Table 6. It is evident from the results in the table that there are no statistically significant differences in the median between groups of varying smell loss severity (mild, moderate, or severe) in different genders, and smell recovery periods

(all p-values > 0.05). Concerning the smell loss severity and the recovery patterns, the result in the table demonstrates that there are significant differences between the group of varying smell loss severity (mild, moderate, severe) and the recovery patterns (p-value=0.011). It also shows that the complete recovery of the smell loss is more frequent in participants with moderate and severe loss than in participants with mild smell loss.

**Table 6. Differences in Smell Loss Severity According to Various Factors**

**Panel (a) Smell Loss Severity and Gender**

Smell Loss Severity	Total Number n (%)	Males n (%)	Females n (%)	P-value
Mild	16 (17%)	4 (4%)	12 (13%)	0.569
Moderate	30 (31%)	11 (11%)	19 (20%)	
Severe	50 (52%)	18 (19%)	32 (33%)	

**Panel (b) Smell Loss Severity and Recovery Patterns**

Smell Loss Severity	Total Number n (%)	Complete Recovery n (%)	Partial or No Recovery n (%)	P-value
Mild	16 (17%)	4 (4%)	12 (13%)	0.011*
Moderate	30 (31%)	17 (18%)	13 (14%)	
Severe	50 (52%)	28 (29%)	22 (23%)	

\*Significant at a 0.05 level.

**Panel (c) Smell Loss Severity and Recovery Period**

Smell Loss Severity	Total Number n (%)	Recovery Period	P-value
Mild	16 (17%)	Range (2-7 Days) Mean=5.4, Median = 7, Std. =2.3	0.587
Moderate	30 (31%)	Range (3-45 Days) Mean=15.6, Median = 14, Std. =11.7	
Severe	50 (52%)	Range (2-70 Days) Mean=24.8, Median = 14.5, Std. =20.5	

The results of whether there are statistically significant differences in the answers related to gender on the one hand and the smell recovery patterns and the recovery period, on the other hand, are presented in Table 7. In terms of smell loss recovery, the results in the table indicate that there is a statistically significant difference between males and females (p-value=0.031). The

complete recovery in males is higher than in females, where 24 male participants out of 33 participants completely recovered from smell loss, while in females it was only 30 participants out of 63. However, when considering the smell loss recovery period, the differences between males and females are not significant (p-value = 0.031).

**Table 7. Smell Loss Recovery and Recovery Period according to Gender**

**Panel (a) Smell Loss Recovery and Gender**

Gander	Total Number <i>n</i> (%)	Complete Recovery <i>n</i> (%)	Partial or No Recovery <i>n</i> (%)	P-value
Male	33 (34%)	24 (25%)	9 (9%)	0.031
Female	63 (66%)	30 (31%)	33 (35%)	

**Panel (b) Smell Loss Recovery Period and Gender**

Gander	Total Number <i>n</i> (%)	Recovery Period	P-value
Male	33 (34%)	Range (2-60 Days) Mean=17, Median = 12, Std. =16	0.713
Female	63 (66%)	Range (2-70 Days) Mean=22, Median = 14, Std. =20	

Lastly, the results of whether there are statistically significant differences in the answers related to age on the one hand and the severity of the smell loss, the smell loss recovery patterns, and the smell loss recovery period, on the other hand, are presented in Table 8. The results show that there is no statistical difference between the age of the

participants on the one hand and the severity of smell loss and the recovery pattern, on the other hand. In contrast, there is a significant difference between the age and the recovery period (p-value=0.008). Participants aged between 20 and 40 years old took a longer time for their smell recovery, contrary to the participants of other ages.

**Table8. Smell Loss Severity, Recovery Patterns and Recovery Period according to Age**

**Panel (a) Age and Smell Loss severity.**

Age	Total Number <i>n</i> (%)	Mild Smell Loss <i>n</i> (%)	Moderate Smell Loss <i>n</i> (%)	Severe Smell Loss <i>n</i> (%)	P-value
More than 60	3 (3%)	2 (2%)	0 (0%)	1 (1%)	0.074
More than 40 and less than 60	44 (46%)	8 (8%)	16 (17%)	20 (21%)	
Between 20 and 40	38 (40%)	6 (6%)	14 (15%)	18 (19%)	
Less than 20	11 (11%)	4 (4%)	5 (5%)	2 (2%)	

**Panel (b) Age and Recovery Patterns.**

Age	Total Number <i>n</i> (%)	Complete Recovery <i>n</i> (%)	Partial or No Recovery <i>n</i> (%)	P-value
More than 60	3 (3%)	1 (1%)	2 (2%)	0.197
More than 40 and less than 60	44 (46%)	18 (19%)	26 (27%)	
Between 20 and 40	38 (40%)	28 (29%)	10 (11%)	
Less than 20	11 (11%)	7 (7%)	4 (4%)	

**Panel (c) Age and Recovery Period.**

Age	Total Number n (%)	Recovery Period	P-value
More than 60	3 (3%)	Range (5-45 Days) Mean=26, Median = 7, Std. =18.40	0.008*
More than 40 and less than 60	44 (46%)	Range (2-70 Days) Mean=15.3, Median = 7, Std. =16.37	
Between 20 and 40	38 (40%)	Range (7-60 Days) Mean=26.6, Median = 21, Std. =18.50	
Less than 20	11 (11%)	Range (2-45 Days) Mean=19, Median = 15, Std. =16	

\*Significant at a 0.05 level

It is worth mentioning that the number of smoker participants is relatively small in this research, as it only represents 8 out of 96 participants. This might be because the majority of participants in the questionnaire are females, and smoking is considered unfashionable among them in Benghazi. Thus, no analysis is conducted to compare the smell loss between smoker participants and non-smoker participants.

**4. DISCUSSION**

A unique and interesting aspect of the COVID-19 pandemic, which is brought on by the new coronavirus SARS-CoV-2, is anosmia, or the loss of smell. Therefore, this research's primary objective is to provide an in-depth understanding of the recovery process and the demographic factors that affect patients with loss of smell post-COVID-19 disease in Benghazi, Libya. Also, to examine respondents' responses differ statistically significantly according to several variables, including gender, age, and the degree of smell loss. In this cohort, the total number of participants was 96, of which 63 were females and 33 were males. The majority of participants were between the ages of 40 and 60 years old, and the minority were found to be older than 60 years old. More than 40% of the participants have no medical history. Regarding other symptoms associated with COVID-19 disease, more than half of the participants 49(51%), had between moderate to severe nasal congestion during their disease this was the same result as shown in another study<sup>8</sup>.

The severe loss smell was only reported in 17.3% of participants in the Hopkins et al. study<sup>9</sup>, while in this study it is reported in 52% of participants. Furthermore, 54 (56%) participants stated that they had completely recovered from the smell loss. Thus, contrary to what Amer et al<sup>10</sup> found, this research found that the majority of participants completely recovered from smell loss. These results are in line with the results of several studies<sup>11,12,13</sup>. The median day of the recovery of smell loss in this research was 14.5 days, which is less than the median of a study in Saudi Arabia, which is 21.76 days<sup>8</sup>. However, the median day of recovery in another study is 7 days<sup>19</sup>.

Similar to other studies conducted in other countries<sup>14,15</sup>, this research found that most of the participants completely regained their sense of smell in one month. Another study found that the majority of participants recovered from smell loss in 3 weeks<sup>19</sup>. Results of other studies asserted that within the first 2 weeks, a substantial improvement in smell loss had occurred<sup>16</sup>.

Unlike AlYahya et al. who found that only 45% of patients reported a sudden loss of smell, this research found that the majority (73%) of participants lost their smell suddenly<sup>8</sup>, and this result is supported by other research<sup>14,10,17,9</sup>. Generally speaking, anosmia is the first or only symptom in asymptomatic COVID-19 carriers. In this context, many studies concluded that the loss of smell should be considered an early indicator of COVID-19 disease<sup>17, 18,19</sup>. Nevertheless, this study found that only 21 (22%) participants completely agreed, 26 (27%) participants partially agreed, and 49 (51%) not agreed. When testing their answers in the One-Sample Wilcoxon Signed Rank test, the results were significantly disagreed (p-value=0.000). Indeed, Trani notes a claim by Professor Evan Reiter, a professor in the Otolaryngology Department at the VCU School of Medicine in the USA, that loss of smell is no longer used as an indicator for infection with COVID-19<sup>20</sup>.

Another study concluded that there is a positive relationship between smell loss severity and the recovery period<sup>11</sup>. It makes sense that the degree of smell loss was linked to a longer recovery time since it could indicate more serious harm to the olfactory structures. This relationship, however, is considered significantly weak in this research since the correlation coefficient was 0.356.

Vaira et al. concluded that there are no differences between males and females concerning smell loss<sup>21</sup>. This research found insignificant differences in the recovery period between males and females (p-value=0.713). However, different studies asserted that the loss of smell was a symptom that affected women more often<sup>1,19,22,23</sup>. Amer et al. emphasised that females need more recovery time than males<sup>10</sup>. Shahzad and Jamil concluded that there

is no difference in a complete recovery between females and males<sup>24</sup>.

In terms of smell loss and age, Lechien et al. found that the loss of smell sense was greater in younger patients<sup>22</sup>. This is in line with Lee et al. argument, who found that younger people demonstrated a propensity to endure smell loss for a longer period, especially those between the ages of 20 and 39 years old<sup>19</sup>. On the other hand, according to Vaira et al, the smell loss was more severe in patients who were older than 50 years old<sup>21</sup>. However, in this research, the results indicate there is no statistical difference between the age of the participants and the recovery pattern, however, participants between 20 and 40 years old took a longer time for their smell recovery, contrary to the participants aged more than 40 years old (P-value=0.008).

## 5. CONCLUSION

In the end, it can be concluded that, although the infection with COVID-19 among the participants was generally of moderate severity, the condition of the loss of the olfactory sense was severe and occurred suddenly, but at the same time, the largest percentage of participants recovered completely from it within the first two weeks of infection. However, it cannot be relied on smell loss as an early indicator of COVID-19 infection.

### Limitation of the Research

Although the researcher made every effort to reduce the limitations of this research to a minimum, there are some of them that the research may have fallen into one or more. These limitations are as follows:

- **Sample Size:** The study's sample size might be limited since it only focuses on patients from Benghazi. As such, the results cannot be applied to the whole Libyan population.
- **Self-Reporting Bias:** Since the questionnaire relies on patients' self-reports, there is a chance that there will be bias or inaccuracies because of memory recall or subjective interpretations.
- **The sample's representativeness** may be impacted by the systematic differences between those who choose to participate and those who do not.
- **The questionnaire** might have missed some crucial elements that could have had an impact on the results, as it may not have included every relevant variable of scent loss and recovery.

## 6. REFERENCES

1. Lechien JR, Chiesa-Estomba CM, De Siati DR, Horoi M, Le Bon SD, Rodriguez A, Dequanter D, Blecic S, El Afia F, Distinguin L, Chekkoury-Idrissi Y. Olfactory and gustatory dysfunctions as a clinical presentation of mild-to-moderate forms of the coronavirus disease (COVID-19): a multicenter European study. *European Archives of Oto-rhinolaryngology*. 2020 Aug;277(8):2251-2261.  
<https://doi.org/10.1007/s00405-020-05965-1>
2. Mao L, Jin H, Wang M, Hu Y, Chen S, He Q, Chang J, Hong C, Zhou Y, Wang D, Miao X. Neurologic manifestations of hospitalized patients with coronavirus disease 2019 in Wuhan, China. *JAMA neurology*. 2020 Jun 1;77(6):683-690.  
<https://doi.org/10.1001/jamaneurol.2020.1127>
3. Brann DH, Tsukahara T, Weinreb C, Lipovsek M, Van den Berge K, Gong B, Chance R, Macaulay IC, Chou HJ, Fletcher RB, Das D. Non-neuronal expression of SARS-CoV-2 entry genes in the olfactory system suggests mechanisms underlying COVID-19-associated anosmia. *Science advances*. 2020 Jul 31;6(31).  
<https://doi.org/10.1126/sciadv.abc5801>
4. Meinhardt J, Radke J, Dittmayer C, Franz J, Thomas C, Mothes R, Laue M, Schneider J, Brünink S, Greuel S, Lehmann M. Olfactory transmucosal SARS-CoV-2 invasion as a port of central nervous system entry in individuals with COVID-19. *Nature neuroscience*. 2021 Feb;24(2):168-175.  
<https://doi.org/10.1101/2020.06.04.135012>
5. Buzgeia AM, Badi NH, Ali FM, Hamad NM. Cross-Sectional Perspective Study of Post-COVID Syndrome Characteristics in Benghazi, Libya. *Open Access Library Journal*. 2023 Dec 4;10(12).  
<https://doi.org/10.4236/oalib.1111004>
6. Taber KS. The use of Cronbach's alpha when developing and reporting research instruments in science education. *Research in science education*. 2018 Dec;48:1273-1296.  
<https://doi.org/10.1007/s11165-016-9602-2>
7. Evans JD. *Straightforward statistics for the behavioral sciences*. Thomson Brooks/Cole Publishing Co; 1996.
8. AlYahya K, Alarfaj AA, AlZahir BZ, Alhelal FM, Al Sultan WA, Almulhim IM, Alhamam AK. Olfactory dysfunction during the COVID-19 era: Prevalence and prognosis for recovery of sense of smell, Eastern region, Saudi Arabia. *Saudi Journal of Otorhinolaryngology Head and Neck Surgery*. 2023 Jan 1;25(1).  
[https://doi.org/10.4103/sjoh.sjoh\\_60\\_22](https://doi.org/10.4103/sjoh.sjoh_60_22)
9. Hopkins C, Surda P, Kumar N. Presentation of new onset anosmia during the COVID-19 pandemic. *Rhinology*. 2020 Jun 1;58(3).  
<https://doi.org/10.4193/rhin20.116>

10. Amer MA, Elsherif HS, Abdel-Hamid AS, Elzayat S. Early recovery patterns of olfactory disorders in COVID-19 patients; a clinical cohort study. *American Journal of Otolaryngology*. 2020 Nov 1;41(6).  
<https://doi.org/10.22541/au.159414621.12510552>
11. Schwab J, Fjaeldstad AW. Recovery rates and parosmia in olfactory loss during the COVID-19 era. *Danish medical journal*. 2022 Aug;69(9).
12. Boscolo-Rizzo P, Guida F, Polesel J, Marcuzzo AV, Antonucci P, Capriotti V, Sacchet E, Cragolini F, D'Alessandro A, Zanelli E, Marzolino R. Self-reported smell and taste recovery in coronavirus disease 2019 patients: a one-year prospective study. *European Archives of Oto-Rhino-Laryngology*. 2022 Jan;279(1):515-520.  
<https://doi.org/10.1007/s00405-021-06839-w>
13. Mitchell MB, Workman AD, Rathi VK, Bhattacharyya N. Smell and Taste Loss Associated with COVID-19 Infection. *The Laryngoscope*. 2023 Sep;133(9):2357-2361.  
<https://doi.org/10.1002/lary.30802>
14. Printza A, Katotomichelakis M, Valsamidis K, Metallidis S, Panagopoulos P, Panopoulou M, Petrakis V, Constantinidis J. Smell and taste loss recovery time in COVID-19 patients and disease severity. *Journal of Clinical Medicine*. 2021 Mar 2;10(5).  
<https://doi.org/10.3390/jcm10050966>
15. Catton G, Gardner A. Relationship between recovery from COVID-19-induced smell loss and general and oral health factors. *Medicina*. 2022 Feb 14;58(2).  
<https://doi.org/10.3390/medicina58020283>
16. Yan CH, Faraji F, Prajapati DP, Ostrander BT, DeConde AS. Self-reported olfactory loss associates with outpatient clinical course in COVID-19. In *International forum of allergy & rhinology* 2020 Jul (Vol. 10, No. 7, pp. 821-831).  
<https://doi.org/10.1002/alar.22592>
17. Haehner A, Draf J, Dräger S, Hummel T. Predictive value of sudden olfactory loss in the diagnosis of COVID-19. *Orl*. 2020 Jul 23;82(4):175-180.  
<https://doi.org/10.1159/000509143>
18. Wee LE, Chan YF, Teo NW, Cherng BP, Thien SY, Wong HM, Wijaya L, Toh ST, Tan TT. The role of self-reported olfactory and gustatory dysfunction as a screening criterion for suspected COVID-19. *European Archives of Oto-Rhino-Laryngology*. 2020 Aug;2389-2390.  
<https://doi.org/10.1007/s00405-020-05999-5>
19. Lee Y, Min P, Lee S, Kim SW. Prevalence and duration of acute loss of smell or taste in COVID-19 patients. *Journal of Korean medical science*. 2020 May 5;35(18).  
<https://doi.org/10.3346/jkms.2020.35.e174>
20. Trani O, Smell and taste loss is no longer a reliable indicator of COVID-19 infection, new research suggests. [Internet]. 2023, July [cited 2024, Mar 1]. Available from:  
<https://www.vcuhealth.org/news/covid-19/smell-and-taste-loss-is-no-longer-a-reliable-indicator-of-covid-19-infection-new-research-suggests#:~:text=%E2%80%9COur%20research%20has%20shown%20that,and%20Taste%20Disorders%20Center%20a>
21. Vaira LA, Deiana G, Fois AG, Pirina P, Madeddu G, De Vito A, Babudieri S, Petrocelli M, Serra A, Bussu F, Ligas E. Objective evaluation of anosmia and ageusia in COVID-19 patients: single-center experience on 72 cases. *Head & neck*. 2020 Jun;42(6):1252-1258.  
<https://doi.org/10.1002/hed.26204>
22. Lechien JR, Chiesa-Estomba CM, Place S, Van Laethem Y, Cabaraux P, Mat Q, Huet K, Plzak J, Horoi M, Hans S, Rosaria Barillari M. Clinical and epidemiological characteristics of 1420 European patients with mild-to-moderate coronavirus disease 2019. *Journal of internal medicine*. 2020 Sep;288(3):335-344.  
<https://doi.org/10.1111/joim.13089>
23. Giacomelli A, Pezzati L, Conti F, Bernacchia D, Siano M, Oreni L, Rusconi S, Gervasoni C, Ridolfo AL, Rizzardini G, Antinori S. Self-reported olfactory and taste disorders in patients with severe acute respiratory coronavirus 2 infection: a cross-sectional study. *Clinical infectious diseases*. 2020 Jul 28;71(15).  
<https://doi.org/10.1093/cid/ciaa330>
24. Shahzad S, Jamil F. Long term recovery assessment of post-COVID-19 loss of taste and smell-A population-based survey. *LIAQUAT MEDICAL RESEARCH JOURNAL*. 2022 Apr 1;4(1):28-32.  
<https://doi.org/10.38106/LMRJ.2022.4.1-05>



## Prevalence of Obesity in Adult Hypertensive Patients and its Effect on Antihypertension Drugs Polypharmacy in Primary Health Care Clinics in Benghazi

Adel Saleh <sup>1\*</sup> - Adela Ebsat <sup>1</sup>

*1 Department of Internal Medicine - Faculty of Medicine - University of Benghazi.*

Received: 28 / 03 / 2024, Accepted: 24 / 05 / 2024

### ABSTRACT

Obesity is one of the most common cardiovascular risk factors that affects blood pressure (BP) control, but there is a lack of data regarding the prevalence of overweight and obesity in hypertensive patients and their relationship in the Libyan population. The aim of this study is to determine the prevalence of obesity and its impact on BP control among hypertensive patients in a primary health care (PHC) unit in Benghazi, Libya. This is a cross-sectional, PHC unit-based study carried out in hypertension clinic of Al-Kish Polyclinic, Benghazi, Libya, between July and December 2017.

A total number of 207 adult patients with systemic hypertension (HTN), comprising 71 males and 136 females with age range from 27-70 years, were studied. The office BP readings along with weight and height were measured and used to calculate the body mass index (BMI) and to classify the participants into obese and nonobese. Abdominal obesity was found through waist-to-hip ratio (WHR) and waist circumference (WC) according to the cut-off points recommended by the World Health Organization (WHO). Data results were coded, entered, and analysed using SPSS version 24.

The mean age of the patients was  $51.7 \pm 09.0$  years. Out of the 207 participants, obesity was found in 136 (65.7%) of the participants. Out of those, 66 (31.9%) had class I obesity, 45 (21.7%) had class II obesity, and class III obesity was found in 25 (12.1%) of patients. BP control was poor in 131 (63.3%) patients, of whom 70% were obese. The BMI correlated positively with each of systolic BP (SBP) with  $r = 0.24$  and  $p=0.005$ ; diastolic BP (DBP) with  $r=0.18$  and  $p= 0.035$ ; and the number of anti-HTN drugs with  $r=0.228$  and  $p=0.008$ .

The prevalence of abdominal obesity determined by WHR and WC was 92.6% and 98.5%, respectively, and it was 88.7% in females and 54.9% in males.

The prevalence of obesity is high in hypertensive patients in Al-Kish Polyclinic and their BP control is poor including those who are obese. Public health measures aimed at reducing obesity should be incorporated into the overall management of systemic hypertensive patients.

**KEYWORDS:** hypertension, obesity, abdominal obesity, body mass index, blood pressure control, waist circumference, waist-to-hip ratio.

### 1. INTRODUCTION

Hypertension (HTN) is characterized by a systolic blood pressure (SBP) equal to or exceeding 140mmHg, a diastolic blood pressure (DBP) equal to or exceeding 90mmHg, or the use of antihypertensive medication <sup>1</sup>.

Worldwide, about 17 million people die from cardiovascular diseases (CVDs) each year. HTN, a major risk factor for CVDs, is estimated to be responsible for at least 45% of heart disease deaths and 51% of stroke deaths <sup>2</sup>.

According to the Seventh Report of the Joint National Committee on Prevention, Detection, Evaluation, and Treatment of High Blood Pressure (JNC 7), a patient has stage I hypertension if his/her SBP is between 140 and 159 mmHg, or DBP is between 90 and 99 mmHg. Stage II hypertension is defined as SBP of 160 mmHg or higher, or DBP of 100 mmHg or higher <sup>3</sup>.

Most patients with HTN are advised to lose weight, increase physical activity, and reduce their salt intake <sup>4</sup>. The 2014 Eighth Joint National Committee (JNC-8) guidelines on HTN recommend starting blood pressure medication for people under 60 years old if their SBP is at least 140 mmHg, or if their DBP is at least 90 mmHg, despite lifestyle modification. For people 60 years and older, blood pressure medication should be started if their SBP is at least 150 mmHg, or their DBP is at least 90

\*Correspondence: Adel Saleh.

[adel.saleh@uob.edu.ly](mailto:adel.saleh@uob.edu.ly)

mmHg<sup>5</sup>. In stage I hypertension, a single agent is generally enough to control BP, whereas in stage II, combined anti-hypertension medications may be required<sup>3</sup>.

Hypertension frequently coexists with obesity, diabetes, or hyperlipidemia; their association with CVD is well established. Because such patients are more prone to end-organ damage, they need their BP to be under control as recommended in the clinical guidelines<sup>6</sup>.

The WHO defines overweight as BMI of 25-29.9kg/m<sup>2</sup>, grade I (mild) obesity as BMI of 30-34.9 kg/m<sup>2</sup>, grade II (moderate) obesity as BMI of 35-39.9kg/m<sup>2</sup>, grade III (severe) obesity as BMI of  $\geq 40$ kg/m<sup>2</sup><sup>7</sup>. Abdominal obesity, on the other hand, is defined by a WHR  $\geq 0.90$  for men and  $\geq 0.85$  for women, or WC  $\geq 102$  cm for men and  $\geq 88$  cm for women<sup>8</sup>.

The obesity-related risks for coronary artery disease and stroke are mediated by its metabolic consequences (i.e. hypertension, dyslipidemia, and diabetes). Among these factors, hypertension appears to have the greatest impact, accounting for 31% of the excess risk of coronary heart disease and 65% of the excess risk of stroke<sup>9</sup>.

In Libya, the prevalence of HTN is 25.5%, and 67% of Libyan adults have BMI  $> 25$  while those with BMI  $> 30$  are 31.9%<sup>10</sup>.

Lifestyle modification, including weight loss, exercise, limited salt intake, and a Mediterranean diet, is usually recommended when managing patients with obesity and hypertension irrespective of BP lowering treatment<sup>11</sup>. The effect of physical activity on BP is crucial, too, independently of the weight loss achievement. Aerobic exercise has the highest impact, lowering BP up to 5-8 mmHg<sup>12</sup>. Recent data highlight the importance of a multicomponent exercise approach to improve cardiometabolic health<sup>13</sup>.

However, following successful weight loss, weight regain over few months is common and can lead to a so-called weight cycling phenomenon. Similarly, adherence to exercise training tends to decline over time<sup>14</sup>. Hence, weighting patients at every visit and self-monitoring need to be encouraged<sup>15</sup>.

The effectiveness of the currently available weight loss monotherapies is still modest, with the exception of GLP-1 RA mainly semaglutide, which in combination with behavioural modification therapy, may achieve more than 15% weight loss<sup>16</sup>.

The shortage of large, prospective, comparative trials in obesity and HTN explains the lack of clear guidelines on how to treat obese hypertensive patients. There is some evidence that managing HTN in obese patients is challenging and that this population received suboptimal treatment in real practice<sup>17, 18</sup>.

Feldstein, et al.<sup>19</sup> evaluated BMI, WC, and WHR to examine the relationship between 24-hour ambulatory blood pressure monitoring in hypertensive patients who are aged 18-86 years in Buenos Aires. The prevalence of overweight and obesity was 56.76% in women and 75.86% in men<sup>19</sup>.

Mufunda, et al.<sup>20</sup> reported a positive association between BMI and SBP, DBP and mean arterial pressure. It was also found that the effect of BMI on BP was higher in males in comparison to females<sup>20</sup>.

Giroto, et al.<sup>21</sup> investigated the prevalence of abdominal obesity in hypertensive patients in a family health unit in Brazil and found that WHR was 87.9% in females and 30.2% in males<sup>21</sup>.

Adamu, et al.<sup>22</sup> conducted a study in Bida, Nigeria, and reported that obesity was found in 44.2% of the participants. The BP control was reasonable in 56%, and the BMI correlated with age, SBP, and DBP<sup>22</sup>.

Whether or not obesity is more prevalent in adult hypertensive patients in Benghazi is still understudied, as there was only one unpublished study conducted in a private clinic. Also, whether a better control of systemic HTN in such patients requires single or multiple antihypertensive drugs still needs further clinical studies.

Faced with the need for more studies to investigate the prevalence of abdominal obesity in patients who already have a risk factor for metabolic syndrome, hypertension, and the importance of determining and preventing the risk factors associated with this condition, this study is designed to investigate the prevalence of obesity and other associated risk factors in patients with systemic HTN.

This study will serve as a base for information and strategies implementation that may reduce such risk factors. It will also encourage the primary health care personnel and physicians to diagnose high-risk patients for appropriate counselling, timely intervention, and proper referral when necessary, aiming to prevent serious complications of systemic hypertension and sudden death.

## 2. OBJECTIVE

This study aims to investigate the prevalence rate of obesity and its correlation with obesity measurements. It also aims to investigate the number of antihypertensive drugs needed for the best control of blood pressure in adult hypertensive patients attending the hypertension clinic at Al-Kish Polyclinic in the City of Benghazi, Libya.

## 3. METHODOLOGY

### 3.1 Design of the Study

This study is a cross-sectional study conducted between June and December 2017 in Al-Kish Polyclinic, a primary health care unit in Benghazi, eastern Libya.

Al-Kish Polyclinic is a primary health care clinic located in Al-Kish neighbourhood. It receives cases from all over Benghazi, the second largest city in Libya which has an estimated population of 800,000 persons. The hypertension clinic is run four days per week. The total cases of adult hypertensive patients registered in the clinic are approximately 402, with an average number of daily attendees of 15 patients.

The study population includes adult hypertensive patients aged 18 to 70 who are registered at Al-Kish Polyclinic in Benghazi. Two hundred and seven adult hypertensive patients were involved and agreed to participate in this study.

#### **Inclusion criteria**

- The study participants are those who are known to have hypertension or were diagnosed with hypertension on the first visit to the HTN Clinic. Participants were divided according to age into an 18 to 50-year-old group and a 51 to 70-year-old group.
- Only patients who gave consent to participate in the study were included.

#### **Exclusion criteria**

- Patients who refused to participate in the study.
- Patients with secondary causes of obesity (e.g., Cushing syndrome), pregnant women, end-stage renal disease, decompensated heart failure or decompensated liver cirrhosis.
- Patients above 70 years old.

### **3.2 Data Collection and Statistical Analysis**

Structured interviews and clinical/biochemical measurements were used for data collection. The structured interview was conducted using an interviewer-administered questionnaire that included demographic characteristics of the subjects, lifestyles, chronic diseases, drugs taken, and risk factors for high blood pressure. Following the interview, the clinical measurements were taken. The BP was measured by the auscultatory method using a mercury sphygmomanometer with an appropriately sized cuff and a 3M Littmann stethoscope. A special thigh cuff was used for BP measurements in obese individuals with a cuff length of 33 cm and cuff width of 20 cm. After resting for about five minutes, the subjects had their blood pressure (BP) measured on either the right or left arm at heart level. The first and fifth Korotkoff sounds marked the systolic and diastolic blood pressures, respectively. Two readings were obtained with five-minute intervals, and the average was calculated and recorded.

Next, the height and weight of each subject were measured using a stadiometer to which an electronic

weighing scale was attached. Measurements were taken while the patients stood erect, wearing light clothing, and with no footwear. Height was measured to the nearest centimetre and weight to the nearest 0.1kg. The BMI was then calculated using the formula:  $BMI = \text{weight (kg)} / \text{height (m)}^2$ .

Waist and hip measurements were obtained with an inextensible measuring tape having a width of 1.0 cm and a minimum unit of 0.1 cm. To take waist and hip measures, the individual remained standing upright, with as little clothing as possible. WC was obtained by positioning the measuring tape on an imaginary median line between the iliac crest and the last rib and was taken at the end of the expiration. Hip circumference was measured at the largest diameter of the buttocks. In both measures, the tape was positioned horizontally without pressing the soft tissues; two measurements were obtained for each, and the average was recorded. The dependent variables analyzed were WC and WHR which the latter was calculated from WC divided by hip circumference.

Serum lipid profile, total cholesterol (TC), triglycerides, low-density lipoprotein cholesterol (LDL-C), and HDL-C, were obtained following an overnight (10-12 hours) fast.

Data were analyzed using SPSS Statistics software for Windows, version 24 (SPSS Inc, Chicago, IL, USA). Descriptive statistics were generated for all variables. Numerical data were expressed as the mean and standard deviation (mean  $\pm$  SD), and categorical data were expressed as percentages. The t-test was used to examine differences in the means of variables (age, BMI, WC, WHR, SBP, and DBP) between study groups, and the  $\chi^2$  test was used to compare the prevalence of general obesity and abdominal obesity between males and females.

Pearson's correlation and linear regression analysis were used to determine the effect of grades of obesity on BP control and the number of drugs needed to control blood pressure. Also, p-values less than 0.05 were considered significant.

### **3.3 Ethical Considerations**

Informed consent was taken from respondents before administering the questionnaire or anthropometry. Names and addresses were excluded to maintain the confidentiality of the respondents. Participants had a brief one-to-one discussion on the health implications of risk behaviours and measures to reduce the risk of noncommunicable diseases. Patients with borderline high BP (i.e., measurements of 140/90mmHg) were counselled on needing further review and follow-up. Those with marked elevations  $\geq$  180/110mmHg were referred to the nearest hospitals for urgent medical treatment and management.

## 4. RESULTS AND DISCUSSION

### 4.1 General Characteristics of Study Subjects

During the study period from July 1<sup>st</sup>, 2017 to December 31<sup>st</sup>, 2017, there were 207 patients with hypertension enrolled in the study, 34.3% (71) of whom were males and 65.7% (136) were females, See Table 1

The female predominance in this study was reported in other studies: 53.7% from Tunisia <sup>23</sup>; 56.5% from Egypt <sup>24</sup>

and 60% from Nigeria <sup>25</sup>. Similarly, multiple studies from different regions of Saudi Arabia showed a similar female predominance: 67% in Jeddah <sup>26</sup>; 52.5% in Riyadh <sup>27</sup>; 56% in Abha <sup>28</sup> and more than 50% in the Aseer region <sup>29</sup>. Moreover, a study from South Africa reported a similar female predominance of 63.8% <sup>30</sup>. However, a different study from the Aseer region found that hypertensive males were more prevalent than females (54% vs 46%) <sup>31</sup>.

**Table 1: Age group distribution among male and female hypertensive patients**

			Gender		Total
			Males	Females	
Age group	18-50 years	Count/percentage	39 (54.9%)	60 (44.1%)	99 (47.8%)
	51-70 years	Count/percentage	32 (45.1%)	76 (55.9%)	108 (52.2%)
Total		Count/percentage	71 (34.3%)	136 (65.7%)	207 (100%)

The mean age for patients was 51.7 years and the age range was from 27 to 70 years. This was higher than the mean age of 45.6 years reported by Ibrahim <sup>24</sup> from Egypt and a mean age of 49.6 years reported from Tunisia <sup>23</sup>. However, the mean age was lower than 60 years reported by Al-Khaldi <sup>31</sup>, 57.2 years reported by Al-Tuwijri and Al-Rukban <sup>27</sup> and 57.8 years reported by Ba-Saikh, et al. <sup>26</sup>, all from Saudi Arabia. The latter had found that the age of their sample ranged from 21 to 84 years. In a study from South Africa, the mean age of the study sample was higher; 60.1 years and the range was from 35 to 90 years <sup>30</sup>. However, in another study from Lagos State Hospital in Nigeria, the mean age was 57 years <sup>25</sup>. More than half of the patients (52.2%) were in the 51 years and above age group, a similar figure shown by Boujnah, et al. <sup>23</sup> and Ba-Saikh, et al. <sup>26</sup>.

The prevalence of current smokers in this study was 46.5%, which is nearly double that (24.3%) reported by Batubenga, et al. <sup>30</sup> from South Africa and it is two times higher than that (20.8%) reported by Boujnah, et al. <sup>23</sup> from Tunisia. A much lower number was reported from Aseer <sup>31</sup> and Riyadh <sup>27</sup> as 3% and 8.3%, respectively. There was a statistically significant difference in smoking status among both males and females' hypertensive patients (p=0.000), where none of the females were current smokers nor had a previous history of smoking, while in males 53.6% were either current or ex-smokers.

The highest co-morbid conditions in this study were dyslipidemia followed by diabetes mellitus (32.9% versus 31.9%). Hyperlipidemia was further subcategorized into high levels of LDL-C in 26.1%, TG in 42%, TC in 32.4% and suboptimal HDL-C level in 43.7% of males and 57.4% of females, see Figure 1.

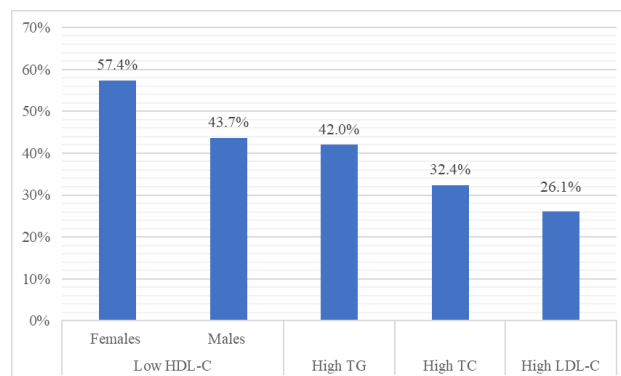


**Figure 1: Pattern of dyslipidemia among the hypertensive patients**

Dyslipidemia is 13.3% higher than that reported by Al-Tuwijri and Al-Rukban <sup>27</sup>, and more than three times that reported by Al-Saleem, et al. <sup>29</sup>. However, it was lower than the prevalence rate found by Al-Khaldi <sup>31</sup> in Saudi hypertensive patients in Aseer region (34-51%). In the latter study, it was shown that 34% of the study sample size have total cholesterol level  $\geq 200$ mg/dl and 51% have TG levels  $\geq 150$  mg/dl. These rates were higher than the results of this study, which showed that abnormal levels of total cholesterol and triglycerides were 32.4% and 42%, respectively. On the other hand, a study from Tunisia has shown that hypercholesterolemia was found in 20.7% of the hypertensive patients <sup>23</sup>.

In a similar fashion, 31.9% of hypertensive patients in this study were diabetics; a prevalence that is similar to what was reported by Al-Saleem, et al. <sup>29</sup>. In addition, such prevalence was lower than results observed in Qatar at 68.9% <sup>32</sup>, in Aseer at 46%<sup>31</sup>, in Riyadh at 38.4% <sup>27</sup>, but it

was more than those reported by another national Saudi study at 22.2%<sup>33</sup>, by Batubenga, et al.<sup>30</sup> from South Africa at 29.5% and by Boujnah, et al.<sup>23</sup> from Tunisia at 19.2%.

The study also shows low frequency of regular physical activity among hypertensive patients under study at 12.1%; this was higher among males (21.1%) than females (7.4 %),  $p=0.004$ . The level of regular physical activity reported by Giroto, et al.<sup>21</sup> was 20% and in a similar fashion it was higher among males than females (26.6% versus 16.3%). This low level of physical activity should not be a surprise considering that sedentary lifestyle is highly prevalent in the Libyan society, where nearly 44% of Libyan adults do not exercise regularly, (51.7% of women and 36% of men)<sup>34</sup>.

**4.2 BMI Distribution of the Hypertensive Patients**

The overall prevalence of obesity was 136 (65.7%), made up of 31 males (22.8%) and 105 females (77.2 %). There was a significant difference in obesity among both genders,  $p$ -value 0.000. This prevalence is higher than the 39% reported from South Africa<sup>30</sup> and lower than the 78.2% reported by Fadupin and Olayiwola<sup>25</sup> among adult hypertensive patients attending the Lagos state hospital, Nigeria. Similarly, it was lower than a study from Saudi Arabia by Barrimah, et al.<sup>35</sup> which showed obesity

rate of 81%. However, some other Saudi studies showed lower rates of 59% and 58% reported by Alzahrani, et al.<sup>36</sup> and Al-Homrany, et al.<sup>28</sup>, respectively. Studies from Tunisia<sup>23</sup> and Egypt<sup>24</sup> showed lower rates in comparison to this study; 26% and 39.8%, respectively.

A study from Aseer region revealed that 47% of the hypertensive patients had obesity of different grades<sup>31</sup>. Another study from Riyadh focused on hypertension control and co-morbidities in primary health care centres<sup>27</sup> showed that 50.4% are obese including a morbid obesity prevalence of 9.2%, which is 3% lower than rate in this study.

The mean BMI of the study subjects was  $32.8 \pm 6.0$  kg/m<sup>2</sup> with a range of 20.4 to 52.8 kg/m<sup>2</sup>. It is worth noting that this mean BMI is higher than that of the general Libyan adult population namely 27.7 kg/m<sup>2</sup><sup>37</sup>. The mean BMI of the nonobese patients was  $26.94 \pm 2.14$  kg/m<sup>2</sup> and that of the obese patients was  $35.89 \pm 5.05$  kg/m<sup>2</sup>,  $p$  value 0.000. They also differed significantly in their SBP ( $137.5 \pm 16.5$  mmHg versus  $142.3 \pm 17.7$  mmHg),  $p < 0.05$  but there was not such difference in their DBP ( $86.6 \pm 12.5$  mmHg versus  $88.4 \pm 11.4$  mmHg)  $p$  value = 0.3, see Table 2.

**Table 2: Clinical and demographic characteristics among obese and non-obese hypertensive patients**

	All (n=207)	Obese (n=136)	Non-obese (n=71)	<i>p</i>
Mean age (years)	51.7±9	51.7±8.4	51.7±10.3	0.9
Gender Male/Female	71/136 (34.3%/65.7%)	31/105 (22.8%/77.2%)	40/31 (56.3%/43.7%)	0.000
Mean BMI (kg/m <sup>2</sup> )	32.8±6	35.9±5	26.9±2.1	0.000
SBP mmHg	140.7±17.4	142.3±17.7	137.5±16.5	< 0.05
DBP mmHg	87.8±11.8	88.4±11.4	86.6±12.5	0.3

Data are shown as mean ± SD or percentage; *p* values refer to comparison of obese and non-obese; BMI=body mass index; SBP=systolic blood pressure; DBP=diastolic blood pressure

Normal BMI was found in 7.7 % of the study subjects. Prevalence of overweight people was 26.6% and most of them were males at 52.7%, a trend being observed worldwide<sup>38</sup>. This rate is similar to that of 26% that was reported by Al-Khaldi<sup>31</sup> but lower than the 35.3% reported by Al-Tuwijri and Al-Rukban<sup>27</sup> and the 29% reported by Al-Homrany, et al.<sup>28</sup>. The different classes of obesity were distributed as follows: 66 (31.9%) with class I obesity, 45 (21.7%) with class II obesity, and class III obesity was found in 25 (12.1%) of the study subjects. Figure 2 shows distribution of hypertensive patients according to their BMI.

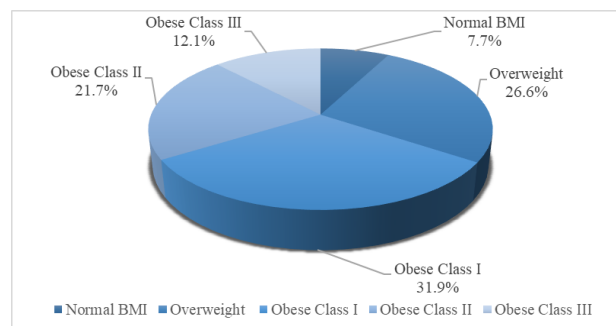


**Figure 2: Distribution of hypertensive patients according to their BMI**

Obesity in this study showed female preponderance. This finding is concurrent with studies in the general Libyan population, which showed that obesity was almost two times more common among Libyan women than men, 21.4% versus 40.1%, respectively<sup>34</sup>. This may be because women tend to have more sedentary lifestyle than men and women in Libya spend much time at home and social events, which are usually associated with consumption of abundant food. In addition, hormonal factors might play a more vital role in accumulation of fat in women than in men<sup>37</sup>. A similar pattern was noted in a study from Egypt that showed obesity was present in 50.3% of hypertensive women<sup>24</sup>.

Considering the age range of obese people in this study, obesity was noted to be more in the age group between 51 and 70 years. The higher BMI for this age group might be due to that elderly people have a higher risk of cardiovascular co-morbidities and less ability to perform regular physical activities because of age-related joint and bone problems. There was no statistical difference in prevalence of obesity or overweight between both age groups, p value > 0.05.

The present study revealed a high association exists between hypertension and obesity. A similar finding was reported in multiple other studies<sup>32, 39-42</sup>. Such association should make physicians working in primary healthcare centres aware of the importance of lifestyle changes (exercise and diet therapy) in the management of HTN through intensive health education programs.

**4.3 Blood Pressure of Hypertensive Patients and its Correlation with Obesity Measurements**

The mean SBP of study subjects was 140.7 ± 17.4 mmHg, whilst the mean DBP was 87.85 ± 11.8 mmHg. The different readings of SBP and DBP of the study sample are shown in Table 3. The mean SBP and DBP for controlled and uncontrolled hypertensive patients are 125.5 and 78.1 mmHg versus 149.6 and 93.6 mmHg, respectively. The overall BP control in all hypertensive patients was “good control” in 36.7%, and 63.3% had poor BP control as can be seen from Figure 3. The prevalence of BP control according to BMI class is illustrated in Figure 4.

**Table 3: Systolic and diastolic blood pressure readings of the hypertensive patients**

		BP level	N	%
Systolic (mmHg)	Controlled	<140	89	43
	Uncontrolled ≥140	140-159	72	34.8
		≥160	46	22.2
Diastolic (mmHg)	Controlled	<90	101	48.8
	Uncontrolled ≥90	90-99	48	23.2
		≥100	58	28

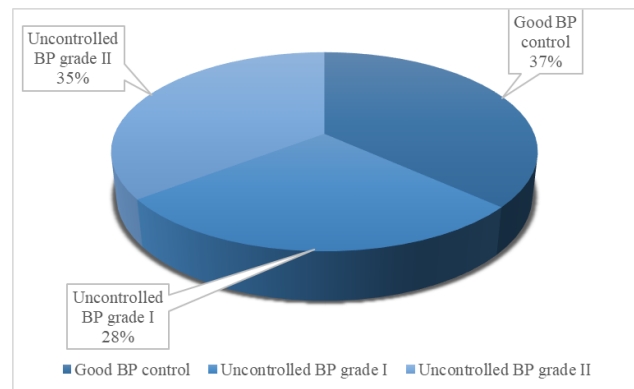


**Figure 3: Prevalence of different BP grades among the hypertensive patients.**

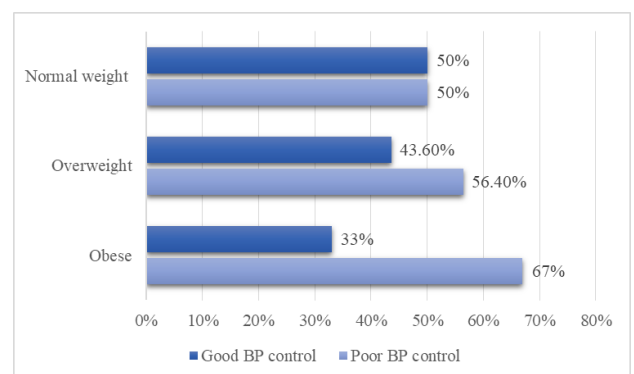


**Figure 4: Blood pressure control in hypertensive patients according to their BMI class**

The good BP control reported in this study is close to the 37.1% reported from Tunisia<sup>23</sup> and 37% from Riyadh in Saudi Arabia<sup>43</sup>; however, it was slightly higher than the 36% found by AL-Shahrani and Al-Khaldi<sup>44</sup> and 35% that was reported from Aseer region<sup>31</sup>. Other studies have shown higher rates of “good control”: 66.5% by Ba-Saikh, et al.<sup>26</sup> from Jeddah, 63% by Al-Homrany, et al.<sup>28</sup> from Abha, 57% by Onwukwe and Omole<sup>45</sup> from South Africa, 56% by Adamu, et al.<sup>22</sup> from Nigeria and 55% by Al-Shidhani, et al.<sup>46</sup> from Oman. Similarly, a study conducted in a specialized healthcare setting in North-western Nigeria showed that good BP control was noted in 42.7%<sup>47</sup> and Al-Saleem, et al.<sup>29</sup> from Aseer showed good BP control in 40% of the study population. On the other hand, other studies had lower control rates as follows: 31.5% by Batubenga, et al.<sup>30</sup> from South Africa, 24.2% by Akpa, et al.<sup>48</sup> from Port Harcourt Nigeria and 15% in Cairo, Egypt<sup>24</sup> and 31% by Hajjar and Kotchen<sup>49</sup> from the USA.

These large differences could be explained by variation of sample sizes, different methods used and definition of cut point of HTN control, along with many other factors that are related to patients, physicians, diseases, and drug efficacy. Regardless of the real reasons for such variations, it is mandatory to reach optimal target of good BP control to prevent long-term serious complications of HTN through intensive health education of patients and

compliance with practical guidelines of HTN care. The need, therefore, for physicians to screen individuals with systemic hypertension for obesity cannot be overemphasized.

It should be also noted that 93.8% of those patients with poorly controlled BP were either overweight or obese as can be seen from Figure 5. This is 15.8% higher than that reported by Adamu, et al. <sup>22</sup> from Nigeria. The relationship between the degree of obesity and BP control should be taken into consideration during management of HTN through raising awareness of healthy lifestyle and weight reduction programs for high-risk hypertension groups.

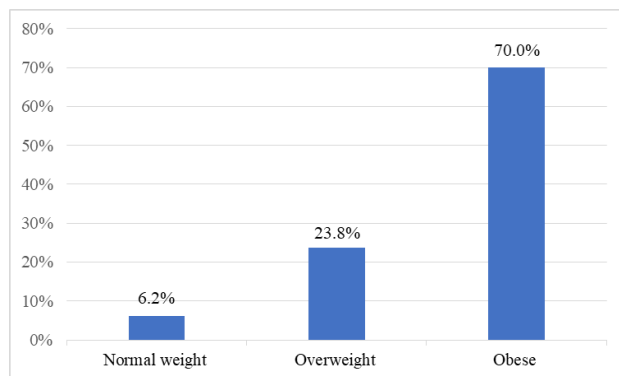


**Figure 5: Distribution of BMI classes among patients with poorly controlled blood pressure.**

Regarding medications prescribed for hypertensive patients, it was found that 61.8% of the patients were on two or more drugs, and more than 70% of them were obese, p- value=0.13. This is in contrast to a study from Oman that reported that about one quarter of the patients (27%) were using two drugs <sup>50</sup>. Al-Rukban, et al. <sup>51</sup> reported that single drug, two drugs and three or more drugs were respectively prescribed for 57%, 26.6% and 10% of hypertensive patients in the capital of Saudi Arabia, Riyadh. These figures were much lower than those reported by Batubenga, et al. <sup>30</sup> who showed that the vast majority of participants (93.6%) in their study in South Africa were on three or more antihypertensive drugs.

Similarly, in a study from Jeddah in Saudi Arabia by Ba-Saikh, et al. <sup>26</sup>, 52.8% of patients were using two or more drugs and the most frequently used drugs were ACEIs (41.9%) and calcium antagonists (38.8%). In this study, calcium antagonists were the most used antihypertensive drugs with 46.3% of patients were using them. Thiazide diuretics and ACEIs were the next most used, at 42% and 37.6%, respectively.

Considering the relationship between BP and obesity measurement, this study showed a positive and statistically significant correlation between BMI and each of SBP (Pearson correlation =0.225, p value= 0.001), DBP (Pearson correlation =0.145, p value= 0.037) and number

of antihypertensive medications used by the patients to control their BP (Pearson correlation =0.216, p value= 0.002). Accordingly, linear regression analysis was studied and confirmed the positive correlation between BMI and each of DBP (Figure 6), SBP (Figure 7) and number of anti-HTN drugs (Figure 8). Similar positive correlation had been shown between WC and SBP (R=.141, p=0.04, B=.209).

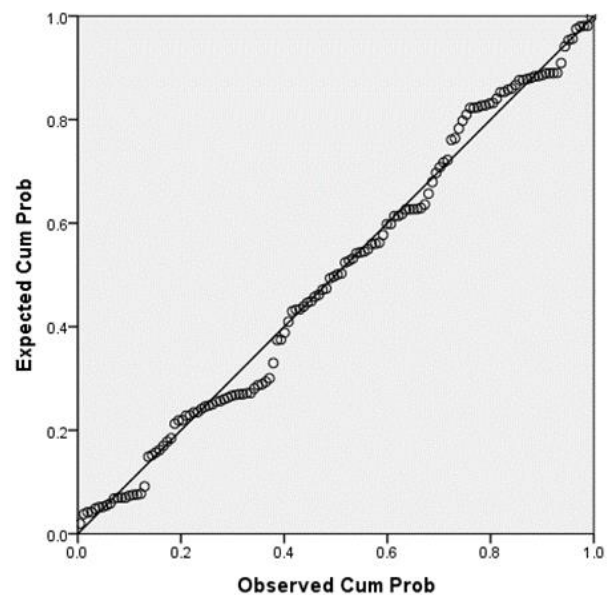


**Figure 6: Linear regression between BMI and DBP among the hypertensive patients (R=0.145, p= 0.037, B=.285).**

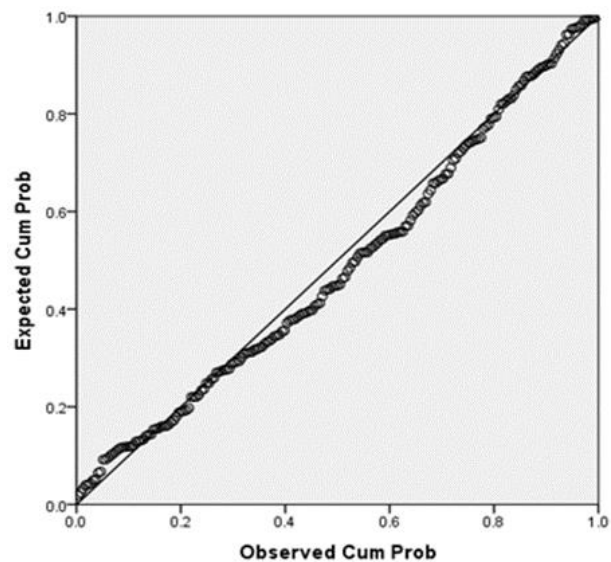


**Figure 7: Linear regression between BMI and SBP among the hypertensive patients (R= 0.225, p=0.001, B=.650).**

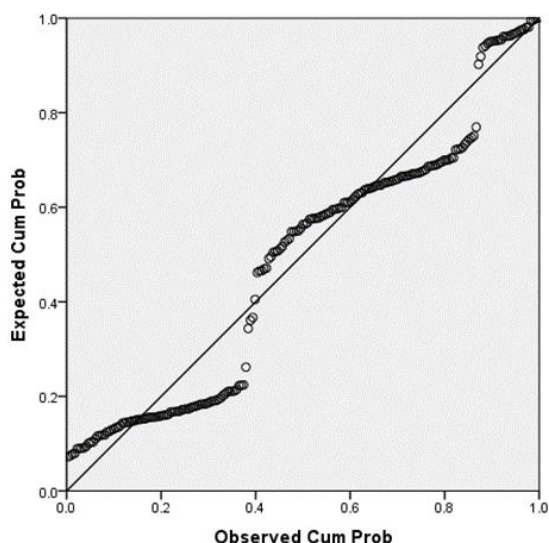


**Figure 8: Linear regression between BMI and the number of used antihypertensive drugs ( $R=0.216$ ,  $p=0.002$ ,  $B=.026$ ).**

#### 4.4 Prevalence of Abdominal Obesity using WC and WHR

The average WHR was  $0.97 \pm 0.05$  for males and  $0.92 \pm 0.06$  for females, whereas WC averaged  $103.1 \text{ cm} \pm 10.6$  and  $108.8 \text{ cm} \pm 11.86$  for men and women, respectively. Importantly, the mean WC for men and women was above the values found in other studies (52-55). As for WHR, Giroto, et al.<sup>21</sup> found close values for men and women, 0.96 and 0.94 respectively, compared to those reported in this study 0.97 and 0.92 respectively. Similarly, Picon, et al.<sup>56</sup> found a mean WHR of 0.93 and 0.98 for women and men, respectively. Such similarities may relate to the fact that the latter study and our study looked at individuals already with a risk factor for the metabolic syndrome such that Picon, et al.<sup>56</sup> considered diabetes, whereas our study considered hypertension. Fadupin and Olayiwola<sup>25</sup> from Nigeria found a higher mean of WHR for both genders; 1.01 for males and 0.97 for females.

This study found high prevalence of abdominal obesity in this population of hypertensive patients measured by both WHR and WC. The prevalence of high WC was higher than that (41%) found by a study from Tunisia<sup>23</sup>.

The prevalence of abdominal obesity determined by WC was higher in females than males (98.5% vs 54.9%,  $p = 0.000$ ). Using WHR, the prevalence was also higher in females (92.6%) than males (88.7%) and  $p > 0.05$ . These results are different from reports from Egypt, which showed that high WHR was more prevalent in males than females<sup>24</sup>.

Comparing both age groups, the prevalence of high WC was higher in the “18-50 years” age group (90.7%) than in the “51-70 years” age group (75.8%),  $p = 0.004$ . Similarly, the prevalence of high WHR was 92.6% and

89.9% for “18-50” and “51-70” age groups, respectively, ( $p > 0.05$ ).

By examining the prevalence of abdominal obesity in both genders, the study found an association between high WHR and each of diabetes mellitus and HDL-C levels, as well as between high WC and uncontrolled blood pressure,  $p=0.03$ . Additionally, High WHR was associated with higher levels of TG and LDL cholesterol in females,  $p=0.03$ .

## 5. CONCLUSION

- This study revealed that general and abdominal obesity is prevalent among hypertensive patients in Al-Kish Polyclinic in Benghazi, Libya.
- More than 75% of the obese hypertensive patients were females, whereas males represented more than 50% of the overweight hypertensive patients.
- The prevalence of co-morbid conditions, namely DM and dyslipidemia, was found in nearly one-third of the hypertensive patients.
- Poor blood pressure control was observed in 63.3% of all hypertensive patients of whom 70% were obese.
- More than 60% of the hypertensive patients were on combined antihypertensive drugs, and more than 70% of them were obese.
- There was a significant positive correlation between BMI and each of SBP, DBP, and the number of antihypertensive drugs used by the patients. A similar correlation was observed between WC and each of SBP and the number of antihypertensive drugs.

## 6. RECOMMENDATIONS

Based on the findings of this study, the authors of this study recommend several actions to be taken by local health authorities, officials, and physicians by:

- Improving the knowledge and the attitude of primary health care physicians towards the importance of achieving the target blood pressure levels according to JNC-8 guidelines and recommendations.
- Identifying obesity through these simple and low-cost measures, which should be part of the routine tasks of primary health care for all hypertensive patients.
- Integrating comprehensive health education regarding lifestyle and behavioural changes into national health policies to avoid obesity comorbidities and to ensure better blood pressure control.

Although the findings of this study suggest a predictive relationship between obesity measurements and BP control, the sample was not nationally representative, and the presence of potential confounders makes it challenging

to suggest meaningful explanations for these relationships. Therefore, similar future research in the field is to be done at larger and better-designed studies aiming to examine and explain the relationships between these variable factors.

## 7. REFERENCES

- Emelia J. Benjamin MJB, Stephanie E. Chiuve, Mary Cushman, Sandeep R. Das, Rajat Deo, Sarah D. de Ferranti, James Floyd, Myriam Fornage, Cathleen Gillespie, Carmen R. Isasi, Monik C. Jiménez, Lori Chaffin Jordan, Suzanne E. Judd, Daniel Lackland, Judith H. Lichtman, Lynda Lisabeth, Simin Liu, Chris T. Longenecker, Rachel H. Mackey, Kunihiro Matsushita, Dariush Mozaffarian, Michael E. Mussolino, Khurram Nasir, Robert W. Neumar, Latha Palaniappan, Dilip K. Pandey, Ravi R. Thiagarajan, Mathew J. Reeves, Matthew Ritchey, Carlos J. Rodriguez, Gregory A. Roth, Wayne D. Rosamond, Comilla Sasson, Amytis Towfighi, Connie W. Tsao, Melanie B. Turner, Salim S. Virani, Jenifer H. Voeks, Joshua Z. Willey, John T. Wilkins, Jason HY. Wu, Heather M. Alger, Sally S. Wong and Paul Muntner. Heart Disease and Stroke Statistics-2017 Update: A Report From the American Heart Association. . *Circulation*. 2017;135(10):e146-e603.  
<https://doi.org/10.1161/CIR.0000000000000485>
- Santulli G. Epidemiology of cardiovascular disease in the 21st century: Updated updated numbers and updated facts. *Journal of Cardiovascular Disease Research*. 2013;1(1).
- Chobanian AV, Bakris GL, Black HR, Cushman WC, Green LA, Izzo Jr JL, Jones DW, Materson BJ, Oparil S, Wright Jr JT. Seventh report of the joint national committee on prevention, detection, evaluation, and treatment of high blood pressure. *hypertension*. 2003;42(6):1206-1252.  
<https://doi.org/10.1161/01.HYP.0000107251.49515.c2>
- Jensen MD, Ryan DH, Apovian CM, Ard JD, Comuzzie AG, Donato KA, Hu FB, Hubbard VS, Jakicic JM. 2013 AHA/ACC/TOS Guideline for the Management of Overweight and Obesity in Adults: A Report of the American College of Cardiology/American Heart Association Task Force on Practice Guidelines and The Obesity Society. *Circulation*. 2014;129(25 Suppl 2):S102.  
<https://doi.org/10.1161/01.cir.0000437739.71477.ee>
- James PA, Oparil S, Carter BL, Cushman WC, Dennison-Himmelfarb C, Handler J, Lackland DT, LeFevre ML, MacKenzie TD, Ogedegbe O. 2014 evidence-based guideline for the management of high blood pressure in adults: report from the panel members appointed to the Eighth Joint National Committee (JNC 8). *Jama*. 2014;311(5):507-520.  
<https://doi.org/10.1001/jama.2013.284427>
- Schmieder RE, Ruilope LM. Blood pressure control in patients with comorbidities. *The Journal of Clinical Hypertension*. 2008;10(8):624-631.  
<https://doi.org/10.1111/j.1751-7176.2008.08172.x>
- Kaess BM, Jozwiak J, Mastej M, Lukas W, Grzeszczak W, Windak A, Piwowarska W, Tykarski A, Konduracka E, Rygiel K. Association between anthropometric obesity measures and coronary artery disease: a cross-sectional survey of 16 657 subjects from 444 Polish cities. *Heart*. 2010;96(2):131-135.  
<https://doi.org/10.1136/hrt.2009.171520>
- WHO. Waist circumference and waist-hip ratio. Report of a WHO Expert Consultation Geneva: World Health Organization. 2008;2008:8-11.
- Lu Y, Hajifathalian K, Ezzati M, Woodward M, Rimm E, Danaei G. Global Burden of Metabolic Risk Factors for Chronic Diseases Collaboration (BMI Mediated Effects). Metabolic mediators of the effects of body-mass index, overweight, and obesity on coronary heart disease and stroke: a pooled analysis of 97 prospective cohorts with 1.8 million participants. *Lancet*. 2014;383(9921):970-983.
- WHO. Global status report on noncommunicable diseases 2014: World Health Organization; 2014.
- Mancia G, Kreutz R, Brunström M, Burnier M, Grassi G, Januszewicz A, Muiesan ML, Tsioufis K, Agabiti-Rosei E, Algharably EAE. 2023 ESH Guidelines for the management of arterial hypertension The Task Force for the management of arterial hypertension of the European Society of Hypertension: Endorsed by the International Society of Hypertension (ISH) and the European Renal Association (ERA). *Journal of hypertension*. 2023;41(12):1874-2071.  
<https://doi.org/10.1097/HJH.0000000000003480>
- Hansen D, Abreu A, Ambrosetti M, Cornelissen V, Gevaert A, Kemps H, Laukkanen JA, Pedretti R, Simonenko M, Wilhelm M. Exercise intensity assessment and prescription in cardiovascular rehabilitation and beyond: why and how: a position statement from the Secondary Prevention and Rehabilitation Section of the European Association of Preventive Cardiology. *European journal of preventive cardiology*. 2022;29(1):230-245.  
<https://doi.org/10.1093/eurjpc/zwab007>
- Batrakoulis A, Jamurtas AZ, Metsios GS, Perivoliotis K, Liguori G, Feito Y, Riebe D, Thompson WR, Angelopoulos TJ, Krstrup P. Comparative efficacy of 5 exercise types on cardiometabolic health in overweight and obese adults: A systematic review and network meta-analysis of 81 randomized controlled trials. *Circulation: Cardiovascular Quality and Outcomes*. 2022;15(6):e008243.  
<https://doi.org/10.1161/CIRCOUTCOMES.121.008243>
- Lopes S, Félix G, Mesquita-Bastos J, Figueiredo D, Oliveira J, Ribeiro F. Determinants of exercise adherence and maintenance among patients with hypertension: a narrative review. *Reviews in Cardiovascular Medicine*. 2021;22(4):1271-1278.  
<https://doi.org/10.31083/j.rcm2204134>

15. Sakane N, Suganuma A, Domichi M, Sukino S, Abe K, Fujisaki A, Kanazawa A, Sugimoto M. The effect of a mhealth app (KENPO-app) for specific health guidance on weight changes in adults with obesity and hypertension: pilot randomized controlled trial. *JMIR mHealth and uHealth*. 2023;11:e43236.  
<https://doi.org/10.2196/43236>
16. Wilding JP, Batterham RL, Calanna S, Davies M, Van Gaal LF, Lingvay I, McGowan BM, Rosenstock J, Tran MT, Wadden TA. Once-weekly semaglutide in adults with overweight or obesity. *New England Journal of Medicine*. 2021;384(11):989-1002.  
<https://doi.org/10.1056/NEJMoa2032183>
17. Banegas JR, Segura J, Ruilope LM, Luque M, García-Robles R, Campo C, Rodríguez-Artalejo F, Tamargo J. Blood pressure control and physician management of hypertension in hospital hypertension units in Spain. *Hypertension*. 2004;43(6):1338-1344.  
<https://doi.org/10.1161/01.HYP.0000127424.59774.84>
18. Goodfriend TL, Calhoun DA. Resistant hypertension, obesity, sleep apnea, and aldosterone: theory and therapy. *Hypertension*. 2004;43(3):518-524.  
<https://doi.org/10.1161/01.HYP.0000116223.97436.e5>
19. Feldstein CA, Akopian M, Olivieri AO, Kramer AP, Nasi M, Garrido D. A comparison of body mass index and waist-to-hip ratio as indicators of hypertension risk in an urban Argentine population: a hospital-based study. *Nutrition, metabolism and cardiovascular diseases*. 2005;15(4):310-315.  
<https://doi.org/10.1016/j.numecd.2005.03.001>
20. Mufunda J, Mebrahtu G, Usman A, Nyarango P, Kosia A, Ghebrat Y, Ogbamariam A, Masjuan M, Gebremichael A. The prevalence of hypertension and its relationship with obesity: results from a national blood pressure survey in Eritrea. *Journal of human hypertension*. 2006;20(1):59-65.
21. Giroto E, Andrade SMD, Cabrera MAS. Prevalence of abdominal obesity in hypertensive patients registered in a Family Health Unit. *Arquivos brasileiros de cardiologia*. 2010;94:754-762.  
<https://doi.org/10.1590/S0066-782X2010005000049>
22. Adamu U, Abdulahi A, Aliyu M, Gbate F, Agboola O, Edem K, Umenze I, Ibok I. Prevalence of Obesity and Its Effect on Blood Pressure Control in Bida, North-Central Nigeria: A Hospital Based Cross-sectional Study. *British Journal of Medicine and Medical Research*. 2017;22(2):1-7.  
<https://doi.org/10.9734/BJMMR2017/33832>
23. Boujnah R, Nazek L, Maalej M, Achhab YE, Nejari C. Hypertension in Tunisian adults attending primary care physicians (ETHNA-Tunisia). *Indian Heart Journal*. 2018;70(4):544-547.  
<https://doi.org/10.1016/j.ihj.2017.11.005>
24. Ibrahim MM. Epidemiology of hypertension in Egypt. *Saudi Journal of Kidney Diseases and Transplantation*. 1999;10(3):352-356.
25. Fadupin G, Olayiwola I. Prevalence of obesity among adult hypertensive patients attending the Lagos State Hospital, Ikeja South West, Nigeria. *Nigerian Journal of Nutritional Sciences*. 2011;32(1).  
<https://doi.org/10.4314/njns.v32i1.67813>
26. Ba-Saikh A, Al-Raddadi RM, Al Dobashi AM, Mohammed E. Hypertension Control and Associated Factors in Patients Attending Primary Health Care Centers in Jeddah, Saudi Arabia. *Imperial Journal of Interdisciplinary Research (IJIR)*. 2017;3(1):2374-2380.
27. Al-Tuwijri AA, Al-Rukban MO. Hypertension control and co-morbidities in primary health care centers in Riyadh. *Annals of Saudi medicine*. 2006;26(4):266-271.  
<https://doi.org/10.5144/0256-4947.2006.266>
28. Al-Homrany MA, Khan MY, Al-Khaldi YM, Al-Gelban KS, Al-Amri HS. Hypertension care at primary health care centers: a report from Abha, Saudi Arabia. *Saudi Journal of Kidney Diseases and Transplantation*. 2008;19(6):990-996.
29. Al-Saleem SA, Al-Shahrani A, Al-Khaldi YM. Hypertension care in Aseer region, Saudi Arabia: barriers and solutions. *Saudi Journal of Kidney Diseases and Transplantation*. 2014;25(6):1328-1333.
30. Batubenga M, Omole OB, Bondo M. Factors associated with blood pressure control among patients attending the outpatient clinic of a South African district hospital. *Tropical Doctor*. 2015;45(4):225-230.  
<https://doi.org/10.1177/0049475515587160>
31. Al-Khaldi YM. Quality of hypertension care in the family practice center, Aseer Region, Saudi Arabia. *Journal of Family and Community Medicine*. 2011;18(2):45.  
<https://doi.org/10.4103/2230-8229.83366>
32. Bener A, Al-Suwaidi J, Al-Jaber K, Al-Marri S, Dagash MH, Elbagi I. The prevalence of hypertension and its associated risk factors in a newly developed country. *Saudi Med J*. 2004;25(7):918-922.
33. Al-Mustafa BA, Abulrahi HA. The role of primary health care centers in managing hypertension. *Saudi med J*. 2003;24(5):460-465.
34. Libyan Ministry of Health. Benghazi diabetes and endocrine center. *Statistics*.; 2009.
35. Barrimah IE, Mohaimed AR, Midhat F, Al-Shobili HA. Prevalence of metabolic syndrome among qassim university personnel in Saudi Arabia. *International journal of health sciences*. 2009;3(2):133.
36. Alzahrani AM, Karawagh AM, Alshahrani FM, Naser TA, Ahmed AA, Alsharif EH. Prevalence and predictors of metabolic syndrome among healthy Saudi Adults. *The British Journal of Diabetes & Vascular Disease*. 2012;12(2):78-80.  
<https://doi.org/10.1177/1474651412441953>

37. Elmehdawi RR, Albarsha AM. Obesity in Libya: a review. *Libyan Journal of Medicine*. 2012;7(1):19086.  
<https://doi.org/10.3402/ljm.v7i0.19086>
38. Flegal KM, Carroll MD, Ogden CL, Curtin LR. Prevalence and trends in obesity among US adults, 1999-2008. *Jama*. 2010;303(3):235-241.  
<https://doi.org/10.1001/jama.2009.2014>
39. Dyer AR, Elliott P. The INTERSALT study: relations of body mass index to blood pressure. INTERSALT Co-operative Research Group. *Journal of human hypertension*. 1989;3(5):299-308.
40. El-Hazmi MA, Warsy AS. Prevalence of hypertension in obese and non-obese Saudis. *Saudi medical journal*. 2001;22(1):44-8.
41. Gupta R, Guptha S, Gupta VP, Prakash H. Prevalence and determinants of hypertension in the urban population of Jaipur in western India. *Journal of hypertension*. 1995;13(10):1193-1200.
42. Kalantan KA, Mohamed AG, Al-Taweel A, Ghani H. Hypertension among attendants of primary health care centers in Al-Qassim region, Saudi Arabia. *Saudi medical journal*. 2001;22:960-963.
43. Saeed AA, Al-Hamdan NA, Bahnassy AA, Abdalla AM, Abbas MA, Abuzaid LZ. Prevalence, awareness, treatment, and control of hypertension among Saudi adult population: a national survey. *International journal of hypertension*. 2011;2011.  
<https://doi.org/10.4061/2011/174135>
44. AL-Shahrani AM, Al-Khalidi YM. Obesity among diabetic and hypertensive patients in Aseer region, Saudi Arabia. *Saudi Journal of Obesity*. 2013;1(1):14-17.  
<https://doi.org/10.4103/2347-2618.119470>
45. Onwukwe SC, Omole OB. Drug therapy, lifestyle modification and blood pressure control in a primary care facility, south of Johannesburg, South Africa: an audit of hypertension management. *South African Family Practice*. 2012;54(2):156-61.
46. Al-Shidhani TA, Bhargava K, Rizvi S. An audit of hypertension at university health center in Oman. *Oman Medical Journal*. 2011;26(4):248.  
<https://doi.org/10.5001/omj.2011.60>
47. Isezuo A, Njoku C. Blood pressure control among hypertensives managed in a specialised health care setting in Nigeria. *African journal of medicine and medical sciences*. 2003;32(1):65-70.
48. Akpa MR, Alasia DD, Emem-Chioma PC. An Appraisal of Hospital Based Blood Pressure Control in Port Harcourt, Nigeria. *Nigerian Health Journal*. 2008;8(1-2):27-30.
49. Hajjar I, Kotchen TA. Trends in prevalence, awareness, treatment, and control of hypertension in the United States, 1988-2000. *Jama*. 2003;290(2):199-206.  
<https://doi.org/10.1001/jama.290.2.199>
50. Al-Awadhi N, Majbour T, Al-Orbany M. Improving hypertension management in primary health care. *Kuwait Med J*. 2007;39:26-30.
51. Al-Rukban MO, Al-Sughair AM, Al-Bader BO, Al-Tolaihi BA. Management of hypertensive patients in primary health care setting, auditing the practice. *Saudi medical journal*. 2007;28(1):85-90.
52. Castanheira M, Olinto MTA, Gigante DP. Associação de variáveis sócio-demográficas e comportamentais com a gordura abdominal em adultos: estudo de base populacional no Sul do Brasil. *Cadernos de Saúde Pública*. 2003;19:S55-S65.
53. Lean M, Han T, Seidell J. Impairment of health and quality of life in people with large waist circumference. *The Lancet*. 1998;351(9106):853-856.  
[https://doi.org/10.1016/S0140-6736\(97\)10004-6](https://doi.org/10.1016/S0140-6736(97)10004-6)
54. Lin S, Cheng TO, Liu X, Mai J, Rao X, Gao X, Deng H, Shi M. Impact of dysglycemia, body mass index, and waist-to-hip ratio on the prevalence of systemic hypertension in a lean Chinese population. *The American journal of cardiology*. 2006;97(6):839-842.  
<https://doi.org/10.1016/j.amjcard.2005.09.133>
55. Pitanga FJG, Lessa I. Associação entre indicadores antropométricos de obesidade e risco coronariano em adultos na cidade de Salvador, Bahia, Brasil. *Revista Brasileira de Epidemiologia*. 2007;10(2):239-248.
56. Picon PX, Leitão CB, Gerchman F, Azevedo MJd, Silveiro SP, Gross JL, Canani LH. Medida da cintura e razão cintura/quadril e identificação de situações de risco cardiovascular: estudo multicêntrico em pacientes com diabetes melito tipo 2. *Arquivos Brasileiros de Endocrinologia & Metabologia*. 2007;51:443-449.  
<https://doi.org/10.1590/S0004-27302007000300013>



## The Analytical Descriptive Study of the Effect of Drinking Water Contamination on the Spread of Hepatitis A Virus in DARAA Governorate-Syria

Wisal Alhommada<sup>1\*</sup> - Tameem Alkrad<sup>2</sup> - khaldon Alkrad<sup>3</sup>

<sup>1</sup> Food Science Department -Agriculture Faculty -Alfurat University.

<sup>2</sup> Educational Science Faculty - Alfurat University.

<sup>3</sup> Assistant Director of Health in Daraa Governorate

Received: 04 / 03 / 2024, Accepted: 27 / 05 / 2024

### ABSTRACT

This study aimed to find out the effect of drinking water pollution on the spread of hepatitis A virus in “Al-Sabil neighborhood” in Daraa governorate in Syria and to know the infection rate in terms of sex (male, female), and age according to age groups (0-12, 13-18, 19-40, 41-60, over 60). Also according to the onset of symptoms (0-10, 11-20 and 21-30) days, and according to the recovery period (less than 100 days - more than 100 days).

The results of the analysis showed that the number of doubtful cases was (6526), where the positive cases were (2118) and the negative cases (4408), As it was shown that males were infected more than females, and the age group from (19-40)year was more susceptible to infection compared to the rest of the age groups, and symptoms began to appear during the first ten days of infection, with a rate of 59.73%, followed by the period from (21-30) days with a rate of 27%, and recovery occurred after one hundred days of infection, at a rate of 59.96%, and it was a significant correlation between the infection and the age, also between one set symptoms and Duration of recovery.

**KEYWORDS:** Hepatitis, Contamination of Drinking Water, Duration of Infection, Recovery Period, Sewage.

### 1. INTRODUCTION

Water is an important element within the ecosystem, as it represents the basic link in food chains, and it is indispensable, and the presence of fresh water is a basic condition for the ecosystem, which constitutes about 2.5% of the total sources of water<sup>1</sup>, but despite the abundance of this component it is exposed to contamination by natural, biological, chemical and radiological pollutants, and this problem is often major in rural areas that depend on wells. The problem of treating wastewater is also a major problem as it contains a large and diverse group of microorganisms that cause harm to humans, animals and plants, while the majority of them, are harmless and may even be beneficial and used to purify water<sup>2,3</sup>.

According to reports from the World Health Organization (WHO), the most common water-borne diseases are enteric viruses, which pose a serious threat to human health in all parts of the world. It causes the death of about two million people, especially in rural areas and children under five years of age, in the absence of sewage treatment and the lack of treatment plants<sup>4</sup>. This water is discharged into marine estuaries, springs and dams, which in turn undergo permanent changes in its physical, chemical and bacteriological composition<sup>5,6</sup>.

Environmental pollution is a public health problem represented by greenhouse gases and acid deposition, which have reached a dangerous level all over the world, as well as industrialization processes that coincide with economic growth and thus more waste discharge<sup>7,8</sup>.

In addition, human activities, chemicals and industrial materials play a major role in water pollution, and WHO reported that 80% of bacterial, viral and parasitic diseases are waterborne, which negatively affects human health and the spread of some diseases such as scabies, asthma, dysentery and respiratory diseases<sup>9,10</sup>, as well as anemia, low platelets, increased risk of cancer, and many skin diseases<sup>11</sup>.

The environmental effects of irrigation with wastewater on soil, plants, animal and human health were also studied, which contain bacteria, protozoa, viruses that cause diseases, or waste from pharmaceutical and pesticide factories, in addition to diseases transmitted through contaminated water as dengue fever, malaria, and yellow fever; Diversity of microbial communities are affected by changes in environmental conditions<sup>12,13</sup>.

In developing countries social and economic inequality are the main reasons for the use of polluted water, such as poverty, the standard of living, health facilities, age, gender, and level of education These factors have a

\*Correspondence: Wisal Alhommada.

[wisal.alhommada@gmail.com](mailto:wisal.alhommada@gmail.com)

prominent role in increasing health awareness and education, as in developed countries<sup>14,15</sup>.

The spread of contemporary viruses, such as Ebola and SARS-Cov-2, has contributed to increasing interest in the issue of water purity, especially water contaminated with viruses, which is the appropriate environment for their spread, as well as in developing countries that are characterized by low social and economic development and thus a low quality of services provided to the population<sup>14</sup>.

The most important causes of intestinal diseases in developing and developed countries are enteric viruses such as cholera, typhoid, and hepatitis (Figure 1). They are of diverse groups and are transmitted by the fecal-oral route, which mainly causes diarrheal diseases.

The average presence of the various Sap virus viruses is  $1.36 \times 10^6$  gc, which was significantly higher compared to Norovirus GII viruses, which reached an average of  $2.94 \times 10^4$  gc.<sup>4,16</sup>

Hepatitis A virus had the highest percentage among the viruses detected in the metagenomic wastewater analysis, as it was significantly associated with an increase in disease cases within one week, as untreated sewage is one of the sure ways for the presence of hepatitis A virus<sup>16</sup>.

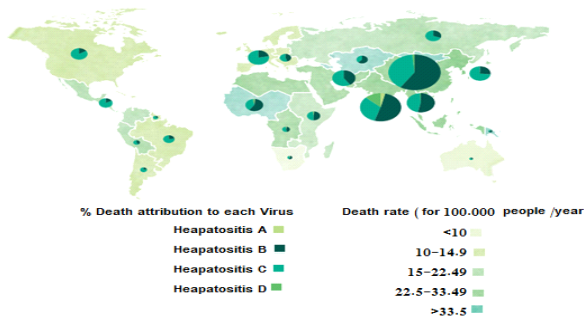


**Figure 1. Regional distribution of hepatitis in the world**

**Source: Global health sector strategy on Viral Hepatitis**

A relationship was also found between water pollution and infection with hepatitis A and waste accumulation, in addition to the fact that males are more infected than females: and those younger than those are more susceptible to infection with hepatitis<sup>14</sup>.

Transmission of the hepatitis A virus occurs through food, as it is one of the most common viruses caused by food-borne infections. Contamination of these foods may occur by those infected without their knowledge. It is capable of resisting food preparation processes, which one of its most important goals is to neutralize pathogenic bacteria. The number of new infections is estimated at about 1.4 million in the world, and developing countries are among the countries where the number of infections is increasing due to the lack of treatment of wastewater or used water<sup>17</sup>.

Hepatitis A is a highly contagious leads to infections that impair liver function, but it is a limited disease that does not cause chronic symptoms. This virus is transmitted in several ways, including eating foods manufactured by a person infected with the virus, drinking water contaminated with sewage, having direct contact with the infected person, even if he does not show symptoms, and having sexual relations with a person infected with hepatitis A .

The symptoms of the disease appear in adults, and range from severe to mild, including yellowing of the skin and eyes, abdominal pain, dark urine, nausea, vomiting, and high temperature.

Therefore, the purpose of this research was to conduct a descriptive and analytical study of the health situation that Al-Sabil neighborhood in the city of Daraa was exposed to, which contributes to developing the ability to respond more quickly to the epidemic and to contain it, and to increase the ability to treat cases of water contamination with hepatitis A type.

## 2. RESEARCH OBJECTIVE

The research aims to conduct a descriptive analytical study of contaminated drinking water and cases infected with hepatitis A in the Al-Sabil area in Daraa Governorate. In addition to analyzing the demographic factors associated with an increased risk of hepatitis A virus infection in the study population. Also, study the extent to which the occurrence of the epidemic is related to the degree of water pollution and the degree of independence of each.

## 3. RESEARCH JUSTIFICATIONS

As a large number of Al-Sabil neighborhood's residents were suffering from several medical cases such as diarrhea, vomiting, and high fever, most cases were admitted to the hospital and they were using the same source of drinking water which appeared to be mixed with sewage due to the occurrence of deterioration and fractures in the sewage system, this work was undertaken to evaluate Al-Sabil drinking water system,

## 4. MATERIALS AND METHODS

The descriptive analytical approach was used for samples and information and was completed through personal interviews of the patients by doctors, and nurses in the Health Directorate and the Syrian Arab Red Crescent branch in the city of Daraa, as well as oral and written reports were obtained by health care workers (doctors, nurses, administrators) to the researchers. Laboratory analyses of samples taken through the mobile clinic affiliated with the Health Directorate from almost all the residents of the Al-Sabil neighborhood, in addition to the patient lists in each city of Daraa for health centers and private clinics.

Analysis of water samples from all regions of Daraa was performed in the laboratories of the Water, Environment and Health Directorates during the period from 30/03/2021 to 30/05/2021.

The specifications of the water that will be pumped from the Water Directorate in the city of Daraa must conform to the Syrian standard specifications and not exceed the permissible values according to table 1.

**Table 1 Water specifications according to Syrian standard specifications**

Analysis	The maximum permitted according to Syrian specifications	
	value	UNIT
Turbidity	5	NTU
Electrical conductivity	2000	Us/cm
Solid phase	1200	mg/l
pH	6.5-9	--
Hardness	700	mg/l
NH4+	0.5	mg/l
Na+	300	mg/l
Ca+	-	mg/l
Mg+	-	mg/l
F-	1.5	mg/l
Cl-	500	mg/l
SO4	500	mg/l
NO3	60	mg/l
NO2	0.2	mg/l
PO4	1	mg/l

## 5. ANALYSIS OF DRINKING WATER

### 1. Devices used in water analysis:

The analysis conducted in the Water, Environment, and Health Directorates in the city of Daraa studied water before, during, and after the occurrence of the pandemic, and Hygiene water bacterial detection device was used, which is a field device to detect bacterial presence in water immediately, as the percentages must be less than 5. It is affiliated with the Health Directorate in Daraa.

### 2. 2- Devices used to analyze blood samples of infected and suspected patients:

The analysis devices used in the comprehensive clinic laboratories of the Daraa Health Directorate, in addition to the laboratories of the Syrian Red Crescent Organization and private laboratories, were SAT 450, an automated chemistry device made in Italy, that measures liver enzymes, MEMMERT dry bacterial sterilizer, German made, sterilizing dishes and tools used in the analysis, A Memmert bacterial incubator at a temperature of 37 °C to incubate the bacterial culture media, A wet sterilizer to sterilize and prepare bacterial media, Bacterial culture media EMB-SS, MacConkey medium, Tryptone medium, and Ptry medium, AST and ALT analysis, which are specific to liver enzymes, as their elevation above 50 indicates infection with hepatitis C, and HAV analysis, which is specific for hepatitis A type.

## 6. STATISTICAL ANALYSIS

SPSS version 23 was used and descriptive statistics, frequency tables, percentages, correlation coefficient, and chi-square will be measured.

## 7. RESULTS AND DISCUSSION

Analysis of the sample was conducted on both contaminated drinking water and blood from people who showed symptoms of hepatitis in the contaminated area (Al-Sabil neighborhood), which were represented by nausea, vomiting, and abdominal pain. It was found that there was contamination of the water with sewage after bacterial and biological cultivation of the water.

According to the Syrian standard specifications for water specifications, the percentage of metals and other pollutants was high, and according to the statistics submitted by the Directorate of Health in Daraa to the Ministry of Health regarding the numbers of final examined cases as in Table (2), the results showed that 2118 out of 6526 were positive case for AST – ALT whereas 4408 cases were negative.

**Table 2 Statistics provided by the Daraa Health Directorate**

Negative cases	Positive cases	Total cases
4408	2118	6526

From Table (3), it is clear that the number of positive male cases was high in the case of the male variant and amounted to and accounted for (55.71%) of the total positive cases, while the percentage of infection among females reached (44.29%) of the total number of positive cases, accounted for (2118) people.

**Table 3 Percentage and frequencies of examined cases according to gender variable**

Variable	Range	Total		Percentage			
				negative		positive	
		%	number	%	Number	%	number
Sex	male	55.9	3648	55.99	2468	55.71	1180
	female	44.1	2872	44.01	1940	44.29	938
overall		100	6526	100	4408	100	2118

Table (4) shows that the age group (19-40) has the highest infection rate with 27.9% of positive infection rate, followed by the age stage (0-12) with the 26.8%, and the lowest infection rate was in the sample with over than 60

years, but the spread of the virus varies from region to another where it reaches 57% for those ranged 15 to 19 in the Caribbean countries and reached to 96% for Andean regions<sup>18</sup>.

**Table 4 Percentage and frequencies of examined cases according to age variable**

Variable	Range	Total		Percentage			
				Negative		Positive	
		%	Number	%	Number	%	Number
Age	0-12	27.9	1821	27.89	1229	27.95	592
	13-18	26.8	1751	26.86	1184	26.77	567
	19-40	41	2675	40.94	1805	41.08	870
	41-60	3.5	226	3.5	154	3.4	72
	60<	0.8	53	0.81	36	0.80	17
Overall		100	6526	100	4408	100	2118

Table (5) shows that the severity of infections with hepatitis A virus began during the first ten days of contamination and reached approximately (59%) with a frequency of (1265) positive cases. The number of people

who showed symptoms of the disease reached 21 days after exposure to contaminated water and continued to increase.

**Table 5 Percentage and frequencies of examined cases according to Onset of symptoms variable**

Variable	Rang	Total		Percentage			
				Negative		Positive	
		%	Number	%	Number	%	Number
Onset of symptoms	0-10	58.5	3820	57.96	2555	59.73	1265
	11-20	13.2	861	13.16	580	13.27	281
	21-30	28.3	1845	28.88	1273	27	572
	Overall	100	6526	100	4408	100	2118

Up to 30 days, there were (572) positive cases, compared to the period from (11-20) days, which was the least in the appearance of symptoms of the disease, and the percentage of positive cases was (13.27%).

As for the cases that were cured, the highest recovery rate occurred 100 days after the infection and accounted for approximately 60% of the infected people, compared to 40% of the infected people who recovered 100 days before the infection, as in Table (6).

**Table 6 Percentage and frequencies of examined cases according to the variable of recovery duration**

Variable	RATE	Percentage	
		%	Number
recovery duration	100>	40.04	848
	100<	59.96	1270
	<b>Total</b>	100	2118

The length of the recovery period also varied. The duration of recovery ranged and differed according to the infected people, their ages, and their gender, as table 7 shows. The percentage of people who recovered before

100 days in the childhood group was 12% compared to the period after 100 days, which amounted to approximately 16%. The same applies to the teenage age group, the youth age group, and the stages of manhood and adulthood.

**Table 7 Statistical analysis of recovery cases according to the relationship between variables**

Variable	Recovery period	%	>100	%	<100
Age	0-12	15.58	330	12.37	262
	13-18	17.85	378	8.92	189
	19-40	23.70	502	17.37	368
	41-60	2.22	47	1.18	25
	>60	0.61	13	0.189	4
Sex	male	33.71	714	22	466
	female	26.25	556	18.04	382
Onset of symptoms	0-10	24.17	512	35.55	753
	11-20	8.88	188	4.4	93
	21-30	26.91	570	0.1	2

In addition, the recovery rate for males 100 days after infection with hepatitis C disease was higher, reaching 33.71% compared to females, and this is due to the higher infection rate for males than for females.

By performing the correlation coefficient between the studied variables, as in table (8), it is apparent that there is a strong positive correlation between the variable of the stage of onset of symptoms and the length of the recovery period. It was also observed that there is a negative significant correlation between the variables of age and the onset of symptoms with the variable of gender, and there was no correlation between age variable and other variables.

**Table 8 Correlation coefficient between the studied variables**

Variables	Age	onset of symptoms	duration of recovery
Sex	*0.048-	*0.049-	ns
Age	--	ns	ns
onset of symptoms	----	---	**0.523

By conducting an analysis of variance, it was observed that there were

significant differences according to the variables of gender, age, the onset of symptoms, and the length of the recovery period. Likewise, the differences were significant between age and gender, and between the period of appearance of symptoms with age, gender, and the length of the recovery period, the differences between them were significant, as shown in Table (9).

**Table 9 significant differences between the studied variables**

Variables	Duration of recovery	ONSET symptoms	Age	Sex
Sex	Un	**	**	**
Age	Un	un	**	**
Onset symptoms	**	**	un	**

Un: insignificant                      \*\*: significant at 0.01

### 8. CONCLUSIONS & RECOMMENDATIONS

1. Males are more susceptible to infection than females, and young people are more susceptible to infection compared to other age groups.
2. Symptoms begin within the first ten days of the disease, and most recovery occurs after one hundred days from the beginning of the infection.
3. The importance of correct sterilization of the equipment used for analysis and not repeatedly using the tools.
4. The locations of sewage pipes must be far from drinking water sources so that if a leak occurs, it does not lead to health risks.
5. Periodic detection of sewage sources and pipes and increasing citizens' awareness of the dangers of pollution and not throwing waste, which in turn leads to an increase in the percentage of pollution.
6. Environmental and health awareness through print and audio media to increase protection, prevention and awareness.

### 9. REFERENCES

1. Kılıç Z. Water pollution: causes, negative effects and prevention methods. *Istanbul Sabahattin Zaim Üniversitesi Fen Bilimleri Enstitüsü Dergisi*. 2021;3(2):129-132.  
<https://doi.org/10.47769/izufbed.862679>
2. Cyprowski M, Stobnicka-Kupiec A, Ławniczek-Wałczyk A, Bakal-Kijek A, Gołofit-Szymczak M, Górny RL. Anaerobic bacteria in wastewater treatment plant. *International Archives of Occupational and Environmental Health*. 2018; 91:571-579.  
<https://doi.org/10.1007/s00420-018-1307-6>.
3. Cyprowski M, Szarapińska-Kwaszewska J, Dudkiewicz B, Krajewski JA, Szadkowska-Stańczyk I. Exposure assessment to harmful agents in workplaces in sewage plant workers. *Medycyna Pracy*. 2005 ;56(3):213-222.
4. World Health Organization .WHO. A regional overview of wastewater. management and reuse in the Eastern Mediterranean Region. 2005.
5. Upfold NS, Luke GA, Knox C. Occurrence of human enteric viruses in water sources and shellfish: A focus on Africa. *Food and Environmental Virology*. 2021 Mar;13(1):1-31.  
<https://doi.org/10.1007/s12560-020-09456-8>.
6. Lamine I, Alla AA, Bourouache M, Moukrim A. Monitoring of Physicochemical and Microbiological Quality of Taghazout Seawater (Southwest of Morocco): Impact of the New Tourist Resort " Taghazout Bay". *Journal of Ecological Engineering*. 2019;20(7).  
<https://doi.org/10.12911/22998993/109873>.
7. Abbasi T, Abbasi SA. Water quality indices based on bioassessment: The biotic indices. *Journal of Water and Health*. 2011 Jun 1;9(2):330-348.  
<https://doi.org/10.2166/wh.2011.133>
8. Loux NT, Su YS, Hassan SM. Issues in assessing environmental exposures to manufactured nanomaterials. *International Journal of Environmental Research and Public Health*. 2011;8(9):3562-3578.  
<https://doi.org/10.3390/ijerph8093562>.
9. Chowdhary P, Bharagava RN, Mishra S, Khan N. Role of industries in water scarcity and its adverse effects on environment and human health. *Environmental Concerns and Sustainable Development: Volume 1: Air, Water and Energy Resources*. 2020:235-256.  
[https://doi.org/10.1007/978-981-13-5889-0\\_12](https://doi.org/10.1007/978-981-13-5889-0_12).
10. Hanif MA, Miah R, Islam MA, Marzia S. Impact of Kapotaksha river water pollution on human health and environment. *Progressive agriculture*. 2020;31(1):1-9.  
<https://doi.org/10.3329/pa.v31i1.48300>.

11. He X, Li P. Surface water pollution in the middle Chinese Loess Plateau with special focus on hexavalent chromium (Cr6+): occurrence, sources and health risks. *Exposure and Health*. 2020 Sep; 12(3):385-401.  
<https://doi.org/10.1007/s12403-020-00344-x>.
12. Singh A. A review of wastewater irrigation: Environmental implications. *Resources, Conservation and Recycling*. 2021 May 1; 168:105454.  
<https://doi.org/10.1016/j.resconrec.2021.105454>.
13. Hassan W. Alibi S. Al-Hadi B M. Assessment of Physico-chemical and Microbial Contamination of Wastewater and Seawater in five Mediterranean Countries. *Arabian Journal of Scientific Research*. 2021 Jun 10; 2021(1): 6.
14. Eljamay SM, Alghazali MA, Younis MM, Ekrouma EM, Taher ZM. Effect of Environmental Pollution on the Spread of the Epidemic Hepatitis A virus in Derna City\Libya and neighbor area, *Al-Hadra Journal for Humanities and Applied Sciences*, fourth issue, 2022, p (176-186).
15. Adelodun B, Ajibade FO, Ighalo JO, Odey G, Ibrahim RG, Kareem KY, Bakare HO, Tihamiyu AO, Ajibade TF, Abdulkadir TS, Adeniran KA. Assessment of socioeconomic inequality based on virus-contaminated water usage in developing countries: a review. *Environmental Research*. 2021; 192:110309.  
<https://doi.org/10.1016/j.envres.2020.110309>
16. McCall C, Wu H, O'brien E, Xagorarakis I. Assessment of enteric viruses during a hepatitis outbreak in Detroit MI using wastewater surveillance and metagenomic analysis. *Journal of Applied Microbiology*. 2021 Sep 1;131(3):1539-1554.  
<https://doi.org/10.1111/jam.15027>.
17. World Health Organization WHO .World Health Association report.2009.
18. World Health Organization WHO. Preventing and controlling viral hepatitis infections.2012.